

**DRAINAGE MORPHOMETRY AND MORPHOTECTONICS OF UPPER TUIRIAL
RIVER BASIN, MIZORAM**

A THESIS SUBMITTED IN PARTIAL FULFILMENT OF THE REQUIREMENTS FOR
THE DEGREE OF DOCTOR OF PHILOSOPHY

BINOY KUMAR BARMAN

MZU REGN. NO. 5604 OF 2013
Ph.D. REGN. NO. MZU/Ph.D./ 998 of 31.05.2017



**DEPARTMENT OF GEOLOGY
SCHOOL OF EARTH SCIENCES AND NATURAL RESOURCES MANAGEMENT**

AUGUST, 2020

**DRAINAGE MORPHOMETRY AND MORPHOTECTONICS OF
UPPER TERTIARY RIVER BASIN, MIZORAM**

BY

**BINOY KUMAR BARMAN
DEPARTMENT OF GEOLOGY**

Research Supervisor

**Prof. K. Srinivasa Rao
Department of Geology, Mizoram University, Aizawl**

Joint Supervisor

**Dr. N.S.R. Prasad
Centre for Geoinformatics Applications in Rural Development,
National Institute of Rural Development and Panchayat Raj, Govt. of
India, Guwahati.**

Submitted

**In Partial fulfilment of the requirement of the degree of
Doctor of Philosophy in Geology of Mizoram University, Aizawl**

CERTIFICATE

This is to certify that this thesis entitled “Drainage Morphometry and Morphotectonics of Upper Tuirial River Basin, Mizoram” submitted by Binoy Kumar Barman for the degree of Doctor of Philosophy to the Mizoram University is based on the results of studies carried out by him under our supervision and guidance. This thesis or any part of this thesis has not been submitted elsewhere for the award of any other degree or diploma.



Joint Supervisor
(Dr. N.S.R. Prasad)



Supervisor
(Prof. K. Srinivasa Rao)

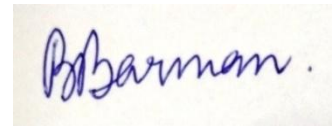
MIZORAM UNIVERSITY

AUGUST, 2020

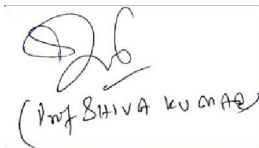
DECLARATION

I Binoy Kumar Barman, hereby declare that the subject matter of this thesis is the record of work done by me, that the contents of this thesis did not form basis of the award of any previous degree to me or to do the best of my knowledge to anybody else, and that the thesis has not been submitted by me for any research degree in any other University/ Institute.

This is being submitted to the Mizoram University for the degree of Doctor of Philosophy in Geology.



(Binoy Kumar Barman)
Candidate



(Prof. Shiva Kumar)
Head



(Prof. K. Srinivasa Rao)
Supervisor

ACKNOWLEDGEMENT

First and foremost, I would like to express my hearty thanks to my Research supervisor **Professor K. Srinivasa Rao**, Department of Geology, Mizoram University, Aizawl for his valuable guidance, continuous encouragement and kind hearted approach that always remained a vital force in the successful completion of my research work. I am obliged to express my sincere thanks and gratitude to my joint supervisor **Dr. N. S. R. Prasad**, Assistant Professor (C-GARD), NIRD & PR, Guwahati, presently posted in Hyderabad for the help and support made throughout the thesis work. I am very much thankful to **Dr. U.B. Rao**, Associate professor, Department of Geography, Mizoram University for his support, suggestions and help throughout this research work. I am very much thankful to **Prof. Shiva Kumar**, Head, Department of Geology, Mizoram University for his encouragement and support during my research work. I am very much thankful to **Mr. Gautom Raz Bawry** and **Miss Liza Gogoi**, Research Scholars, Department of Geology for their valuable support and helping me in each and every aspect of this research work during my research career.

I am always be indebted to my mother **Mrs. Khuki Barman**, my father **Mr. Poresh Barman**, my brothers and sisters for their financial support and love and all my relatives whose love and support have been a constant source of inspiration and encouragement.

I also extend my thanks to my friend **Mr. Sankar Singha** for his constant encouragement throughout my research work.

Finally, I wish to express my sincere thanks to Mizoram University, Aizawl, for providing considerable support and laboratory facilities during the course of this research work.



(Binoy Kumar Barman)

Abstract

Upper Tuirial watershed is the western tributary of Barak River of Assam which covers an area of 534.81 km², originates in the state of Mizoram, NE India. This study was carried out to understand the sub surface lithological characteristics, morphology and evolution of the landforms also to explore various important natural resources using conventional, Remote Sensing and GIS based analysis. The morphometric analysis of an area is an important criterion to monitor and understand the hydrological behaviour of the basin and to carry out management strategies of the watershed based on prioritization. A total of 19 sub-watersheds were delineated and calculated the various morphometric parameters. Following the computation of morphometric parameters and their significant values, prioritisation of Sub-watershed was done through geo-statistical techniques for immediate remedies.

This study reveals that the Upper Tuirial River is a six order river basin. The study is mainly focused on basin morphometric parameter such as linear aspects [Stream Order, Bifurcation Ratio, Stream length, Stream frequency and areal aspects [Form factor, Circulatory Ratio, Elongation Ratio and Drainage density] and Relief aspects [Relief, Relative relief, Relief ratio and Ruggedness Number]. During the study, relationships among the linear morphometric indices hold true for Horton's Law of drainage composition.

Based on the detail analysis of the linear, areal and relief aspects of morphometric parameters, it is found that upper Tuirial watershed, as well as those of the nineteen sub basins are characteristics of resistant and impermeable sub surface having homogeneous lithology, late youth to mature stage of erosional development and less storage capacity of water. Lower-order streams mostly dominate each basin. Based on mean weighted bifurcation ratio values it is found that sub watershed Kailian (5.34), Ngharum (5), Zilpui (5.49), Muthi (5.36) and Tuipawl (5) are structurally controlled basin. Sub watershed sakei, suibual, Belkhui, Nghalrawh, Tuiphu, Tuizual and Chite are slightly structurally distorted and the sub watersheds Nghathup, Sherbawk, Tuirial, Tulrital, Darkhuang, Suanghuan and SW18 are geologically controlled basin. High values of drainage density and drainage frequency with coarse to mostly medium texture ratio suggesting impermeable sub surface lithology, less infiltration rate, rugged topography, and high run off with high rate of erosion and dissection. Lg values for different sub watershed ranges from 0.09 km for Darkhuang to 0.20 km for Nghathup indicating high runoff, less infiltration and high rate of erosion. As the

length of overland flow is very short, construction of artificial recharge structures is not feasible in the region. The constant of channel maintenance value is $0.25 \text{ km}^2/\text{km}$ i.e., only 250 square meters of area is needed to run 1000 meters of stream indicating that the area is characterized by high surface runoff, low permeability, less infiltration and closely dissected. The circularity ratio values ranges from 0.44 for Kailian to 0.67 for Muthi indicates that the area is characterized by high to moderate relief, mature stage of geomorphic development and elongated in shape. The values of Relief ratio, gradient ratio and average slope angle indicate that the discharge capability of the watersheds is very high and ground water potential is meagre. The hypsometric integral value ranges from 0.5 to 0.55 indicating that all the sub watersheds have attained the steady state condition (mature geologic stage).

As an applied aspect of morphometric analysis, identification and prioritization of soil erosion prone zones and groundwater potential zones were also demarcated in the study area.

Prioritisation of different sub watersheds were carried out using Compound Factor (CF) model as Multi Criteria Decision Making (MCDM) techniques and the results showed that sub-watershed Tulrital is highly susceptible to erosion followed by sub watersheds Zilpui, Tuiphu, SW18, Belkhui, Darkhuang, sakei, Chite, Ngharum, Muthi, Tuipawl, Nghalrawh, Kailian, Suanghuan, Suibual, Nghathup, Sakei, Sherbawk and the least erosive sub watershed is Tuirial.

For the identification of groundwater potential zones, TOPSIS (Technique of Order Preference Similarity to the Ideal Solution) based multi criteria decision making tool was performed on selected morphometric parameters. The result of this analysis revealed that sub watershed Kailian is the best potential zones for groundwater resources and sub watershed Tulrital is found to be the most deficit zone of groundwater.

The second aspect of the study is the Morphotectonic study of Upper Tuirial watershed for investigating geomorphic signatures of active tectonics using geographical information system (GIS). Most commonly used geomorphic indices for morphotectonic analysis; viz. Basin elongation ratio (Re), Transverse topographic symmetry (T), Asymmetric factor (AF), Valley floor width to valley height ratio (Vf), Mountain front sinuosity (Smf), Longitudinal profile and Stream length gradient index (SL) have been used in this study. From the analysis of various morphotectonic parameters, it is found that there is a strong relationship between topography and active deformation and is reflected in the geological and

geomorphological set-up of the Upper Tuirial Basin. The lineament analyses indicate that there is only one set of prominent lineaments trending almost N-S direction and few lineaments oriented in all directions. The development of N-S oriented Faults/lineaments is expected in this region as the basin is under East-West tectonic compression due to collision of Indo-Burmese plates. The elongation ratio values found to be 0.56 indicating that the basin is slightly tectonically active. The Hypsometric Integral values vary from 0.50 for Suibual to 0.55 for Ngharum and 0.51 for the whole watershed indicating mature landscape and slightly tectonically active. Exceptionally high value of stream length gradient index is shown as knick zones along the longitudinal profile of sub watershed Chite, Muthi, Suanghuan, Tuizual, Ngharum and Tulrital. These anomalous high values cannot be due to rock resistance to erosion only, but there must be some strong tectonic activity. The values of valley floor to valley height ratio indicate deep, narrow, V-shaped valleys due to intense incision and gradual uplift signifies strong tectonic activity. The mountain-front sinuosity values for different sub watersheds measured at different sections are found to be in the ranges of 1.02 to 1.52. These low values are the indication of active tectonism in the watershed. The values of asymmetry factor revealed that all the major channels have been shifted downstream to either right tilt or left tilt. This downstream shifting of river is possibly due to the obstruction by faulting.

Soil loss assessment was also carried out in the present study. Soil erosion is a major problem in the present world which affects the agricultural production, soil fertility, excessive siltation and sedimentation in lakes and rivers. Though it is a natural process but due to anthropogenic intervention in over exploitation of natural resources, this process has been accelerated in the recent past. Degradation of land cover due to shifting cultivation is one of the triggering factors in accelerating the soil erosion in this region. A comprehensive methodology that is Revised Universal Soil Loss Equation (RUSLE) was adopted in the present study in order to estimate the soil loss of Tuirial river basin of Mizoram. The various thematic layers generated and utilized for the RUSLE model are rainfall erosivity factor (R), soil erodibility factor (K), slope length (L), slope steepness factor (S), crop management factor (C) and practice management factor (P). For analysis of each layer, rainfall data collected from Directorate of Agriculture and Crop Husbandry, govt. of Mizoram, soil textural map was generated based on the National Bureau of Soil Survey and Land Use Planning (NBSS & LUP), CARTOSAT DEM of 30 m spatial resolution for L and S factors, and Sentinel 2A multispectral satellite data for C and P factors were used. The estimated

average annual soil loss from the study area is found to be $115.4 \text{ Mg ha}^{-1} \text{ yr}^{-1}$. The estimated total loss of sediments is 6.161 million Mg yr^{-1} . From this study it is also found that the severe erosion zones are mostly in areas with high slope values. While slight erosions are mostly observed in areas with low slope values. The prominent cause of soil erosion in the study area is high intensity of rainfall, mountainous terrain with steep slopes and unscientific practices of shifting cultivations.

Land use and land cover change detection for a period of 2000 to 2018 was analysed to monitor LULC transformation. The overall accuracy assessment and kappa coefficient values showed accepted accuracy limit. Over the study period, there is a significant changes observed in LULC classes, as evidenced by a sharp increase in built-up from 1.51% in 2000 to 4.02 % in 2018 and a net increase of 14.04% of scrubland within the landscape. The period 2000-2018 has shown a sharp decrease of jhumland from 19.65 % to 2.02% and the forest cover remains almost unchanged. This study will be useful for the forest department to carry out forestation activities in the spatially distributed scrubland and also useful in monitoring the changes that area happening in our ecosystem and environment.

CONTENTS

Details			Page No.
Acknowledgements			i
Abstract			ii
Contents			vi
List of Tables			viii
List of Figures			ix
List of Plates			xi
Chapter 1	Introduction		1 – 14
	1.1	Introduction	1
	1.2	Description of the study area	3
	1.2.1	Study area	3
	1.2.2	Climate	3
	1.2.3	Rainfall	5
	1.2.4	Topography	6
	1.2.5	Drainage	6
	1.3	Review of Literature	7
	1.4	Significance of the study	12
	1.5	Scope and objectives of Research work	13
	1.6	Outline of Thesis	14
Chapter 2	Existing Geological setup		15-25
	2.1	Regional Geology and Stratigraphy	15
	2.2	Structure and Tectonic settings	18
	2.3	Geology	19
	2.4	Geomorphology	20
	2.4.1	Structural Hill	20
	2.4.2	Structural Valley	20
	2.4.3	Valley fills	21

	2.5	Slope Analysis	22
	2.6	Vegetation Analysis	24
Chapter 3	Morphometric analysis		26 - 94
	3.1	Drainage morphometry	26
	3.2	Methodology	26
	3.3	Linear aspects of morphometric analysis of a watershed	30
	3.3.1	Stream order	30
	3.3.2	Stream number	31
	3.3.3	Stream length	32
	3.3.4	Mean stream length	32
	3.3.5	Stream length ratio	33
	3.3.6	Bifurcation ratio	33
	3.3.7	Weighted mean Bifurcation ratio	34
	3.3.8	Rho coefficient	38
	3.3.9	Relation between stream order and stream number	41
	3.3.10	Relation between stream order and stream length	42
	3.3.11	Relation between stream order and mean stream length	42
	3.4.0	Areal aspects of morphometric analysis of sub-watersheds	43
	3.4.1	Basin area	43
	3.4.2	Basin perimeter	43
	3.4.3	Basin length	43
	3.4.4	Drainage density	45
	3.4.5	Stream frequency	47
	3.4.6	Relationship between Drainage density and Stream frequency	49
	3.4.7	Texture Ratio	50
	3.4.8	Constant of Channel Maintenance	50
	3.4.9	Length of Overland Flow	51
	3.5.0	Geometric aspects of morphometric analysis of watershed	52
	3.5.1	Form Factor	53
	3.5.2	Circularity Ratio	53
	3.5.3	Elongation ratio	54
	3.5.4	Relationship of form factor, circulatory ratio, and elongation	54

		ratio	
	3.6.0	Relief aspects of the morphometric analysis of a watershed	55
	3.6.1	Basin relief	55
	3.6.2	Relative relief	56
	3.6.3	Absolute relief	58
	3.6.4	Dissection Index	60
	3.6.5	Relief Ratio	61
	3.6.6	Gradient ratio	62
	3.6.7	Ruggedness Index	63
	3.6.8	Slope analysis	65
	3.6.9	Hypsometric Analysis of erosional topography	67
	3.6.10	Percentages of Hypsometric Curves	67
	3.6.11	Plots of hypsometric curves	67
	3.6.12	Methods of generating Hypsometric data	68
	3.6.13	Hypsometric Integral	77
	3.6.14	Inter-correlation among geomorphic parameters	80
	3.6.15	Watershed prioritization for soil and water conservation measures	82
	3.7	Prioritization of groundwater potential zones using Multi Criteria Decision Making techniques	86
	3.7.1	Introduction	86
	3.7.2	Methodology	86
	3.7.3	Results and Discussions	92
Chapter 4	Tectonic Geomorphology		94-118
	4.1	Introduction	94
	4.2	Materials and Methodology	94
	4.3	Results and Discussion	97
	4.3.1	Tectonic lineament analysis	97
	4.3.2	Basin elongation ratio	98
	4.3.3	Hypsometric Integral	100
	4.3.4	Asymmetry Factor	101
	4.3.5	Transverse Topographic Symmetry Factor	103

	4.3.6	Stream length-gradient index	107
	4.3.7	The ratio of valley floor width to valley height	112
	4.3.8	Mountain-front Sinuosity Index	114
Chapter5	Estimation of Soil Loss using RUSLE Model		119-132
	5.1	Introduction	119
	5.2	Materials and methodology	120
	5.3	Soil erosion modeling	121
	5.4	Rainfall-runoff erosivity factor	121
	5.5	Soil Erodibility factor	123
	5.6	Slope length and slope steepness factors	124
	5.7	Crop Management factor	125
	5.8	Practice Management factor	128
	5.9	Average annual soil loss	129
	5.10	Erosion Risk zones	129
	5.11	Results and Discussions	130
	5.12	Summary and findings	131
Chapter6	Temporal Change Detection of Land use and Land cover		133-140
	6.1	Introduction	133
	6.2	Materials and Methodology	133
	6.3	Image classification scheme	135
	6.4	Classification accuracy assesment	135
	6.5	Accuracy assessment analysis	137
	6.6	Results and discussions	139
Chapter7	Summary and Conclusions		142-129
	7.1	Conclusion about the Morphometry analysis	141
	7.2	Conclusion about Soil and water conservation measures	142
	7.3	Conclusion about Groundwater potential zones	142
	7.4	Conclusion about Morphotectonic study	143
	7.5	Conclusion about Soil erosion assesent	144
	7.6	Conclusion about LULC change detection	144
		References	146-166

List of Tables

Table No.	Description of Tables	Page No.
3.1	Monthly mean temperature and rainfall data.	4
3.2	Annual rainfall data in mm for the year 2007-2016.	5
3.3	Generalized stratigraphic succession of Mizoram.	17
3.4	Slope classification in the study area	23
3.5	The broad classification of land use / land covers in the study area.	25
3.1	List of data products utilized in this study.	27
3.2	Methodology for calculation of morphological parameters.	27
3.3	Method of deriving weighted mean Bifurcation ratio.	35
3.4	Linear aspects of Upper Tuirial basin and its Sub watersheds.	38
3.5	Textural aspects of watershed.	44
3.6	Classification of Drainage Density statistics in the study.	46
3.7	Classification of stream frequency statistics in the study area	49
3.8	Geometric aspects of Upper Tuirial watershed.	52
3.9	Relief Aspects of Upper Tuirial watershed.	55
3.10	Classification of Relative relief and its statistics.	58
3.11	Classification of Absolute relief and its statistics.	59
3.12	Classification of Dissection Index and its statistics.	61
3.13	Gradient ratio and Ruggedness Index of upper Tuirial watershed.	63
3.14	Classification of Ruggedness Index and its statistics.	65
3.15	Methods of calculating Hypsometric curves.	69
3.16	Computation of Hypsometric Integral for Tuirial basin.	78
3.17	Spearman's correlation matrix of the morphometric parameters.	81
3.18	Estimated compound parameters with priority ranking.	85
3.19	Calculated morphometric parameters and weightage values	87
3.20	Normalised matrix	88
3.21	Weighted normalised matrix	89
3.22	Ideal best and ideal worst value	90
3.23	Values of Euclidean distance and performance scores	91

4.1	Morphotectonic indices and their mathematical formulae.	95
4.2	The computed elongation ratios of upper Tuirial watershed.	99
4.3	Hypsometric Integral values of the Tuirial watershed.	101
4.4	The computed values of Asymmetry factor for study area.	103
4.5	Magnitude and direction of Transverse Topographic Symmetry Factor	105
4.6	The computed ratios of valley floor width to valley height for Upper Tuirial watershed and its sub watersheds.	113
4.7	Computation of Mountain front sinuosity Index at selected locations in the upper Tuirial watershed.	116
5.1	Materials to be used for the study	120
5.2	Annual rainfall of 9 years of surrounding stations	122
5.3	Soil erodibility factor values	123
5.4	Image classification details and corresponding C and P factor value	127
5.5	Spatial distribution of soil loss and erosional risk classes	130
6.1	Image classification details	135
6.2	Confusion matrix of 2000 LULC map	136
6.3	Confusion matrix of 2018 LULC map	137
6.4	Land use categories for 2000 and 2018 and their statistics	139

List of Figures

Fig. No.	Description of figures	Page No.
1.1	Location map of the study area	3
1.2	Climograph of monthly mean temperature (°c) and mean rainfall (mm).	4
1.3	Rainfall distribution map of the study area.	5
1.4a	Drainage map of the study area.	6
1.4b	Major types of drainage patterns (Figs. A, B, C, D) in the study area.	6
2.1	Schematic geological cross section across the fold belt of Mizoram	16
2.2	Lithology with major faults inferred and mapped in the state of Mizoram	18
2.3	Geological map of the study area.	19
2.4	3D model of the study area showing the dissected ridges and valleys.	21
2.5	Geomorphology map of the study area.	21

2.6	Slope distribution map of the study area	22
2.7	Land use/land cover classification in the Tuirial watershed area	24
3.1	Flow chart for calculating the morphometric parameters.	30
3.2	Relation between Stream Order and Stream Number.	41
3.3	Relation between Stream Order and Stream Number.	41
3.4	Relationship of stream order, mean stream length of watershed.	42
3.5	Schematic diagram defining the basin length, area and perimeter.	44
3.6	Spatial distribution of Drainage density of upper Tuirial Watershed.	46
3.7	Spatial distribution of Stream frequency of upper Tuirial Watershed.	48
3.8	Relation between Drainage density (Dd) and Stream frequency (Sf).	49
3.9	Relationship between form factor, elongation ratio, and circulatory ratio.	54
3.10	Spatial distribution of Relative relief/sq.km. in the study area.	57
3.11	Spatial distribution of absolute relief per 1 km ² of Upper Tuirial Watershed.	59
3.12	Spatial distribution of dissection index of upper Tuirial Watershed.	60
3.13	Spatial distribution of Ruggedness index of upper Tuirial Watershed.	64
3.14	Spatial distribution of average slope of upper Tuirial Watershed.	66
3.15	Schematic representation of Hypsometric analysis.	68
3.16	Hypsometric curves of upper Tuirial basin.	76
3.17	Construction of Hypsometric curve preparation for basin area vs. height.	77
3.18	Prioritization map for soil and water conservation practices.	83
3.19	Sub-watershed wise prioritisation based on morphometric parameters	93
4.1	Flow chart for Morphotectonic analysis	96
4.2	Digital elevation Model of Tuirial watershed with 13 selected basins.	97
4.3	Rose diagram showing azimuthal distribution of the tectonic lineaments.	98
4.4	Lineaments interpreted from Hill shade map from the satellite imagery.	98
4.5	The schematic diagram showing the 3D view of tectonic tilt.	102
4.6	The tectonic tilting of the selected sub watersheds in the study area.	102
4.7	Transverse topographic profile reflecting the terraces in the study area.	104
4.8	Diagram of transverse topographic symmetry factor in the study area.	105
4.9	Google Earth image of terraces in the remnant beds on both the banks.	105
4.10	Aerial view of the study area from the Google Earth showing terraces.	109
4.11	Longitudinal stream profiles of upper Tuirial basin and sub-watersheds.	110

4.12	Profile locations across Tuirial River	112
4.13	Transverse profiles of selected locations in the study area.	112
4.14	Map showing the Mountain front Sinuosity values at different sections.	115
5.1	Flowchart showing procedure for RUSLE – based soil erosion modeling	121
5.2	Rainfall distribution map in mm	122
5.3	Rainfall-runoff erosivity factor map	122
5.4	Soil Textural Map	124
5.5	Map of soil erodibility factor	124
5.6	LS factor Map	126
5.7	LULC Map of the study area	127
5.8	Crop management factor map	127
5.9	Practice management factor map	128
5.10	Spatially distributed soil loss Map of upper Tuirial Watershed	128
5.11	Spatial distribution of soil erosion and soil erosion risk map of the study area	129
6.1	Flowchart demonstrating the methodology followed in present study	134
6.2	FCC images for the year 2000 and 2018	136
6.3	LULC classified map for the year 2000 and 2018	139

List of Plates

Plate No.	Description of plates	Page No.
2.1	Alternate beds of sandstones, siltstones and shales of Bhuban Unit.	19
2.2	Massive Sandstone formations of upper Bhuban unit.	19
2.3	Narrow valley running parallel to the Ridges	22
2.4	Dissected ridge of Tlangnaum Hill, western part of the study area.	22
2.5	Field photograph showing boulders, cobbles, pebbles, gravel, sand and silt as valley fills.	22

4.1	Highly jointed sandstone beds of almost vertical inclination	117
4.2	Deeply incised V-shaped valley	117
4.3	Development of Cracks on horizontal bed	118
4.4	Strath terraces on Chite river bank (T1&T2)	118
4.5	Field evidence of knick points and development of waterfalls due to tectonic activity.	118
5.1	A common phenomenon in the mountainous region shows the burning and clearing of forest cover through Jhum activity for cultivation.	131
5.2	Terrace farming (Top of the Photo) is more common in the hilly terrain and current jhum land (below the photograph) ready for cultivation.	131
5.3	Manual sand seiving is common hilly rievrr beds for construction purpose extracted form the Tuirial river bed in the study area.	132
5.4	Huge deposition of sediments on the river bed of Chite Lui sub-watershed, Eastern part of the Aizawl city area in Tuirial basin	132

CHAPTER- 1

INTRODUCTION

1.1 Introduction

Watersheds are the hydrological units which are designed for planning purposes focused on conservation of natural resources such as land, forest soil and water resources. Watersheds are natural hydrologic entities that cover a specific areal extent of landforms where rainwater is accumulated and flows to a defined gully, stream or river at particular outlet. The size of watershed is depending on the size of river and the number of tributaries connecting the main channel, longer the river is larger the watershed area and vice-versa.

The upper Tuirial watershed is the western tributary of Barak River of Assam which covers an area of 534.81 km², originates in the central part of Mizoram state, NE India. A large number of villages, an eastern part of the Aizawl city, small towns and hamlets are present within the study area are directly or indirectly depend on natural resources available within the watershed. It plays a vital role for their surrounding hamlets livelihood, water supply, food security in terms of agricultural and horticultural products and economic development of the region as a whole and the neighbouring localities.

MORPHOMETRY (from Greek μορφή morphe, "shape, form", and -μετρία metria, "measurement") is the measurement and mathematical analysis of the configuration of the Earth's surface, shape and dimensions of its landforms (Clarke, 1966). The drainage basin morphology is the study of distribution of various drainage network on the surface of the earth which are numerically analyze or mathematically quantify to understand the evolution of present day landforms. The Drainage characteristics that can be measured and for comparative-study among different watersheds are streams numbers, average stream length, total stream length, bifurcation ratio, basin shape, basin perimeter, drainage density, stream frequency, basin relief, basin area, etc. Therefore, it is necessary to delineate watershed boundaries at various levels of hierarchy to identify particular watersheds for developmental activities under various schemes. Strahler's stream ordering technique (1964) was used for delineation and analysis of drainage basin for conservation measures and management practices. The drainage basin analysis is an important tool for analyzing the hydrological investigations like assessment of groundwater potential, groundwater management, pedology, environmental assessment and also lithological investigations like permeability and porosity of the of the litho column. Soil and water conservation is the key issues in the watershed

management. However, watershed conservation work for the basin as a whole is not feasible and hence the study area has been divided into several smaller units as sub watersheds or micro watersheds by considering its drainage system.

Morphotectonic aspects are the study of landforms produced by tectonic processes (Keller and Pinter, 1996). Analysis of active tectonics depends upon the use of morphotectonic indices which are sensitive to rock resistance, climatic change and tectonic process resulting into landscape evolution. Basin elongation ratio (Re), transverse topographic symmetry (T), asymmetric factor (AF), valley floor width to valley height ratio (Vf), mountain front sinuosity (Smf), longitudinal profile and stream length gradient index (SL) are the most common geomorphic indices of active tectonics which are considered as an evidence of ongoing tectonic activity in this area.

Tectonic geomorphology is the study of the interplay between tectonic and surface processes that shape the landscape in regions of active deformation and at the time scales ranging from short span of time to millions of years. Tectonics plays a very important role in the morphological evolution of any drainage basin and is well reflected by structural, fluvial and morphotectonic parameters (Bhatt, et al., 2007). Morphotectonic analysis using geomorphic indices has been developed as a basic reconnaissance tool in order to identify areas experiencing rapid tectonic deformation or to estimate the relative variations of tectonic activity in a specific area. Thus based on the analysis of river basins and related drainage networks by calculating the geomorphic indices will be able to attain valuable information about tectonic history of an area. The information about tectonic history of an area can be retrieved by quantification of different morphotectonic indices derived from topographic maps and satellite image data (Keller, 1986). An integrated multidisciplinary approach by using the geomorphological, structural and neotectonics are very useful in evaluation of active tectonics (Wells, et al., 1988).

The Remote sensing (RS) and Geographical Information System (GIS) techniques are widely applied tools for studying the morphometric and morphotectonic aspects of the watershed. Processing of Remote sensing data in GIS platform enhance the accuracy of analytical parameters for morphometry and morphotectonic study, which is the latest technique applied to any catchment area at a large extent within accessible field areas for fieldwork / ground truth. Remote sensing plays a significant role in procuring updated spatial information needed for computation of these indices. The GIS is a set of tools for collecting, storing, retrieving and analysing the geospatial data with the real world coordinates.

1.2 Description of the study area

1.2.1 Study area

The study area is located in the eastern part of Aizawl district in the Mizoram state. The geographical location of the study area lies between longitudes 92°42'E - 92° 52'E and latitudes 23°26'N - 23°52'N which falls in the parts of Survey of India Toposheet numbers such as 84A/9, 84A/10, 84A/11, 84A/13, 84A/14 and 84A/15, covering an area of about 534.816 km². The Tuirial River originates near the spring Hmuifang and flowing towards north direction. The highest altitude in the study area is about 1690 m above MSL and lowest altitude is about 76 m above MSL and is surrounded by river Mat in the South, River Tlawng in the West, River Tuirini in the East and in the North, River Tuirial itself flows to the lower part of the state. The important villages are situated in and around study area are Aibawk, Thiak, Sialsuk, Seling, Tlungvel, Baktawng, Chhingchhip, and Lamchhip. The location of study area is shown in Figure 1.1.

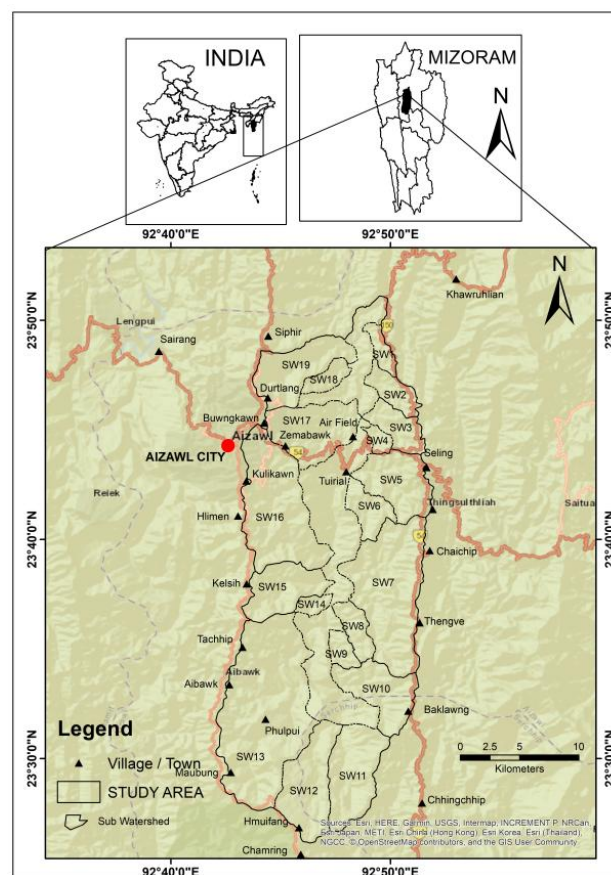


Figure 1.1 Location map of the study area.

1.2.2 Climate

In terms of climate, Mizoram is known as natural air-conditioning state due to its pleasant and favourable climatic condition. Mizoram experiences a moderate humid climate

which is characterized by short winters and long summer with heavy rainfall. The temperature varies from 11°C to 23°C during winter, 21°C to 35°C during summer (Rintluanga, 1994). The state is under direct influence of southwest monsoon with an annual average precipitation of about 2500 mm, with the onset of this monsoon being the early month of May. However, July and August months are considered to be the wettest months while December and January form the driest months of the year. Rainfall and temperature data collected from Aizawl station for a period of 2007 to 2018 as shown in the Table 1.1 and Fig. 3.4 bellow indicate that the average monthly temperature is 21.24⁰ C and maximum and minimum temperature is 15.39⁰ C and 27.19⁰ C respectively while the average monthly rainfall is 193 mm.

Table 1.1 Monthly mean temperature and rainfall data for the year 2007 to 2018.

	Jan	Feb	Mar	Apr	May	Jun	Jul	Aug	Sept	Oct	Nov	Dec	Mean
Rainfall in mm	10.53	14.84	44.51	149.46	301.34	425.76	348.89	439.28	362.56	178.81	32.35	7.69	193.00
Minimum T (°c)	10.25	12.14	15.21	16.01	16.78	17.70	17.68	17.73	18.08	17.28	14.31	11.45	15.39
Mean T(°c)	17.20	19.19	22.01	22.20	22.52	22.65	22.67	22.60	22.84	22.52	20.63	17.83	21.24
Maximum (°c)	24.14	26.24	28.81	29.19	28.26	27.59	27.66	27.53	27.95	27.75	26.96	24.22	27.19

(Source. Meteorological Centre, Directorate of Science and technology, Mizoram)

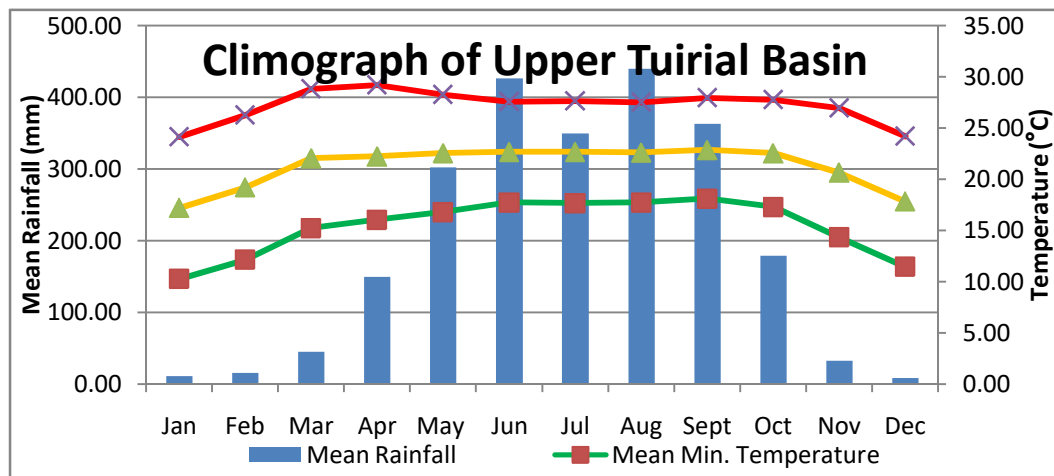


Figure 1.2 Climograph of monthly mean temperature (°c) and mean rainfall (mm)

The air is highly humid throughout the year. Relative humidity is highest during southwest monsoon, reaches above 90 %. Wind speed is generally gentle except in March to July. During those days, the disturbances in Bay of Bengal also affect the Mizoram in general and Aizawl in particular. Mizoram comes under the influence of monsoon with the beginning of May. Therefore, the maximum rain is received in between the months of May and September (Fig. 1.2).

1.2.3 Rainfall

Annual rainfall data of 9 years (2007-2016) collected from Directorate of Agriculture and Crop Husbandry, Mizoram. These data were recorded in 6 different rain gauges in an around the study area namely Aizawl, Sialsuk, Neihbawi, Darlawn, Khawruhlian and Sairang. Using inverse distance weighted (IDW) interpolation method in GIS environment, rainfall distribution map was prepared for the study area (Fig.1.3). Map shows that rainfall intensity varies from 2416.26 mm to 3878.6 mm per year and the northern part of the watershed received more precipitation.

Table 1.2 Annual rainfall data in mm for the year 2007-2016.

Rainfall	2007	2008	2009	2010	2011	2012	2013	2014	2015	2016	Average
Aizawl	2485.5	1569.5	1591.8	4378.4	2155.9	2543.6	2078.2	1913.7	2551.3	2844.3	2411.22
Sialsuk	4650.6	2986.7	2458.2	3276	3163	3606	3000	2993	3249.3	3162.6	3254.54
Neihbawi	4859	3784	3217	4404.3	3864	4057	4275	2976	3501	3848.7	3878.6
Darlawn	2922.6	2084.9	1921.9	2454.4	2287.4	3030.4	1697	1089	1691	2391.8	2157.04
Khawruhlian	2844.6	1894	1516	2485	1857	2128	2180	1997	2423	3010	2233.46
Sairang	2489	1661	1579	2679	2137	2266	2810	2733	2977	3217.4	2454.84

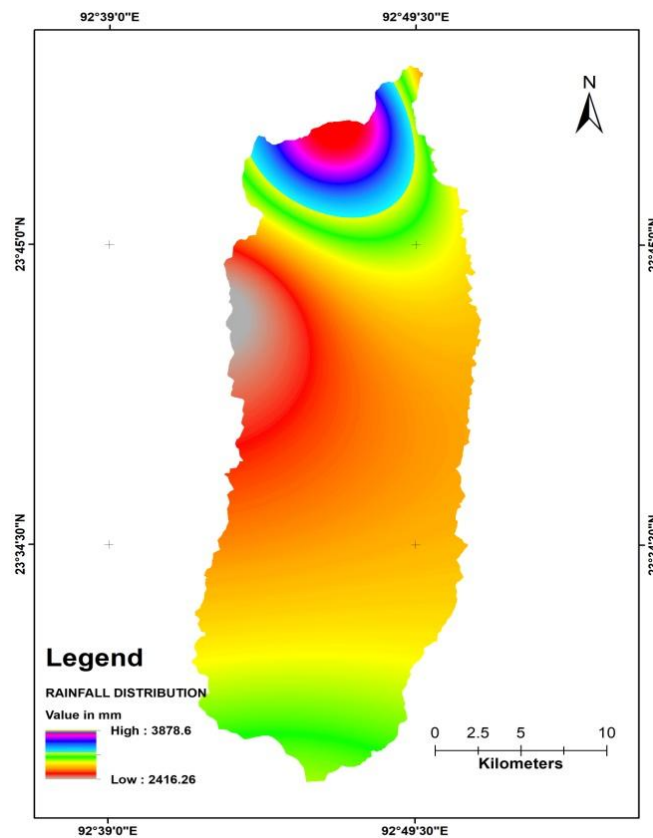


Fig.1.3 Rainfall distribution map of the study area.

1.2.4 Topography

Topographically Mizoram has a hostile terrain characterized by its highly undulated, steep and rugged terrain. Almost all the hill ranges and valleys are mostly trending in the N-S to NNE-SSW directions. The average elevation in Mizoram is about 900 meters above Mean Sea Level. The elevation ranges from 40 meters at Bairabi (north western of Mizoram) to 2157 meters above MSL at Phawngpui (The Blue Mountain) along the Myanmar border at the east. Thus, the general elevation increases from west to east. The ridges are characterized by relatively compact and resistant older rock units, whereas the valleys and the synclinal trough are composed of younger and softer formations (Ganguly, 1983).

The study area exhibits undulating terrain with multiple long and linear to arcuate shape ridges with intermittent valleys. Various streams passing through these valleys finally join the Tuirial river and flows to the north. The hill ranges are mostly oriented in north south direction. The maximum elevation of about 1690 m above mean sea level is found in the southern part of the area while the minimum elevation of about 76 m is seen at its confluence where it meets river Tuirini in the north.

1.2.5 Drainage

Study of Drainage pattern is an important recognisance tool to understand the subsurface geology of an area and the evolution of the landscape (Zernitz, E. R., 1932).

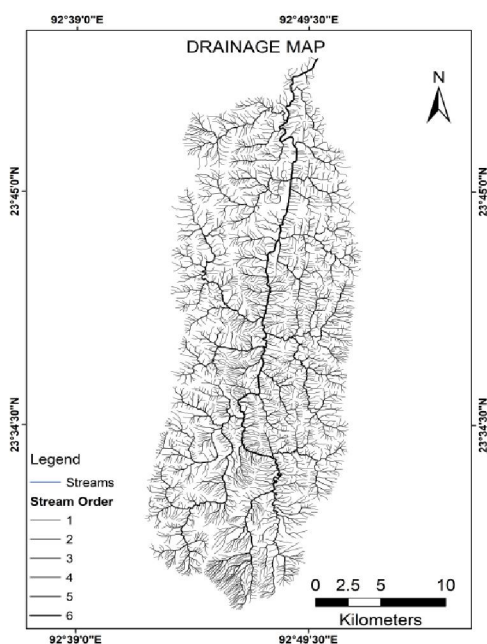


Figure 1.4.a Drainage map of the study area

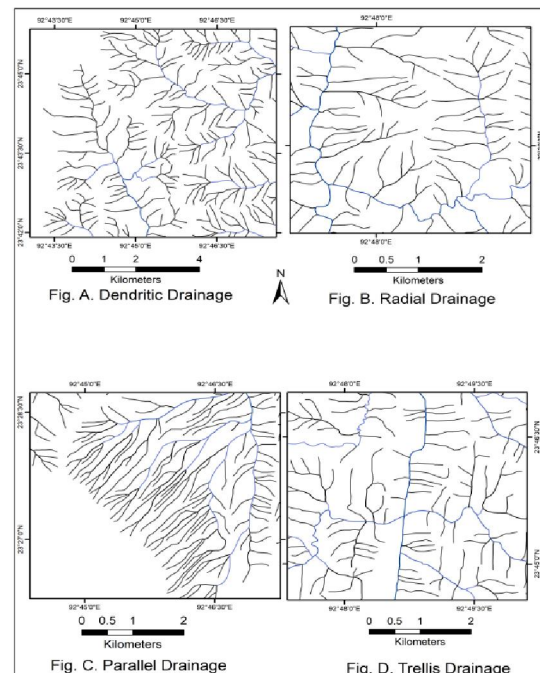


Figure 1.4.b Major types of drainage patterns (Figs. A, B, C, D) in the study area.

Different drainage patterns are responsible for topographical variation of different landforms. The river Tuirial runs over a length of about 60 km within the study area. Number of tributaries such as river Chie, Muthi, Tulrital, Zilpui, Suanghuan etc feed this watershed which is an elongated basin (Fig. 1.4.a). As a whole dendritic to sub dendritic pattern is seen as the predominant type in the area but due to local variation in topography other types of drainage pattern are also found in some areas. In the study area four types of drainage patterns are observed which are Dendritic, Trellis, Radial and Parallel drainage patterns (Fig.1.4. b). Existence of different types of drainage pattern within a small area is an indication of strong structural controls of drainage evolution.

1.3 Review of Literature

The concept of quantitative geomorphology and the drainage basin morphometry has been initiated by Horton (1932, 1945) and developed further by Smith (1950), Strahler (1952, 1954, 1956 & 1964), Schumm (1956 & 1963), Miller (1953), Chorley (1957), Melton (1958), Morisawa (1962) and others. A number of studies have been carried out for various drainage basins particularly quantitative studies on landforms and their litho-tectonic controls (Tandon, 1974). Morisawa (1985) analyzed the effect of different shape parameters on run-off rainfall ratios. It has been observed that the shape parameters showed a negative correlation with run-off rainfall ratio.

Rai, et al., (2014) carried out drainage morphometric analysis of Kanhar River Basin using GIS and inferred that increase in stream length ratio from lower to higher order indicate that the study area has reached a mature geomorphic stage.

Gajbhiye and Sharma, (2015) worked on Prioritization of watershed through morphometric parameters using PCA and the results showed that sub-watershed 7 and 5 are possibly having high erosion. Hence, suitable soil erosion control measures are required in these watersheds to preserve the land from further erosion

Gajbhiye, et al., (2014) have studied on prioritization of erosion-prone area through morphometric analysis. The results of morphometric analysis show that sub-watershed 13 and 11 are prone to relatively higher erosion and soil loss.

Sreedevi, et al., (2009) have worked on morphometric analysis of watershed using SRTM data and GIS and inferred that mean Rb of the entire basin is 3.89 which indicate that the drainage pattern is not much influenced by geological structure.

Akram, et al., (2012) and Gopinath, et al., (2014) briefly described the automated extraction of watershed boundary from DEM using Arc GIS and compared with survey of India toposheet.

Yadav, et al., (2016) have worked on Prioritization of sub-watersheds based on earth observation data and the result showed that SW-2, 1, 3, 5 and SW-10 were more – deficit zones of groundwater. SW-8, 4 and SW-6 were identified better groundwater potentialities.

Rahaman, et al. (2015) have prioritized different sub watershed of Kallar basin based on morphometric characteristics using GIS and statistical method like, fuzzy logic and analytical hierarchical process (AHP) for determination of controlling factors.

Vittala, et al., (2004) have carried out Morphometric analysis of sub-watersheds using remote sensing and GIS techniques and inferred that variation in values of bifurcation ratio among the sub-watersheds is due to the difference in topography and geometric development.

Arefin, et al., (2020); Gurmessa and Bárdossy (2009); Brown (1992), Pandžić and Trninić (1992) have used PCA analysis for their works in different fields of scientific research.

Jaiswal et al. (2014), used morphometric indices and the fuzzy analytical hierarchy, including the Saaty analytical hierarchy process (AHP) to prioritize watersheds for determination of the controlling factor.

Javed, et al., (2011) have carried out watershed prioritization using morphometric analysis and land use/land cover (LULC) parameters and showed that only SW 14 is highly susceptible to erosion and prioritized for immediate implementation of soil and water conservation measures.

Puno and Puno, (2019) have carried out watershed prioritization using morphometric analysis and land use/land cover (LULC) parameters and showed that from 14 sub-watersheds, SW 13, SW 14 and SW 4 were observed as the most susceptible to land degradation and soil erosion; therefore, immediate attention for soil and water conservation is important for these watersheds

Mishra, et al., (1994) have studied the effect of different topo elements such as drainage area, drainage density and form factor compared with the sediment production rate of the sub watersheds in the upper Damodar valley and inferred that the increase of form factor reduces the sediment production rate.

Tiwari and Jha, (1997) have estimated run-off and sediment yield for various watersheds in Mizoram and concluded that almost all the watersheds are highly elongated, steep and composite ground slope with high sediment yield rate due to intense erosion.

Agarwal, (1998) has inferred the sub-basins of Karamnasha river in Naugarh area of Varanasi district, Uttar Pradesh, better scope for artificial recharge due to more infiltration with less run off gives deep ground water exploration.

Based on the morphometric analysis of drainage basins using remote sensing and GIS techniques was studied by Biswas, et al., (1999) in the Midnapur district of West Bengal suggest that the low bifurcation ratios and low drainage densities virtually indicates the drainage not affected by structural disturbances.

Ravishankar, (1994) and Saxena, et al., (2000) based on the study of remote sensing data of watersheds inferred that remotely sensed spatial databases can form the basis of appropriate and convenient hydrologic simulation.

Arya, et al., (2002) have prepared various thematic maps of the Ghaggar watershed to develop the land and water resources management plans for sustainable development of the area.

A study on characterization and management of watersheds in Ganeshapur watershed of Nagpur district was carried out by Solanke, et al., (2005) and suggested that the sloping areas and wastelands need urgent soil conservation measures such as contour bounding, gully plugging and small check dams to prevent the risk of soil erosion hazard.

Nooka Ratnam, et al., (2005) have carried out morphometric analysis by using remote sensing and GIS in Midnapur district of West Bengal by integrating the sediment Yield Index (SYI) model and micro-watersheds morphometric analysis an efficient techniques for prioritization of suitable sites for check dam construction.

Arun, et al., (2005) have attempted a rule-based physiographic characterization of a drought-prone watershed applying remote sensing and GIS techniques for Gandeshwari watershed in Bankura district of West Bengal and generated database through the spatial information about agricultural suitability, emphasizing the availability of water and conservation practices can be improved to utilize the potential of Agricultural Hydrologic Response Units (AHRU).

Udayabhaskara, R. Ch., (2011) has computed some of the significant drainage morphometric parameters of lower Tlawng sub-watershed located in Aizawl district. It is inferred based on the values of various morphometric parameters obtained in this study that the watershed is elongated, with highly permeable rocks and coarse drainage texture

indicating humid tropical climate, with high rainfall and the presence of sandy-clayey type of soils with high infiltration capacity. The drainage pattern appears to be controlled by sedimentary nature of rocks and the watershed is showing strong relief with steep slopes and tectonically active due to faulting and tilting.

Ganju, (1975) have studied the structure and stratigraphy of Mizoram based on photogeological methods with limited field checks. The study reveals that the area is composed of a series of longitudinal en-echelon folds with asymmetric and tight anticlines and broad synclines. A large number of lineaments mostly oriented in NW-SE, N-S, NNE-SSW directions are seen in this areas of which the prominent one is aligned in NW-SE direction named as Mat fault after the Mat river as it follows the trend of the fault across Mizoram. It is inferred that the Tipam formations are exposed only in the northwestern part and the rest of the area is covered by Surma group of rocks, the younger sediments in Mizoram. Further, he revealed that the N-S trending Lushai hills have come into existence in the Post Pliocene or in the Quaternary period showing neotectonic traces.

Das and Mukherjee, (2005) have carried out on drainage morphometry using satellite data and GIS in Raigad district of Maharashtra and concluded that the watersheds with low infiltration numbers have high infiltration capacity and thus better scope for artificial recharge.

More recently Zaidi, (2011) has carried out the drainage basin morphometry of Gaga river in Almora district, Uttarakhand to propose recharge structures in the basin.

Das and Gupta, (2019) have studied on morphotectonic analysis of Sali river basin and found that there is a strong correlation between structural geology (i.e. lineaments, faulting, etc.) and channel orientation in the basin.

Dar, et al., (2017) have studied on tectono-geomorphic of the Karewa Basin of Kashmir Valley and suggested that the basin experiences relatively high degree of tectonic activity along the Pir Panjal side.

El Hamdouni, et al., (2008) worked on assessment of relative active tectonics, southwest border of Sierra Nevada and suggested that geomorphic indices of active tectonics are useful tools to analyze the influence of active tectonics.

Derakshani, et al., (2010) have evaluated tectonic activity of Babakouhi anticline in Zagros folded belt in Iran using morphometric parameters. The morphometric indices such as mountain front sinuosity, facet percentage and valley floor width to depth ratio have been used to evaluate the stage of tectonic activity. Based on the geomorphic and morphometric evidences it is inferred that the Babakouhi is morphotectonically active fold.

Ahmed and Bhat, (2012) studied on tectonic geomorphology of the Rambiarra basin and inferred from the geomorphic indices and presence of unpaired fluvial terraces that the Rambiarra basin is tectonically active.

Singh and Awasthi, (2010) studied on Stream profiles and concluded that anomalous high value of SL gradient index, low value of mountain front sinuosity and low valley width to height ratios reflect active tectonic deformation along the IFT due to reactivation.

Crosby and Whipple, (2006); Pavano, et al., (2016) studied on Knickpoints as geomorphic markers of active tectonics and suggested that anomalous high value of SL index as Knickpoint is a useful geomorphic indicator of rock upliftment due to tectonic activity,

Cuong and Zuchiewicz, (2001) studied the morphotectonic properties of Lo River fault near Tam Dao in North Vietnam and suggested that the Tam Dao segment of the Lo River fault is an oblique active fault which is tectonically active.

Raj, et al., (2003) have applied morphotectonic analysis to substantiate the field observations on active tectonic activity in the Karjan river basin of Lower Narmada valley. They have inferred that the gradual decrease in the value of ruggedness number of the topography towards south and two phases of the river incision could be due to uplift in the Early and Late Holocene.

Wani, et al., (2019) have worked on Drainage Characteristics of tectonically active Mawar basin and based on computed geomorphic indices, geomorphology and the structures present in the Karewas (Plio Pleistocene) deposits they inferred that the basin has shown activity in Pleistocene period, suggesting that basin is tectonically active.

Azor, et al., (2002) have studied tectonic geomorphic analysis using several indices of active tectonics concerning fold Growth. Based on the values of Mountain-front sinuosity; Valley floor width to valley height ratios; hypsometric integral and Drainage density they concluded that the lateral and vertical fold growth were likely produced by westward decrease in fault slip along the buried Oak Ridge fault.

Verrios, et al., (2004) carried out morphotectonic analysis in Elike fault Zone to correlate active tectonics and erosional processes by using topographic maps and aerial photographs. Based on the obtained values of geomorphic indices the Elike fault zone has been ranked as tectonically very active. It is inferred that the intensity of tectonic activity is increasing towards east and gradually decreasing towards west.

Zizioli, (2008) has evaluated morphotectonic indices to understand the influence of tectonic activity in the evolution of drainage basins in the western Lingurian Alps using 5 m resolution digital elevation models acquired by TERRA 4 ASTER satellite. It is inferred based on the analysis of computed parameters that some of the ancient structures in the area are still active at present experiencing tectonic activity by folding and faulting.

Derakshani, et al., (2010) have evaluated tectonic activity of Babakouhi anticline in Zagros folded belt in Iran using morphometric parameters. Based on the geomorphic and morphometric evidences it is inferred that the Babakouhi is morphotectonically active fold in Iran.

Recently, Delacailau, et al., (2006) has used digital elevation model (DEM) to study the landforms, fluvial anomalies, structural features and quantified morphotectonic parameters in Siwalik foothills. They have carried out the systematic drainage basin asymmetry in the Chandigarh anticline ridge and it propagates laterally from NW to SE.

Jain and Verma, (2009) have studied drainage characteristics of tectonically active areas by using the remote sensing and GIS techniques to integrate the geomorphology, slope, vegetation index and morphotectonic aspects to assess the neotectonic potential. The study reveals that the cross faults present in Bundi-Indergarh sector are the younger tectonic elements and are focal centers of the present day tectonic activity.

Bhatt, et al., (2007) have evaluated the morphotectonic analysis through satellite data and GIS in Anandpur Sahib Region in Punjab and their study substantiate the role of active tectonics in the area.

1.4 Significance of the study

Morphometric analysis of a basin provides important parameters about the watershed characteristics that help in understanding the topography, geology and hydrology of the area. The drainage pattern of the watershed gives information about topography and sub surface geological structures. The present study is also useful for natural resources management and development, improvement of irrigational facilities for agricultural development, soil conservation and to mitigate the risk of natural hazards like landslides and flash floods particularly in its lower reaches.

As the study area is located in a tectonically active region of eastern Himalayas, the landscape changes are quite prevalent. Therefore, it is essential to understand the terrain characteristics for formulating proper hazard mitigative measures. Further, the area has scarcity of surface water resources due to rugged topographic and high relief terrain. The

present study is expected to provide information which is useful for proposing various water harvesting structures and to improve ground water recharge conditions in this area.

1.5 Scope and objectives of research work

In the proposed study, an attempt has been made to understand and evaluate the geomorphic attributes such as topography, slope, drainage-network, geologic setting, valley type, base-level controls, lithological characters, etc. to understand the evolution of Tuirial watershed. Landforms as the products of several endogenetic (internal) and exogenetic (external) processes provide clues to understand the influence of ongoing tectonic activity in the development of landscape (Bishop, et al., 2002). Therefore, it is essential to identify and map the landforms in the area using survey of India toposheets and satellite imagery. The study is based on the usage of the most advanced tools and techniques of GIS and remote sensing to arrive at reasonable conclusions. Hypsometric analysis was also carried out to understand the stage of drainage and landscape development of the basin. In order to synthesize the genesis of various landform features, interpretation of satellite imagery followed by field observations were carried out to interpret the various landforms mapped in the watershed area. Generation of various thematic maps such as geology, geomorphology, slope and lineaments were generated for better understanding the terrain conditions and further developmental activities in the study area. A number of studies have been carried out in this region to study the morphometric characteristics of the drainage (Ahmed and Rao, 2015; Barman, et. al., 2019; Tiwari and Jha, 1996; Dutta and Sarma, 2015 & 2016). However, till to date no detailed work on morphometric and drainage network analysis of the Tuirial River basin with implications on tectonic activity has been carried out. The major objectives of the present study as follows:

1. To compute the morphometric aspects of Upper Tuirial watershed.
2. Prioritization of sub-watersheds for soil and water conservation measures.
3. Prioritization of groundwater potential zones using Multi Criteria Decision Making Techniques.
4. To compute the morphotectonic aspects of Upper Tuirial watershed.
5. To quantify the soil loss in the watershed area using RUSLE model.
6. To assess the land use / land cover change detection for a period of 2000 to 2018.

1.6 Outline of thesis

This thesis is divided into 7 chapters. The first chapter comprises of introductory part of the research work with detail information about the title of the thesis. Description about the study area, review of the relevant literature published in reputed journals, Significance of the study, Scope and objectives of research work and outline of the thesis is included in this chapter. The second chapter comprises of existing Geological set up such as Regional geology and stratigraphy of Mizoram, Structure and tectonic settings, local Geology, Geomorphology, slope analysis and vegetation analysis. The third chapter discussed about the various morphometric parameters, methodology to calculate these parameters and the significance of their values. An applied aspect of morphometric analysis in prioritizing different sub watershed for soil and water conservation measures and identification of groundwater potential zones is also covered in this chapter. Chapter four discussed about the Morphotectonic aspects and the evolutionary history of the watershed. Estimation of soil erosion using RUSLE model is discussed in chapter five. Temporal change detection of land use and land cover is kept in chapter six. Summary and conclusions are presented in chapter seven. Methodology for each objective is explained separately in each chapter.

CHAPTER- 2

EXISTING GEOLOGICAL SETUP

2.1 Regional geology and stratigraphy of Mizoram

The Mizoram part is entirely covered by thick pile of Surma Group of sedimentary rocks belong to the Tertiary age with a total thickness of around 8000 meters or more (Ganguly, 1993). The Tertiary succession in the Mizoram part has been divided into three groups namely, the Barail, the Surma and the Tipam groups in the ascending order (Nandi, et al., 1983). Barail group is exposed only in the eastern part of the state bordering Myanmar. However, there are two schools of thought for the presence of Barail Group in Mizoram and it remains controversial till date. Many workers from Geological Survey of India like Munshi, (1964), Nandy, (1972) and Nandy, et al., (1983) are of the opinion that the rocks exposed in the eastern part of Mizoram belong to Barail Group. On the other hand, workers from ONGC like Ganju (1975), Ganguly (1975), Shrivastava, et al. (1979) and Ram and Venkataraman (1984) are of the view that the Barails do not occur in Mizoram and the rocks of eastern Mizoram undoubtedly belong to the Surma Group of rocks. According to them the entire sedimentary succession of Mizoram consists of a rhythmic alteration (rhythmites) of arenaceous and argillaceous rocks belongs to Paleogene and Neogene age thinning upward sequence. Silty-sandstone, siltstone, shale, mudstone, sandstone, silt and their admixture of varying proportion along with a few pockets of shell-limestone, calcareous sandstone and intraformational conglomerates are some of the rocks which are commonly found in this area.

The Surma Group, named after its type locality in surma valley by Evans (1932) has been sub divided into Bhuban Subgroup (Lower, Middle and upper Bhuban Formations) and Bokabil Formation on the basis of relative abundance of shale and sandstones as observed in their Bhuban subgroup type areas.

The Bhuban subgroup has been named after its type area of Bhuban Range in the western Manipur Hills and is well developed in Mizoram. The subgroup has been further divided into Lower Bhuban Formation which is arenaceous predominating with sandstone, silty shale, Middle Bhuban Formation consists of Argillaceous predominating with shale alterations and sandstone and the upper Bhuban Formation consist of arenaceous predominating with sandstone, shale and siltstone (Karunakaran, C. 1974; Ganju, J. L. 1975).

Conformably overlying the upper Bhuban Formation is the Boka Bil Formation named after its type section near Boka Bil village in Hailakandi valley, Assam. This is a

dominantly argillaceous formation and comprises soft, grey, laminated claystone, siltstone/shale alteration and sandstone.

In general, Lower Bhuban is confined to the anticlinal cores of high amplitude folds, while middle Bhuban succession is mostly found on the limbs of folds and it also occupy the cores of low amplitude anticlines. The Upper Bhuban rocks form anticlines in the western Mizoram part, but are confined to the synclinal cores in central and eastern Mizoram area. The Bokabil Formation of Surma and Tipam Groups are confined to the cores of synclines in the western and northwestern part of the state (Ram and Venkataraman, 1984).

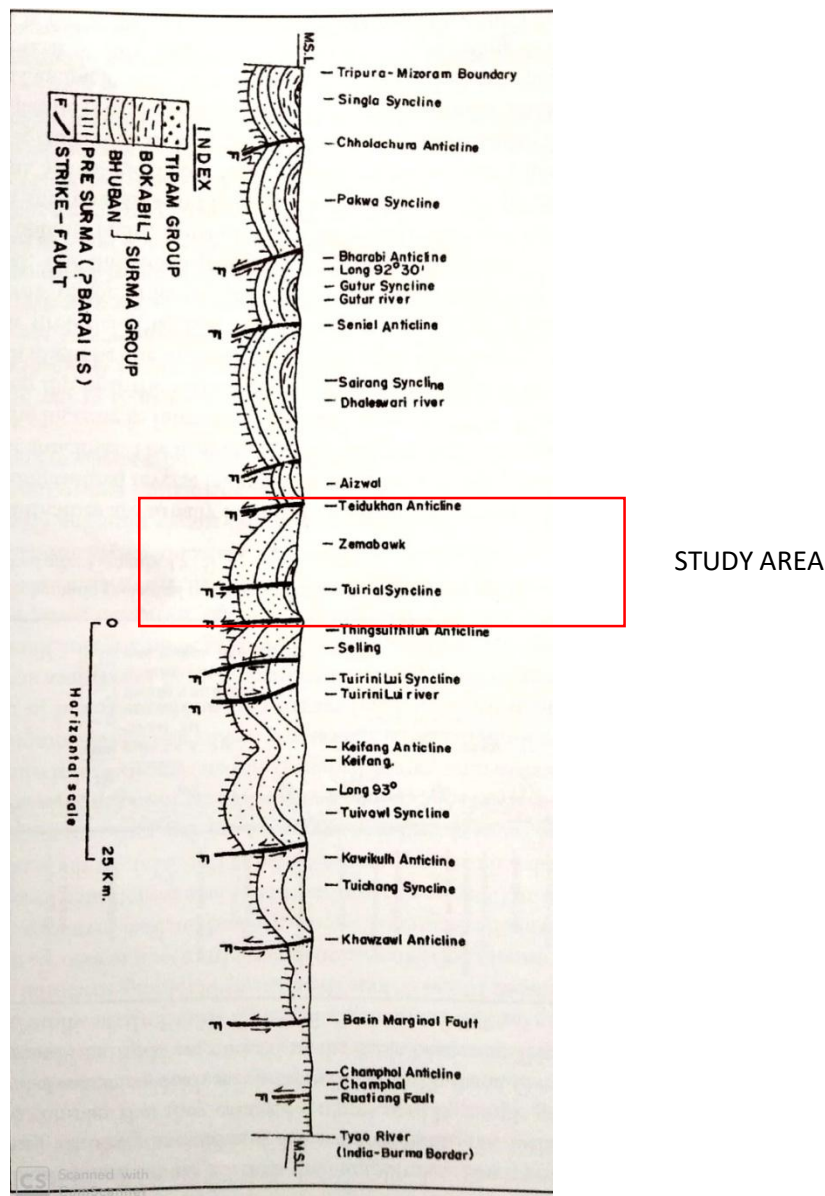


Figure 2.1 Schematic geological cross section across the fold belt of Mizoram, Surma basin (Modified after Ganguly, 1983)

The succession of sandstone and mottled clay overlying the Boka Bil was named as the Tipam ‘series’ after the name of Tipam river in the type area by Mallet, 1876. The Tipam

group consisting of medium to course ferruginous sandstone with plenty of fossil woods occurs only on the northern and western part of the surma basin. The generalized stratigraphic succession as work out by Karunakaran (1974) and Ganju (1975) is shown in Table 2.1.

Table 2.1 Generalized stratigraphic succession of Mizoram (After Karunakaran, 1974; Ganju, 1975; Tiwari and Kachhara, 2003 & Mandokar, 2000; Duhawma, et.al., 2016).

Age	Group/Formation	Thickness	Gross Lithology	Depositional Environment	
Recent	-	-	Gravel, silts and clays	Fluvial and alluvial	
-----Unconformity-----					
Early Pliocene to Late Miocene	Tipam	+ 900 m.	Friable sandstone with occasional clay bands	Fluvial	
-----Conformable and transitional contact -----					
Miocene To Upper Oligocene	S	B o k a b i l	+ 950 m.	Shale, siltstone and sandstone	Shallow marine
		-----Conformable and transitional contact -----			
	U R	B H U	Upper (+1100 m.)	Arenaceous predominating with sandstone, shale and siltstone	Shallow marine, near shore to lagoonal
			-----Conformable and transitional contact -----		
	M A N	A	Middle (+1000m.)	Argillaceous predominating with shale alterations and sandstone	Deltaic
			-----Conformable and transitional contact -----		
		Lower (+900 m.)	Arenaceous predominating with sandstone, silty shale	Shallow marine	
-----Unconformity obtained by faults-----					
Oligocene	B a r a i l	(+ 3000 m)	Shale, siltstone and sandstone	Shallow marine	
----- Lower contact not exposed -----					

2.2 Structure and tectonic settings

Structurally, the Mizo Hills are characterized by a series of continuous and discontinuous N-S, N 15° E - S 15° W, sub-parallel doubly plunging, en-echelon anticlinal ridges and synclinal valleys formed of rocks belongs to Surmas and Tipams (Sarkar and Nandy, 1977).

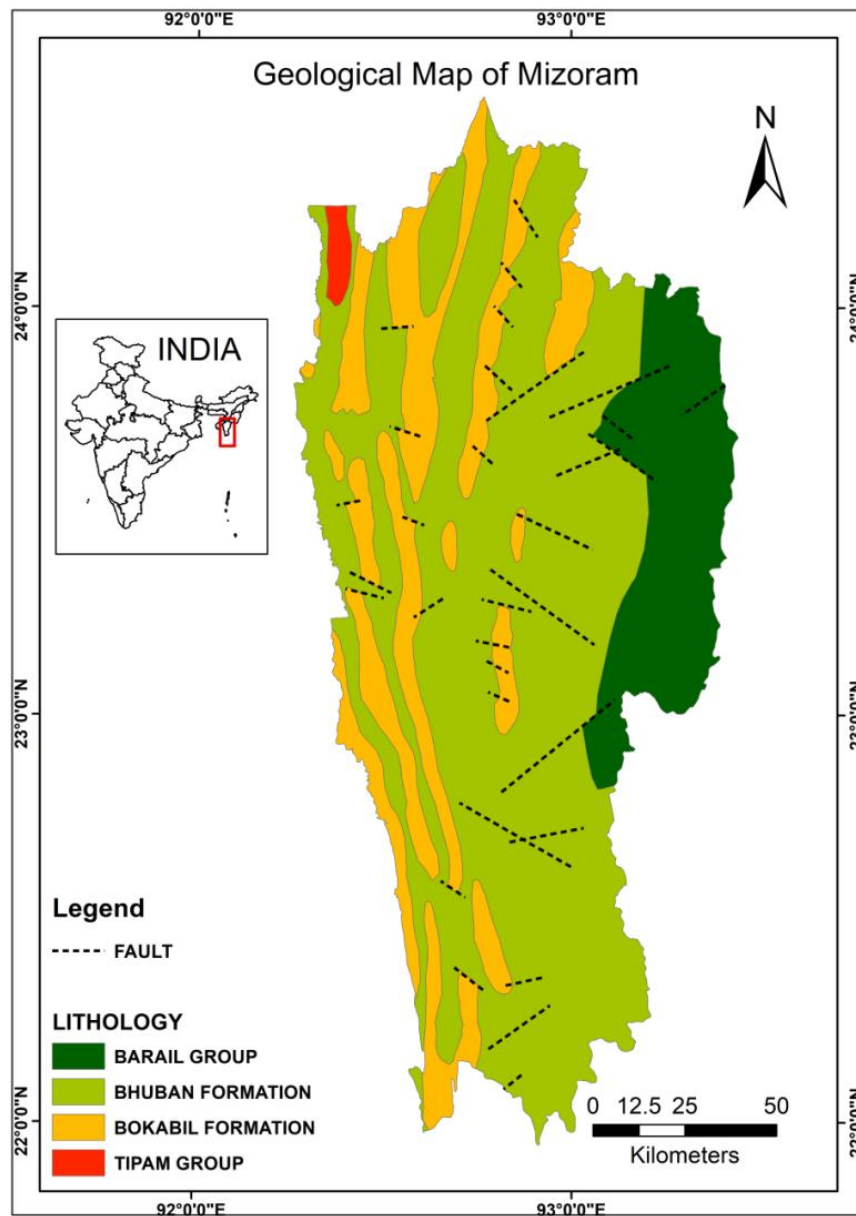


Figure 2.2 Lithology with major faults inferred and mapped in the state of Mizoram (After Ganju, 1975).

The general strike direction of the rock formation is N-S with dip amount varying from 20°-50° either towards east or west. The fold belt is slightly arcuate in shape with westward convexity (Srivastava, et al., 1979). The hill ranges mainly comprise of compact and resistant older rock units exposed in the anticlinal crests, whereas the valleys are composed of younger and softer formations exposed in the synclinal troughs (Ganguly, 1983). There are around 15 major long and arcuate anticlines and corresponding synclines in the region (Nandy, et al., 1983). These anticlines and synclines are commonly dislocated by numerous longitudinal faults and thrusts (Ram and Venkataraman, 1984).

2.3 Geology

The geological succession of Mizoram is composed of sedimentary rocks of Tertiary age (Ganju, 1975) belongs to Surma group. The Surma Group was subdivided into two subgroups, the Bhuban and the Bokabil (Evans, 1932). No formal stratigraphic formations are proposed systematically. However, based on Landsat imagery, five lithostratigraphic units, i.e., Lower, Middle, and Upper Bhuban, Bokabil and Tipam formations are identifiable. In general, Lower Bhuban is confined to the anticlinal cores of high amplitude folds, while middle Bhuban succession is mostly found on the limbs of folds and it also occupy the cores of low amplitude anticlines (Ram and Venkataraman, 1984).

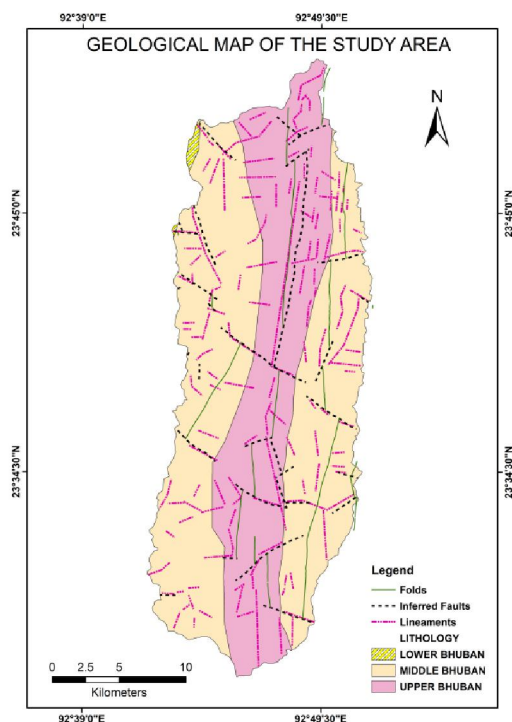


Figure 2.3 Geological map of the study area



Plate 2.1 Alternate beds of sandstones, silt-stones and shales of Middle Bhuban Unit.



Plate 2.2 Massive Sandstone of Upper Bhuban unit.

The study area consist of middle Bhuban rocks at the synclinal zone and upper Bhuban rocks are exposed on both the limbs with little exposure of lower Bhuban rocks in the North western part of the basin (Fig. 2.3). The contact between the middle and upper members are gradational, where there is a gradual change from argillaceous to arenaceous rocks. The major litho-units identified in the area are sandstones, silt-stones and shales with their admixtures in various proportions belong to Upper and Middle Bhuban formations, respectively (Plate 2.1 & 2.2).

2.4 Geomorphoogy

Geomorphology is the study of landforms such as rivers, hills, plains, beaches, sand dunes etc. and the processes that create them. Bloom, A. L. (1978) also defined geomorphology as the systematic description and analysis of landscapes and the processes that changes them. Landforms present in the study area include highly dissected hills and valleys on both the limbs (Fig. 2.5), moderately dissected hills and valley along the synclinal zones and water body as river (GSI). Most of the ridges are elongated and narrow crested, though few of these are broad crest types. Highly dissected valleys are the product of intense vertical erosion which is occupied by the streams and flowing in all direction parallel to the strike ridges (Plate 2.3). The geomorphic features observed locally in the study area are structural valleys, structural hills and valley fills.

Structural landforms are developed due to endogenetic forces like uplift, folding and faulting and shaped by exogenetic processes like weathering and erosion. The prominent structural landforms identified in the area are (i) structural hills and (ii) structural valleys.

2.4.1 Structural Hill

Structural hill is a linear or arcuate shaped hill which runs parallel to valleys showing a definite structural trend lines. These are usually associated with folding and faulting which show lithological variations and usually acts as run-off zone and contribute certain amount of run-off to the adjoining valleys and plains depending up on the lithology. Majority of the structural hills run parallel to each other generally in north-south direction and separated by narrow and deep valleys. A few hills are aligned in NW-SE directions as seen on the geomorphic map (Fig. 2.5).

2.4.2 Structural Valley

It is a narrow linear or curvilinear feature formed along the structurally weak planes like fault, fractures and lithological contacts (Bates and Jackson, 1987). The structural valleys act as good recharge zones and show excellent groundwater potential. The recharge capacity

of valleys depends up on the nature of underlying bedrock, structures and the thickness and the composition of valley fill deposits. The structural valleys follow the general trend of structural hills. A majority of the valleys are controlled by the underlying faults and fractures to the large extent. A majority of the third and fourth order streams which follow these valleys in the area are structurally controlled as seen on the satellite image.

2.4.3 Valley fills

Valley fill is the only fluvial landform identified in the study area. Valley fill constitutes boulders, cobbles, pebbles, gravel, sand and silt which are developed by streams or rivers normally in a narrow fluvial valley which is partly weathered as shown in plate 2.5. Valley fills are mostly fracture controlled and act as good groundwater potential zones depending up on the thickness.

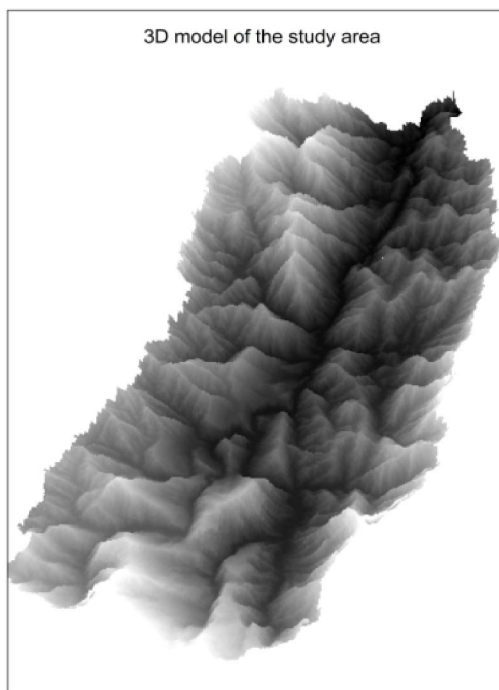


Figure 2.4. 3D model of the study area showing the dissected ridges and valleys

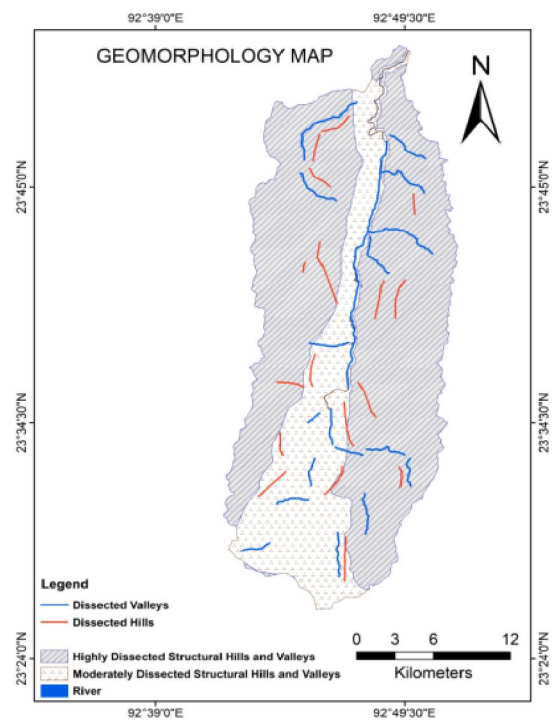


Figure 2.5 Geomorphology map of the study area



Plate 2.3 Narrow valley running parallel to the Ridges photo view from western part the Chite basin boundary looking towards south



Plate 2.4 Dissected hill running N-S in the western boundary of Chite Lui watershed.



Plate 2.5 Field photograph showing boulders, cobbles, pebbles, gravel, sand and silt as valley fills.

2.5 Slope Analysis

Slope analysis is an important parameter in geomorphic studies. Slopes are the fundamental unit of physiographic landscape. In a broad sense, slope can be defined as an angular variation between different elevations. It is an important aspect in assessing landslides because the influence of slope steepness on landslide occurrence is the easiest factor to understand. Depending upon the resistivity of underlying rocks and orientation of bedding planes, slope angle also vary from place to place. A better understanding of slope distribution is essential, as a slope map provides data for planning, settlements, mechanization of agriculture, afforestation, deforestation, planning of engineering structures, conservation practices, etc. (Sreedevi, 2009). Slope map of the study area has been prepared using DEM in GIS environment (Fig. 2.6).

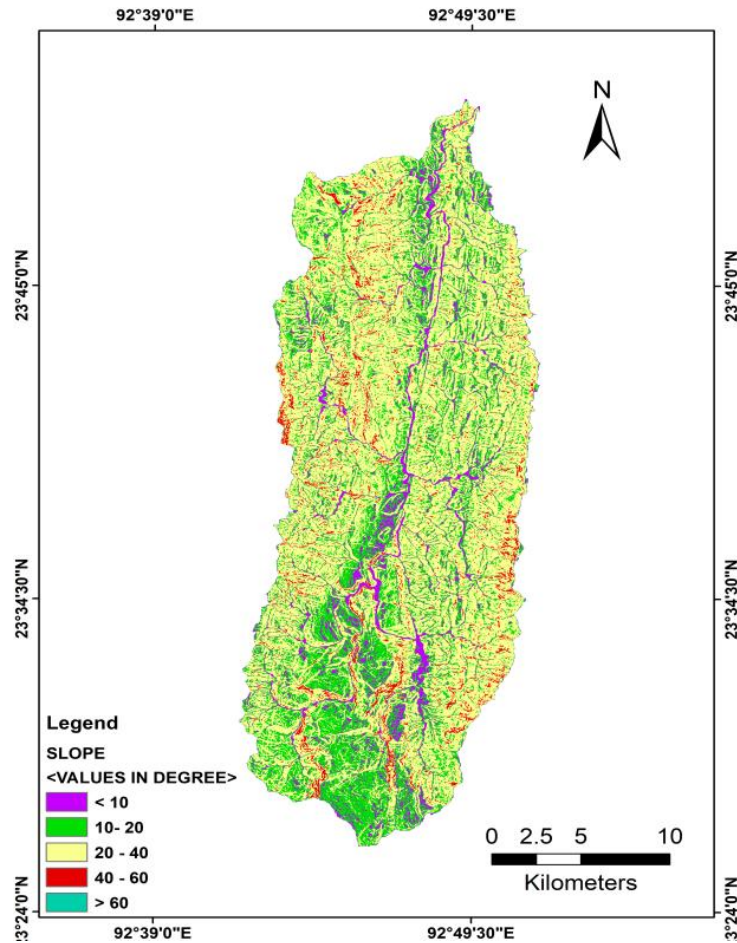


Figure 2.6 Slope distribution map of the study area

Table 2.4 The slope classification in the study area covered by different Slope Angles.

Serial No.	Slope in degree	Area in km ²	Area in %
1	< 10 ⁰	45.52	8.50
2	10 ⁰ -20 ⁰	141.24	26.38
3	20 ⁰ -40 ⁰	325.12	60.74
4	40 ⁰ -60 ⁰	23.21	4.34
5	>60 ⁰	0.14	0.02

According to above statistics (Table 2.4) about 8.5% of the study area falls under the category less than 10⁰ slope covering mostly the valleys, about 26.38 % area falls under category 10⁰-20⁰ slope covering mostly the southern part of the basin and partly in the northern valley side which are suitable for agricultural activities. About 60.74% of the area falls under category 20⁰-40⁰ slope and about 4.34 % area falls under 40⁰-60⁰ slope category

which are landslide prone zones (Barman et al., 2019). Only 0.02 % area is under $>60^{\circ}$ slope category (Fig. 2.6).

2.6 Vegetation Analysis

For vegetation analysis NDVI (Normalized Difference Vegetation Index) was performed using Landsat 8 imagery acquired on 30 March 2019. NDVI is a measure of the state of plant health based on how the plant reflects light at certain frequencies (some waves are absorbed and others are reflected). Chlorophyll (a health indicator) strongly absorbs red light, and the cellular structure of the leaves strongly reflect near-infrared light. An NDVI map of the study area was produced using Equation.

$$\frac{(NIR-R)}{(NIR+R)}$$

Where, NIR is the near infrared portion of the electromagnetic spectrum and R is the red portion of the electromagnetic spectrum. Its value always ranges from -1 to +1. Negative values correspond to water body, value close to zero indicates barren land, moderate values represent shrub and grassland and value close to +1 indicating thick forest. The NDVI value for the study area was found to be -0.0082984 to 0.551859.

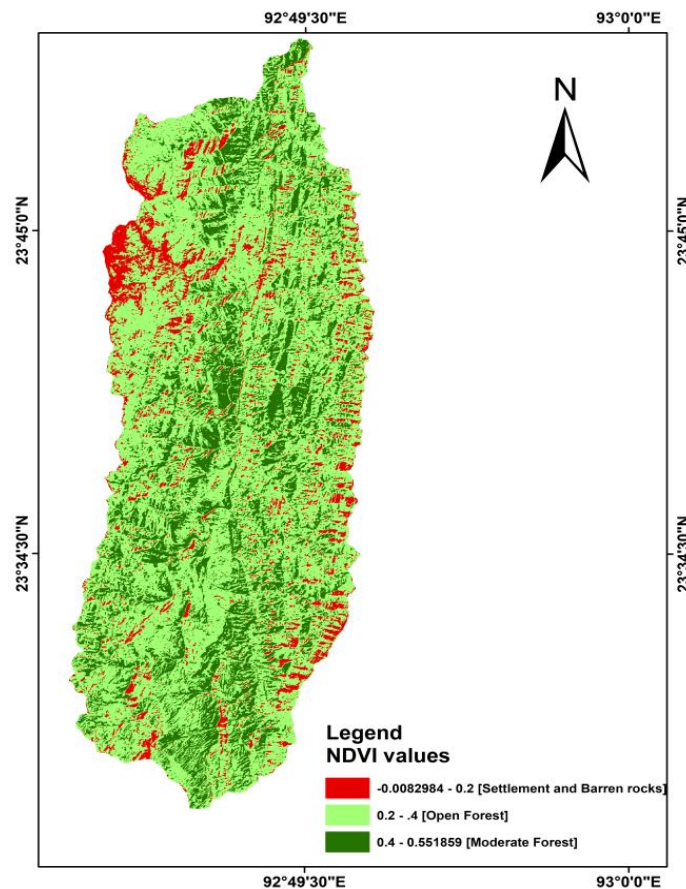


Figure 2.7 Land use/land cover classification in the Tuirial watershed area.

These values clearly indicate the absence of water or negligible amount of water in the area because the negative value is very close to zero. Accordingly the study area has been divided into three classes based on the NDVI equation. Here the barren lands identified are rock exposure and Jhum fallow land. Based on limited field verification, settlement and barren lands are assigned with threshold value <0.2 , for open forests as $0.2-0.4$ and moderate forests as >0.4 as shown in Table 2.5.

Table 2.5 The broad classification of land use/land cover in the study area covered.

Classes	NDVI values	Area in km²	Area in %
Settlement & Barren land	-0.0082984 - 0.2	55.8072	10.4346
Open Forest	0.2 - 0.4	345.667	64.6314
Moderate Forest	0.4 - 0.551859	133.354	24.934

According to above statistics (Table 2.5) about 10% of the study area covers Settlement & Barren land, about 65 % area falls under the category of open forest and about 25% of the area falls under category Moderate forests. The distribution of these land cover classes are shown in figure 2.7.

CHAPTER- 3

MORPHOMETRIC ANALYSIS OF WATERSHED

3.1 Drainage morphometry

The morphometric characteristics of the various basins in different parts of the globe have been studied by different authors using conventional method (Horton, 1945; Smith, 1950, Leopold and Maddock, 1953; Schumm, 1956; Strahler, 1964; Rahaman, et al., 2015; Krishnamurty, et al., 1996; Biswas, et al., 1999; Sreedevi, et. al., 1999 & 2005; Rai et al. 2014, 2017a; Barman, et al., 2019). Literature review shows that morphometric analyses involve evaluation of linear, aerial and relief parameters (Choudhari, et al., 2018; Farhan, et al., 2017; Singh, et al., 2014; Meshram and Sharma, 2015, Ahmed and Rao, 2015). For the present study, morphological characterization analysis was carried out for 19 sub-watersheds of Upper Tuirial watershed through the measurement of linear, areal, and relief aspect). The primary morphometric parameters like, stream number, stream length, basin area, basin perimeter, the length of main channel and basin length were obtained from the natural drainage system of topographical map. The morphometric parameters in accordance with statistical correlation analysis using SPSS software was carried out for prioritizing and ranking the severity of erosion status in different sub watershed (Gajbhiye, et al., 2014; Rai, et al., 2017b, 2018, 2019; Magesh, et al. 2012; Sharma, et al., 2018).

3.2 Methodology

The drainage network of the watershed has been delineated from the Survey of India toposheets (SoI) of 84A/9, 84A/10, 84A/11, 84A/13, 84A/14 and 84A/15 on 1:50,000 scale and the altitude variation have been delineated from terrain corrected ALOS PALSAR DEM of 12.5 m resolution (Table 3.1). A total of 19 Sub watersheds have been delineated from the whole watershed for its detailed morphometric analysis. Ranking of stream orders has been adopted based on stream ordering method developed by Horton (1945) and modified by Strahler, (1964). The length of the streams, basin length, basin perimeter and basin area have been calculated in GIS environment. The basic parameters like drainage density, stream frequency, bifurcation ratio, stream length ratio, constant of channel maintenance, stream frequency, length of overland flow, Texture ratio, Circulatory ratio, elongation ratio, form factor and the relief aspects such as Basin relief, Relief ratio, Ruggedness number were calculated based on formulae shown in Table 3.2.

The various methods used for the present study and arrived to get the confirmed conclusions (Tables 3.1 and 3.2).

Table 3.1 List of data products utilized in this study

Sl. No.	Type of Data	Source	Purpose
1	Toposheet (1: 50,000) of 1986	Survey of India (SOI),	Base map, Drainage, and Sub-watershed boundary map preparation.
2	Satellite data LANDSAT -8 Satellite data Sentinel 2A	United States Geological Survey (USGS)	Land use/Land cover, Geomorphology, and Lineament mapping
3	ALOS PALSAR DEM (12.5m) (2009)	Alaska satellite facility, USA	DEM, Slope, Hill shade map.
5	Geology (1:50,000)	Geological Survey of India (GSI)	Geology map.
4	Climate data (2007-2018)	Meteorological Centre, Directorate of Science and technology, Mizoram	Climograph
6	Rainfall data (2007-2016)	Directorate of Agriculture and Crop Husbandry, Mizoram	Rainfall Distribution map

Table 3.2 Methodology for calculation of morphological parameters

Aspects	Morphometric parameters	Definition/formula	References
Linear Aspects	Stream order (Nu)	Hierarchical order	Strahler (1964)
	Stream number (Nu)	$Nu = N1 + N2 + \dots + Nn$ Where, Nu = Total number of streams, N1 = First order stream N2 = Second order stream	Horton (1945)
	Stream length (Lu)	$Lu = \text{Length of the stream}$	Horton (1945)
	Mean stream length (Lsm)	$Lsm = Lu / Nu$	Strahler (1964)
	Stream length ratio (RL)	$RL = Lu / Lu - 1$ where Lu = total	

		stream length of order 'u', L_{u-1} = the total stream length of its next lower order	Horton (1945)
	Bifurcation ratio (R_b)	$R_b = N_u/N_{u+1}$ where N_u = total no. of stream segments of order 'u', N_{u+1} = number of segments of the next higher order	Schumm (1956)
	Mean bifurcation ratio (R_{bm})	$R_{bm} = (R_{b1} + R_{b2} + \dots + R_{bn})/n$	Schumm (1956)
	Length of main channel (L_m)	Length along longest water course from the outflow point to the upper limit of catchment boundary	Horton (1945)
	Rho coefficient	R_L/R_b	Horton (1945)
Areal Aspects	Basin area (A)	Area enclosed within the boundary of watershed divide	Schumm (1956)
	Basin perimeter (P)	Length of watershed divide which surrounds the basin	Schumm (1956)
	Basin length (L_b)	Distance between outlet and farthest point on the basin boundary	Schumm (1956)
	Drainage density (D_d)	$D_d = L_u/A$	Horton (1945)
	Stream frequency (S_f)	$S_f = N_u/A$	Horton (1932)
	Texture ratio (T)	$T = N_u/P$	Smith (1950)
	Constant of channel maintenance (C)	$C = 1/D_d$	Schumm (1956)
	Length of overland flow (L_g)	$L_g = 1/(D_d \times 2)$	Horton (1945)
	Form factor (F_f)	$R_f = A/L_b^2$	Horton (1945)
	Circulatory ratio (R_c)	$R_c = 4\pi A/P^2$	Miller (1953)
	Elongation ratio (R_e)	$R_e = 2(\sqrt{A}/\pi) / L_b$	Schumm (1956)
	Basin relief	Maximum vertical distance between the lowest and highest points on the watershed	Schumm (1956)

Relief Aspects	Relative relief (Rr)	$Rr = (h - h') / A$ where, h = Maximum height and h' = Minimum height	Smith (1935)
	Absolute relief (Ar)	Maximum height of any region	Dove Nir's (1957)
	Dissection index (D.I)	$D.I = Rr / Ar$ where Rr = Relative relief and Ar = Absolute relief	Dove Nir's (1957)
	Relief ratio (Rh)	$Rh = H / Lb$	Schumm (1956)
	Gradient ratio (Rg)	$Rg = (a - b) / L$ Where Rg is the Gradient ratio, "a" is the elevation at the source of the river "b" is the elevation at mouth of the river and "L" is the length of main stream.	Sreedevi, et al., (2005)
	Ruggedness index (Rn)	$Rn = Rr \times Dd$	Patton and Baker (1976)
	Slope	$\tan Q = (ACC \times C.I) / 636.6$ Where, Q = The angle of slope in degrees. ACC = Average contour crossing per sq.km. C.I = Contour Interval, which is 20 m in this case and 636.6 = Constant value.	Wentworth's (1930)
	Hypsometric integral (HI)	$HI = (EL_{mean} - EL_{min}) / (EL_{max} - EL_{min})$ Where, EL _{mean} is the mean elevation, EL _{min} . the minimum and EL _{max} . the maximum elevation	Pike and Wilson in (1971)

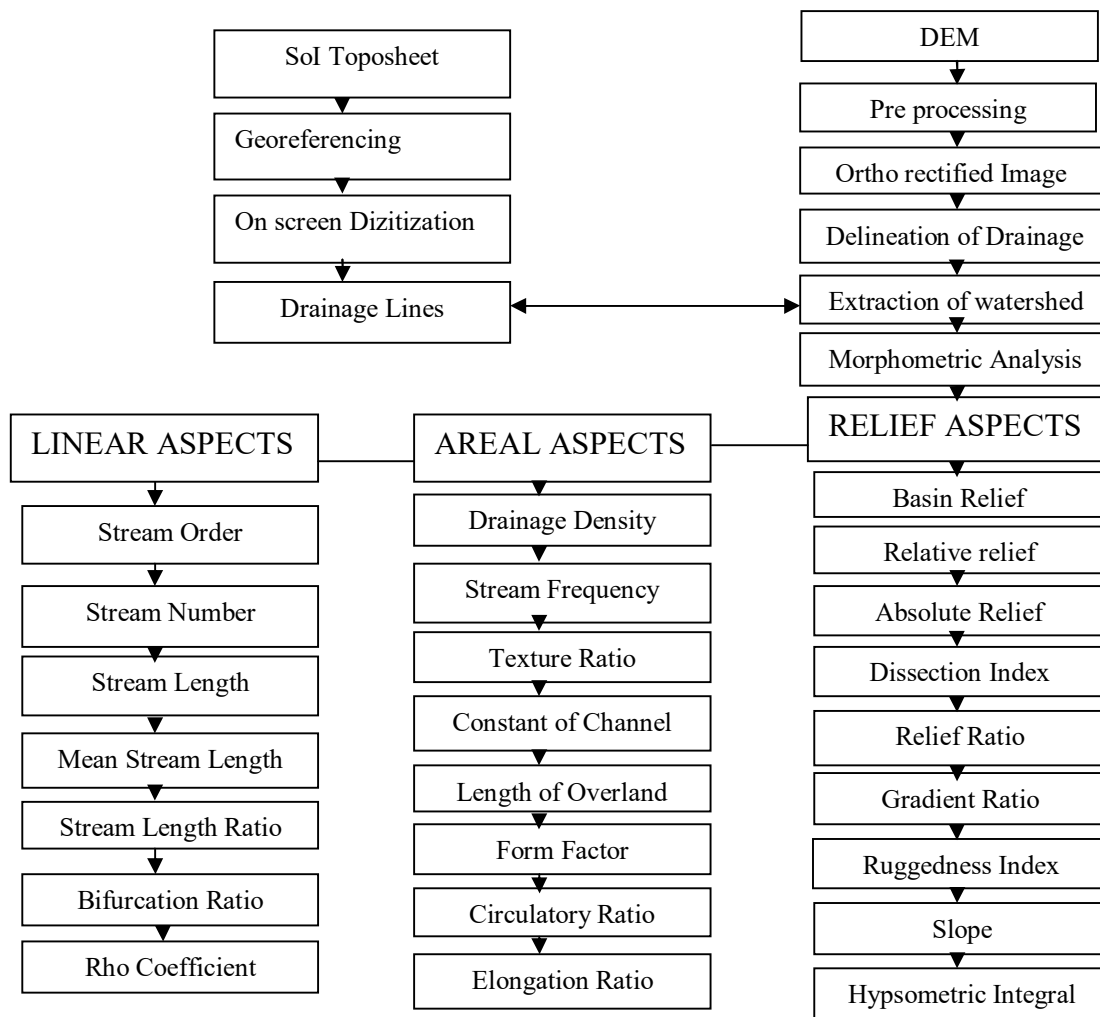


Figure 3.1 Flow chart for calculating the morphometric parameters.

3.3 Linear aspects of morphometric analysis of watershed

The linear aspect of a drainage network reveals the behaviour of a river and its tributaries from head to mouth with respect to lithological and structural controls of the drainage basin (Resmi, et al., 2019). The linear aspects include Stream order, stream number, stream length, mean stream length, stream length ratio, bifurcation ratio and Rho coefficient which were calculated and the results are presented in Table 3.3 and 3.4

3.3.1 Stream Order (u)

The first step in drainage basin analysis is the order designation where different streams are assigned with numeric values so that an universal counting pattern can be followed for any drainage basin called as stream ordering system. Several authors have proposed the ordering system of a drainage basin in their own way (Horton, 1945; Strahler, 1964 & Shreve, 1967).

In Strahler's method (1964), the smallest and furthest upstream un-branched fingertip streams are designated as 1st order, the confluence of two 1st order channels give a channel segments of 2nd order, two 2nd order streams join to form a segment of 3rd order and so on. The main assumption behind this ordering system is that when two similar order streams join to create the next higher order stream, mean discharge capacity is doubled.

After reviewing the stream ordering system, it is found that Strahler's method of stream ordering is the most convenient and widely applied system by different authors worldwide. Hence, Strahler (1964) stream ordering system has been adopted for the present study. One of the important applications of this ordering system is that it is directly proportional to relative watershed dimensions, channel size and stream discharge in a basin i.e., higher order streams produces higher discharge and also give a clue about the size of the watershed.

In all, there are 3598 number of streams that identified within the study area of which 2836 first order, 597 second order, 126 third order, 32 fourth order and 6 fifth order streams, 1 of sixth order.

3.3.2 Stream Number (Nu)

The number of stream segments in each order is known as stream number. The number of streams usually decreases as the stream order increases. Thus stream number and stream order are inversely proportional to each other (Horton, 1945). The upper Tuirial River is a sixth order drainage basin in which 78.82 % of the total number of streams belong to first order, 16.59 % of the total number of streams belong to second order, 3.5 % of the total number of streams belongs to third order, 0.89 % of the total number of streams belongs to fourth order, 0.17 % of the total number of streams belongs to fifth order and 0.03 % of the total number of streams belongs to sixth order. This large percentage of first order stream segments indicates complex geomorphic terrain and impermeable sub surface lithology (Pakhmode, et al., 2003; Vincy, et al., 2011). It also indicates that there is a possibility of flash floods after heavy rainfall in the down streams (Chitra, et al., 2011). A logarithmic regression of a number of streams of each order against stream orders usually gives a straight line plot with very little scatter (Maxwell, 1955; Samal, et al., 2015). The geometric relationship of stream order and stream number for all the sub watersheds show negative correlation (Fig.3.2) that validates the law of stream number defined by Horton in 1945

which states that the number of stream segment of each order form an inverse geometric sequence with order number. Generally it is denoted by the formula

$$N_u = N_1 + N_2 + N_3 + \dots$$

Where, N_u = Total number of streams, N_1 = First order stream N_2 = Second order stream and so on.

3.3.3 Stream Length (Lu)

Stream length is one of the fundamental linear properties of drainage network and is measured as the total length of streams in a particular order (Horton, 1945). Stream length is one of the most important hydrological characters of the area as it gives information about surface runoff characteristics (Rai, et al., 2017). The river of fairly smaller length is characteristics of regions with steep slopes and less permeable rock formation and Rivers having longer lengths are commonly suggestive of smoother slope. The L_u values for different sub watershed are given in Table 3.4.

The total stream length of upper Tuirial river basin was found to be 2162.24 km out of which 1459.46 km of the first order, 347.28 km second order, 166.46 km third order, 91.70 km fourth order, 49.41 km fifth order and 47.93 km length of sixth order. It is observed that as the stream order increases the stream length of successive order decreases and this relation between stream order and stream length is called Horton's second law "law of stream lengths". It states that the total length of stream segment is the maximum in the first order stream and decreases as the stream order increases.

3.3.4 Mean stream length (Lsm)

The mean stream length is an attribute that characterizing the size aspects of drainage network and its associated surface (Strahler, 1964). It is obtained by dividing the total length of streams of a particular order by the total number of segments in that orders and is directly proportional to topography (rough topography shorter length and smoother topography longer length) and size of river basin. The L_{sm} values for the upper Tuirial watershed range from 0.515 for first order streams to 47.93 km for sixth order streams (Table 3.4). These vast differences in mean length indicating that the lower order streams are originated from higher altitude with steep slopes and highly fractured topography (Rai, et. al., 2017; Singh and Singh, 1997). It is noted that L_{sm} value of any stream order is greater than that of the lower order and less than that of its next higher order in the basin that means

stream order and mean stream length shows positive correlation (Fig. 3.4). The L_{sm} values differ with respect to different basins, as it is directly proportional to the size and topography of the basin. Mean stream length of different sub-watershed of upper Tuirial watershed is shown in the Table 3.4.

3.3.5 Stream Length Ratio (R_L)

Stream length ratio (R_L) may be defined as the ratio of the cumulative mean length of given stream order to the cumulative mean length of next lower order of stream segment (Horton 1945).

Changes in stream length ratio from one order to another indicate the late youth to mature stage of geomorphic development (Rai, et al., 2014; Singh and Singh, 1997). This variation might be due to changes in slope and topography (Kumar, et al., 2001; Sudheer, 1986; Sreedevi, 1999 and Sreedevi, et al., 2005). Low R_L values are the indication of moderately resistant rocks (Pandey and Das, 2016). Thus R_L values for the upper Tuirial watershed ranges from 2.12 to 4.55 (Table 3.4) and these differences in length ratio is due to changes in slope and topography within the study area. And the mean R_L value of 2.72 is quite low value suggesting the occurrence of resistant rock in the terrain. The R_L value of 2.72 means in an average the length of higher order streams are 2.72 times longer than the lower order streams. The R_L has an important relationship with the surface flow discharge and erosional stage of the basin. Lower value of stream length ratio indicates high discharge and high rate of erosion. The mean stream length ratio is calculated as the mean of the stream length ratio. The R_L values of different sub watersheds are listed in Table 3.4.

3.3.6 Bifurcation Ratio (R_b)

Bifurcation ratio is related to the branching pattern of a drainage network and is the ratio of number of given order streams to the next higher order streams (Schumm, 1956). The higher values of R_b indicate a strong structural control in the drainage pattern produces elongated narrow basin whereas the lower values are the characteristics of structurally less disturbed watershed without any distortion in the drainage pattern (Strahler, 1964; Vittala, et al., 2004; Chopra, et al., 2005). If the bifurcation ratio of a stream network is low then there is higher chance of flooding as the water will be concentrated in the channel rather that spread out as a higher bifurcation. The bifurcation ratio also shows which parts of the drainage basin are more likely to be flooded. According to Horton (1945), the bifurcation ratio varies from a minimum of 2 in flat or rolling drainage basins to 3 or 4 in mountainous or highly dissected

drainage basins. The Rb values of greater than 5 which indicate that the lithologically and structurally controlled drainage. The mean Rb of the present study is found to be 4.72 (Table 3.3) indicates that highly mountainous terrain and the drainage pattern is slightly influenced by geological structures. Bifurcation ratio of 4.72 means that on an average there are 4.7 times as many streams of one order as of the next higher order.

The formula of the bifurcation ratio is

$$R_b = N_u / N_{u+1}$$

Where, Rb is the bifurcation ratio

Nu is the number of stream of order u

Nu+1 is the number of stream of the next higher order.

3.3.7 Weighted Mean of Bifurcation Ratio

Because of chance irregularities, bifurcation ratio between successive pairs of orders differs within the same basin due to differences in the stage to their erosional development and also due to topographic variations. To arrive at a more representative bifurcation number, Strahler (1953) used a weighted-mean bifurcation ratio obtained by multiplying the bifurcation ratio for each successive pair of orders by the total number of streams involved in the ratio and taking the mean of the sum of these values (Table 3.3).

The Rb values for the 19 sub basins are listed in Table 4.3. Based on mean weighted Rb values it is found that sub watershed Kailian, Ngarum, Zilpui, Muthi and Tuipawl are strongly influenced by structure. Sub watershed Sakei, Suibual, Belkhui, Nghalrawh, Tuiphu, Tuizual and Chite are slightly structurally distorted and the sub-watersheds Nghathup, Sherbawk, Tuirial, Tulrital, Darkhuang, Suanghuan and SW18 are geologically controlled and has attained mature stage of erosional development.

Table 3.3 Method of deriving weighted mean Bifurcation ratio

Name of the Basin	Stream order	Number of Streams	Bifurcation Ratio (Rb)	No. of streams involved in ratio (N)	Products of Rb and N.	Sum of streams involved in ratio (P)	Sum of product (R)	weighted mean Rb = (R/P)
Upper Tuirial watershed	I	2836	-	-	-	-	-	-
	II	597	4.75	3433	16306.8	-	-	-
	III	126	4.7	723	3398.1	-	-	-
	IV	32	3.93	158	620.94	4359	20570.33	4.72
	V	6	5.33	38	202.54	-	-	-
	VI	1	6	7	42	-	-	-
Kailian	I	27	-	-	-	-	-	-
	II	5	5.4	32	172.8	38	202.8	5.34
	III	1	5	6	30	-	-	-
Nghathup	I	48	-	-	-	-	-	-
	II	11	4.36	59	257.24	-	-	-
	III	3	3.66	14	51.24	77	320.48	4.16
	IV	1	3	4	12	-	-	-
Sakei	I	53	-	-	-	-	-	-
	II	10	5.3	63	333.9	80	389.19	4.86
	III	3	3.33	13	43.29	-	-	-
	IV	1	3	4	12	-	-	-
Sherbawk	I	15	-	-	-	-	-	-
	II	5	3	20	60	-	-	-
	III	2	2.5	7	17.5	30	83.5	2.78
	IV	1	2	3	6	-	-	-
Suibual	I	134	-	-	-	-	-	-
	II	27	4.96	161	798.56	-	-	-
	III	6	4.5	33	148.5	201	989.06	4.92
	IV	1	6	7	42	-	-	-

Ngharum	I	69	-	-	-	-	-	-
	II	15	4.6	84	386.4	-	-	-
	III	2	7.5	17	127.5	104	519.9	5.0
	IV	1	2	3	6	-	-	-
Zilpui	I	361	-	-	-	-	-	-
	II	63	5.73	424	2429.52	-	-	-
	III	14	4.5	77	346.5	522	2867.24	5.49
	IV	3	4.66	17	79.22	-	-	-
	V	1	3	4	12	-	-	-
Belkhui	I	72	-	-	-	-	-	-
	II	14	5.14	86	442.04	-	-	-
	III	4	3.5	18	63	109	525.04	4.82
	IV	1	4	5	20	-	-	-
Nghalrawh	I	42	-	-	-	-	-	-
	II	8	5.25	50	262.5	-	-	-
	III	3	2.66	11	29.26	65	303.76	4.67
	IV	1	3	4	12	-	-	-
Tuiphu	I	142	-	-	-	-	-	-
	II	31	4.58	173	792.34	-	-	-
	III	5	6.2	36	223.2	215	1045.54	4.86
	IV	1	5	6	30	-	-	-
Tuirial	I	119	-	-	-	-	-	-
	II	28	4.25	147	624.75	-	-	-
	III	7	4	35	140	194	802.25	4.14
	IV	2	3.5	9	31.5	-	-	-
	V	1	2	3	6	-	-	-
Tulrital	I	169	-	-	-	-	-	-
	II	42	4.02	211	848.22	-	-	-
	III	9	4.66	51	237.66	280	1135.13	4.05
	IV	4	2.25	13	29.25	-	-	-
	V	1	4	5	20	-	-	-
	I	470	-	-	-	-	-	-

Tuizual	II	103	4.56	573	2612.88	-	-	-
	III	22	4.68	125	585	733	3342.36	4.56
	IV	6	3.66	28	102.48	-	-	-
	V	1	6	7	42	-	-	-
Darkhuang	I	24	-	-	-	-	-	-
	II	6	4	30	120	-	-	-
	III	2	3	8	24	41	150	3.66
	IV	1	2	3	6	-	-	-
Suanghuan	I	104	-	-	-	-	-	-
	II	28	3.71	132	489.72	-	-	-
	III	6	4.66	34	158.44	177	678.16	3.83
	IV	2	3	8	24	-	-	-
	V	1	2	3	6	-	-	-
Chite	I	239	-	-	-	-	-	-
	II	49	4.87	288	1402.56	-	-	-
	III	10	4.9	59	289.1	364	1746.95	4.8
	IV	3	3.33	13	43.29	-	-	-
	V	1	3	4	12	-	-	-
Muthi	I	127	-	-	-	-	-	-
	II	23	5.52	150	828	-	-	-
	III	5	4.6	28	128.8	184	986.8	5.36
	IV	1	5	6	30	-	-	-
SW18	I	32	-	-	-	-	-	-
	II	7	4.57	39	178.23	-	-	-
	III	2	3.5	9	31.5	51	215.73	4.23
	IV	1	2	3	6	-	-	-
Tuipawl	I	105	-	-	-	-	-	-
	II	21	5	126	630	-	-	-
	III	4	5.25	25	131.25	156	781.25	5.0
	IV	1	4	5	20	-	-	-

3.3.8 Rho Coefficient (ρ)

It is defined as the ratio of stream length ratio to the bifurcation ratio and it is an important parameter relating drainage density to physiographic development of a watershed which evaluates the water storage capacity of the basin (Horton, 1945). Higher values indicate high and low value indicates low storage capacity of water in the watershed (Pande and Moharir, 2017). The value of Rho coefficient for the upper Tuirial watershed is 0.54 suggesting low water storage capacity basin and for its sub watersheds ranges from 0.49 to 0.81 as shown in Table 3.4. The value of Rho coefficient for the Sub watershed Kailian, Ngharum, Sherbawk and Chite shows relatively higher storage capacity of water than the rest of the sub watershed. The formula of the Rho coefficient is

$$P=R_L/R_b$$

Where, ρ is rho coefficient, R_L = the stream length ratio and R_b = the bifurcation ratio

Table 3.4 Linear aspects of Upper Tuirial basin and its Sub watersheds

Sub-Basin/ watershed Name	Stream order	Number of Streams	Bifurcation Ratio (R_b)	Total length of segments (km)	Mean Stream length (km)	Cumulative mean length (km)	Length Ratio (R_L)	Mean R_L	Rho coefficie nt	Mean Rho
Upper Tuirial	1	2836	-	1459.46	0.52	0.52	-	-	-	-
	2	597	4.75	347.28	0.58	1.09	2.12	-	0.45	-
	3	126	4.7	166.46	1.32	2.41	2.21	2.72	0.47	0.54
	4	32	3.93	91.70	2.87	5.28	2.19	-	0.56	-
	5	6	5.33	49.41	8.24	13.51	2.56	-	0.48	-
	6	1	6	47.93	47.93	61.44	4.55	-	0.76	-
Kailian	1	27	-	13.09	0.49	0.49	-	-	-	-
	2	5	5.4	2.16	0.43	0.92	1.89	-	0.35	-
	3	1	5	4.94	4.94	5.86	6.40	4.14	1.28	0.81
Nghathup	1	48	-	21.36	0.45	0.45	-	-	-	-
	2	11	4.36	5.89	0.54	0.98	2.20	-	0.51	-
	3	3	3.66	2.60	0.87	1.85	1.88	2.36	0.51	0.67
	4	1	3	3.67	3.67	5.51	2.99	-	1.00	-
	1	53	-	26.29	0.50	0.50	-	-	-	-
	2	10	5.3	7.31	0.73	1.23	2.47	-	0.47	-

Sakei	3	3	3.33	2.18	0.73	1.96	1.59	2.36	0.48	0.65
	4	1	3	3.92	3.92	5.88	3.01	-	1.00	-
Sherbawk	1	15	-	7.86	0.52	0.52	-	-	-	-
	2	5	3	1.63	0.33	0.85	1.62	-	0.54	-
	3	2	2.5	0.82	0.41	1.26	1.48	1.78	0.59	0.75
	4	1	2	1.56	1.56	2.82	2.23	-	1.12	-
Suibual	1	134	-	58.52	0.44	0.44	-	-	-	-
	2	27	4.96	17.43	0.65	1.08	2.48	-	0.50	-
	3	6	4.5	8.40	1.40	2.48	2.29	2.75	0.51	0.53
	4	1	6	6.17	6.17	8.65	3.48	-	0.58	-
Ngharum	1	69	-	30.46	0.44	0.44	-	-	-	-
	2	15	4.6	8.80	0.59	1.03	2.33	-	0.51	-
	3	2	7.5	3.77	1.89	2.91	2.84	2.56	0.38	0.71
	4	1	2	4.42	4.42	7.33	2.52	-	1.26	-
Zilpui	1	361	-	162.65	0.45	0.45	-	-	-	-
	2	63	5.73	41.13	0.65	1.10	2.45	-	0.43	-
	3	14	4.5	20.26	1.45	2.55	2.31	-	0.51	-
	4	3	4.66	11.81	3.94	6.49	2.54	2.33	0.55	0.54
	5	1	3	6.65	6.65	13.14	2.03	-	0.68	-
Belkhui	1	72	-	29.47	0.41	0.41	-	-	-	-
	2	14	5.14	5.37	0.38	0.79	1.94	-	0.38	-
	3	4	3.5	2.96	0.74	1.53	1.94	2.58	0.55	0.63
	4	1	4	4.41	4.41	5.94	3.87	-	0.97	-
Nghalrawh	1	42	-	17.47	0.42	0.42	-	-	-	-
	2	8	5.25	3.80	0.48	0.89	2.14	-	0.41	-
	3	3	2.66	1.19	0.40	1.29	1.44	2.29	0.54	0.68
	4	1	3	2.93	2.93	4.22	3.27	-	1.09	-
Tuiphu	1	142	-	63.92	0.45	0.45	-	-	-	-
	2	31	4.58	16.90	0.55	1.00	2.21	-	0.48	-
	3	5	6.2	8.80	1.76	2.75	2.77	2.51	0.45	0.48
	4	1	5	5.25	5.25	7.01	2.54	-	0.51	-
	1	119	-	73.72	0.62	0.62	-	-	-	-

Tuirial	2	28	4.25	19.94	0.71	1.33	2.15	-	0.51	-
	3	7	4	11.60	1.66	2.99	2.24	1.96	0.56	0.60
	4	2	3.5	5.07	2.54	5.53	1.85	-	0.53	-
	5	1	2	3.29	3.29	8.82	1.60	-	0.80	-
Tulrital	1	169	-	110.25	0.65	0.65	-	-	-	-
	2	42	4.02	26.68	0.64	1.29	1.97	-	0.49	-
	3	9	4.66	12.29	1.37	2.65	2.06	2.10	0.44	0.57
	4	4	2.25	3.84	0.96	3.61	1.36	-	0.61	-
	5	1	4	7.21	7.21	10.82	3.00	-	0.75	-
Tuizual	1	470	-	232.84	0.50	0.50	-	-	-	-
	2	103	4.56	57.59	0.56	1.05	2.13	-	0.47	-
	3	22	4.68	24.34	1.11	2.16	2.05	-	0.44	-
	4	6	3.66	16.41	2.74	4.90	2.27	2.68	0.62	0.56
	5	1	6	16.09	16.09	20.99	4.29	-	0.71	-
Darkhuang	1	24	-	15.98	0.67	0.67	-	-	-	-
	2	6	4	1.16	0.19	0.86	1.29	-	0.32	-
	3	2	3	1.69	0.85	1.70	1.98	1.73	0.66	0.65
	4	1	2	1.58	1.58	3.29	1.93	-	0.96	-
Suanghuan	1	104	-	56.14	0.54	0.54	-	-	-	-
	2	28	3.71	11.46	0.41	0.95	1.76	-	0.47	-
	3	6	4.66	7.00	1.17	2.12	2.23	-	0.48	-
	4	2	3	3.54	1.77	3.89	1.84	1.95	0.61	0.64
	5	1	2	3.75	3.75	7.63	1.96	-	0.98	-
Chite	1	239	-	124.50	0.52	0.52	-	-	-	-
	2	49	4.87	31.40	0.64	1.16	2.23	-	0.46	-
	3	10	4.9	12.70	1.27	2.43	2.09	2.63	0.43	0.73
	4	3	3.33	2.27	0.76	3.19	1.31	-	0.39	-
	5	1	3	12.42	12.42	15.61	4.89	-	1.63	-
Muthi	1	127	-	68.95	0.54	0.54	-	-	-	-
	2	23	5.52	17.99	0.78	1.33	2.44	-	0.44	-
	3	5	4.6	9.48	1.90	3.22	2.43	2.48	0.53	0.49
	4	1	5	5.05	5.05	8.27	2.57	-	0.51	-

SW18	1	32	-	17.24	0.54	0.54	-	-	-	-
	2	7	4.57	2.97	0.42	0.96	1.79	-	0.39	-
	3	2	3.5	3.71	1.86	2.82	2.93	1.97	0.84	0.61
	4	1	2	0.55	0.55	3.37	1.19	-	0.60	-
Tuipawl	1	105	-	66.47	0.63	0.63	-	-	-	-
	2	21	5	14.53	0.69	1.33	2.09	-	0.42	-
	3	4	5.25	4.73	1.18	2.51	1.89	2.89	0.36	0.65
	4	1	4	9.27	9.27	11.77	4.70	-	1.17	-

3.3.9 Relation between Stream order and stream number

Each stream order is plotted against the corresponding number of streams as shown in Fig. 3.2. It is observed from the plot that the number of streams of a given order decreases systematically with increase in stream order, i.e. the relationship shows a negative correlation and this is in conformity with the law of stream numbers (Horton, 1945) also known as Horton's first law.

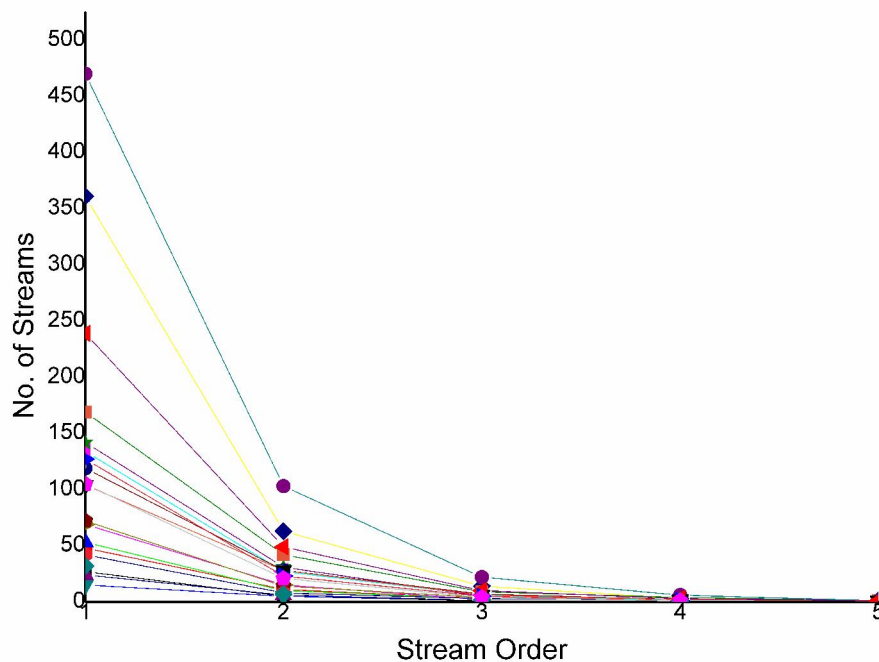


Figure 3.2 Relations between Stream Order and Stream Number

Each order of stream is plotted against its corresponding length as shown in Fig. 3.3. It is observed from the graph that the length of streams decreases systematically with increase

in stream order, i.e. the relationship shows a negative correlation and it also validates the Horton's (1932) second law (law of stream lengths) which states that the total length of stream segment is the maximum in the first order stream and decreases as the stream order increases.

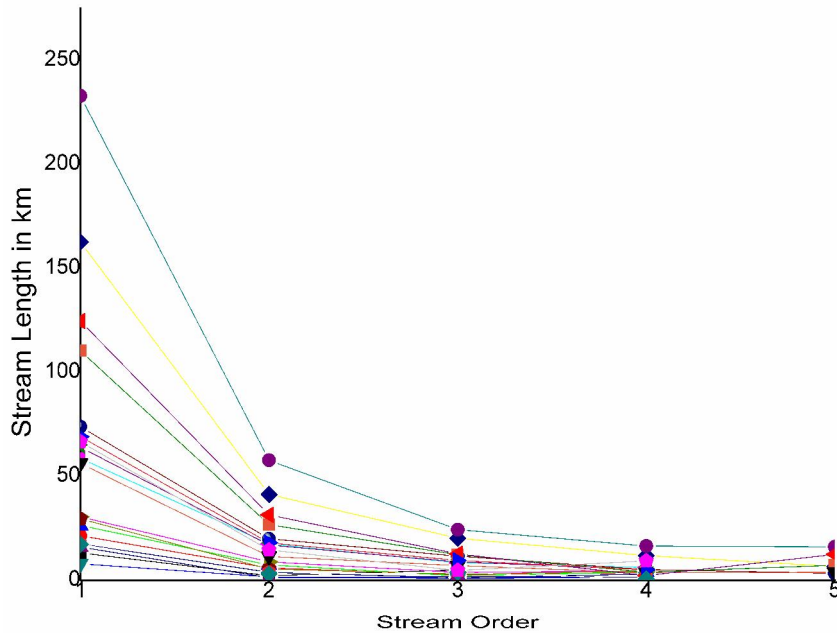


Figure 3.3 Relation between Stream Order and Stream length of watersheds.

3.3.11 Relation between stream order and mean stream length

The mean length of stream of a given order is plotted against the corresponding stream order on a graph as shown in Fig. 3.4. It is evident from the plot that the mean length of the streams of a given order increases systematically with increase in order and thus shows positive correlation. Similar relation will follow for the sub watershed also.

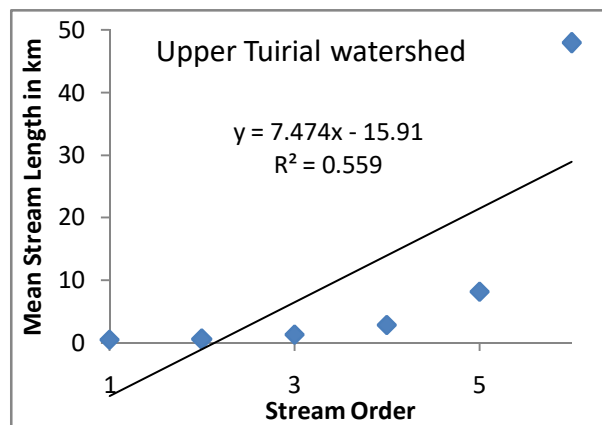


Figure 3.4. Relationship between stream order and mean stream length of watershed.

3.4 Areal aspects of morphometric analysis of sub-watersheds in the study area

Areal aspect of morphometric analyses has been divided into textural and geometric aspects whose parameters are Drainage density, Stream frequency, Texture ratio, Length of overland flow, Constant of channel maintenance, Form factor, Circularity ratio and elongation ratio which were calculated and the results are given in Table 3.5 and Table 3.8.

Textural aspects of morphometric analysis of watershed

3.4.1 Basin Area (A)

Basin area is defined as an area enclosed within the boundary of watershed divide (Schumm, 1956). It is an important parameter for hydrologic characteristics of watershed because the basin area which determines the volume of water that can be accumulated from the rainfall. Watershed area is comprised of two sub-components; Stream areas and Inter-basin areas. The inter-basin areas are the surface elements contributing flow directly to streams of order higher than 1. Stream areas are those areas that would constitute the area draining to a pre-determined point in the stream or outlet. The basin area of upper Tuirial watershed is about 531.40 km² and the drainage areas for the 19 sub-watersheds is listed in the Table 3.5.

3.4.2 Basin perimeter (p)

Basin perimeter can be defined as the linear distance along the watershed boundary encircling the basin. The perimeter of Upper Tuirial watershed is 124.9 km and for the sub watersheds are presented in the Table 3.5.

3.4.3 Basin Length (Lb)

Basin length can be defined in more than one way as shown in the Fig. 3.7

1. The maximum straight-line distance between any two points on the perimeter
2. The longest distance between the outlet and any point which is farthest on the basin boundary.
3. The length of the main stream from its source (projected to the perimeter) to the outlet

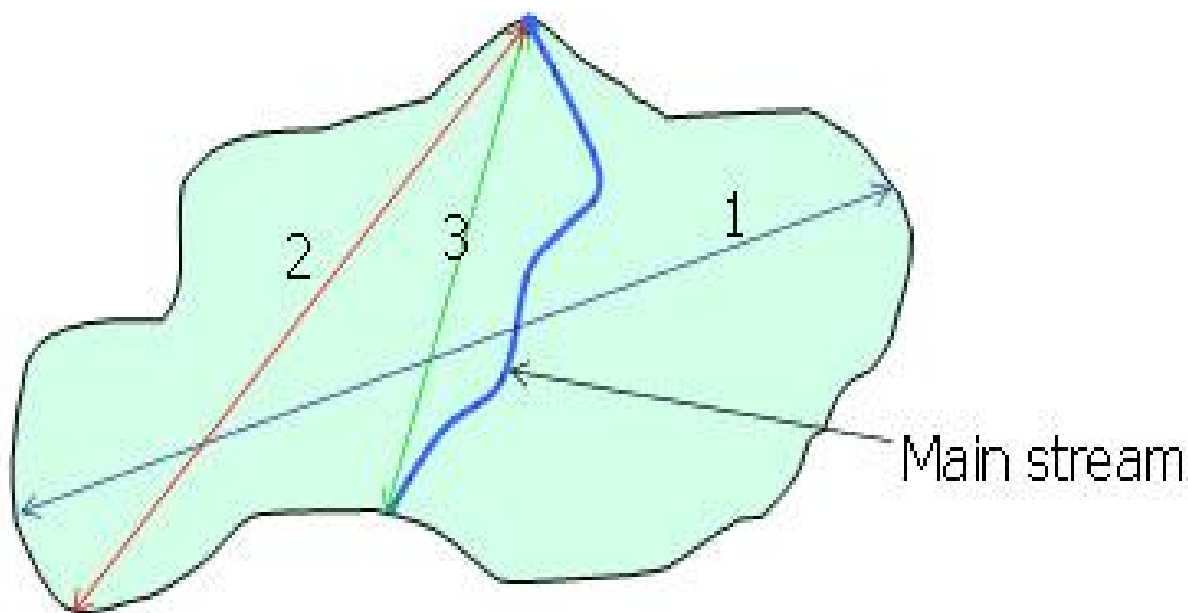


Figure 3.5 Schematic diagram defining the basin length, area and perimeter. (After Zavoianu, 2011).

Basin length is basically calculated for time parameter, which is a measure of the travel time of water through a watershed. For the present study basin length was measured along the flow path from the watershed outlet to the farthest point on the basin boundary assuming that the greatest volume of water would travel by this path. Length of the basin calculated for the upper Tuirial watershed is 46.35 km and for the sub-watersheds are listed in the Table 3.8.

Table 3.5 Textural aspects of upper Tuirial watershed.

Name of watershed/ Sub watershed	Area in km ²	Perimeter in km	Drainage Density (km/ km ²)	Stream Frequency (streams /km ²)	Texture Ratio (streams/km)	Constant of channel maintenance in km ² /km	Length of overland flow in km
Upper Tuirial	531.40	124.89	3.6	10.27	28.81	0.28	0.14
Kailian	5.31	12.26	2.63	7.3	2.69	0.38	0.19
Nghathup	9.31	15.58	2.53	8.25	4.04	0.40	0.20
Sakei	11.65	16.81	3.08	8.86	3.99	0.32	0.16

Sherbawk	3.40	8.63	3.65	11.11	2.66	0.27	0.14
Suibual	24.14	22.65	3.31	10.21	7.42	0.30	0.15
Ngharum	11.03	17.60	4.08	12.23	4.94	0.25	0.12
Zilpui	56.10	39.00	3.75	11.53	11.33	0.27	0.13
Belkhui	8.83	14.65	4.6	16.05	6.21	0.22	0.11
Nghalrawh	5.47	10.59	4.84	16.38	5.10	0.21	0.10
Tuiphu	22.90	24.60	3.73	11.57	7.28	0.27	0.13
Tuirial	29.18	24.46	3.42	9.1	6.42	0.29	0.15
Tulrital	29.91	26.93	4.61	12.27	8.36	0.22	0.11
Tuizual	88.42	46.13	3.63	10.7	13.05	0.28	0.14
Darkhuang	3.66	8.46	5.31	15.37	3.90	0.19	0.09
Suanghuan	21.37	21.78	3.84	10.56	6.47	0.26	0.13
Chite	51.47	36.81	3.12	8.93	8.20	0.32	0.16
Muthi	28.59	23.2	3.27	9.1	6.72	0.31	0.15
SW18	6.06	11.25	3.69	9.66	3.73	0.27	0.14
Tuipawl	25.71	25.61	2.79	7.45	5.11	0.36	0.18

3.4.4 Drainage density (Dd)

The Drainage density indicates the closeness of spacing of channels and it is dependent on several factors like presence of exposed bedrocks, surface ruggedness, permeability or impermeability of the sub-surface geology etc., (Kelson and Wells, 1989; Morisawa, 1958). Low values of drainage density indicate presence of a permeable subsurface material and low relief (Reddy, et al., 2004; Chow, 1964; and Das, 2014) and the high values are the indication of resistant sub surface and impermeable strata. Drainage density is the ratio of total stream length per unit area (Horton, 1945). By this method one can obtain only a single value which represents the drainage density of the whole basin. This method is applicable satisfactorily only for the comparative study of drainage densities among the basins, not for a macro level study of a drainage basin. Thus Drainage density has been calculated by dividing the watershed into 1 km x 1 km grids which has been selected as the smallest unit of the area for the purpose of areal analysis. Total length of the streams present within a single grid has been calculated and each value is plotted at the center of the grid. Then isopleths lines have been drawn using IDW (Inverse Distance Weighted)

interpolation methods in ArcGIS for depicting the Drainage density for each Grid of the study area. The drainage density map (Fig. 3.6) displays the areal distribution of drainage density, which has been further classified into five groups as Low Dd. (Below 2 km/km²), Moderate Dd. (2-4 km/km²), Moderate high Dd. (4-6 km/km²), High Dd. (6-8 km/km²) and Very high Dd. (Above 8 km/km²) (Table 3.6). Higher drainage densities (> 4km/km²) are observed in the southern tip and the central portion of the catchment whereas moderate to lower values (< 4km/km²) are confined mainly in the Northern and peripheral part of the basin. The drainage density of upper Tuirial River basin is 3.6 km/km² which is considered to be moderate drainage density and the drainage densities for the 19 sub-watersheds are shown in Table 3.5.

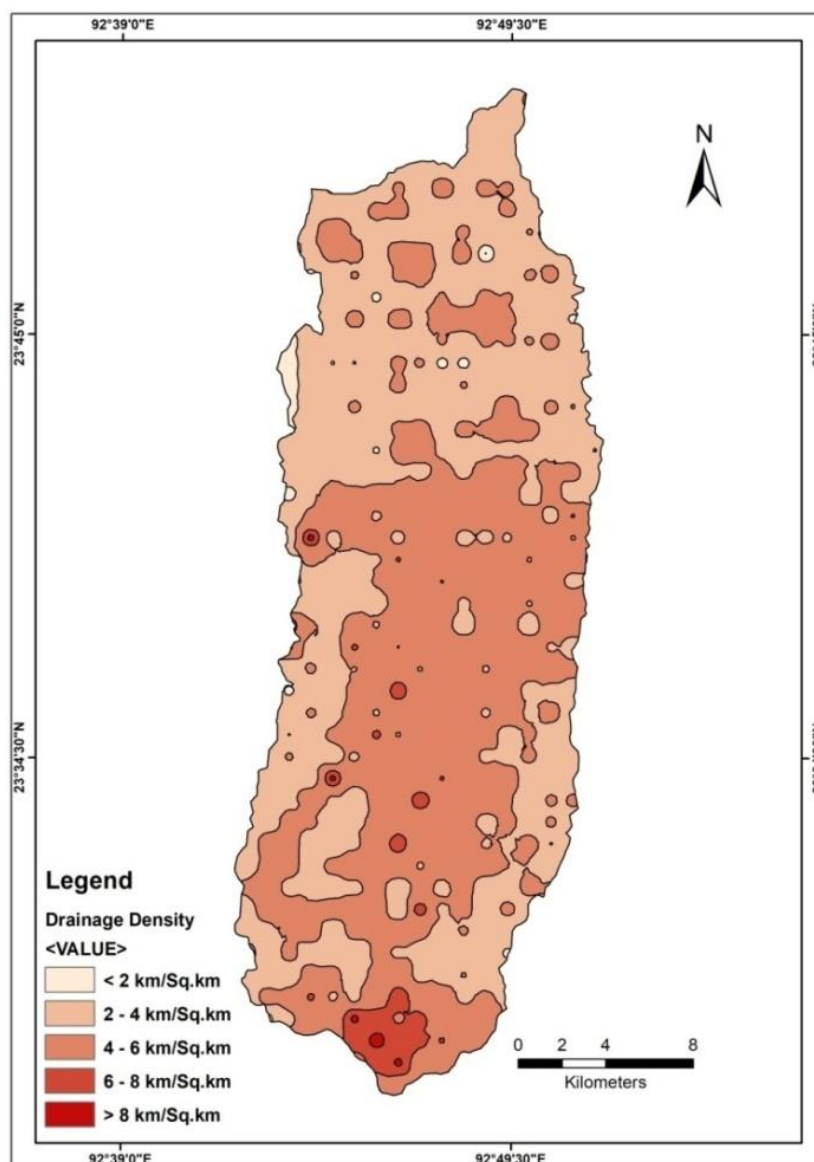


Figure 3.6 Spatial distribution of Drainage density of Upper Tuirial Watershed.

Table 3.6 Classification of Drainage Density statistics in the study area.

Drainage Density Classes	Frequency of Classes (km/km²)	Area in (km²)	Area (%)
Low	<2	3.90	0.73
Moderate	2-4	259.97	48.92
Moderate to high	4-6	254.96	47.98
High	6-8	11.95	2.25
Very high	>8	0.60	0.11

Among all the Sub watersheds Kailian, Nghathup and Tuipawl shows relatively low drainage density than the remaining sub watershed whose values are considered to be moderate to high drainage density suggesting greater run-off, impermeable subsurface material, sparse vegetation, high relief and low infiltration rate. The drainage density is calculated by using the following formula:

$$Dd=Lu/A$$

where, Dd is the drainage density, Lu is the total stream length and A is the area of the basin.

3.4.5 Stream frequency (Sf)

Stream frequency is the ratio between the total numbers of stream segments of all order per unit area (Horton, 1932). For macro level analysis, the study area has been divided into number of grids of 1 km x 1 km and the total number of streams in each grid has been calculated and the values are plotted at the center of each grid. Then isopleth lines have been drawn using IDW interpolation methods in ArcGIS for depicting the Drainage frequency for each Grid of the study area. The stream frequency map (Fig. 3.7) displays the areal distribution of drainage frequency, which has been further classified into five groups as Low Sf. (Below 7 streams/km²), Moderate Sf. (7-11 streams/km²), Moderate high Sf. (11-15 streams/km²), High Sf. (15-19 streams/km²) and Very high Sf. (above 19 streams/km²) (Table 3.5). High drainage frequency values are observed in the southern tip and the central portion of the catchment whereas moderate to low values are confined mainly in the Northern and peripheral part of the basin. The value of stream frequency of upper Tuirial watershed is found to be 10.27 streams/ km² which is classified as moderate frequency and is found in areas having the characteristics of resistant subsurface strata, high relief with low

permeability of rock formation and sparse vegetation. The higher values of Sf also indicate high run off and intense erosion (Horton, 1945). Sub watershed Kailian, Nghathup and Tuipawl shows relatively lower frequency than the rest of the sub watershed. In case of drainage density also it was found that the Sub watershed Kailian, Nghathup and Tuipawl shows low value, thus it is confirmed that these three sub watersheds are mature stage of geomorphic development and are potential zones for ground water availability. The stream frequency is calculated by using the following formula

$$Sf = Nu/A$$

Where, Sf is the drainage frequency, Nu is the number of stream and A is the area of the basin.

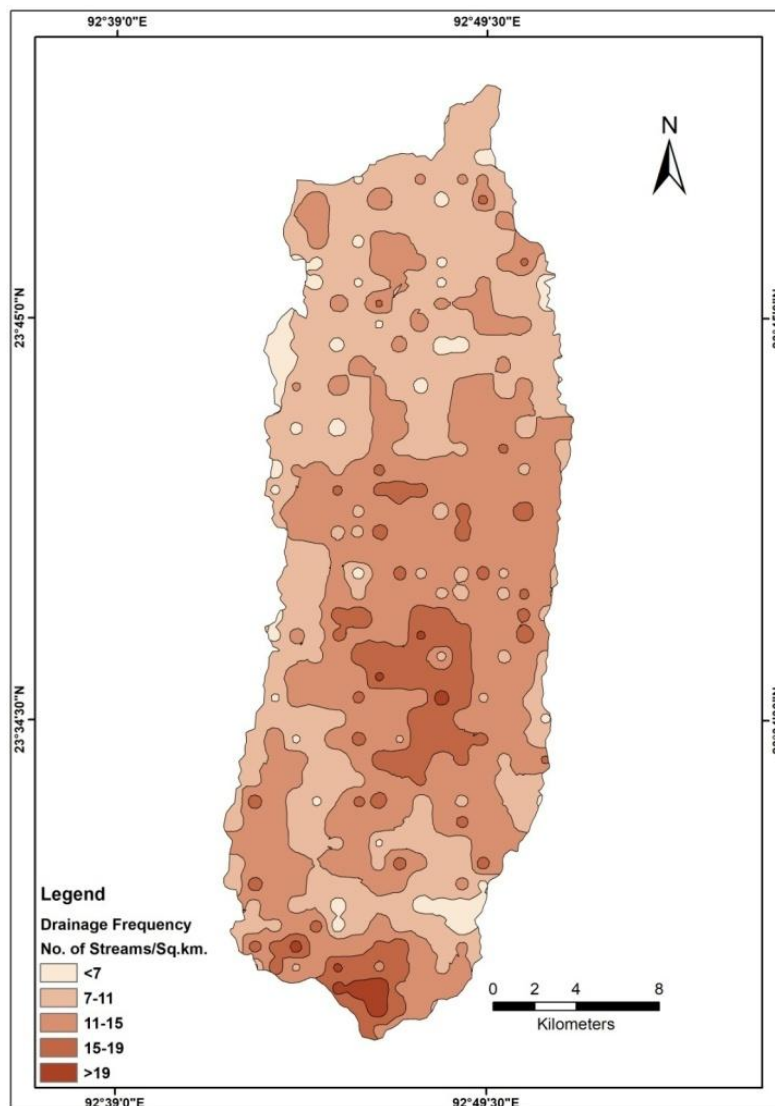


Figure 3.7 Spatial distribution of Stream frequency of Upper Tuirial Watershed

As per as areal distribution pattern of Drainage frequency, it is observed that more than 96 % of the total area is having the characteristics of moderate to very high drainage frequencies indicating that the lithology is very hard and steep topography with very little infiltration capacity of water.

Table 3.7 Classification of Stream frequency statistics in the study area.

Stream frequency Classes	Frequency Range	Area in (km ²)	Area (%)
Low	< 7	17.58	3.31
Moderate	7-11	216.34	40.71
Moderate high	11-15	244.23	45.96
High	15-19	49.39	9.30
Veryhigh	> 19	3.82	0.32

3.4.6 Relation between Drainage density and Stream frequency

The drainage densities of all the watersheds are plotted against the Stream frequencies as shown in figure 3.8. It is evident from the plot that the drainage density increases systematically with increase in drainage frequency and thus shows very strong positive correlation suggesting that similar geological conditions prevailed in the study area.

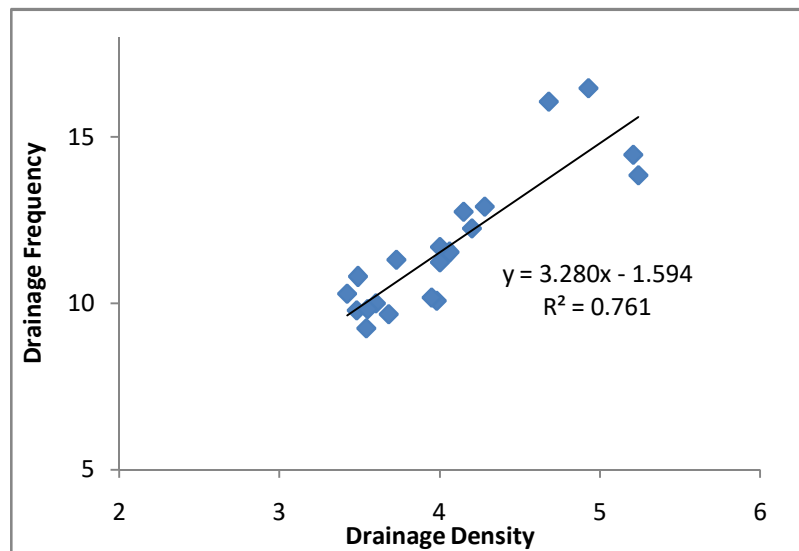


Figure 3.8 Relation between Drainage density (Dd) and Stream frequency (Sf).

3.4.7 Texture Ratio (T)

Texture ratio is the total number of stream segments of all orders per perimeter of the area and is the expression of relative spacing of drainage lines in a river basin (Smith, 1950). It is the coarseness or fineness of the dissection of the drainage network. The drainage texture depends on number of factors such as climate, rainfall, vegetation, rock and soil type, infiltration capacity, relief, and stage of development of the basin (Dornkamp and King, 1971). Smith (1950) classified drainage texture into four different classes i.e. coarse (<4), medium (4-10), fine (10-100) and ultrafine (>100). Generally coarse texture resemble permeable sub surface and fine texture resemble impermeable sub surface with high rate of erosion and dissection (creation of cuts in a landscape due to erosion). In the present study, the drainage texture value of upper Tuirial watershed is 28.81 indicating fine texture, suggesting impermeable sub surface lithology, less infiltration rate, rugged topography, and high run off with high rate of erosion and dissection. According to Smith (1950) classification method Sub watershed Kailian, Sakei, Sherbawk, Darkhuang and SW18 are course texture, sub-watersheds Nghathup, Ngharum, Nghalrawh, Suibual, Belkhui, Tuiphu, Tulrital, Chite, Tuirial, Suanghuan, Muthi and Tuipawl are moderate textures and sub-watersheds Zilpui and Tuizual are fine textures.

The texture ratio is calculated by using the following formula:

$$T = Nu / P$$

Where, T is the texture ratio

Nu is the total number of stream segments of all orders.

P is the perimeter of the watersheds

3.4.8 Constant of Channel Maintenance

Constant of channel maintenance is defined as the area of the watershed surface needed to maintain a unit length of stream channel and is expressed by the reciprocal of drainage density (Schumm, 1956). The value of constant of channel maintenance is high in areas having the characteristics of permeable sub surface geology, low relief and thick vegetation. The Stream value for upper Tuirial basin is 0.25 km²/km i.e., only 250 square meters of area is needed to run 1000 meters of stream which is very low indicating that the area is characterized by high surface runoff, low permeability, less infiltration and closely

dissected. The sub watershed wise constant of channel maintenance values ranges from 0.19 to 0.40 sq.km/km indicating similar topographic and geologic conditions in those areas as shown in Table 3.5. The constant of channel maintenance for sub watershed Kailian, Nghathup and Tuipawl shows relatively high as compare to the rest of the sub watershed suggesting relatively permeable lithology. The constant of channel maintenance is calculated by the following formula:

$$C_m = 1/D_d$$

Where, C_m is the constant of channel maintenance, and D_d is the drainage density.

3.4.9 Length of Overland Flow (L_g)

Rainfall which precipitates on surfaces before reaching a channel as runoff is called overland flow which is synonymous to sheet flow. The average length of overland flow is approximately half of the average distance between channels and is approximately equal to half the reciprocal of drainage density. Horton (1945) defined the term length of overland flow as the length of flow path, projected to a horizontal plane of the rain flow from a point on the drainage that divide to a point on the adjacent stream channel. The length of overland flow is inversely proportional to the surface runoff, i.e., lower the value of length of overland flow quicker the surface runoff from the streams and higher the value longer the flow path and thus gentle ground slopes. In the study area, L_g value is found to be 0.12 km which means an average length of flow path is 120 meters. This low value of L_g indicating quicker surface runoff due to steep ground slope and it is one of the major factors for less infiltration of water on the surface. The L_g values for different sub watershed (Table 3.5) ranges from 0.09 km for Darkhuang to 0.20 km for Nghathup indicating high runoff, less infiltration and high rate of erosion. As the length of overland flow is very short, construction of artificial recharge structures is not possible in the region. Among all the sub watersheds, Kailian, Nghathup and Tuipawl sub watershed shows relatively high value as compare to the rest of the sub watershed suggesting more infiltration rate due to longer path of surface flow of water and hence more permeability in these three sub watersheds. The length of overland flow is calculated by the following formula:

$$L_g = 1/(D_d \times 2)$$

Where L_g = Length of overland flow, D_d = Drainage density.

3.5 Geometric aspects of morphometric analysis of watershed

The geometric parameters include form factor, circulatory ratio and elongation ratio which are basically shape factors. These parameters have been calculated to understand the shape of the basin as these are important morphometric parameters to predict the erosion rate, tectonic activity, stage of geomorphic cycle and forecasting flash flood within the basin. Generally basins of circular shape are less prone to erosion than a basin of an elongated shape.

Table 3.8 Geometric aspects of Upper Tuirial watershed.

Watershed Name	Basin Length in km	Form Factor	Circulatory Ratio	Elongation ratio
Upper Tuirial	46.35	0.25	0.43	0.56
Kailian	5.04	0.21	0.44	0.52
Nghathup	5.87	0.27	0.48	0.59
Sakei	5.48	0.39	0.52	0.70
Sherbawk	3.10	0.35	0.57	0.67
Suibual	6.96	0.50	0.59	0.80
Ngharum	5.83	0.32	0.45	0.64
Zilpui	13.54	0.31	0.46	0.62
Belkhui	5.39	0.30	0.52	0.62
Nghalrawh	3.92	0.36	0.61	0.67
Tuiphu	7.83	0.37	0.48	0.69
Tuirial	9.32	0.34	0.61	0.65
Tulrital	10.44	0.27	0.52	0.59
Tuizual	17.00	0.31	0.52	0.62
Darkhuang	3.35	0.33	0.64	0.64
Suanghuan	7.55	0.37	0.57	0.69
Chite	13.08	0.30	0.48	0.62
Muthi	7.50	0.51	0.67	0.80
sw18	4.47	0.30	0.60	0.62
Tuipawl	8.44	0.36	0.49	0.68

3.5.1 Form Factor (Ff).

Form factor is a dimensionless parameter which defined as the ratio of the area of a drainage basin to the square of the basin length (Horton, 1945). Thus, the form factor (Ff) is expressed as $Ff = A/Lb^2$

Where, Ff= Form factor; A= Area of the basin; and Lb = length of the basin.

The form factor (Ff) value varies from 0 in highly elongated basin to 1 for perfectly circular basin. Hence, lesser the value of form factor more elongated the shape of the basin and vice-versa. The form factor of upper Tuirial watershed is 0.25 which indicate highly elongated basin while the Ff of sub watersheds ranges from 0.21 for Kailian to 0.51 for Muthi as shown in Table 3.8. The Form factor value can be used as an indicator for flash flood formation in a watershed. Basins with high form factor have high peak flows of shorter duration, whereas elongated watersheds with low form factor value have lower peak flow of longer duration. Management of floods is easier in elongated basin than those of the circular basin (Nautiyal, 1994). This parameter is also used as an indicator of sediment production rate (Morisawa, 1985). It has been observed that the shape parameters showed a negative correlation with runoff-rainfall ratio. Thus the decrease in form factor increases sediment production rate.

3.5.2 Circularity Ratio (Rc)

Miller (1953) defined the term ‘Circularity Ratio’ as the ratio of the area of the basin to the area of the circle having same circumference as the basin perimeter. Higher the value represents more circularity in the shape of the basin and if the value is low the basin is an elongated shape. The Rc ratio influenced by length of the basin, frequency of streams, geological structures, climate, land use/land cover, relief and slope of the basins (Vittala, et al., 2004). Low, medium and high values of Rc indicate the young, mature, and old stages of geomorphic development of cycle of erosion (John, et al., 2012). The circularity ratio of the upper Tuirial basin is 0.43 and the various sub basins ranges from 0.44 for Kailian to 0.67 for Muthi indicates that the area is characterized by high to moderate relief, mature stage of geomorphic development and elongated in shape (Table 3.8). It is calculated by using the formula-

$$Rc = 4\pi A/P^2$$

Where, Rc = Circularity ratio; P = Basin perimeter and A=Area of the Basin.

3.5.3 Elongation ratio (Re)

The elongation ratio (Re) is a representation of the shape of the river basin. According to Schumm (1956), elongation ratio is defined as the ratio of the diameter of a circle having the same area as the basin and the maximum basin length (Lb). Strahler (1964) reported that Re value close to 1.0 are found in typical regions of low relief and circular basin and as the value decreases the shape of the basin changes to elongate in nature and are generally associated with strong relief and steep ground slopes. Higher values of elongation ratio show high infiltration capacity and low runoff, whereas lower Re values which are characterized by high susceptibility to erosion and sediment load (Reddy, et al., 2004; Singh and Singh, 1997). Thus, the basin can be classed as (i) Circular (above 0.9), (ii) Oval (0.8-0.9), (iii) Less elongated (0.7-0.8), and (iv) Elongated (below 0.7). The upper Tuirial watershed Re value is 0.56 which is classified as elongated basin. For the sub basins Re values ranges from 0.52 for Kailian to 0.80 for Muthi (Table 3.8) indicating strong to moderate relief , steep ground slopes, elongated to less elongated in shape. It is also evident from the table that the sub watersheds suibual, sakei and Muthi show higher value of elongation ratio indicating less erosive than the rest of the sub watersheds. The elongation ratio may be obtained by using the formula

$$Re = 2(A/ \Pi)^{0.5}/ Lb$$

Where ‘Re’ is the elongation ratio, ‘2’ is a constant, A= area, and ‘Lb’ = maximum basin length.

3.5.4 Relationship of form factor, circulatory ratio, and elongation ratio

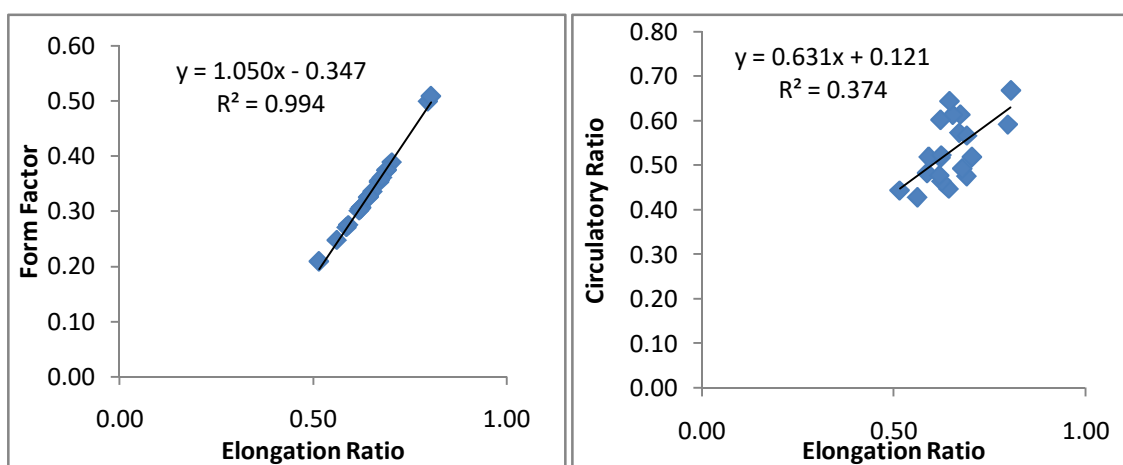


Figure 3.9 Relationship of form factor, circulatory ratio, and elongation ratio

Based on physical observation of the plots it is clear that these parameters are strongly correlated positively indicating similar geomorphological characteristics.

3.6 Relief aspects of morphometric analysis of watershed

Relief aspects of watershed consist of the parameters such as Basin relief, Relative Relief, Absolute Relief, Dissection Index, Relief ratio, Gradient ratio, Ruggedness index, slope analysis and Hypsometric analysis. These parameters help us to understand the flow direction of streams and the denudation progression occurring within the watershed, based on the geophysical and topographic conditions of the terrain.

3.6.1 Basin relief

The difference in elevation from the highest point on the basin to the lowest point at the mouth of the basin is called Basin relief (Schumm, 1956). It is an important parameter to understand the slope characteristics, degree of denudation and the rate of infiltration. Higher value indicates steeper slope, high rate of erosion and low rate of infiltration of water. The value of basin relief for upper Tuirial watershed is 1614 m which is very high relief and for the sub watershed the values ranges from 554 m for Kailian to 1349 m for Tulrital as shown in Table 3.9.

Table 3.9 Relief Aspects of Upper Tuirial watershed.

Watershed name	Highest Elevation (h)/ Absolute Relief (Ar) in m.	Lowest Elevation (h') in m.	Relative Relief (h-h') in m.	Dissection Index	Relief Ratio
Upper Tuirial	1690.00	76.00	1614.00	0.96	0.03
Kailian	630.00	76.00	554.00	0.88	0.12
Nghathup	840.00	120.00	720.00	0.86	0.15
Sakei	960.00	120.00	840.00	0.88	0.15
Sherbawk	706.00	140.00	566.00	0.80	0.18
Suibual	952.00	145.00	807.00	0.85	0.12
Ngharum	797.00	145.00	652.00	0.82	0.11

Zilpui	1220.00	160.00	1060.00	0.87	0.10
Belkhui	940.00	170.00	770.00	0.82	0.14
Nghalrawh	720.00	170.00	550.00	0.76	0.14
Tuiphu	1423.00	255.00	1168.00	0.82	0.20
Tuirial	1290.00	270.00	1020.00	0.79	0.11
Tulrital	1619.00	270.00	1349.00	0.83	0.13
Tuizual	1511.00	210.00	1301.00	0.86	0.09
Darkhuang	760.00	170.00	590.00	0.78	0.18
Suanghuan	1010.00	170.00	840.00	0.83	0.11
Chite	1310.00	150.00	1160.00	0.89	0.09
Muthi	1383.00	120.00	1263.00	0.91	0.17
SW 18	1120.00	100.00	1020.00	0.91	0.23
Tuipawl	1383.00	100.00	1283.00	0.93	0.15

3.6.2 Relative relief (Rr)

Maxwell in 1960 defined the term relative relief as the ratio of maximum relief to the basin perimeter. Melton's (1967) proposed the definition of relative relief is as follows:

$$\text{Relative relief} = H/P$$

Where, H is the difference between the highest and lowest points of the basin, P = Perimeter of the basin.

Smith in 1935 postulated the term Relative relief as the difference in elevation between the heights point and the lowest point per unit area.

Smith's method of relative relief has been adopted for this study. The other two methods give only a single value for the whole basin which is applicable for comparative study of relative relief among the basins and not for a macro level study of a drainage basin. Hadley and Schumm (1961) also revealed that residuals or abnormally high points on the divide should be ignored when obtaining the total relief of a basin. Hence, the area has been divided into 1km by 1 km grids which have been selected as the smallest unit of the area for the purpose of relief analysis. The differences in elevations between the highest and lowest points within the grid have been calculated and each value is plotted at the centers of each

grid. Then isopleth lines have been drawn using IDW interpolation method for depicting the relative relief of each grid. For a more comprehensive and detailed study of the relative relief, the values plotted in the grids have been categorized into five groups as displayed in figure 3.10. The value ranges from 49.05 m to 1061.30 m. Higher value of relative relief in the area can be seen in the central, north western and south eastern part of catchment. Higher relative relief values correspond with uplands indicating shallow and comparatively immature soil, on the other hand, lower relative relief correlates with low lying areas showing deep and more mature soil. Low values are the region of low run off and more infiltration of water on the surface and high values indicate high runoff and faster erosion on the surface (Pandey and Das, 2016). Basically it determines the slope gradient which is useful to estimate the runoff and sediment transport with in a basin.

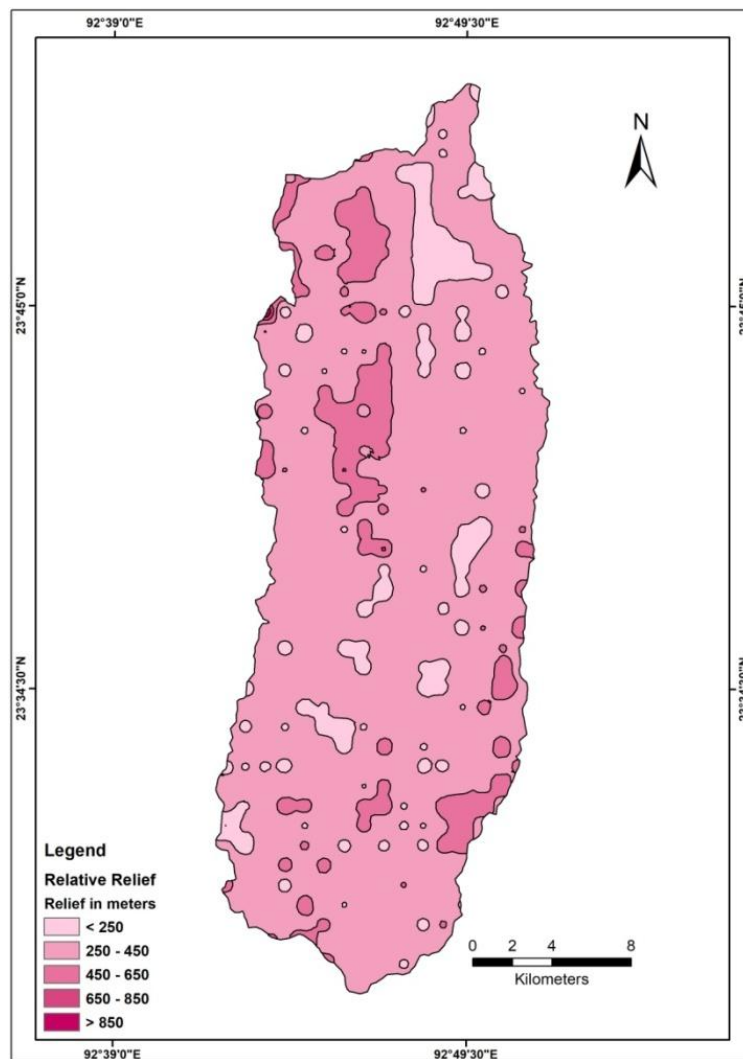


Figure 3.10 Spatial distribution of Relative relief per sq.km. of Upper Tuirial Watershed.

Table 3.10 Classification of Relative relief and its statistics.

Classes	Frequency of Classes (meters)	Area in (km²)	Area (%)
Low	<250	44.49	8.37
Moderate	250-450	432.29	81.35
Moderate high	450-650	54.369	10.23
High	650-850	0.19	0.04
Very high	>850	0.069	0.01

Table 3.10 shows that, the maximum area (81.35 %) of the basin falls in the relief group of 250 -450 m followed by 450-650 m i.e. 10.23 % of the area, less than 250 m relief covering 8.37 %, 650-850m of relief covering 0.04 % and the highest relief of more than 850 m covers only 0.01 % (Fig.4.10).

3.6.3 Absolute relief (Ar)

Absolute relief means the maximum height of any region above mean sea level (Dove Nir's, 1957).

The distribution of absolute altitude is attempted here with a specific purpose that it should give some idea regarding the nature of existing topography prior to the dissection by various denudational processes. Absolute relief of a region may be analyzed in two ways. First with the help of contour map divided in zones and second by regional distribution discrepancies based on different profiles drawn (Bhunja, et al., 2012). For the present study the area has been divided into grid units of one sq. km and the absolute value of each grid is plotted at the center. Using IDW interpolation method isopleth lines have been drawn and classified the basin into five classes as shown in the Table 3.11 and figure 3.11. Lower values are observed near the confluence towards North and the central part of the basin and the values increases towards the basin boundary. Absolute relief for the upper Tuirial watershed ranges from 260.20 m – 1616.85 m.

Table 3.11 Classification of Absolute relief and its statistics.

Classes	Frequency of Classes (meters)	Area in (km ²)	Area (%)
Low	<530	79.87	15.03
Moderate	530-800	212.88	40.06
Moderate high	800-1070	178.43	33.58
High	1070-1340	52.59	9.90
Very high	>1340	7.63	1.44

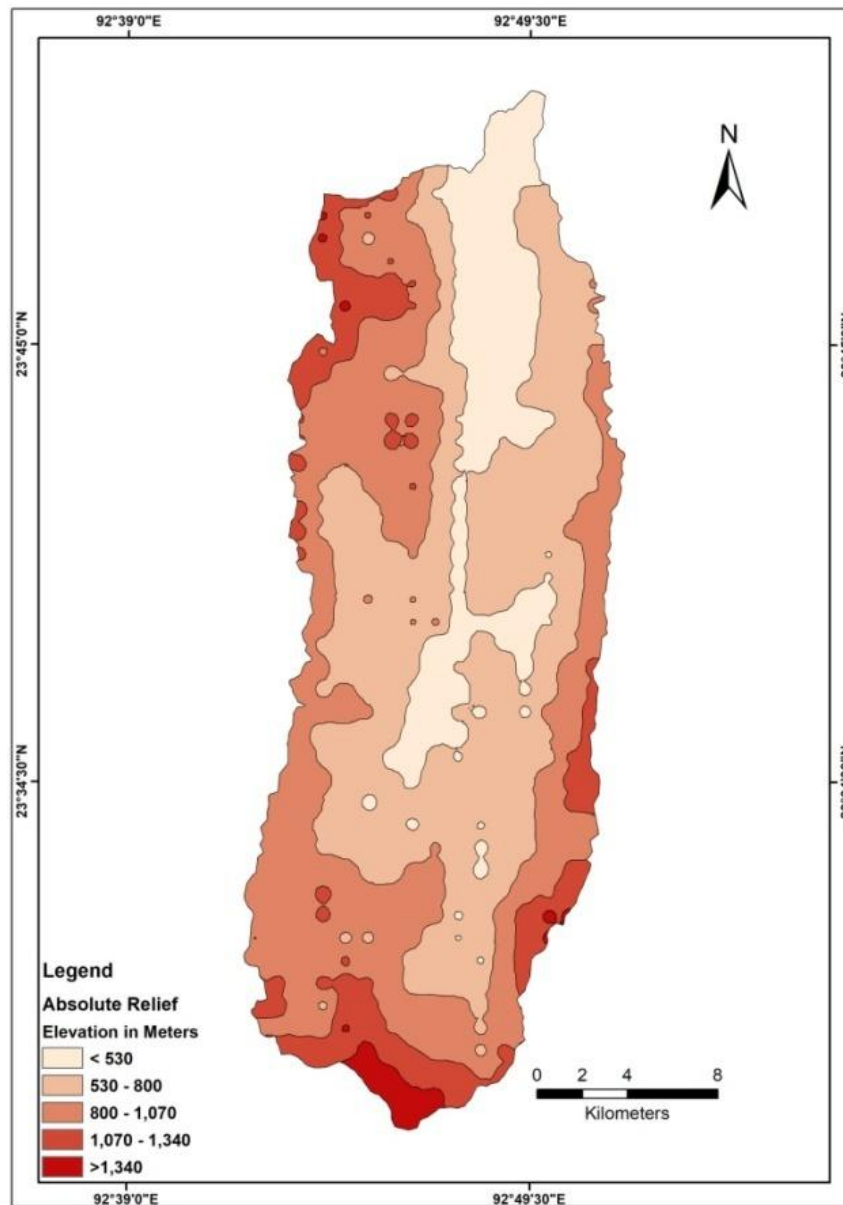


Figure 3.11 Spatial distribution of absolute relief per 1 km² of Upper Tuirial Watershed.

3.6.4 Dissection Index (DI)

Dove Nir's (1957) defined the term Dissection Index as the ratio of relative relief and absolute relief of an area and gives clue about stages of the landscape's evolution and degree of dissection or vertical erosion of a region. For the analysis of D.I., the area has been divided into grids of 1 Km by 1 km and the dissection index values are computed for each grid unit and plotted them in the centers of each grid. Using IDW interpolation method in GIS environment the D.I. of the whole area is prepared and further classified into five classes to show a clear picture of the distribution of dissection index (Fig. 3.12).

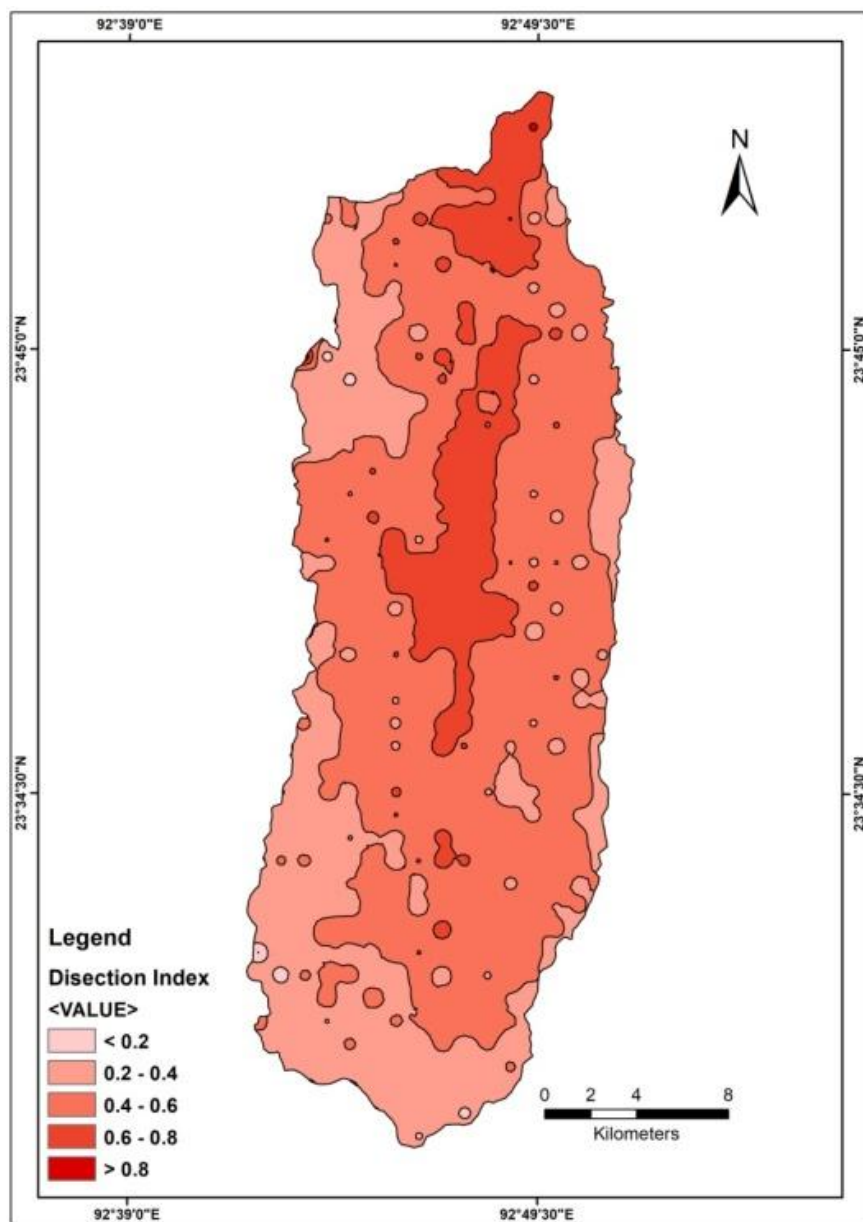


Figure 3.12 Spatial distribution of dissection index of Upper Tuirial Watershed.

These categories are Low dissection index (<0.2), Moderate (0.2-0.4), Moderately high (0.4-0.6), High (0.6-0.8) and Very high (>0.8). The value of D.I. close to Zero indicates absence of dissection while the value close to 1.0 indicates vertically dissected. The dissection index of the upper Tuirial basin ranges from 0.06 - 0.9 with a mean index of 0.47 suggesting moderately high dissection index. Table 3.12 reveals highest area is covered by the group of moderate high dissection index which is 304.95 km² or 57.39 percent of the total area followed by moderate index of 28.75 %, high 13.57 % and the lowest dissection index is under the group of below 0.02 which is 0.07% of the total area. D.I. values can also be correlates with soil thickness. Areas having lower D.I. correspond with deeper soil, while the higher values correspond to shallow skeletal soils. Accordingly, the present study in the Tuirial watershed, horticulture/ agricultural activities are expected to be more productive in the region having low dissection Index because these areas are less erosive in nature. Overall, the study suggests that the study area is moderate to high dissected indicating very high erosion in the central and Northern part of the basin.

Dissection index values of Upper Tuirial and all the sub-watersheds ranges from 0.7 to 0.96 (Table 3.12) indicating highly dissected terrain and high susceptible to erosion.

Table 3.12 Classification of Dissection Index and its statistics.

Classes	Frequency of Classes (meters)	Area in (km ²)	Area (%)
Low	< 0.2	1.43	0.27
Moderate	0.2-0.4	152.79	28.75
Moderate high	0.4-0.6	304.95	57.39
High	0.6-0.8	72.10	13.57
Very high	> 0.8	0.12	0.02

3.6.5 Relief Ratio (Rh)

Relief ratio is the ratio between the total relief of a basin and the horizontal distance along the longest dimension of the basin parallel to the principle drainage line (Schumm, 1956). It is a dimensionless height-length ratio equal to the tangent of an angle formed by two planes intersecting at the mouth of a basin, one representing the horizontal and the other passing through the highest point of the basin. It denotes the overall steepness of drainage basin and is an indicator of the intensity of denudational processes operating on slopes of that

particular basin. Higher the value of relief ratio indicating high slope angle, for example if the Rh value is found to be 1 which means the slope angle is 45° ($\tan 45^{\circ}=1$). The Rh value normally increases with decreasing drainage area as the basin length also decreases (Gottschalk, 1964). Glock (1932) reported in his study that an area of available high relief has relief ratio greater than 0.15, an area of moderate relief has relief ratio of 0.04 and an area of low relief has relief ratio of 0.009. High relief ratios are the characteristic features of high resistant rocks and low relief ratio are characteristic features of less resistant rocks of the area (Sudheer, 1986; Sreedevi, 1999, Sreedevi, 2005). The high relief ratio indicates higher kinetic energy on the slopes and hence quicker runoff with high rate of erosion. The relief ratio of the upper Tuirial watershed is 0.03 whose angular dimension is 1.72° indicating gentle slope of depression and mature topography (Moderate Relief). Relief ratio of different sub-watersheds of Upper Tuirial basin ranges from 0.09 for Chite to 0.23 for SW18 is shown in the Table 3.9 suggesting younger to early mature topography and high rate of erosion. In terms of prioritization of the different sub watersheds of Nghathup, Sakei, Sherbawk, Tuiphu, Darkhuang, Muthi, SW 18 and Tuipawl are more prone to erosion and needs immediate attention to arrest the soil erosion.

3.6.6 Gradient ratio (Rg)

It is the Ratio of the vertical distance to the actual distance along the slope (i.e. sine of the slope angle). Gradient ratio is an indication of channel slope from which an assessment of the runoff volume could be evaluated (Sreedevi, et al., 2005 & 2009). The high value of gradient ratio high will be the flow velocity and as the ratio decreases, the slope angle also decreases and hence flow velocity reduces. The basin has a gradient ratio of 0.03, while that of the nineteen sub-basins are 0.05 for Tuizual to 0.18 for Sub watershed 18, showing moderate to high gradients (Table 3.13). Gradient ratio is calculated by the following formula

$$R_g = (a-b)/L$$

Where Rg is the Gradient ratio, “a” = elevation at the source of the river “b” = elevation at mouth of the river and “L”= length of main stream.

In general, the gradient ratio will be less than the relief ratio due to lack of channel straightness and meandering nature increases the channel length beyond the drainage basin length.

Table 3.13 Gradient ratio and Ruggedness Index of Upper Tuirial watershed.

Watershed	Elevation at source 'a' in m	Elevation at Mouth 'b' in m	Fall in height (a-b) in km	Length of main stream 'L' in km	Gradient ratio (a-b/L)	Ruggedness Index
Tuirial	1600	76	1.52	60.89	0.03	5.81
Kailian	600	77	0.52	5.88	0.09	1.46
Nghathup	800	120	0.68	5.67	0.12	1.82
Sakei	640	120	0.52	5.69	0.09	2.59
Sherbawk	600	120	0.48	3.58	0.13	2.07
Suibual	940	145	0.80	8.42	0.09	2.67
Ngharum	700	145	0.56	7.94	0.07	2.66
Zilpui	1040	160	0.88	14.64	0.06	3.98
Belkhui	720	170	0.55	6.29	0.09	3.54
Nghalrawh	620	170	0.45	4.37	0.10	2.66
Tuiphu	1200	260	0.94	9.11	0.10	4.36
Tuirial	1104	270	0.83	10.53	0.08	3.49
Tulrital	1600	270	1.33	12.12	0.11	6.22
Tuizual	1126	210	0.92	19.57	0.05	4.72
Darkhuang	700	170	0.53	3.26	0.16	3.13
Suanghuan	900	170	0.73	9.50	0.08	3.23
Chite	1100	150	0.95	16.93	0.06	3.62
Muthi	1320	120	1.20	11.12	0.11	4.13
SW 18	940	100	0.84	4.62	0.18	3.76
Tuipawl	1120	100	1.02	11.32	0.09	3.58

3.6.7 Ruggedness Index (Rn)

The Ruggedness Index (Rn) also popularly known as Ruggedness Number is the product of basin relief (H) and drainage density (Dd). This Index is also used in identifying the characteristics of land surfaces. It is the property of roughness of the land surface. The basin having low ruggedness values infers less prone to erosion and the high ruggedness value implies highly susceptible to erosion (Sujatha, et al., 2013). For the macro level

analysis of ruggedness index of Upper Tuirial watershed, the area has been divided into 1 Km² grids and the values of each grid are thus plotted at the center of each grid. Then isopleths lines are drawn for depicting the zonal variation of ruggedness in the area. The values are then grouped into five broad categories as shown in Table 3.14. The ruggedness index of the study area ranges from 0.09 to 4.23. From the spatial distribution map (Fig. 3.13) of Rn values, it is observed that the maximum values are concentrated at the central portion and the southern tip of the basin. The lowest value (<2) covers mainly the northern part and the western extremity of the basin.

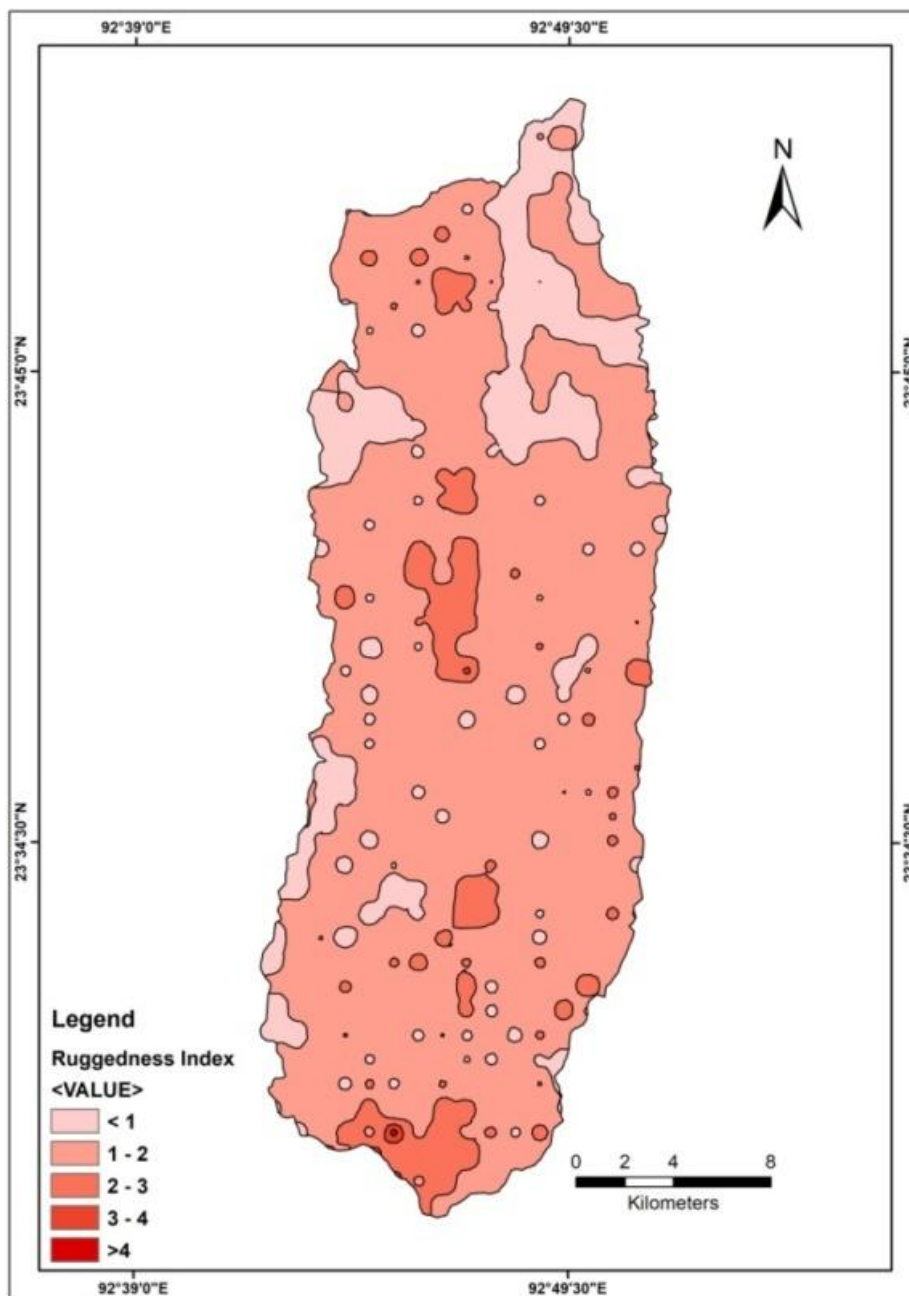


Figure 3.13 Spatial distribution of Ruggedness index of Upper Tuirial Watershed.

Pandey and Das (2016) reported homogenous lithology, gentle regional slope and lack of structural control were responsible for low values of Rn in the Chhotanagpur plateau. Samal, et al., (2015) reported high Rn values indicates structural complexity of a terrain and highly susceptible to erosion in the Western Ghats. Ruggedness number of upper Tuirial watershed is 5.81 and such high value is expected generally in mountainous region of tropical climate with higher rainfall (Schumm, 1956) and also indicating susceptible to high erosion. All the sub-basins Rn value ranges from 1.46 for Kailian to 6.22 for Tulrital, as shown in Table 3.13. Ruggedness index is calculated by the following formula:

$$\text{Ruggedness Index} = \text{Relative Relief} \times \text{Drainage Density}$$

Table 3.14 Classification of Ruggedness Index and its statistics.

Classes	Frequency of Classes (meters)	Area in (km ²)	Area (%)
Low	< 1	80.74	15.19
Moderate	1-2	410.11	77.18
Moderate high	2-3	39.92	7.51
High	3-4	0.57	0.11
Very high	> 4	0.05	0.01

3.6.8 Slope analysis

Slope analysis is an important parameter in geomorphic studies. Depending upon the resistivity of underlying rocks and orientation of bedding planes, slope angle also vary from place to place. A better understanding of slope distribution is essential, as a slope map provides data for planning, settlements, mechanization of agriculture, afforestation, deforestation, planning of engineering structures, conservation practices, etc. (Sreedevi, 2009). Though various methods are used to carry-out the slope analysis, Wentworth's (1930) average slope method was employed in this study using topographic maps on a scale of 1:50,000 (Fig. 3.14). The area has been divided into grids of 1 km by 1 km and the average slope values are computed for each grid unit and plotted them in the centers of each grid. Using IDW interpolation method in GIS environment the average slope of the whole area is prepared and further classified into five classes to show a clear picture of the distribution of slope within the watershed. The upper Tuirial watershed area slope varies from 12.84° to

33.41°. A high degree of slope is noticed in the Northwestern and southeastern parts of the basin. The formula adopted by Wentworth for computing the average slope is as follow

$$\text{Tan } Q = (\text{ACC} \times \text{C.I.})/636.6$$

Where Q= The angle of slope in degrees.; ACC= Average contour crossing per sq.km.; C.I.= Contour Interval, which is 20 m in this case and 636.6= Constant value.

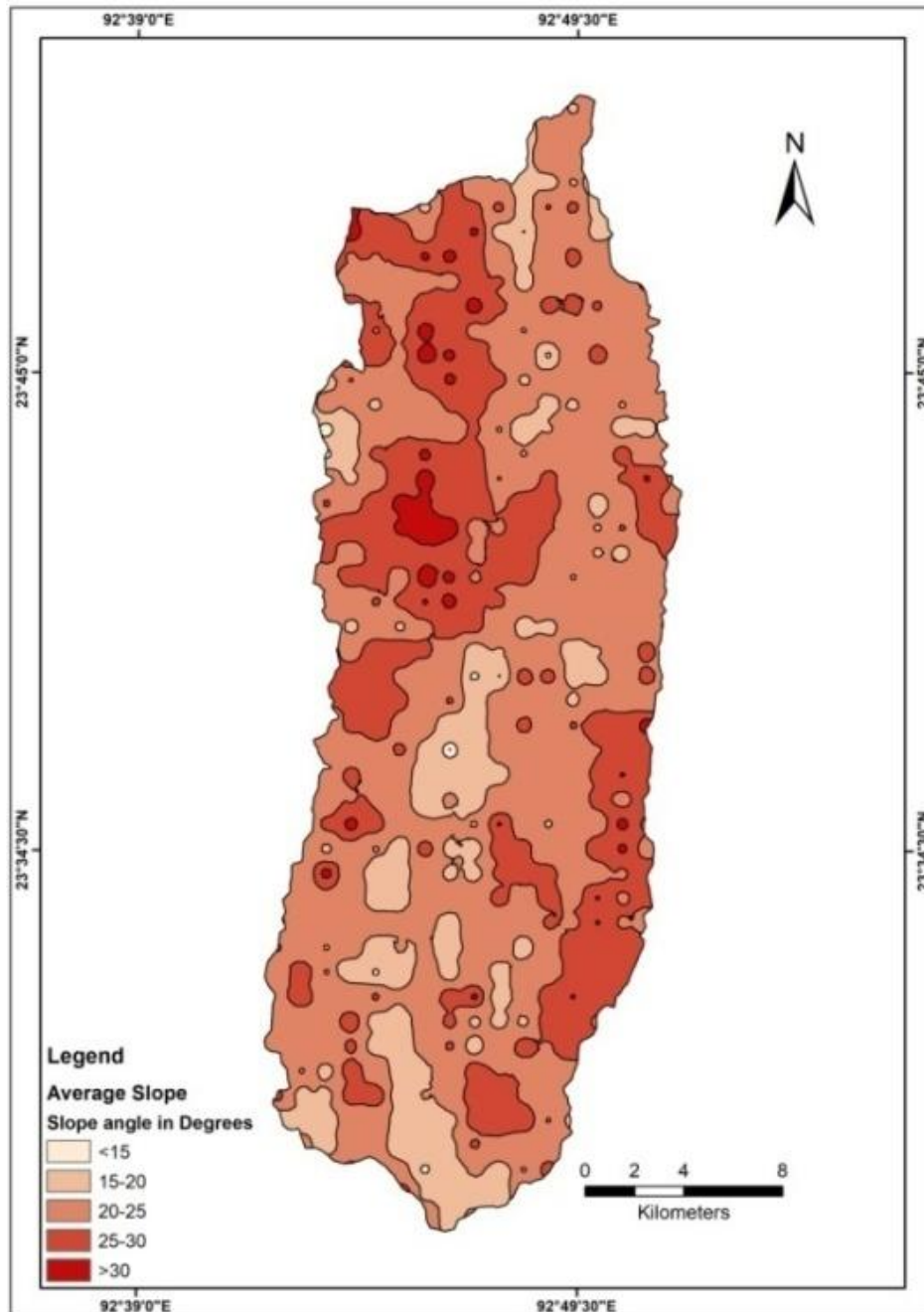


Figure 3.14 Spatial distribution of average slope of Upper Tuirial Watershed.

3.6.9 Hypsometric Analysis of erosional topography

Hypsometric analysis or the relationship of horizontal cross-sectional drainage basin area to elevation (Area altitude analysis) was developed by Langbein, et al., 1947, where he applied this method to determine how the land mass is distributed within a basin from confluence to origin. Initially the analysis was carried out for large watersheds and later on this technique was also used for small drainage basins of low order to estimate the proportion of landmass available within the basin (Strahler, 1952; Miller, 1953; Schumm, 1956; Coates, 1956; and Pike and Wilson, 1971). These values help to find out the erosional state or geomorphic stage of a basin and also show the area-height relationship, which is quite significant in geomorphic analysis

3.6.10 Percentage Hypsometric Curves

The percentage hypsometric curve is a plot of the continuous function $[y=f(x)]$ corresponding to relative height 'y' to relative area 'x' with respect to the total height and total area of a drainage basin. This curve is essentially a graph that shows the proportion of land area that exists at various elevations by plotting relative area against relative height. The relative height is the ratio of height of a given contour 'h' to total basin height H. Relative area is the ratio of horizontal cross-sectional area 'a' to the entire basin area A (Figure 3.15). Three curves shown on the right hand side figure implies the stages of geologic development within the basin. If the curve is convex outward the stage of development is young or in-equilibrium stage and convex inward indicates old or monadnock phase. The middle curve shows "S" shape with upper concavity and lower convexity indicating mature or equilibrium stage of geologic development.

3.6.11 Plotting of percentage hypsometric curves

The two variables used for drawing the hypsometric curves are:

- i) Relative area or a/A ('a' is the area enclosed between the contour and the upper perimeter and 'A' is the total basin area) represented along the abscissa, and
- ii) Relative height or h/H ('h' is the height of the contour above the base and 'H' is the total basin height) plotted along ordinate.

The curve must always originate in the upper left-hand corner of the square ($x = 0, y = 1$) and reach the lower right hand corner ($x = 1, y = 0$). It may, however, take any one of a

variety of paths between these points, depending upon the distribution of the landmass from base to top.

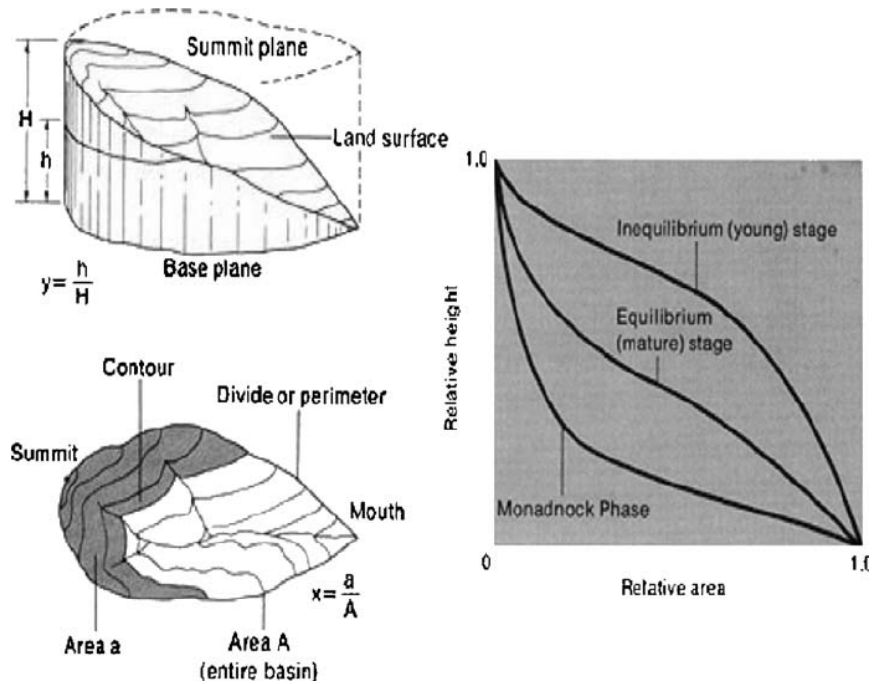


Figure 3.15 Schematic representation of Hypsometric analysis (Strahler 1954).

3.6.12 Methods of obtaining Hypsometric data

The hypsometric analysis was carried out using ALOS PALSAR Digital Elevation Model (DEM) of 12.5 meters spatial resolution. The methodology involves generation of contour lines of 100 meter interval for all the sub watersheds. The measure of the total area of each basin in GIS platform, then measure the area between each contour interval. Tabulate these values in one column representing the partial area above the bottom of the lower interval i.e., the areas enclosed between each contour and the upper perimeter. The relative area thus obtained as a ratio of the area above a particular contour to the total area of the watershed and the value ranges from 1.0 to 0.0. Similarly, the relative elevation is calculated as the ratio of the height of a given contour (h) from the base plane to the maximum basin elevation (H) whose value ranges from 0.0 to 1.0 as shown in Table 3.15. Thus hypsometric curve is obtained by plotting the relative area (a/A) along the abscissa and relative elevation (h/H) along the ordinate (Figure 3.15). This provided a measure of the distribution of landmass volume remaining beneath or above a basal reference plane.

Table 3.15 Methods of calculating Hypsometric curves.

Basin Name	Contour Interval in meters	Area within Interval in sq.km.	Area above the bottom of lower interval (a)	Relative Area (a/A)	Lower Interval - Elevation at the mouth of the river (h)	Relative Height (h/H)
Upper Tuirial	81-181	20.32	535.24	1.00	0.00	0.00
	181-281	56.50	514.92	0.96	100.00	0.07
	281-381	73.32	458.42	0.86	200.00	0.14
	381-481	80.37	385.09	0.72	300.00	0.20
	481-581	75.68	304.73	0.57	400.00	0.27
	581-681	64.25	229.05	0.43	500.00	0.34
	681-781	58.04	164.79	0.31	600.00	0.41
	781-881	44.01	106.75	0.20	700.00	0.47
	881-981	27.83	62.74	0.12	800.00	0.54
	981-1081	17.33	34.91	0.07	900.00	0.61
	1081-1181	8.65	17.58	0.03	1000.00	0.68
	1181-1281	4.86	8.92	0.02	1100.00	0.74
	1281-1381	2.66	4.06	0.01	1200.00	0.81
	1381-1481	1.27	1.41	0.00	1300.00	0.88
	1481-1558	0.14	0.14	0.00	1400.00	0.95
	>1558	-	0.00	0.00	1477.00	1.00
Kailian	110-210	0.29	5.45	1.00	0.00	0.00
	210-310	0.70	5.17	0.95	100.00	0.20
	310-410	0.91	4.47	0.82	200.00	0.40
	410-510	2.13	3.56	0.65	300.00	0.61
	510-604	1.43	1.43	0.26	400.00	0.81
	>604	-	0.00	0.00	494.00	1.00
	114-214	0.25	9.16	1.00	0.00	0.00
	214-314	1.61	8.91	0.97	100.00	0.14
	314-414	2.59	7.30	0.80	200.00	0.27

Nghathup	414-514	2.36	4.70	0.51	300.00	0.41
	514-614	1.42	2.34	0.26	400.00	0.54
	614-714	0.63	0.92	0.10	500.00	0.68
	714-814	0.27	0.28	0.03	600.00	0.81
	814-852	0.01	0.01	0.00	700.00	0.95
	>852	-	0.00	0.00	738.00	1.00
Sakei	115-215	0.74	11.56	1.00	0.00	0.00
	215-315	2.10	10.83	0.94	100.00	0.13
	315-415	2.78	8.72	0.75	200.00	0.26
	415-515	2.18	5.94	0.51	300.00	0.39
	515-615	1.85	3.76	0.33	400.00	0.51
	615-715	1.08	1.91	0.17	500.00	0.64
	715-815	0.74	0.83	0.07	600.00	0.77
	815-894	0.10	0.10	0.01	700.00	0.90
	>894	-	0.00	0.00	779.00	1.00
Sherbawk	135-235	0.16	3.41	1.00	0.00	0.00
	235-335	1.01	3.25	0.95	100.00	0.19
	335-435	1.48	2.24	0.66	200.00	0.38
	435-535	0.49	0.76	0.22	300.00	0.57
	535-635	0.26	0.27	0.08	400.00	0.77
	635-657	0.01	0.01	0.00	500.00	0.96
	>657	-	0.00	0.00	522.00	1.00
Suibual	124-224	1.21	24.24	1.00	0.00	0.00
	224-324	3.91	23.03	0.95	100.00	0.13
	324-424	5.68	19.12	0.79	200.00	0.25
	424-524	5.00	13.43	0.55	300.00	0.38
	524-624	3.85	8.43	0.35	400.00	0.50
	624-724	2.49	4.57	0.19	500.00	0.63
	724-824	1.57	2.08	0.09	600.00	0.75
	824-924	0.51	0.51	0.02	700.00	0.88
	>924	-	0.00	0.00	800.00	1.00
Ngharum	126-216	0.61	11.00	1.00	0.00	0.00

	216-316	1.12	10.39	0.94	100.00	0.17
	316-416	3.30	9.27	0.84	200.00	0.33
	416-516	3.46	5.97	0.54	300.00	0.50
	516-616	2.22	2.51	0.23	400.00	0.66
	616-716	0.28	0.29	0.03	500.00	0.83
	716-731	0.01	0.01	0.00	600.00	0.99
	>713	-	0.00	0.00	605.00	1.00
Zilpui	142-242	4.53	56.35	1.00	0.00	0.00
	242-342	9.67	51.82	0.92	100.00	0.09
	342-442	9.38	42.15	0.75	200.00	0.18
	442-542	9.11	32.77	0.58	300.00	0.28
	542-642	7.79	23.66	0.42	400.00	0.37
	642-742	5.73	15.87	0.28	500.00	0.46
	742-842	4.09	10.14	0.18	600.00	0.55
	842-942	3.11	6.05	0.11	700.00	0.65
	942-1042	1.83	2.94	0.05	800.00	0.74
	1042-1142	0.84	1.12	0.02	900.00	0.83
	1142-1224	0.27	0.27	0.00	1000.00	0.92
	>1224	-	0.00	0.00	1082.00	1.00
Belkhui	162-262	0.74	8.82	1.00	0.00	0.00
	262-362	2.10	8.08	0.92	100.00	0.19
	362-462	2.85	5.99	0.68	200.00	0.38
	462-562	2.15	3.14	0.36	300.00	0.57
	562-662	0.98	0.99	0.11	400.00	0.76
	662-686	0.01	0.01	0.00	500.00	0.95
	>686	-	0.00	0.00	524.00	1.00
Nghalrawh	162-262	0.83	5.57	1.00	0.00	0.00
	262-362	1.95	4.74	0.85	100.00	0.23
	362-462	1.94	2.79	0.50	200.00	0.46
	462-562	0.83	0.85	0.15	300.00	0.69
	562-596	0.03	0.03	0.00	400.00	0.92
	>596	-	0.00	0.00	434.00	1.00

Tuiphu	215-315	2.03	23.25	1.00	0.00	0.00
	315-415	3.52	21.21	0.91	100.00	0.09
	415-515	3.78	17.70	0.76	200.00	0.18
	515-615	3.17	13.92	0.60	300.00	0.26
	615-715	2.69	10.75	0.46	400.00	0.35
	715-815	2.53	8.06	0.35	500.00	0.44
	815-915	2.20	5.54	0.24	600.00	0.53
	915-1015	1.51	3.34	0.14	700.00	0.61
	1015-1115	1.01	1.83	0.08	800.00	0.70
	1115-1215	0.56	0.82	0.04	900.00	0.79
	1215-1315	0.24	0.26	0.01	1000.00	0.88
	1315-1355	0.02	0.02	0.00	1100.00	0.96
	>1355	-	0.00	0.00	1140.00	1.00
Tuirial	216-316	1.59	29.42	1.00	0.00	0.00
	316-416	3.36	27.82	0.95	100.00	0.09
	416-516	3.81	24.47	0.83	200.00	0.18
	516-616	3.45	20.65	0.70	300.00	0.26
	616-716	3.57	17.20	0.58	400.00	0.35
	716-716	3.03	13.63	0.46	500.00	0.44
	816-916	3.47	10.60	0.36	600.00	0.53
	916-1016	3.77	7.13	0.24	700.00	0.62
	1016-1116	2.05	3.36	0.11	800.00	0.71
	1116-1216	0.97	1.31	0.04	900.00	0.79
	1216-1316	0.32	0.33	0.01	1000.00	0.88
	1316-1350	0.02	0.02	0.00	1100.00	0.97
	>1350	-	0.00	0.00	1134.00	1.00
Tulrital	215-315	0.92	30.54	1.00	0.00	0.00
	315-415	1.60	29.62	0.97	100.00	0.07
	415-515	2.30	28.02	0.92	200.00	0.15
	515-615	3.23	25.72	0.84	300.00	0.22
	615-715	3.35	22.49	0.74	400.00	0.30
	715-815	3.10	19.14	0.63	500.00	0.37

	815-915	2.89	16.04	0.53	600.00	0.45
	915-1015	2.67	13.15	0.43	700.00	0.52
	1015-1115	2.57	10.49	0.34	800.00	0.60
	1115-1215	2.59	7.92	0.26	900.00	0.67
	1215-1315	2.52	5.32	0.17	1000.00	0.74
	1315-1415	2.08	2.80	0.09	1100.00	0.82
	1415-1515	0.67	0.72	0.02	1200.00	0.89
	1515-1558	0.05	0.05	0.00	1300.00	0.97
	>1558	-	0.00	0.00	1343.00	1.00
Tuizual	193-293	2.91	88.70	1.00	0.00	0.00
	293-393	6.43	85.79	0.97	100.00	0.08
	393-493	8.87	79.36	0.89	200.00	0.16
	493-593	13.22	70.50	0.79	300.00	0.24
	593-693	17.24	57.27	0.65	400.00	0.32
	693-793	17.33	40.03	0.45	500.00	0.40
	793-793	12.94	22.70	0.26	600.00	0.48
	893-893	5.47	9.76	0.11	700.00	0.56
	993-1093	2.96	4.29	0.05	800.00	0.64
	1093-1193	0.83	1.33	0.01	900.00	0.71
	1193-1293	0.34	0.50	0.01	1000.00	0.79
	1293-1393	0.13	0.16	0.00	1100.00	0.87
	1393-1452	0.02	0.02	0.00	1200.00	0.95
	>1452	-	0.00	0.00	1259.00	1.00
Darkhuang	142-242	0.93	3.99	1.00	0.00	0.00
	242-342	1.19	3.06	0.77	100.00	0.17
	342-442	0.82	1.87	0.47	200.00	0.34
	442-542	0.46	1.04	0.26	300.00	0.51
	542-642	0.36	0.58	0.15	400.00	0.68
	642-728	0.22	0.22	0.05	500.00	0.85
	>728	-	0.00	0.00	586.00	1.00
Suanghuan	142-242	1.08	21.60	1.00	0.00	0.00
	242-342	2.32	20.52	0.95	100.00	0.13

	342-442	3.96	18.19	0.84	200.00	0.26
	442-542	4.83	14.23	0.66	300.00	0.39
	542-642	4.57	9.39	0.43	400.00	0.51
	642-742	3.38	4.82	0.22	500.00	0.64
	742-842	1.29	1.44	0.07	600.00	0.77
	842-920	0.14	0.14	0.01	700.00	0.90
	>920	-	0.00	0.00	778.00	1.00
Chite	142-242	1.01	51.98	1.00	0.00	0.00
	242-342	3.58	50.96	0.98	100.00	0.09
	342-442	6.08	47.38	0.91	200.00	0.19
	442-542	8.58	41.30	0.79	300.00	0.28
	542-642	8.20	32.72	0.63	400.00	0.38
	642-742	8.83	24.52	0.47	500.00	0.47
	742-842	7.76	15.70	0.30	600.00	0.57
	842-942	4.60	7.94	0.15	700.00	0.66
	942-1042	2.65	3.33	0.06	800.00	0.76
	1042-1142	0.66	0.68	0.01	900.00	0.85
	1142-1199	0.02	0.02	0.00	1000.00	0.95
	>1199	-	0.00	0.00	1057.00	1.00
Muthi	114-214	2.80	28.99	1.00	0.00	0.00
	214-314	3.96	26.19	0.90	100.00	0.08
	314-414	2.69	22.22	0.77	200.00	0.16
	414-514	3.12	19.53	0.67	300.00	0.25
	514-614	3.39	16.41	0.57	400.00	0.33
	614-714	3.48	13.01	0.45	500.00	0.41
	714-814	3.49	9.54	0.33	600.00	0.49
	814-914	2.95	6.05	0.21	700.00	0.57
	914-1014	1.65	3.09	0.11	800.00	0.65
	1014-1114	0.82	1.44	0.05	900.00	0.74
	1114-1214	0.48	0.62	0.02	1000.00	0.82
	1214-1314	0.13	0.14	0.00	1100.00	0.90
	1314-1336	0.01	0.01	0.00	1200.00	0.98

	>1336	-	0.00	0.00	1222.00	1.00
SW18	104-204	0.87	6.22	1.00	0.00	0.00
	204-304	1.18	5.35	0.86	100.00	0.10
	304-404	0.96	4.18	0.67	200.00	0.21
	404-504	0.92	3.22	0.52	300.00	0.31
	504-604	0.61	2.30	0.37	400.00	0.41
	604-704	0.50	1.69	0.27	500.00	0.52
	704-804	0.45	1.19	0.19	600.00	0.62
	804-904	0.36	0.74	0.12	700.00	0.73
	904-1004	0.32	0.39	0.06	800.00	0.83
	1004-1068	0.07	0.07	0.01	900.00	0.93
	>1068	-	0.00	0.00	964.00	1.00
Tuipawl	104-204	1.79	26.27	1.00	0.00	0.00
	204-304	1.64	24.48	0.93	100.00	0.08
	304-404	1.68	22.85	0.87	200.00	0.16
	404-504	2.37	21.16	0.81	300.00	0.24
	504-604	2.48	18.79	0.72	400.00	0.33
	604-704	2.64	16.31	0.62	500.00	0.41
	704-804	2.99	13.68	0.52	600.00	0.49
	804-904	3.16	10.68	0.41	700.00	0.57
	904-1004	2.65	7.52	0.29	800.00	0.65
	1004-1104	2.28	4.87	0.19	900.00	0.73
	1104-1204	1.61	2.59	0.10	1000.00	0.81
	1204-1304	0.98	0.98	0.04	1100.00	0.90
	1304-1333	0.00	0.00	0.00	1200.00	0.98
	>1333	-	0.00	0.00	1229	1.00

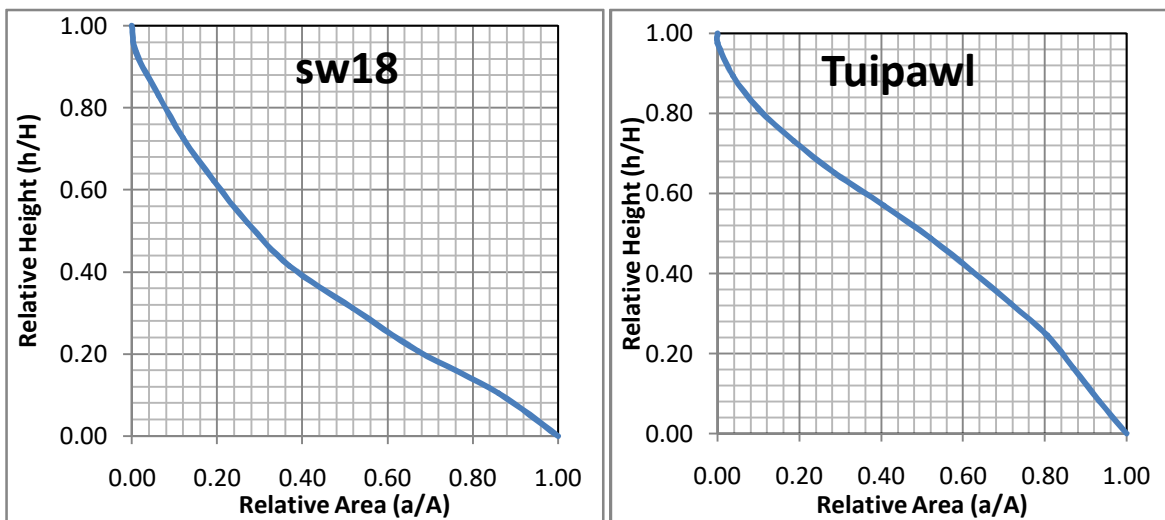
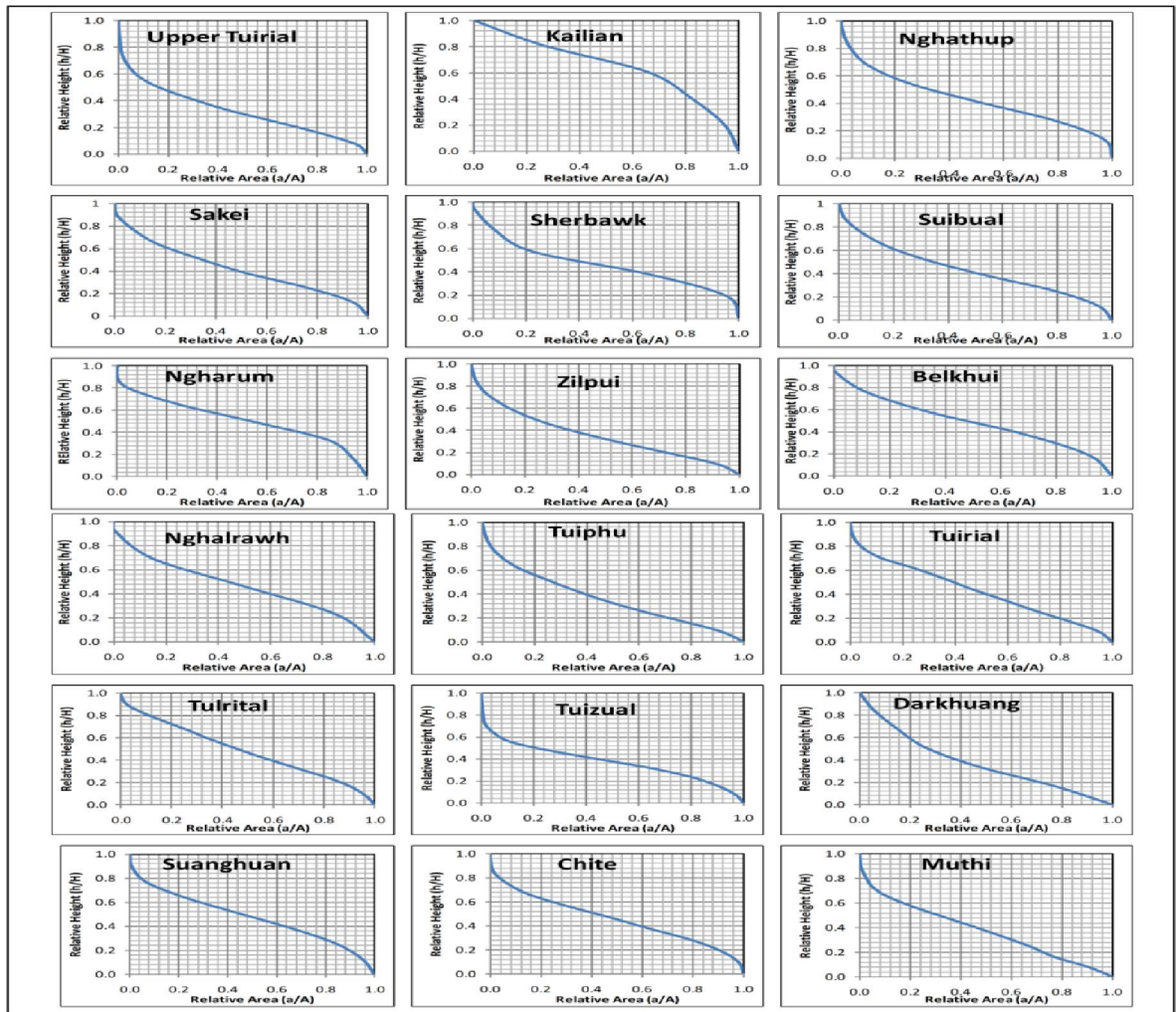


Figure 3.16 Hypsometric curves of Upper Tuirial watershed and its sub watersheds.

The Hypsometric curve of the upper Tuirial watershed matches with the hypothetical curve of equilibrium stage given by Strahler (1952) in figure 3.16. This suggests that the

watershed is undergoing steady state of geomorphic development. The hypsometric curves of the various sub watersheds shows the shape almost similar with hypothetical curve of mature stage except sub watershed Kailian, which is the modified hypsometric curve probably resulting from the presence of a massive resistance formation above a weaker rock that resulted the drainage basins steep inner slopes but very gentle slopes on the extensive divides which is expected in horizontal sedimentary strata due to differences in rate of rock weathering at low and high altitudes.

The mature stage of development of the topography is achieved by long-continued fluvial erosion over the land surface that has removed all traces of flat inter-stream uplands and it is assumed that the basins are stable in form and that the total regimen of erosion and transportation processes is in a steady state.

3.6.13 Hypsometric Integral

Integration of the hypsometric curve is called the hypsometric integral. The hypsometric integral is defined as the area below the hypsometric curve ($x=f(y)$) that has not been eroded and; therefore, it can be calculated by the exact integration of $f(y)$ between the limits of the unit square (Strahler, 1952).

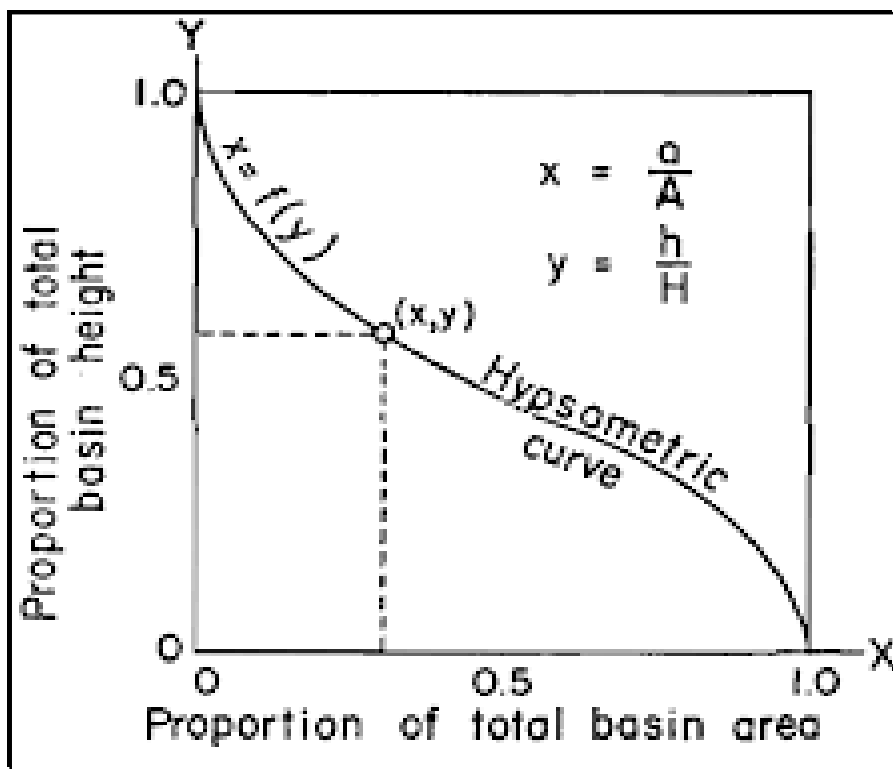


Figure 3.17 Construction of Hypsometric curve preparation for basin area vs. height.

Similar study was also carried out by Pike and Wilson in 1971, where they proposed a simpler formula to calculate the hypsometric integral of a watershed. It is defined as:

$$HI = (EL_{\text{mean}} - EL_{\text{min}}) / (EL_{\text{max}} - EL_{\text{min}})$$

Where, EL_{mean} is the mean elevation, EL_{min} the minimum and EL_{max} the maximum elevation within the drainage basin as extracted from a DEM.

Hypsometric integral has three threshold values, each representing the distinctive stages of the geomorphic cycle (Strahler, 1952). These are

1. Inequilibrium or young stage ($HI \geq 0.60$)
2. Equilibrium or mature stage ($0.35 \leq HI \leq 0.60$)
3. Monadnock or old stage ($HI \leq 0.35$)

Figure 3.16 shows hypsometric curves plotted for each basin in the sequence. Using these hypsometric curves, it is possible to read the percentage of total basin area above any percentage of total height. Area under the hypsometric curve is the hypsometric integral, expressed as percentage. An integral value of upper Tuirial watershed is 0.51 which can be interpreted as 49 percent of rock masses is eroded and 51 percent of rock masses still exist in the basin between reference planes passing through summit and base. The hypsometric integral value is high in the youthful stage; it decreases as the landscape is denuded towards a stage of maturity and old stage (Strahler, 1952). The hypsometric integral of the 19 sub-Watersheds ranges from 0.5 to 0.55 as shown in Table 3.16, thus indicating that all the drainage basins have attained the steady state condition.

Table 3.16 Computation of Hypsometric Integral for Tuirial basin.

Name of watershed	Maximum Elevation	Minimum elevation	Mean elevation	Hypsometric Integral	Percent of landmass available	Geologic stage
Upper Tuirial	1558	81	830	0.51	51 %	Mature
Kailian	604	110	359	0.504	50 %	Mature
Nghathup	852	114	507.11	0.530	53 %	Mature
Sakei	894	115	513	0.511	51 %	Mature
Sherbawk	657	135	424	0.554	55 %	Mature

Suibual	924	124	524	0.500	50 %	Mature
Ngharum	731	126	457	0.547	55 %	Mature
Zilpui	1224	142	691	0.507	51 %	Mature
Belkhui	686	162	451	0.552	55 %	Mature
Nghalrawh	596	162	401	0.551	55 %	Mature
Tuiphu	1335	215	810.38	0.520	52 %	Mature
Tuirial	1350	216	811	0.525	52 %	Mature
Tulrital	1558	215	911	0.518	52 %	Mature
Tuizual	1452	193	840	0.514	51 %	Mature
Darkhuang	728	142	440	0.509	51 %	Mature
Suanghuan	920	142	540	0.512	51 %	Mature
Chite	1199	142	688	0.517	52 %	Mature
Muthi	1336	114	758	0.527	53 %	Mature
SW18	1068	104	601	0.516	52 %	Mature
Tuipawl	1333	104	748.93	0.520	52 %	Mature

Hypsometric analysis is an important parameter for morphometric studies because it is a dimensionless parameter and therefore allows different sub watershed to be compared irrespective of scale. Based on the integral values, different sub watershed can be prioritize for conservation and management aspects of natural resources. The low integral values represent old eroded landscapes in the late stages of geomorphic evolution, while high values indicate young, less eroded landscapes where the surface denudational processes is strong and much of the volume of rock in the basin is still to be removed. Study of integrated watershed management planning involves suitable soil and water conservation measures and enhancing biomass production in the catchment for sustainable management of natural resources. Hypsometry analysis or assessment of erosional status and geologic stage of development is the first criteria for selection of sites to carry out the management activity.

Secondly the hypsometric analysis is also useful to calculate the sediment load derived from a small drainage basin in relation to slope (Strahler, 1953). Because the hypsometric curve combines the value of slope and surface area at any elevation of the basin, it might help to obtain more precise calculations to locate the expected source of maximum sediment derived from surface runoff in a typical basin of a given order of magnitude. Thus, it

is expected that sub watershed Tuiphu, Tuirial, Tulrital, Muthi, SW 18 and Tuipawl will produce a maximum sediment load along with the surface runoff because the hypsometric curves are very steep in those sub watershed as compare to the remaining sub watersheds.

3.6.14 Inter-correlation among geomorphic parameters

After understanding the dimensional characteristics of different sub basins through detail analyses of the linear, relief and aerial aspects of the Upper Tuirial watershed, it is found that some important parameters such as Drainage density, Stream frequency, Texture Ratio, Relative relief, Dissection Index, Gradient Ratio, Relief ratio, Ruggedness Index and Weighted Bifurcation ratio are directly proportional to land and water degradation factors whereas Constant of Channel maintenance, Length of overland flow, Form factor, Circulatory ratio, Elongation ratio and Hypsometric Integral are inversely proportional to land and water degradational factors. To understand the existing interrelationship among these morphometric parameters Correlation matrix was carried out using SPSS software. Meshram and Sharma (2015) have described that when correlation coefficient value >0.9 , the parameter is strongly correlated, when correlation coefficient value >0.75 , the parameter has good correlation, when correlation coefficient value >0.6 , the parameter is moderately correlated, and when correlation coefficient value is 0.6 to <0.6 , the parameter has poor correlation.

Based on Pearson's coefficient correlation matrix information, 11 most important morphometric parameters were taken into consideration in sub-watershed prioritization. These parameters are **Dd**– Drainage density, **Sf**- Stream frequency, **T**–Texture Ratio, **C**- Constant of Channel maintenance, **Lg** – Length of overland flow, **Re**- Elongation ratio, **H**- Maximum basin relief, **Rh**- Relief ratio, **Rg**-Gradient Ratio, **Rb**– Weighted Bifurcation ratio and **ρ** - Rho coefficient.

Table 3.17 Pearson's Correlation Matrix

Parameters	Dd	Sf	T	C	Lg	Ff	Rc	Re	H	DI	Rh	Rg	Rn	HI	Slope	Rb	Rho
Dd	1																
Sf	.933**	1															
T	.089	.078	1														
C	-.969**	-.887**	-.173	1													
Lg	-.973**	-.902**	-.194	.994**	1												
Ff	-.036	-.020	.084	-.065	-.087	1											
Rc	.370	.264	-.146	-.398	-.372	.588**	1										
Re	-.027	-.011	.068	-.079	-.099	.995**	.568**	1									
H	-.194	-.332	.658**	.109	.108	.151	-.051	.154	1								
DI	-.693**	-.732**	.101	.664**	.656**	.064	-.263	.054	.518*	1							
Rh	.130	.087	-.547*	-.115	-.100	.157	.377	.179	-.085	.044	1						
Rg	.252	.145	-.621**	-.185	-.154	-.004	.502*	.004	-.254	-.069	.871**	1					
Rn	.347	.172	.679**	-.412	-.410	.044	.088	.051	.835**	.101	-.032	-.104	1				
HI	.331	.477*	-.274	-.320	-.315	-.029	.069	.004	-.283	-.386	.190	.113	-.119	1			
Slope	-.455	-.334	.161	.355	.335	.359	-.110	.385	.356	.353	-.021	-.330	.037	.192	1		
Rb	-.308	-.198	.318	.312	.241	.135	-.373	.096	.274	.494*	-.295	-.497*	.069	-.216	.438	1	
Rho	-.138	-.093	-.600**	.224	.247	-.550**	-.309	-.541**	-.631**	-.096	-.154	.036	-.665**	.231	-.272	-.247	1

** . Correlation is significant at the 0.01 level (2-tailed).

* . Correlation is significant at the 0.05 level (2-tailed).

Dd– Drainage density, **Sf**- Stream frequency, **T**–Texture Ratio, **C**-Constant of Channel maintenance, **Lg** – Length of overland flow, **Ff**-Form factor, **Rc**- Circulatory ratio, **Re**- Elongation ratio, **H**-Maximum basin relief, **Di**-Dissection Index, **Rh**- Relief ratio, **Rg**-Gradient Ratio, **Rn**- Ruggedness Index, **HI**- Hypsometric Integral, **Rb**– Weighted Bifurcation ratio., **Rho**- Rho coefficient.

3.6.15 Watershed prioritization for soil and water conservation measures

The analyses of morphometric parameters are significant in prioritizing and identifying the zones of high soil erosion activity (Yadav, et al., 2016; Gopinath, et al., 2016; Arefin, et al., 2020; Choudhari, et al., 2018, Gajbhiye, et al., 2014). Soil erosion and water conservation measure for a large area is difficult. Therefore, large area is divided into sub-watershed using drainage network (Meshram and Sharma, 2015). For the prioritization of 19 sub watersheds of the Upper Tuirial watershed, important morphometric parameters used such as Drainage density, Stream frequency, Texture Ratio, Relative relief, Dissection Index, Gradient Ratio, Relief ratio, Ruggedness Index and Weighted Bifurcation ratio which are directly proportional to high erosion whereas, Constant of Channel maintenance, Length of overland flow, Form factor, Circulatory ratio, Elongation ratio and Hypsometric Integrals are inversely proportional to soil and water degradation.

Compound factor (CF) model as one of the MCDM techniques was applied for the prioritisation of watersheds (Farhan, et al., 2016; Nitheshnirmal, et al., 2019, 2020). The CF is computed using the formula given by Biswas, et al., 1999.

$$CF = \frac{1}{a} \sum_{i=1}^a R_i$$

Where ‘a’ and **R** denote the number of attributes and the ranking, respectively. Accordingly, rating is given to the parameters which are directly proportional to soil and water degradation by assigning highest priority, i.e., 19 for the sub watersheds having maximum value of the parameter, and least priority ranking i.e. 1 is given to the sub watershed having minimum value of impact. Similarly, ranking is given to the parameters which have inverse relationship with the land and water degradation factors by assigning highest priority, i.e., 19 for the sub watershed having minimum value of the parameter, and least priority i.e. 1 is given to the sub watershed having maximum value of impact (Table 3.18). After ranking, the ranked values for each sub-watershed were averaged to find compound parameter (Cp). The Cp values ranges from 7.33 (Tuirial) to 14.13 (Tulrital). Final priority Rp that has been taken for sub watershed Tulrital is 1 (one) as highest rank which is the most susceptible zones of erosion, and for sub watershed Tuirial, Rp value has been taken 19 (nineteen) as a lowest rank which is least susceptible zone of erosion. Figure 3.18 shows the final priority map in terms of severity of erosion.

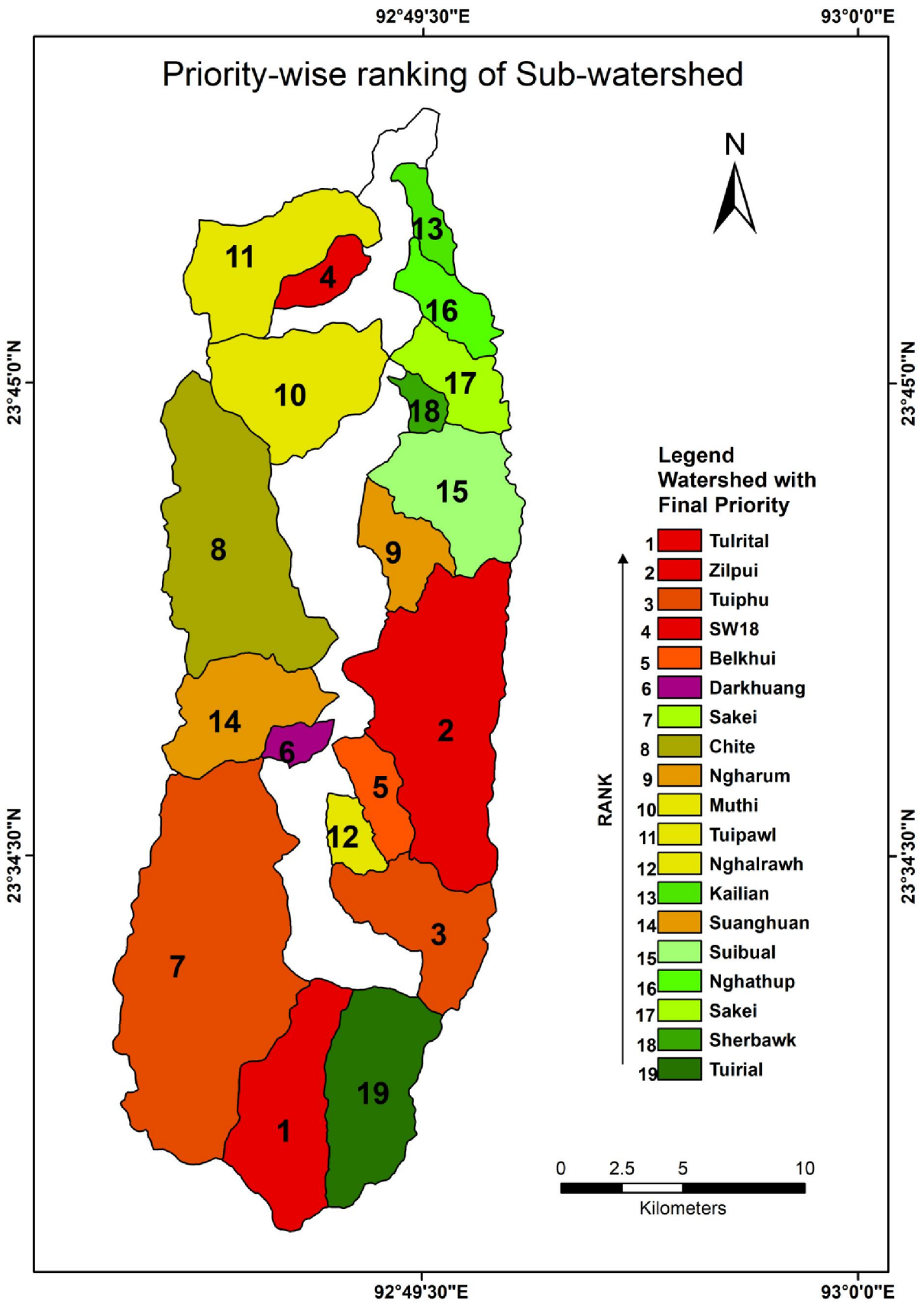


Figure 3.18 Prioritisation map for soil and water conservation practices.

Therefore, sub-watershed wise prioritisation result showed that sub-watershed Tulrital is highly susceptible to erosion followed by sub watersheds Zilpui, Tuiphu, WS18, Belkhui, Darkhuang, sakei, Chite, Ngharum, Muthi, Tuipawl, Nghalrawh, Kailian, Suanghuan, Suibual, Nghathup, Sakei, Sherbawk and the least erosive sub watershed is Tuirial. The proposed technique for identification of soil erosion prone zones is a viable approach for the planers and the decision makers to protect the natural resources for sustainable develoment of the region.

Table 3.18 Estimated compound parameter with priority ranking.

watershed	Dd	Sf	T	C	Lg	H	Di	Rh	Rb	Re	Ff	Rc	Rg	Rn	HI	Compound parameter (Cp)	Final Priority (Rp)
Kailian	2	1	2	2	2	2	14	8	17	20	19	19	11	1	18	9.2	13
Nghathup	1	3	6	1	1	6	11	12	6	19	18	14	16	2	5	8.07	16
Sakei	4	4	5	4	4	9	15	13	13	4	3	10	8	4	15	7.67	17
Sherbawk	10	12	1	11	10	3	4	17	1	9	8	7	17	3	1	7.60	18
Suibual	7	9	15	7	8	8	10	7	14	3	2	6	9	7	19	8.73	15
Ngharum	15	15	7	15	15	5	5	5	15	12	11	18	4	5	4	10.07	9
Zilpui	13	13	18	13	14	13	13	3	19	13	12	17	3	15	17	13.07	2
Belkhui	16	18	10	17	17	7	6	11	11	15	14	12	7	11	2	11.60	5
Nghalrawh	18	19	8	18	18	1	1	10	9	8	7	3	12	6	3	9.40	12
Tuiphu	12	14	14	12	13	15	7	18	12	6	5	16	13	17	9	12.20	3
Tuirial	8	7	11	8	7	11	3	4	5	10	9	4	6	10	7	7.33	19
Tulrital	17	16	17	16	16	19	9	9	4	18	17	11	14	19	10	14.13	1
Tuizual	9	11	19	9	11	18	12	1	8	14	13	9	1	18	13	11.07	7
Darkhuang	19	17	4	19	19	4	2	16	2	11	10	2	18	8	16	11.13	6
Suanghuan	14	10	12	14	12	10	8	6	3	5	4	8	5	9	14	8.93	14
Chite	5	5	16	5	5	14	16	2	10	17	16	15	2	13	11	10.13	8
Muthi	6	6	13	6	6	16	18	15	18	2	1	1	15	16	6	9.67	10
SW18	11	8	3	10	9	12	17	19	7	16	15	5	19	14	12	11.80	4
Tuipawl	3	2	9	3	3	17	19	14	16	7	6	13	10	12	8	9.47	11

(**Dd**– Drainage density, **Sf**- Stream Frequency, **T**–Texture Ratio, **C**-Constant of Channel maintenance, **Lg** – Length of overland flow, **Ff**- Form factor, **Rc**- Circulatory ratio, **Re**- Elongation ratio, **H**- Relative Relief, **Di**-Dissection Index, **Rh**- Relief ratio, **Rg**-Gradient Ratio, **Rn**-Ruggedness Index, **HI**- Hypsometric Integral, , **Rb**– Weighted Bifurcation ratio).

3.7 Prioritization of groundwater potential zones using Multi-Criteria Decision-Making (MCDM) techniques

3.7.1 Introduction

Conservation and management of natural resources cannot be taken simultaneously for an entire catchment due to several resource constraints (Panda, et al., 2005; Yadav, et al., 2018; Biswas, et al., 1999; Gajbhiye, et al., 2014). Watershed prioritization is, therefore, essential for identifying the most suitable or vulnerable sub watershed to carry out conservation measures (Vittala, et al., 2004; Kumar, et al., 2011). This study aims to identify the most suitable groundwater potential zones by prioritizing 19 sub watersheds of upper Tuirial basin based on morphometric parameters. Multi-Criteria Decision-Making (MCDM) techniques have been widely used to prioritise different sub watersheds by several researchers in the past (Meshram, et al., 2020; Rahaman, et al., 2015; Makhdumi and Dwarakish, 2019; Farhan, et al., 2018; Choudhari, et al., 2018; Meshram, et al., 2019; Vivien, et al., 2011; Asl-Rousta and Mousav, 2018; Patel, et al., 2012; Saaty, 1980; Jain and Ramsankaran, 2019; Singh, et al., 2019). MCDM is a generic term for all methods that exist for helping people makes decisions according to their preferences, in cases where there is more than one conflicting criterion (Mardani, et al., 2015). This study presents the application of TOPSIS (Technique of Order Preference Similarity to the Ideal Solution) based multi criteria decision making tool for prioritization of potential areas for groundwater resources. TOPSIS is a mathematical model which can be used to deal with complex problems by breaking the problems into smaller pieces.

3.7.2 Methodology

The methodology to calculate the various morphometric parameters such as linear, areal and relief aspects have already been discussed above. In this study, we carried out watershed prioritization starting with the calculated morphometric parameters of different sub-watersheds. For this analysis a total of 11 morphometric parameters were taken into consideration in our sub-watershed prioritization. These parameters are **Dd**– Drainage density, **Sf**- Stream frequency, **T**–Texture Ratio, **C**-Constant of Channel maintenance, **Lg** – Length of overland flow, **Re**- Elongation ratio, **H**-Maximum basin relief, **Rh**- Relief ratio, **Rg**-Gradient Ratio, **Rb**– Weighted Bifurcation ratio and **ρ**- Rho coefficient (Table 4.19)

Table 3.19 Calculated morphometric parameters and weightage values (in %) assigned for each parameter.

Weightage	0.1	0.1	0.1	0.1	0.1	0.1	0.1	0.1	0.05	0.05	0.1
watershed ↓	Dd	Sf	T	C	Lg	H	Rh	Rb	Re	ρ	Rg
Sherbawk	3.650	11.110	2.660	0.270	0.140	0.566	0.180	2.783	0.671	0.75	0.130
Kailian	2.630	7.300	2.690	0.380	0.190	0.554	0.120	5.337	0.516	0.81	0.090
sw18	3.690	9.660	3.730	0.270	0.140	1.020	0.230	4.230	0.622	0.61	0.180
Darkhuang	5.310	15.370	3.900	0.190	0.090	0.590	0.180	3.659	0.645	0.65	0.160
Sakei	3.080	8.860	3.990	0.320	0.160	0.840	0.150	4.865	0.703	0.65	0.090
Nghathup	2.530	8.250	4.040	0.400	0.200	0.720	0.150	4.162	0.587	0.67	0.120
Ngharum	4.080	12.230	4.940	0.250	0.120	0.652	0.110	4.999	0.643	0.71	0.070
Nghalrawh	4.840	16.380	5.100	0.210	0.100	0.550	0.140	4.673	0.673	0.68	0.100
Tuipawl	2.790	7.450	5.110	0.360	0.180	1.283	0.150	5.008	0.678	0.65	0.090
Belkhui	4.600	16.050	6.210	0.220	0.110	0.770	0.140	4.817	0.622	0.63	0.090
Tuirial	3.420	9.100	6.420	0.290	0.150	1.020	0.110	4.135	0.654	0.6	0.080
Suanghuan	3.840	10.560	6.470	0.260	0.130	0.840	0.110	3.831	0.691	0.64	0.080
Muthi	3.270	9.100	6.720	0.310	0.150	1.263	0.170	5.363	0.805	0.49	0.110
Tuiphu	3.730	11.570	7.280	0.270	0.130	1.168	0.200	4.863	0.689	0.48	0.100
Suibual	3.310	10.210	7.420	0.300	0.150	0.807	0.120	4.921	0.797	0.53	0.090
Chite	3.120	8.930	8.200	0.320	0.160	1.160	0.090	4.799	0.619	0.73	0.060
Tulrital	4.610	12.270	8.360	0.220	0.110	1.349	0.130	4.054	0.591	0.57	0.110
Zilpui	3.750	11.530	11.330	0.270	0.130	1.060	0.100	5.493	0.625	0.54	0.060
Tuizual	3.630	10.700	13.050	0.280	0.140	1.301	0.090	4.560	0.624	0.56	0.050

Multi-Criteria Decision Making (MCDM) Techniques

TOPSIS as one of the MCDM method widely used techniques is explained here.

The TOPSIS is one of the separation based techniques which was first presented by Hwang and Yoon (1981). This technique helps people make decisions according to their preferences, in cases where there is more than one conflicting criterion. Since the value of morphological parameters considered for watershed prioritization may vary in diverse range, and hence require normalization as first step to be used in TOPSIS to restrict the variation in

a defined range of 0 to 1 for comparison amongst them. The standard methodology for normalization of different parameters used by Hwang and Yoon, 1981 is given below.

$$X_{ij} = \frac{R_{ij}}{\sqrt{\sum_{j=1}^n R_{ij}^2}} \dots\dots\dots \text{Equation 1.}$$

Where, X_{ij} is the normalised value of a morphometric parameter for i^{th} row and j^{th} column ($i=1,2,3,\dots,19$, & $j=1,2,3,\dots,11$) and R is the observed value of parameters for i^{th} watershed.

Table 3.20 Normalised matrix

watershed	Dd	Sf	T	C	Lg	H	Rh	Rb	Re	ρ	Rg
Sherbawk	0.223	0.228	0.091	0.214	0.223	0.135	0.284	0.139	0.234	0.233	0.290
Kailian	0.161	0.150	0.092	0.302	0.303	0.132	0.189	0.266	0.180	0.138	0.201
sw18	0.226	0.198	0.127	0.214	0.223	0.244	0.363	0.211	0.217	0.200	0.401
Darkhuang	0.325	0.315	0.133	0.151	0.143	0.141	0.284	0.182	0.225	0.215	0.357
Sakei	0.188	0.182	0.136	0.254	0.255	0.201	0.237	0.243	0.245	0.256	0.201
Nghathup	0.155	0.169	0.138	0.318	0.319	0.172	0.237	0.207	0.204	0.178	0.267
Ngharum	0.250	0.251	0.168	0.199	0.191	0.156	0.174	0.249	0.224	0.214	0.156
Nghalrawh	0.296	0.336	0.174	0.167	0.159	0.131	0.221	0.233	0.234	0.235	0.223
Tuipawi	0.171	0.153	0.174	0.286	0.287	0.306	0.237	0.250	0.236	0.238	0.201
Belkhui	0.281	0.329	0.211	0.175	0.175	0.184	0.221	0.240	0.217	0.200	0.201
Tuirial	0.209	0.187	0.219	0.230	0.239	0.244	0.174	0.206	0.228	0.221	0.178
Suanghuan	0.235	0.217	0.220	0.206	0.207	0.201	0.174	0.191	0.241	0.247	0.178
Muthi	0.200	0.187	0.229	0.246	0.239	0.302	0.268	0.267	0.280	0.335	0.245
Tuiphu	0.228	0.237	0.248	0.214	0.207	0.279	0.316	0.242	0.240	0.246	0.223
Suibual	0.202	0.209	0.253	0.238	0.239	0.193	0.189	0.245	0.278	0.329	0.201
Chite	0.191	0.183	0.279	0.254	0.255	0.277	0.142	0.239	0.216	0.198	0.134
Tulrital	0.282	0.252	0.285	0.175	0.175	0.322	0.205	0.202	0.206	0.181	0.245
Zilpui	0.229	0.237	0.386	0.214	0.207	0.253	0.158	0.274	0.217	0.202	0.134
Tuizual	0.222	0.219	0.444	0.222	0.223	0.311	0.142	0.227	0.217	0.202	0.111

The second step is to calculate weighted normalised matrix. Weightage of 10% is assigned for all the parameters except for the parameters **Re** and **ρ** where the weightage assigned is 5%. The weightage is assigned in such a way that sum of the weightage must be equal to 100%. Methodology used to calculate weighted normalised matrix is given by the equation

$$V_{ij} = X_{ij} \times W_{ij} \dots\dots\dots \text{Equation 2.}$$

Where, V_{ij} = Weighted normalised value of a parameters for i^{th} row and j^{th} column

X_{ij} = Normalised value of a morphometric parameter for i^{th} row and j^{th} column and

W_{ij} = Weightage assigned for each parameter.

Table 3.21 Weighted normalised matrix

watershed	Dd	Sf	T	C	Lg	H	Rh	Rb	Re	ρ	Rg
Sherbawk	0.022	0.023	0.009	0.021	0.022	0.014	0.028	0.014	0.012	0.014	0.029
Kailian	0.016	0.015	0.009	0.030	0.030	0.013	0.019	0.027	0.009	0.015	0.020
sw18	0.023	0.020	0.013	0.021	0.022	0.024	0.036	0.021	0.011	0.011	0.040
Darkhuang	0.032	0.032	0.013	0.015	0.014	0.014	0.028	0.018	0.011	0.012	0.036
Sakei	0.019	0.018	0.014	0.025	0.026	0.020	0.024	0.024	0.012	0.012	0.020
Nghathup	0.015	0.017	0.014	0.032	0.032	0.017	0.024	0.021	0.010	0.012	0.027
Ngharum	0.025	0.025	0.017	0.020	0.019	0.016	0.017	0.025	0.011	0.013	0.016
Nghalrawh	0.030	0.034	0.017	0.017	0.016	0.013	0.022	0.023	0.012	0.012	0.022
Tuipawl	0.017	0.015	0.017	0.029	0.029	0.031	0.024	0.025	0.012	0.012	0.020
Belkhui	0.028	0.033	0.021	0.017	0.018	0.018	0.022	0.024	0.011	0.011	0.020
Tuirial	0.021	0.019	0.022	0.023	0.024	0.024	0.017	0.021	0.011	0.011	0.018
Suanghuan	0.023	0.022	0.022	0.021	0.021	0.020	0.017	0.019	0.012	0.012	0.018
Muthi	0.020	0.019	0.023	0.025	0.024	0.030	0.027	0.027	0.014	0.009	0.025
Tuiphu	0.023	0.024	0.025	0.021	0.021	0.028	0.032	0.024	0.012	0.009	0.022
Suibual	0.020	0.021	0.025	0.024	0.024	0.019	0.019	0.025	0.014	0.010	0.020
Chite	0.019	0.018	0.028	0.025	0.026	0.028	0.014	0.024	0.011	0.013	0.013
Tulrital	0.028	0.025	0.028	0.017	0.018	0.032	0.021	0.020	0.010	0.010	0.025
Zilpui	0.023	0.024	0.039	0.021	0.021	0.025	0.016	0.027	0.011	0.010	0.013
Tuizual	0.022	0.022	0.044	0.022	0.022	0.031	0.014	0.023	0.011	0.010	0.011

The third step is to calculate the ideal best and ideal worst value. This value is to be determined by selecting the maximum value or minimum value from weighted normalised parameters. In this case the maximum value is selected as ideal best and minimum value is selected as ideal worst for the parameter C-constant of channel maintenance, **Lg**- Length of overland flow, **Re**- Elongation ratio and **ρ**- Rho coefficient. As the value of these parameters increases the chances of groundwater recharge / percolation of water will also increase and vice versa. Similarly, minimum value is selected as ideal best and maximum value is selected as ideal worst for the parameters **Dd**- Drainage density, **Sf**- Stream frequency, **T**-Texture Ratio, **H**-Maximum basin relief, **Rh**- Relief ratio, **Rg**-Gradient Ratio, **Rb**- Weighted Bifurcation ratio. As the values of these parameters decreases the chances of storing water in these areas also increases because the low value of these parameters is the indication of high permeability of the sub surface lithology (Choudhari, et al., 2018; Meshram, et al., 2019; Gajbhiye, et al., 2014; Yadav, et al, 2018; Biswas, et al., 1999). Table 3.22 shows the ideal best and ideal worst value. To determine the positive and negative ideal solutions, the following Equations have been used.

$$A^+ = \{(maxv_{ij}/j \in J1), (minv_{ij}/j \in J2)/i=1, 2, \dots, m\} \dots\dots\dots \text{Equation 3}$$

$$A^- = \{(maxv_{ij}/j \in J1), (minv_{ij}/j \in J2)/i=1, 2, \dots, m\} \dots\dots\dots \text{Equation 4}$$

Where, $A^+ = (v_1^+, v_2^+, v_3^+, \dots, v_n^+)$; $A^- = (v_1^-, v_2^-, v_3^-, \dots, v_n^-)$

$J1 = \{1, 2, \dots, n\}$ is associated with the positive criteria

$J2 = \{1, 2, \dots, n\}$ is associated with the negative criteria

Table 3.22 Ideal best and ideal worst value.

Ideal best (A^+)	0.015	0.015	0.009	0.032	0.032	0.013	0.014	0.014	0.014	0.015	0.011
Ideal worst (A^-)	0.032	0.034	0.044	0.015	0.014	0.032	0.036	0.027	0.009	0.009	0.040

Step four is to calculate the Euclidean distance from the ideal best value. The best option would be the one that is closest to the positive-perfect arrangement and most remote from the negative perfect arrangement (Meshram, et al., 2020). The methodology adopted for this calculation is given by the equations

$$S_i^+ = [\sum_{j=1}^n (V_{ij} - V_j^+)^2]^{0.5} \quad (i=1, 2, \dots, m) \dots\dots\dots \text{Equation 5}$$

$$S_i^- = [\sum_{j=1}^n (V_{ij} - V_j^-)^2]^{0.5} \quad (i=1, 2, \dots, m) \dots\dots\dots \text{Equation 6}$$

The calculated parameters for these two equations are shown in Table 3.23.

The last step in the TOPSIS procedure is to calculate the relative intimacy to the perfect result and rank the performance Score. The performance score is calculated by the equation

$$P_i = \frac{S_i^-}{S_i^+ + S_i^-} \dots\dots\dots \text{Equation 7}$$

Where, $i=1, 2, 3, \dots, m$

Since $S_i^- \geq 0$ and $S_i^+ \geq 0$, then clearly $P_i \in [0, 1]$. The greater the index value, the improved the performance of the substitutes. Thus highest P_i score is given rank as 1 (Groundwater potential zone) and lowest P_i score is given rank as 19 (Groundwater deficit zone) (Table 3.23)

Table 3.23 values of Euclidean distance and performance scores of sub watersheds.

watershed	S_i^+	S_i^-	Pi Score	Rank	Prioritization
Kailian	0.017165	0.058662986	0.773629112	1	Very good groundwater potential zone
Nghathup	0.021055	0.052103541	0.712203338	2	
Sakei	0.02143	0.048431619	0.693247162	3	
Tuirial	0.024377	0.044652304	0.646862491	4	
Tuipawl	0.026533	0.04774201	0.64277784	5	Good groundwater potential zones
Ngharum	0.026943	0.046920258	0.635235092	6	
Suanghuan	0.025856	0.043426005	0.62679645	7	
Sherbawk	0.02885	0.048211509	0.625619678	8	
Chite	0.028134	0.046646153	0.623779793	9	
Suibual	0.026949	0.041820518	0.608129298	10	
Nghalrawh	0.037193	0.040822546	0.52326386	11	Moderate groundwater potential zones
Muthi	0.034154	0.037260589	0.521750504	12	
Belkhui	0.036489	0.037343418	0.505785886	13	
Zilpui	0.041136	0.038647722	0.484404263	14	Poor groundwater potential zones
Tuizual	0.044244	0.041374981	0.483248061	15	
sw18	0.042586	0.03884655	0.477042057	16	
Tuiphu	0.037408	0.032179487	0.462435168	17	
Darkhuang	0.04478	0.038511927	0.462371567	18	
Tulrital	0.041325	0.030138813	0.421733707	19	

3.7.3 Results and Discussions

The result of TOPSIS model demonstrated that sub-watersheds Kailian show the highest score of 0.773629112 which is assigned with rank 1. This sub watershed is considered to be the utmost potential zone for groundwater. On the other hand it is found that sub watershed Tulrital has the least score of 0.421733707, which is assigned with rank 19 and is considered to be the poorest potential zone of groundwater. These sub watersheds are again classified into four classes based on performance scores. Kailian, Nghathup and Sakei shows the highest scores (corresponding numerical values: 0.773629112, 0.712203338, 0.693247162) are ranked 1 to 3 and thought to be very good groundwater potential zones. Sub watershed Tuirial, Tuipawl, Ngharum, Suanghuan, Sherbawk, Chite and Suibual shows performance scores of 0.646862491, 0.64277784, 0.635235092, 0.62679645, 0.625619678, 0.623779793 and 0.608129298 which are ranked 4 to 10 are classified as good groundwater potential zones. Sub watershed Nghalrawh, Muthi and Belkhui having performance scores of 0.52326386, 0.521750504 and 0.505785886 which are ranked 11 to 13 are classified as moderate groundwater potential zones.

Sub watershed Zilpui, Tuizual, sw18, Tuiphu, Darkhuang and Tulrital whose corresponding performance scores are 0.484404263, 0.483248061, 0.477042057, 0.462435168, 0.462371567 and 0.421733707. These low performance scores are categorised ranked as 14 to 19 and are considered to be poor groundwater potential zones. The spatial distribution of these sub watersheds are shown in Figure 3.19.

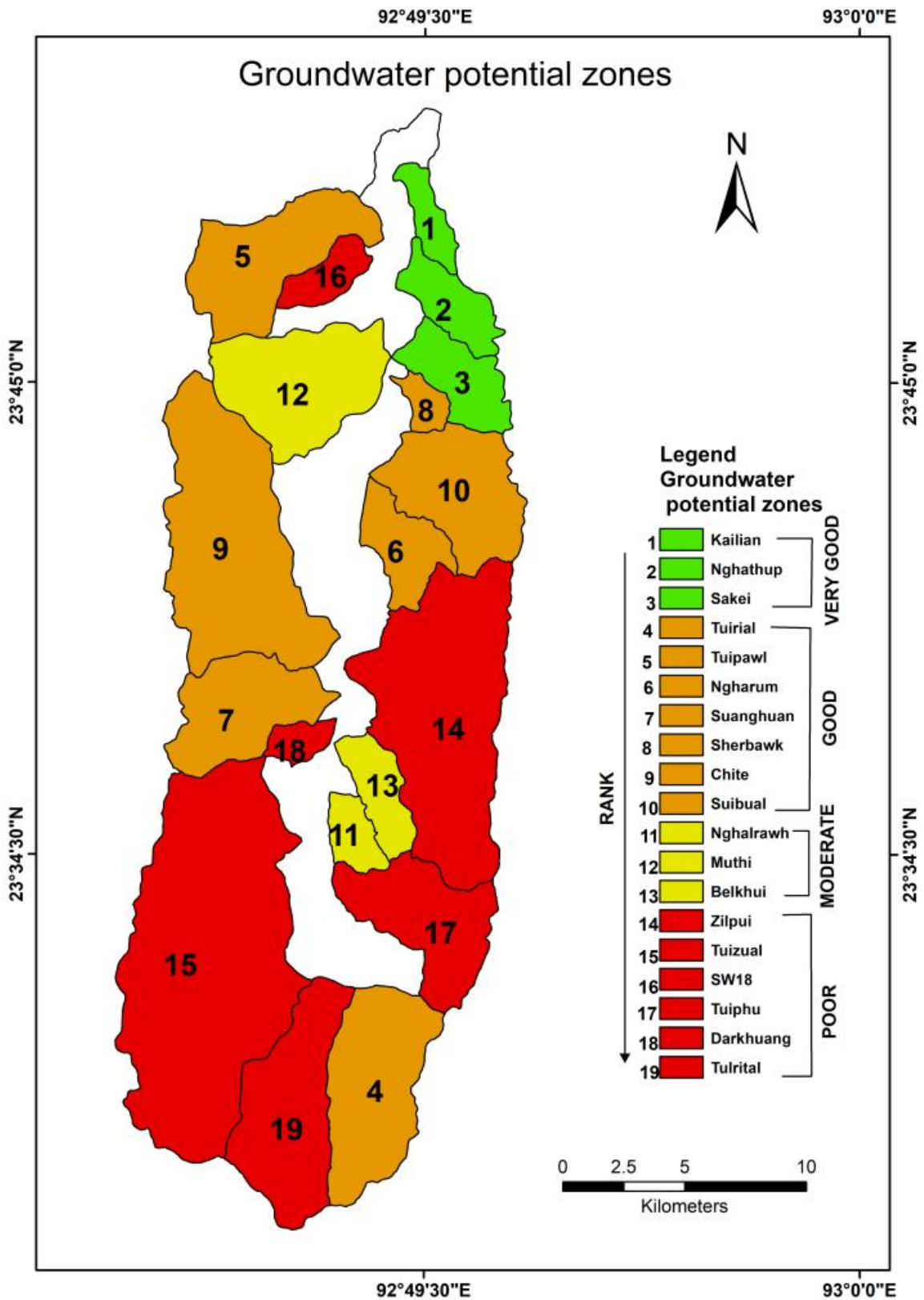


Figure 3.19 Sub-watershed wise prioritisation based on morphometric parameters (i.e. '1' rank indicate very good groundwater potential zone).

CHAPTER- 4

T E C T O N I C G E O M O R P H O L O G Y

4.1 Introduction

From the tectonic point of view, upper Tuirial watershed of Mizoram is situated in a tectonically active region. There are many anticlinal and synclinal structures formed by the collision of Indian and Burmese plates. Morphotectonic analysis of drainage system is widely applied to understand the evolutionary history of landscape development due to tectonic deformation (Cuong and Zuchiewicz, 2001, Bhatt, et al., 2007). In order to identify the tectonic activity of the study area, morphotectonic analysis have been carried out by performing a tectonic lineaments analysis and analyses of different geomorphic indices like hypsometric integral, elongation ratio, asymmetry factor, transverse topography asymmetry factor, stream length-gradient index, river profile, ratio of valley floor width to valley height, and mountain front sinuosity index (Wani, et al., 2019; Verrios, et al., 2004; Jain and Verma 2006; Raj, et al., 2003; Das and Gupta, 2019). Geomorphic indices are particularly useful in tectonic studies (El Hamdouni, et al., 2008) because the necessary data can be obtained from topographic maps and aerial photographs and they can be used for rapid evaluation of large areas. Quantitative measurements and the calculation of geomorphic indices have been previously tested as valuable tools in various tectonically active areas around the world (Bull and McFadden, 1977; Keller, 1986; Silva, et al., 2003; Zovoili, et al., 2004; Dehbozorgi, et al., 2010; Rockwell, et al., 1984).

On the basis of evaluation of above mentioned parameters, an attempt has been made to trace out the plausible phases of the geomorphic evolution of the upper Tuirial basin by using remote sensing and GIS techniques. For morphotectonic analysis, the study area has been divided into 13 sub basins symbolically assigned names as W1 to W13 (Fig. 5.2) to decipher the tectonic activity along the major tributaries of the watershed. The application of tectonic geomorphology is significant in terms of deciphering the ongoing tectonic activity in an area and earthquake hazard management and mitigation.

4.2. Materials and Methods

To study the morphotectonic indices, it is necessary to have some primary maps to calculate the indices, and the most important of which are: Topographic map of 1:50,000 scale prepared by GSI (1986), Digital Elevation Model (DEM), Multispectral satellite

imagery (Sentinel 2 and Landsat 8) the drainage network and the sub-basins map of the basin that have been extracted from DEM and Toposheet. And the methodology involves determining the various indices (Table 4.1) are shown in the flow chart below.

Table 4.1 Morphotectonic indices and their mathematical formulae.

Geomorphic indices	Mathematical formulae	Explanation	Reference
Basin elongation ratio	$Re = 2(A/\Pi)^{0.5}/Lb$	'Re' is the elongation ratio, '2' is a constant, A is area, and 'Lb' is the maximum basin length.	Schumm, 1956
Asymmetry factor	$AF = (A_r / A_t) \times 100$	AF = Asymmetry Factor A _r = right hand side of the drainage basin looking downstream A _t = total area of the drainage basin	Gardner, et. al., 1985
Transverse topographic asymmetry factor	$T = D_a / D_d$	T= Topographic Symmetry Factor. D _a = distance from mid line of the drainage basin to the active channel. D _d = distance from basin midline to basin divide.	Cox, 1994
Stream length gradient index	$SL = (\Delta H/\Delta L) \times L$	ΔH is the drop in elevation of the reach and ΔL is the length of the reach) and L is the total channel length from drainage divide to the centre of the reach measured along the channel.	Hack, 1973
Valley floor to valley width ratio	$Vf = 2Vfw / [(Eld - Esc) + (Erd - Esc)]$	Vf is the valley-floor width to height ratio, Vfw is the width of valley floor, Eld and Erd are elevations of the left and right	Bull & McFadden, 1977

		valley divides respectively, and Esc is the elevation of valley floor	
Mountain-front Sinuosity Index	$Smf = Lmf/Ls$	Smf is the mountain-front sinuosity, Lmf is the length of the mountain front along the foot of the mountain, at the pronounced break in slope; and Ls is the straight line length of the mountain front	Bull, 1977,1978
Hypsometric Integral	$HI = (EL_{mean} - EL_{min}) / (EL_{max} - EL_{min})$	EL_{mean} is the mean elevation, EL_{min} the minimum and EL_{max} the maximum elevation	Pike and Wilson, 1971

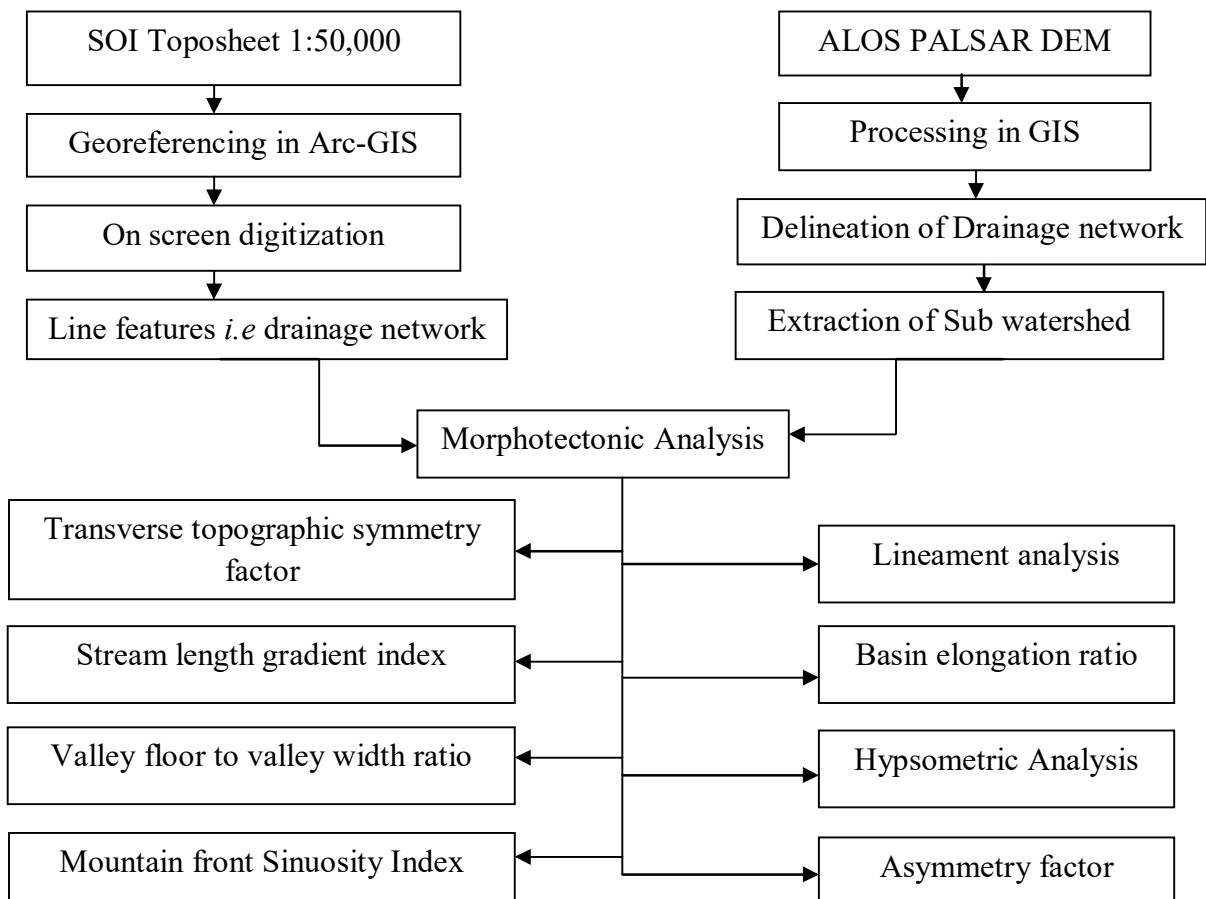


Figure 4.1 Flow chart for Morphotectonic analysis

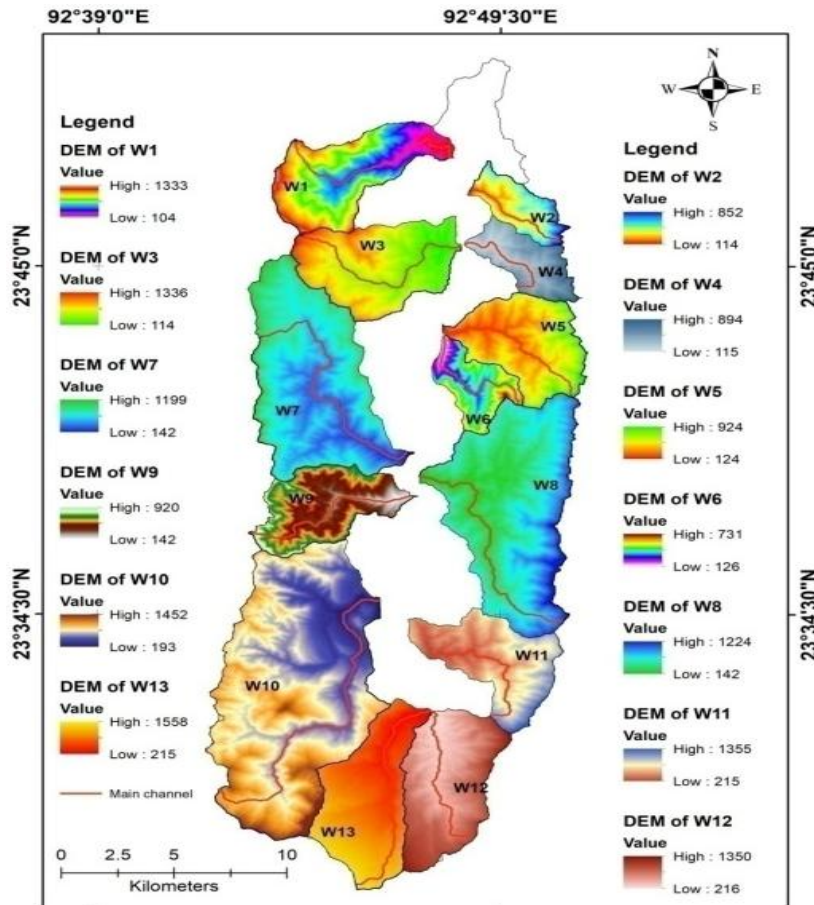


Figure 4.2 Digital elevation Model of 13 selected basins.

4.3 Result and Discussion

4.3.1 Tectonic lineament analysis

Tectonic lineaments are linear features of tectonic origin that are identified on satellite imagery as straight tonal variations aligned and long narrow surface elements which are represented by sub surface structures like fractures and faults. In the study area, 153 lineaments have been identified through visual interpretation of FCC satellite imagery, hill shade map (Fig.4.4), lineament map prepared by GSI and physical observation during field investigation. The lineament features are of varying in length, the longest length of lineament is 13.96 km and the smallest length of lineament is 0.45 km. The longest lineament lies in middle catchment of the upper Tuirial watershed which is oriented in almost North South direction. Among the lineaments identified in the study area, majority of the lineaments oriented in N-S direction as shown in the figure below and there are also cross cutting lineaments that occur along the tributaries of the main channel. The lineament study has been applied successfully to structural geology and tectonic study by various authors such as

Arlegui and Soriano 1998; Hung, et al., 2005 & Das and Gupta, 2019. On plotting various lineaments in Rose diagram, it is found that there is only one predominant set of lineament observed trending almost N-S and other lineaments are trending haphazardly in all directions (Fig. 4.3).

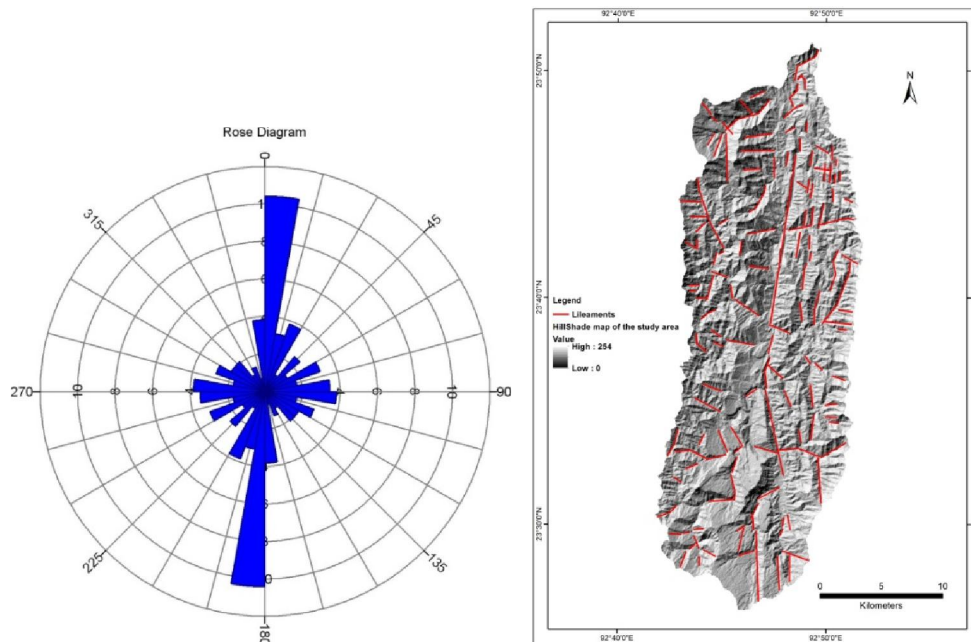


Fig. 4.3 Rose diagram showing the azimuthal distribution of the tectonic lineaments from the study area.

Figure 4.4. Lineaments interpreted from Hill shade map.

The geomorphic indices that are most widely used to understand the active tectonics of a region are:

4.3.2 Basin elongation ratio (Re)

The elongation ratio is a representation of the shape of a river basin. According to Schumm (1956), elongation ratio is defined as the ratio of the diameter of a circle having the same area as the basin and the maximum basin length. The parameter is calculated by using the following equation (Schumm1956).

$$Re = 2(A/ \Pi)^{0.5}/ Lb$$

Where 'Re' is the elongation ratio, '2' is a constant, A is area, and 'Lb' is the maximum basin length.

Higher the value of Re more circular the basin is. Accordingly the basin can be classed as (i) Circular (above 0.9), (ii) Oval (0.8-0.9), (iii) Less elongated (0.7-0.8), and (iv) Elongated (below 0.7). Basin elongation ratio also reflects competing roles of tectonics versus erosion i.e. tectonically active basins are elongated in shape and prone to erosion (Strahler, 1964; Das and Gupta, 2019). Low value of basin elongation ratio is a proxy indicator of recent tectonic activity (Bull and McFadden 1977; Cuong and Zuchiewicz, 2001). Accordingly the Re values are classified into three categories.

Re < 0.50, tectonically active.

Re = 0.50–0.75, slightly active and

Re > 0.75, inactive setting.

Table 4.2 The computed elongation ratios of upper Tuirial watershed.

Watershed Name		Basin area in sq. Km.	Basin Length in km	Elongation ratio (Re)
Upper Tuirial		531.40	46.35	0.56
Suanghuan	W9	21.37	7.55	0.69
Zilpui	W8	56.10	13.54	0.62
Chite	W7	51.47	13.08	0.62
Ngharum	W6	11.03	5.83	0.64
Suibual	W5	24.14	6.96	0.80
Sakei	W4	11.65	5.48	0.70
Muthi	W3	28.59	7.50	0.80
Nghathup	W2	9.31	5.87	0.59
Tulrital	W13	29.91	10.44	0.59
Tuirial	W12	29.18	9.32	0.65
Tuiphu	w11	22.90	7.83	0.69
Tuizual	W10	88.42	17.00	0.62
Tuipawi	W1	25.71	8.44	0.68

The computed Re values of all the sub basins of the study area are given in Table 4.2. The Re values for sub watersheds of Nghathup, Sakei, Ngharum, Zilpui, Tuipawl, Chite, Suanghuan, Tuizual, Tulrital, Tuirial and Tuiphu pointing to slightly tectonically active setting and for the sub watersheds of Suibual and Muthi shows Re value of 0.8 suggesting

inactive setting. However, the watershed as a whole is elongated in shape and basin elongation ratio of 0.56 indicating slightly active basin.

4.3.3 Hypsometric Integral (HI)

The hypsometric integral indicates an area lying below the hypsometric curve is computed to determine the hypsometric integral (HI) that represents the percentage of landmass available as compare to the total landmass with in the basin. The area that lies above the hypsometric curve is called Erosional integral (Ei) and it indicates the volume of area which has been eroded by erosional processes. This parameter is calculated to determine the erosional status of cycle of erosion and is calculated by using the equation (Pike and Wilson, 1971).

$$HI = (EL_{\text{mean}} - EL_{\text{min}}) / (EL_{\text{max}} - EL_{\text{min}})$$

Where EL_{mean} is the mean elevation, EL_{min} the minimum and EL_{max} the maximum elevation within the drainage basin as extracted from a DEM.

Hypsometric integral has three threshold values, each representing the distinctive stages of the geomorphic cycle (Strahler, 1952; Mayer, 1986; Keller and Pinter, 2002). These are given as

1. In equilibrium or young stage ($HI \geq 0.60$)
2. Equilibrium or mature stage ($0.35 \leq HI \leq 0.60$)
3. Monadnock or old stage ($HI \leq 0.35$)

Hypsometric integral reflects a competition between erosion and tectonics with respect to base level erosion. Basin characterized by uniform lithology and climatic conditions, with high values in HI is an indication of active tectonic deformation, whereas low values of Hi suggesting tectonically stable basin (Keller and Pinter, 1996; El Hamdouni et al. 2008; Gajbhiye, et al., 2014). Therefore, hypsometric integral would be expected to have a higher value for younger or youthful stage of landscapes and lower value for older ones as the landscape is denuded towards a stage of maturity and old stages (Strahler, 1952; Keller and Pinter, 2002). The calculated HI values given in Table 4.3 vary from 0.50 (Suibual) to 0.55 (Ngharum) and 0.51 for the whole watershed indicating mature landscape, suggesting that the studyarea is slightly tectonically active.

Table 4.3 Hypsometric Integral values of the Tuirial watershed.

Name of watershed/ Sub watershed	Maximum Elevation (m)	Minimum elevation(m)	Mean elevation(m)	Hypsometric Integral
Upper Tuirial	1558	81	830	0.51
Nghathup	852	114	507.11	0.53
Sakei	894	115	513	0.51
Suibual	924	124	524	0.50
Ngharum	731	126	457	0.55
Zilpui	1224	142	691	0.51
Tuiphu	1335	215	810.38	0.52
Tuirial	1350	216	811	0.52
Tulrital	1558	215	911	0.52
Tuizual	1452	193	840	0.51
Suanghuan	920	142	540	0.51
Chite	1199	142	688	0.52
Muthi	1336	114	758	0.53
Tuipawi	1333	104	748.93	0.52

4.3.4 Asymmetry Factor (AF)

The asymmetry factor was developed to detect tectonic tilting transverse to flow at drainage basin or larger scales (Gardner, et al., 1985). The drainage network often has a distinct pattern and geometry in a region developed by tectonic deformation. In the study area also it shows that asymmetry nature in some of the sub watersheds (Fig. 4.6) indicating the presence of tectonic activity in this region.

It is the ratio of right-hand side area of the drainage basin facing downstream of the trunk stream (A_r) to the total area of the drainage basin (A_t) i.e.

$$AF = (A_r / A_t) \times 100$$

Where, AF = Asymmetry Factor, A_r = right hand side of the drainage basin looking downstream and A_t = total area of the drainage basin

For a stable setting and uniform lithology, AF is 50. It is sensitive to tilting perpendicular to the trend of the trunk stream (Keller and Pinter, 2002). When AF is greater than 50, the channel has shifted towards the downstream left side of the drainage basin. On the other hand, when AF value is less than 50, it indicates that the channel has shifted towards the downstream right side of the drainage basin.

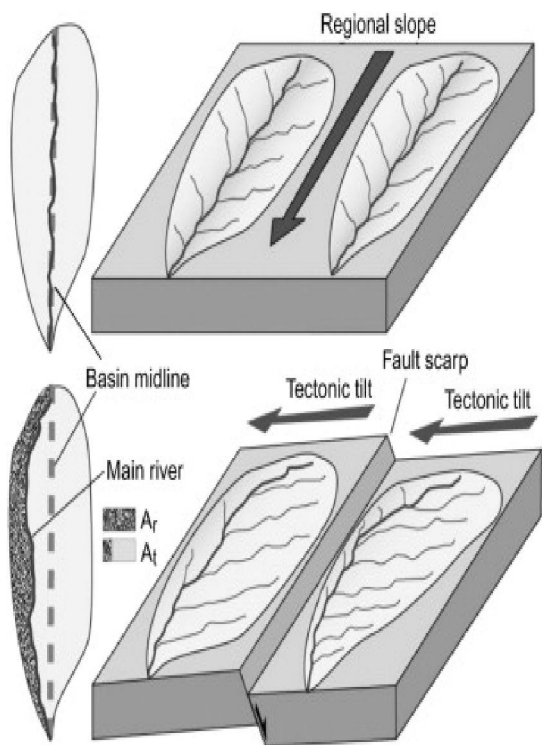


Figure 4.5. The schematic diagram showing the 3D view of tectonic tilt.

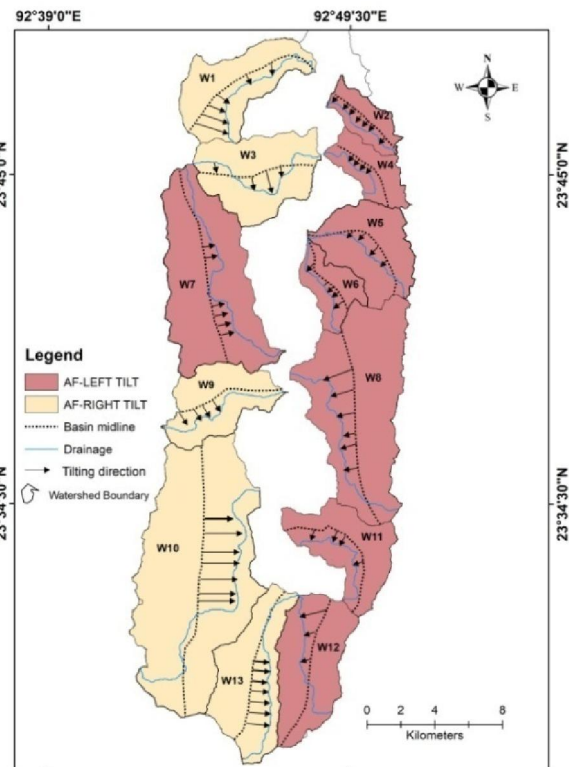


Figure 4.6. The tectonic tilting of the selected sub watersheds in the study area..

This parameter allows determination of the general tilt of the basin landscape, irrespective of whether the tilt is due to local or regional tectonic deformation (Hare and Gardner, 1985).

Following the Strahler's (1964) stream ordering scheme, the AF for 13 sub watersheds were calculated and presented in Table 4.4. The AF values indicate that all the major channels have shifted downstream to either right tilt or left tilt. This downstream shifting of all rivers is possibly due to the obstruction by faulting.

Table 4.4 The computed values of Asymmetry factor for upper Tuirial watershed.

watershed		Ar	At	AF=(Ar/At)x100	Interpretation
Upper Tuirial		251.748	531.431	47.37	Right Tilt
Tuipawi	W1	6.10	26.27	23.22	Right Tilt
Nghathup	W2	6.84	9.16	74.68	Left Tilt
Muthi	W3	13.94	28.99	48.08	Right Tilt
Sakei	W4	9.34	11.57	80.79	Left Tilt
Suibual	W5	14.73	24.24	60.76	Left Tilt
Ngharum	W6	7.67	11.00	69.72	Left Tilt
Chite	W7	27.96	51.98	53.78	Left Tilt
Zilpui	W8	45.51	56.35	80.76	Left Tilt
Suanghuan	W9	7.78	21.60	36.04	Right Tilt
Tuizual	W10	24.62	88.70	27.76	Right Tilt
Tuiphu	W11	18.88	23.26	81.17	Left Tilt
Tuirial	W12	15.57	29.42	52.94	Left Tilt
Tulrital	W13	7.07	30.55	23.14	Right Tilt

4.3.5 Transverse Topographic symmetry Factor (T)

Transverse Topographic Symmetry Factor is also one of the quantitative index to evaluate the basin symmetry and is defined as the ratio between distance from the midline of the drainage basin to the active meander belt (D_a) and the distance from the basin midline to the basin divide (D_d)(Cox, 1994). It is calculated by the following formula:

$$T = D_a / D_d$$

Where, T= Topographic Symmetry Factor.

D_a = distance from mid line of the drainage basin to the active channel.

D_d = distance from basin midline to basin divide.

For a given perfect Symmetry basin, $T=0$. As symmetry increases, T increases and approaches a value of 1. Thus, T is a vector with a bearing (direction) and magnitude from 0 to 1.

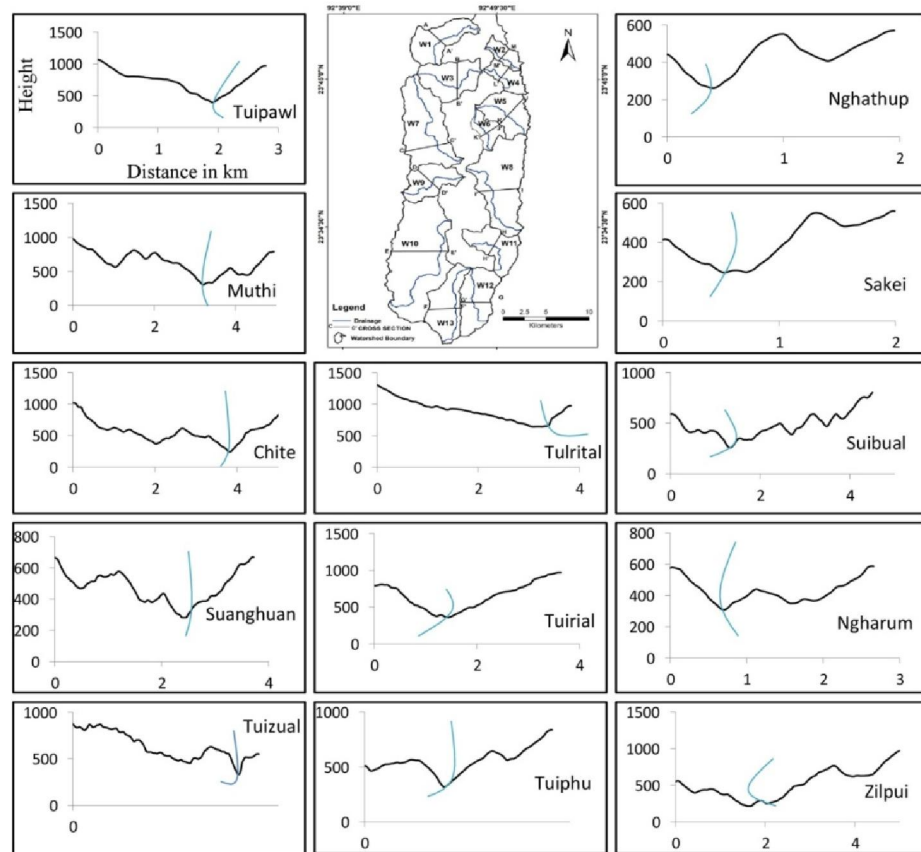


Figure 4.7 Transverse topographic profile reflecting terraces of each sub-watershed.

This method does not give the direct evidence of tectonic tilt rather it gives the possible tilting orientation. From the analysis of transversely topographic profile (Farooqi and Desai, 1974; Bhatt, 1989; Bhat and Ahmed, 2012) drawn for all the sub-watersheds (Fig. 4.7), it is observed that sub watersheds of Tuipawl, Muthi, Chite, Suanghuan, Tuizual and Tuirital which are located on the left bank of the Upper Tuirial basin shows unpair terraces tilting downstream eastward. The other sub watersheds namely Nghathup, Sakei, Suibual, Ngharum, Zilpui, Tuiphu and Tuirial, which are located on the right bank of the Upper Tuirial watershed also shows an unpaired terraces tilting westward. The magnitude and bearing of tilting measured randomly at four places on each sub watershed and taken the average value is shown in Table 4.5.

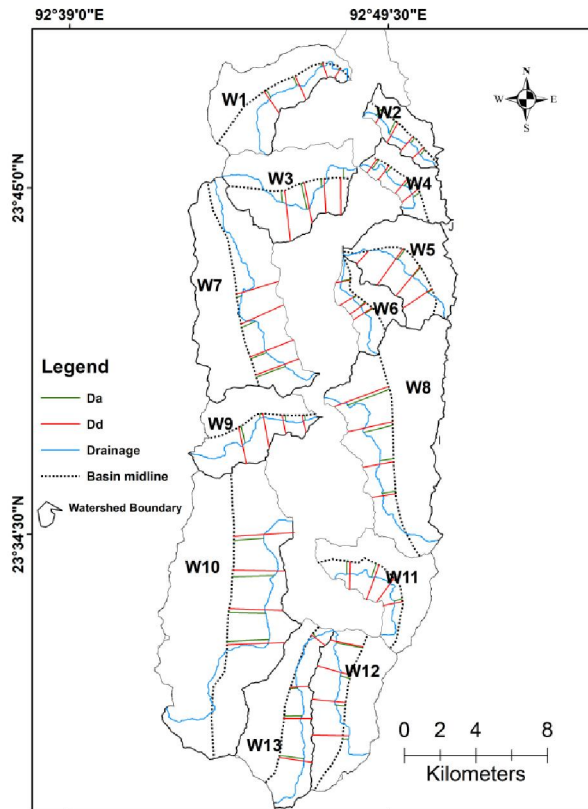


Figure 4.8 Diagram showing the parameters calculated for transverse topographic symmetry factor (T)

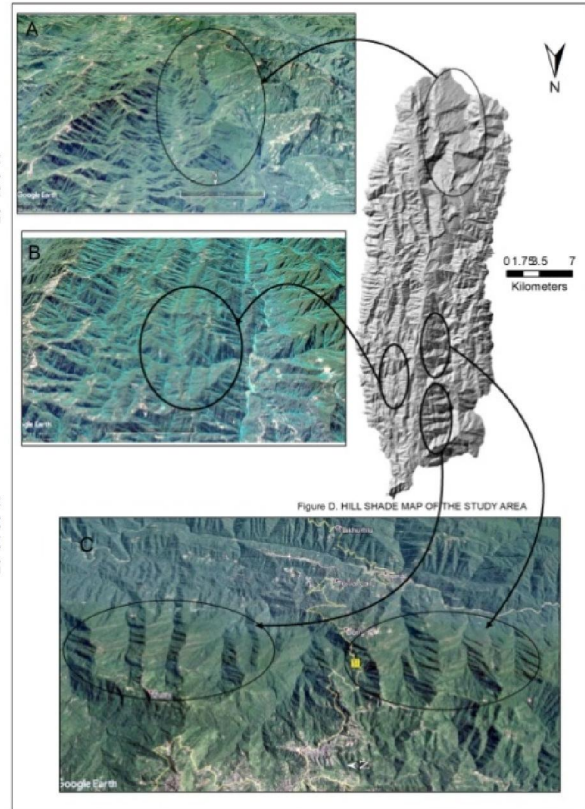


Figure 4.9 Google earth image showing the terraces of remnant beds on both the banks.

Table 4.5 Computation of magnitude and direction of Transverse Topographic Symmetry Factor in the study area

Sub watersheds	Da	Dd	T	Orientation of T in °	Average value of T	Average Orientation of T in °
W1	0.132	0.618	0.213592	212	0.200913	155(SE)
	0.176	0.876	0.200913	155		
	0.513	1.47	0.34898	154		
	0.461	1.499	0.307538	158		
W2	0.398	0.774	0.514212	217	0.615139	210(SW)
	0.772	1.255	0.615139	210		
	0.344	1.018	0.337917	222		
	0.409	0.858	0.47669	228		

W3	0.545	2.075	0.262651	180	0.24739	178 (S)
	0.474	1.916	0.24739	178		
	1.488	2.292	0.649215	168		
	0.679	2.844	0.238748	174		
W4	0.606	0.932	0.650215	215	0.415133	215(SW)
	0.406	0.978	0.415133	218		
	0.458	1.096	0.417883	220		
	0.453	1.146	0.395288	231		
W5	0.032	1.007	0.031778	194	0.301085	194(SW)
	0.694	2.479	0.279952	216		
	0.666	2.212	0.301085	220		
	0.276	1.929	0.143079	237		
W6	0.5	0.842	0.593824	262	0.195392	238(SW)
	0.212	1.085	0.195392	238		
	0.347	1.104	0.314312	236		
	0.515	1.233	0.41768	242		
W7	1.695	2.992	0.566511	253	0.326287	251(SW)
	0.937	2.425	0.386392	247		
	0.849	2.602	0.326287	250		
	0.28	2.469	0.113406	251		
W8	2.448	3.219	0.760485	250	0.496158	263(WSW)
	1.772	2.913	0.608308	251		
	0.904	1.822	0.496158	260		
	0.729	1.476	0.493902	263		
W9	0.276	0.971	0.284243	164	0.120122	170(SE)
	0.31	1.071	0.289449	169		
	0.237	1.973	0.120122	170		
	0.955	2.07	0.461353	169		
W10	1.681	3.368	0.499109	88	0.70074	90(E)
	2.333	2.905	0.803098	90		
	2.084	2.974	0.70074	92		
	2.367	3.266	0.72474	91		

W11	0.737	1.561	0.472133	183	0.409217	202(SW)
	0.795	2.05	0.387805	202		
	0.408	1.638	0.249084	216		
	0.444	1.085	0.409217	255		
W12	1.479	1.856	0.796875	261	0.163096	277(WNW)
	0.533	1.906	0.279643	287		
	0.55	1.863	0.295223	277		
	0.335	2.054	0.163096	272		
W13	0.247	0.947	0.260824	122	0.512011	100 (ESE)
	0.426	0.998	0.426854	88		
	1.003	1.593	0.62962	90		
	1.376	1.883	0.730748	99		
UPPER TUIRIAL	1.62	4.978	0.325432	94	0.007387	93(E)
	0.66	6.839	0.096505	93		
	0.05	6.769	0.007387	89		
	2.007	6.846	0.293164	82		

4.3.6 Stream length-gradient index

The stream length-gradient index (SL index) is a measure of identifying the probable zones of tectonic uplift or rock resistance which can be interpreted from the analysis of river profile (Hack, 1973; Azor, et al., 2002; Keller and Pinter, 2002; Dar, et al., 2014; Pérez-Peña, et. al., 2010). Anomalous high values of SL index are highlighted as nick point due to change in gradient in the river profile indicates tectonic deformation or change in rock resistance (Keller, 1986; Keller and Pinter, 2002). It is defined and mentioned below:

$$SL = (\Delta H / \Delta L) \times L$$

Where, SL is the stream-gradient index, $\Delta H / \Delta L$ is the local gradient of the stream reach where the index is computed (ΔH is the drop in elevation of the reach and ΔL is the length of the reach) and L is the total channel length from the drainage divide to the centre of the reach measured along the channel.

Analysis of longitudinal river profile is a tool to understand the geological setup, structural information, and tectonic deformations in an area (Snyder, et al., 2000; Crosby and

Whipple, 2006; Singh and Awasthi, 2010; Dar, et al., 2014; Roy and Sahu, 2015; Pavano, et al., 2016). Thus longitudinal river profile and SL index has been drawn in a single plot using the contour interval of 20 meters generated from ALOS PALSAR DEM. The SL values are high in areas where rocks are particularly resistant or where active tectonics has resulted in vertical deformation at the earth's surface (Bhat and Ahmed, 2012). Therefore, it is useful parameter to evaluate, if the changes in stream slope are caused due to rock resistance or tectonic deformation. Generally, the SL value increases with increase in elevation from river mouth to source which can be correlated positively with increasing intensity of erosion. The differential weathering occurs due to change in rock resistance over intercalated soft and hard rocks (Fig.4.11) resulting the development of nick points along the river profile. Another possibility of development of terraces / nick points at the higher altitude is due to compressional stress on the basin from East-West direction developing cracks and joints over hinge zones parallel to anticline (Fig. 4.10).

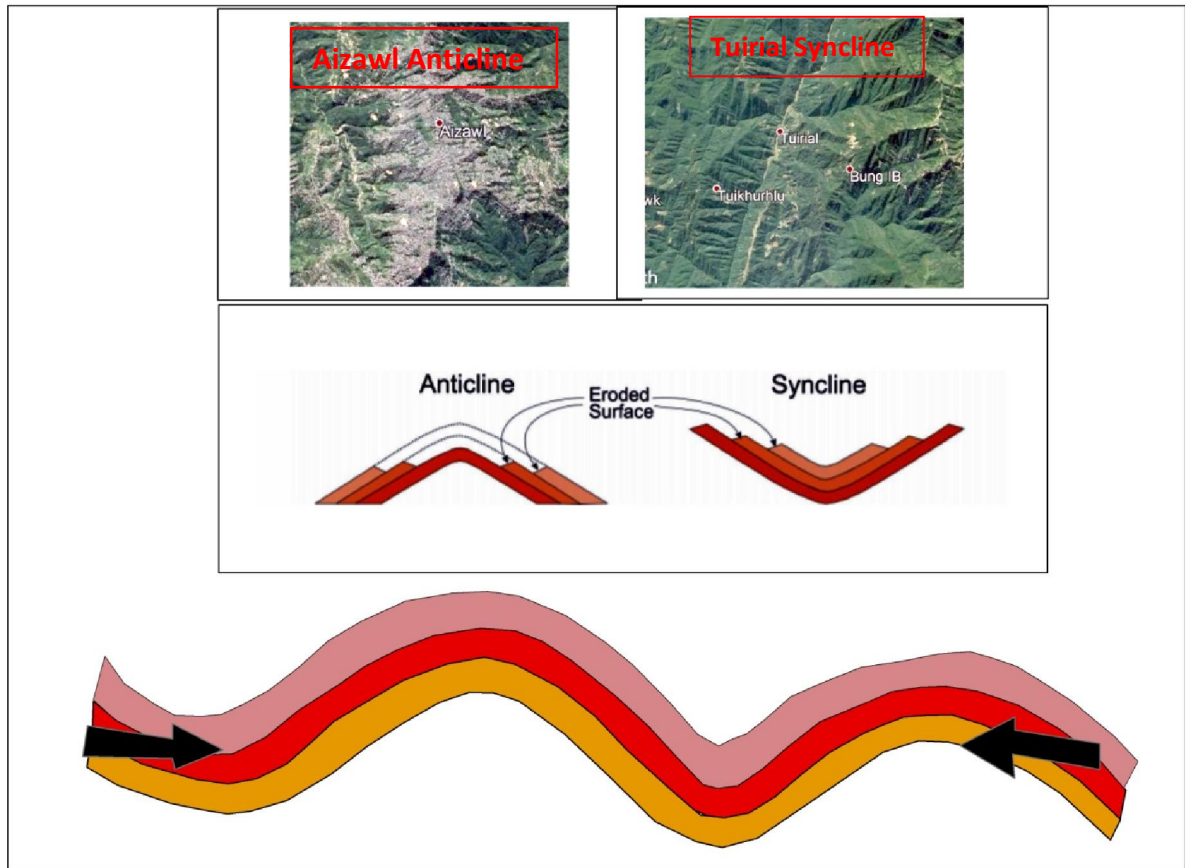
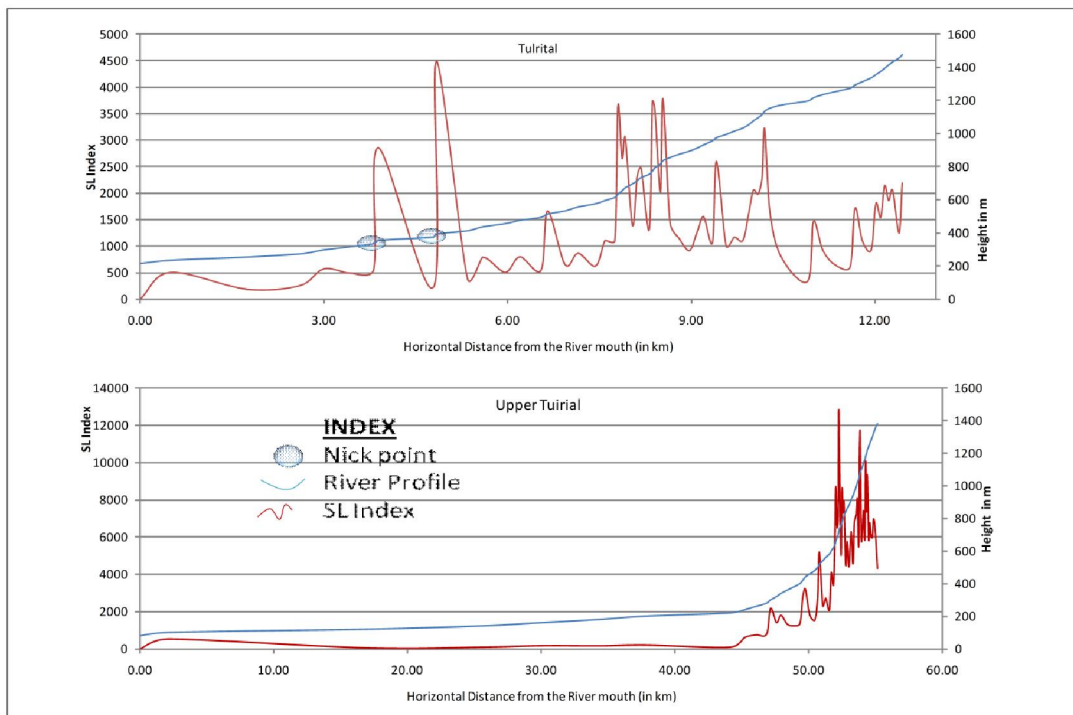


Figure 4.10 Aerial view of the study area from the Google earth and schematic Compressional stress model for the development of terraces (Eroded Surface) in the limbs of a fold belt.



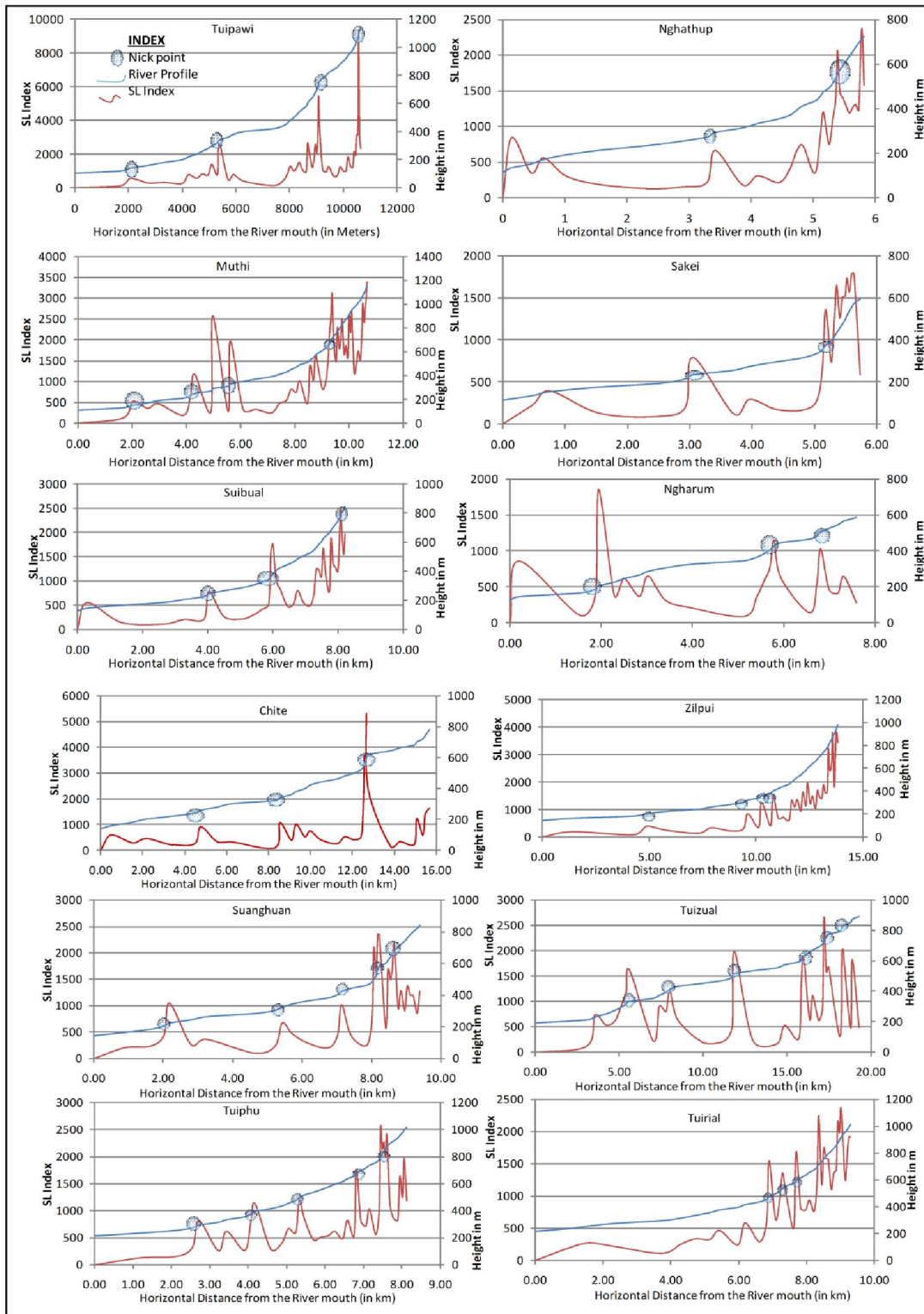


Figure 4.11 Longitudinal profiles of different sub watersheds of upper Tuirial watershed and SL value.

Sub watershed Tuipawl has four prominent nick points on its longitudinal profile where the SL values are 559.48, 2625.72, 5481.09 and 9345.35 between the contour intervals 120–140 m, 320–340 m, 720–740 and 1080–1100. The SL values are increasing with increased in elevation from river mouth to source which may be due to change in rock resistance to erosion. Sub watershed Nghathup, Sakei, Suibual, Zilpui, Tuiphu and Tuirial shows similar trend of increasing value from river mouth to source suggesting these nick zones on the longitudinal profile are due to change in rock resistance to erosion.

In sub watershed Muthi, a series of nick zones observed in the longitudinal profile but there is sudden increase of SL values of 2585.99, 1973.71 and 3121 between the contour intervals of 274-294 m, 314-334 m and 694-714 m. These anomalous high values cannot be due to rock resistance to erosion only, but there must be some tectonic activity. Longitudinal profile of sub watershed chite has a nick point between the contour intervals 582-602 m where the SL index value exceptionally high (5289.34), which indicating that may be caused due to vertical tectonic deformation. Sub watershed Suanghuan has several nick points on the longitudinal profile of which nick points between the contour intervals 202-222 m and 542-562 m, where the SL index value is relatively high (1047.76 and 2352.20) suggesting that may cause due to tectonic deformation. Longitudinal profile of Sub watershed Tuizual has multiple nick points at different heights. Three prominent nick points observed that in between the contour intervals of 313-333 m, 493-513 m and 713-733 m where the corresponding SL values are 1613.72, 1993.05 and 2657.04. Comparing the other values of SL index, these four values are anomalously high suggesting that may cause due to tectonic deformation. Sub watershed Ngharum has exceptional high value of SL index (1860.46) between the contour intervals of 186-206 m indicating the tectonic activity. Longitudinal profile of Sub watershed Tulrital also has series of nick zones at different contour intervals but anomalously high index value of 4496.58 between the contour intervals of 375-395 m which indicate strong tectonic activity.

The longitudinal profile of the whole basin (Upper Tuirial) has a series of nick points only at higher altitudes towards the river source. First prominent nick point observed along the profile at a distance of 47.137 km from the basin mouth between the contour intervals 281-301 m and the corresponding SL value is 2184.73. Subsequently the values increase with the increasing in altitude towards the source. The development of prominent knick points at higher altitude indicating change in rock resistance rather than tectonic deformation.

4.3.7 Ratio of valley floor width to valley height

The ratio of valley floor width to valley height (Vf) may be expressed as:

$$Vf = 2Vfw / [(Eld - Esc) + (Erd - Esc)]$$

Where Vf is the valley-floor width to height ratio, Vfw is the width of valley floor, Eld and Erd are elevations of the left and right valley divides respectively, and Esc is the elevation of valley floor (Bull, 1977, 1978 and Bull & Mc Fadden, 1977). The left and right valley divide is determined by looking downstream.

This index differentiates between U-shaped valleys of broad-floored canyons, where the Vf value is high indicating low tectonic activity and V-shaped valleys (Vf values close to 0), where the river is down cutting in response to tectonic uplift that signifies relatively high tectonic activity. The high values of Vf characterize low tectonic activity, while low value of Vf characterizes high tectonic activity (Bull and McFadden, 1977; Keller and Pinter, 1996 & 2002).

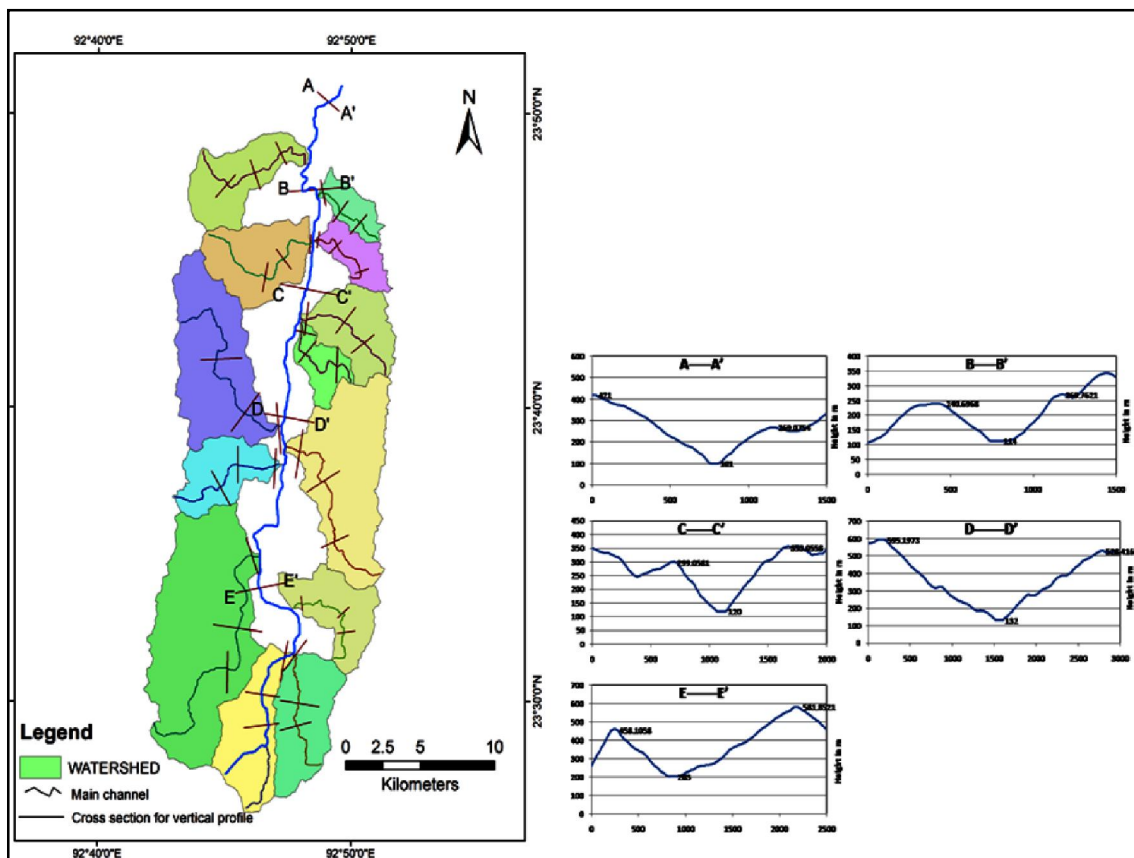


Fig. 4.12. Plots of longitudinal profiles along selected cross sections in the upper Tuirial River Basin.

The Vf values of the Upper Tuirial watershed has been calculated for five cross sections namely AA', BB', CC', DD', EE' (Fig. 4.12). The calculated values are 0.08, 0.07, 0.07, 0.07 and 0.11, respectively. The calculated values and profiles shows that the basin is V-shaped, deeply incised, associated with upliftment which in turn reflects that basin is tectonically active. Similarly, the Vf values for the 13 sub watersheds have been calculated across the main channel at three random locations for each sub-watershed as shown in the figure 4.12 and Table 4.6. The calculated values of Vf for all the sub watershed ranges from 0.06 to 0.25 which represent deep, narrow V-shaped valleys and also indicate ongoing incision and gradual uplifting due to strong tectonic activity.

Table 4.6 The computed ratios of valley floor width to valley height values for Upper Tuirial watershed and its sub watersheds.

Sub watershed	Profile no.	Vwf	Eld	Erd	Esc	Vf	Mean Vf
Upper Tuirial Watershed	AA'	19.30	421.00	269.07	101.00	0.08	0.08
	BB'	10.00	240.69	269.76	114.00	0.07	
	CC'	14.00	299.05	353.05	120.00	0.07	
	DD'	32.00	595.19	528.41	132.00	0.07	
	EE'	34.00	458.10	581.85	203.00	0.11	
Tuipawl	1	5.20	364.52	250.48	162.26	0.04	0.08
	2	6.92	469.33	507.34	313.15	0.04	
	3	27.68	642.61	593.07	438.52	0.15	
Nghathup	1	5.72	369.04	369.27	199.50	0.03	0.09
	2	10.25	388.45	397.65	312.26	0.13	
	3	10.80	412.81	450.00	337.00	0.11	
Muthi	1	8.00	224.39	223.26	124.56	0.08	0.08
	2	12.30	297.85	300.48	193.97	0.12	
	3	10.17	517.77	596.03	298.00	0.04	
Sakei	1	15.00	291.22	229.49	124.00	0.11	0.07
	2	6.60	313.46	301.39	180.33	0.05	
	3	15.00	510.81	594.63	304.72	0.06	
Suibual	1	6.20	287.33	250.93	151.26	0.05	0.07
	2	11.70	360.85	452.31	207.51	0.06	
	3	19.20	570.43	457.00	307.18	0.09	

Ngharum	1	15.70	316.52	200.90	153.00	0.15	0.11
	2	12.50	385.51	448.83	242.41	0.07	
	3	14.00	602.41	557.98	437.37	0.10	
Chite	1	12.70	233.25	188.46	142.00	0.18	0.12
	2	12.90	449.90	509.91	221.23	0.05	
	3	25.80	545.30	492.99	309.00	0.12	
Zilpui	1	12.63	348.14	381.44	151.00	0.06	0.08
	2	15.50	345.53	374.43	198.00	0.10	
	3	26.80	624.93	544.01	298.00	0.09	
Suanghuan	1	16.86	250.02	205.63	155.00	0.23	0.13
	2	20.36	451.38	435.69	257.00	0.11	
	3	7.58	443.00	540.40	314.81	0.04	
Tuizual	1	18.80	342.82	419.03	193.00	0.10	0.08
	2	15.80	604.86	574.71	338.00	0.06	
	3	12.36	581.22	650.25	452.50	0.08	
Tuiphu	1	10.16	336.87	329.74	222.18	0.09	0.08
	2	19.28	536.93	668.36	368.04	0.08	
	3	12.35	749.65	728.88	522.59	0.06	
Tuirial	1	18.50	263.89	253.29	226.93	0.58	0.25
	2	11.75	475.39	464.55	296.00	0.07	
	3	28.00	679.39	560.56	363.34	0.11	
Tulrital	1	8.40	351.30	273.80	236.00	0.11	0.06
	2	9.00	671.46	605.13	335.00	0.03	
	3	10.50	554.66	821.33	450.00	0.04	

4.3.8 Mountain-front Sinuosity Index (Smf)

Mountain front sinuosity index is defined as follows:

$$Smf = Lmf/Ls$$

Where, Smf is the mountain-front sinuosity, Lmf is the length of the mountain front along the foot of the mountain, at the pronounced break in slope; and Ls is the straight line length of the mountain front (Bull, 1977,1978).

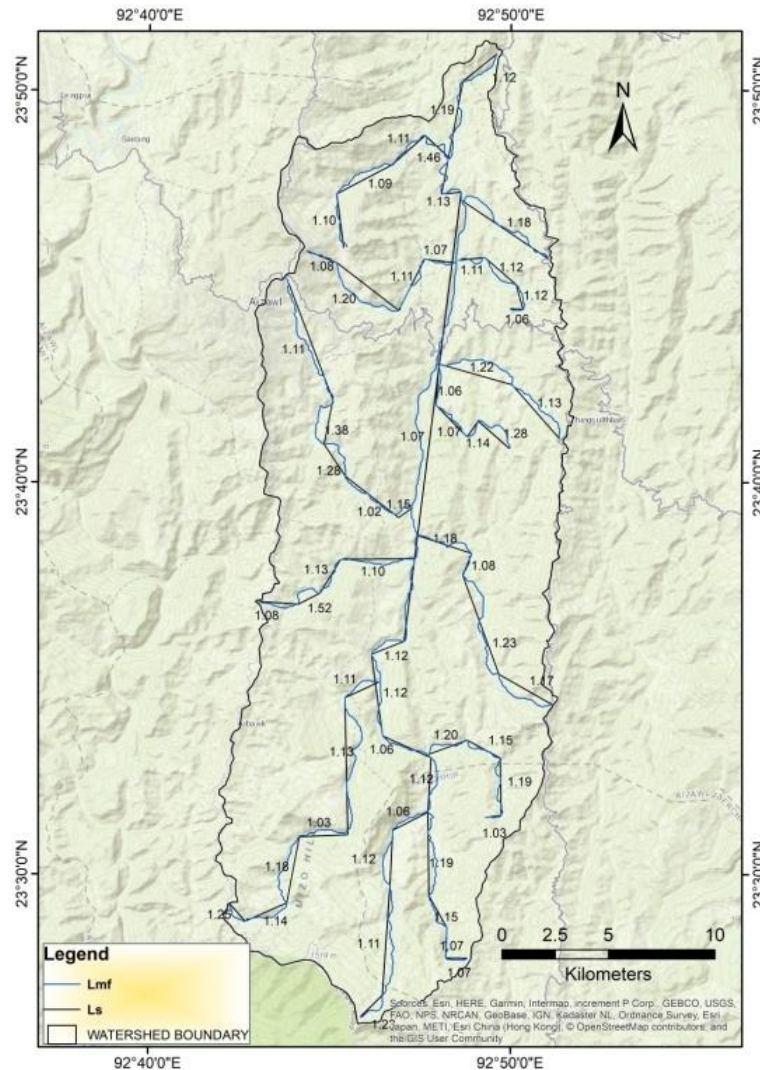


Figure 4.13 Map showing the Mountain front Sinuosity values at different sections.

This index reflects the erosional forces that tend to produce sinuous mountain front and tectonic forces that tend to produce a straight mountain front coincident with an active range bounding fault. Those mountain fronts associated with active tectonics and uplift are relatively straight, with low values of S_{mf} whereas higher values of S_{mf} indicate irregular mountain front and are associated with less tectonic activity (Bull, 1977 & 1978, Bull and McFadden, 1977, Killer and Pinter, 2002).

The S_{mf} value less than 1.4 indicate tectonically active areas, S_{mf} values between 1.4 to 3.0 indicate slightly active areas and S_{mf} values greater than 3.0 indicate inactive setting (Bull and McFadden, 1977). The S_{mf} values for different sub watersheds are measured at different sections (Fig. 4.13) and the values are found to be in the ranges from 1.02 to 1.52 shown in Table 4.7. These low values are the indication of active tectonism in the watershed.

Table 4.7 Computation of Mountain front sinuosity Index at different sections in the upper Tuirial watershed.

watershed	Number of distinct breaks in slope	Straight length	Mountain front	Mountain front Sinuosity
Tuipawl	1	2.56	2.81	1.10
	2	2.92	3.19	1.09
	3	2.09	2.33	1.11
	4	1.61	2.36	1.46
Nghathup	1	4.84	5.72	1.18
Muthi	1	1.51	1.63	1.08
	2	3.65	4.37	1.20
	3	2.69	3.00	1.11
	4	1.47	1.57	1.07
Sakei	1	0.63	0.67	1.06
	2	1.21	1.36	1.12
	3	1.95	2.17	1.11
	4	1.24	1.53	1.23
Suibual	1	3.38	3.84	1.13
	2	3.63	4.42	1.22
Ngharum	1	1.98	2.53	1.28
	2	0.91	1.03	1.14
	3	2.09	2.25	1.07
	4	1.93	2.04	1.06
Chite	1	6.17	6.88	1.11
	2	2.13	2.94	1.38
	3	1.82	2.33	1.28
	4	3.15	3.22	1.02
	5	0.81	0.93	1.15
Zilpui	1	2.87	3.35	1.17
	2	4.95	6.11	1.23
	3	1.12	1.21	1.08
	4	2.71	3.20	1.18
Suanghuan	1	1.87	2.01	1.08
	2	1.15	1.75	1.52
	3	1.86	2.09	1.13
	4	3.44	3.77	1.10
	1	1.08	1.35	1.25

Tuizual	2	2.14	2.44	1.14
	3	3.17	3.73	1.18
	4	2.28	2.35	1.03
	5	6.45	7.31	1.13
	6	1.77	1.97	1.11
Tuiphu	1	0.76	0.78	1.03
	2	2.70	3.20	1.19
	3	1.77	2.04	1.15
	4	1.92	2.30	1.20
Tuirial	1	1.04	1.11	1.07
	2	1.43	1.53	1.07
	3	1.72	1.98	1.15
	4	3.93	4.66	1.19
Tulrital	1	1.45	1.79	1.23
	2	5.20	5.76	1.11
	3	2.59	2.91	1.12
	4	1.86	1.97	1.06
Upper Tuirial	1	2.58	2.89	1.12
	2	2.50	2.64	1.06
	3	3.90	4.11	1.05
	4	1.65	1.85	1.12
	5	21.30	22.87	1.07
	6	0.92	1.04	1.13
	7	5.40	6.41	1.19
	8	2.07	2.31	1.12

Geomorphic field evidences of tectonic activity



Plate 4.1. Highly jointed sandstone beds of almost vertical inclination



Plate 4.2. Deeply incised V-shaped valley.



Plate 4.3 Development of Cracks on horizontal bed

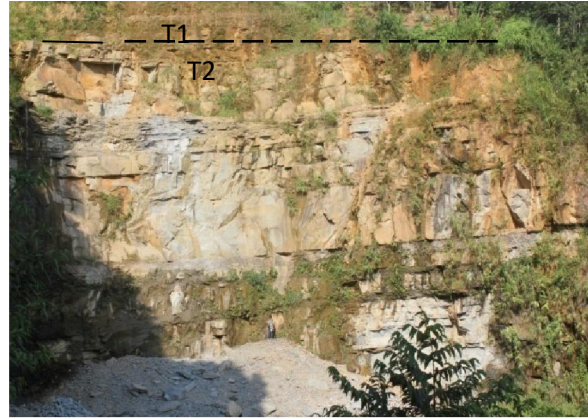


Plate 4.4. Strath terraces on Chite river bank (T1&T2)



Plate 4.5 Field evidence of knick points and development of waterfalls due to tectonic activity.

CHAPTER- 5

Estimation of soil loss using RUSLE model.

5.1 Introduction

Soil erosion is a major problem in the present world which affects the agricultural production, soil fertility, excessive siltation and sedimentation in lakes and rivers. Each year, due to erosion, million tons of soil is removed mostly from agricultural practices in steep slopes (Debral, et al., 2008; Pandey, et al., 2009; Zonunsanga, R. 2016). Soil degradation problem of the study area is assessed to identify exact location of different types of degradation and suggest proper preventive measures. Although soil erosion is a natural process, but it often accelerated by anthropogenic activities (Adornado, et al., 2009). A comprehensive methodology that is Revised Universal Soil Loss Equation (RUSLE) was adopted in the present study in order to estimate the average soil loss (tons per unit area) and also to identify the spatial distribution of soil erosion prone zones with in the upper Tuiriul river basin of Mizoram. Similar study was carried out by different authors in the past (Farhan and Nawaiseh, 2015; Pandey, et al., 2007; Fagbohun, et al., 2016; Parveen and Kumar 2012; Bera, A. 2017; Das, et al., 2018; Pradeep, et al., 2014). The various thematic layers used for RUSLE model are rainfall erosivity factor (R), soil erodibility factor (K), slope length(L), slope steepness factor (S), crop management factor (C) and practice management factor (P). For analysis of each layer, rainfall data collected from Directorate of Agriculture and Crop Husbandry, Govt. of Mizoram, soil textural map was generated based on the National Bureau of Soil Survey and Land Use Planning (NBSS & LUP), CARTOSAT DEM of 30 m spatial resolution for L and S factors, and Sentinel 2A multispectral satellite data for C and P factors were used. The major soil problems of the area are shifting cultivation practices and landslides in hill slopes. On the other hand, the parent materials for the formation of soils are mostly fine grained sandstones and clayey to silty sedimentary rocks, which are prone to erosion due to high precipitation in this region.

Revised universal soil loss equation (RUSLE) is a well-known empirical method developed by Renard, et al., in 1997, which is an updated version of universal soil loss equation (USLE) of Wischmeier and Smith (1978). In this method the annual average soil loss of an area is calculated by multiplying five factors, viz. rainfall erosivity factor (R), soil erodibility factor (K), slope length and steepness factor (LS), cover management factor (C) and conservation practice (P) factor.

5.2 Materials and methodology

Materials used for the present study is shown in Table 5.1

Table 5.1 Materials to be used for the study.

Sl. No.	Type of Data	Source	Purpose
1	Toposheet	Survey of India	Base Map
2	Soil Map	NBSS & LUP	Soil Textural map
3	Satellite data Sentinel 2A (10 m resolution), 30/03/19	United States Geological Survey (USGS)	Land use/Land cover mapping
4	CARTOSAT DEM (2009)	Bhuban portal	Slope map and Flow accumulation map
5	Rainfall (2007-2016)	Directorate of Agriculture and Crop Husbandry, Mizoram	Rainfall Distribution map

Methodology involved integration of different thematic layer such as land cover map, DEM, rainfall, and soil map in GIS environment (Figure 5.1). Soil textural map of 1:250,000 scale was collected from NBSS & LUP (National Bureau of Soil Survey and Land Use Planning) which was then digitized in Arc GIS to generate soil erodibility factor map (K). Rainfall data of nine years for six stations covering the study area were collected from Directorate of Agriculture and Crop Husbandry, Mizoram. These point data were then interpolated using IDW interpolation method in GIS to generate the rainfall distribution map and finally the rainfall erosivity factor map (R). For generation of L and S factors CARTOSAT DEM of 30 m spatial resolution was used to generate slope and flow accumulation map. Sentinel 2A multispectral satellite data of 10 m spatial resolution acquired on 30 March 2019 was used to prepare land use and land cover map of the study area in order to generate the crop management factor (C) and practice management factors (P).

5.3 Soil erosion modeling

For the estimation of average annual soil loss of an area a commonly used model called RUSLE is widely used where multiple components responsible for soil erosion are integrated in GIS environment. These components are rainfall runoff erosivity factor (R), soil erodibility factor (K), slope length (L), slope steepness (S), cover management factor or crop management factor (C), and practice management factor (P) (Renard, et al., 1997).

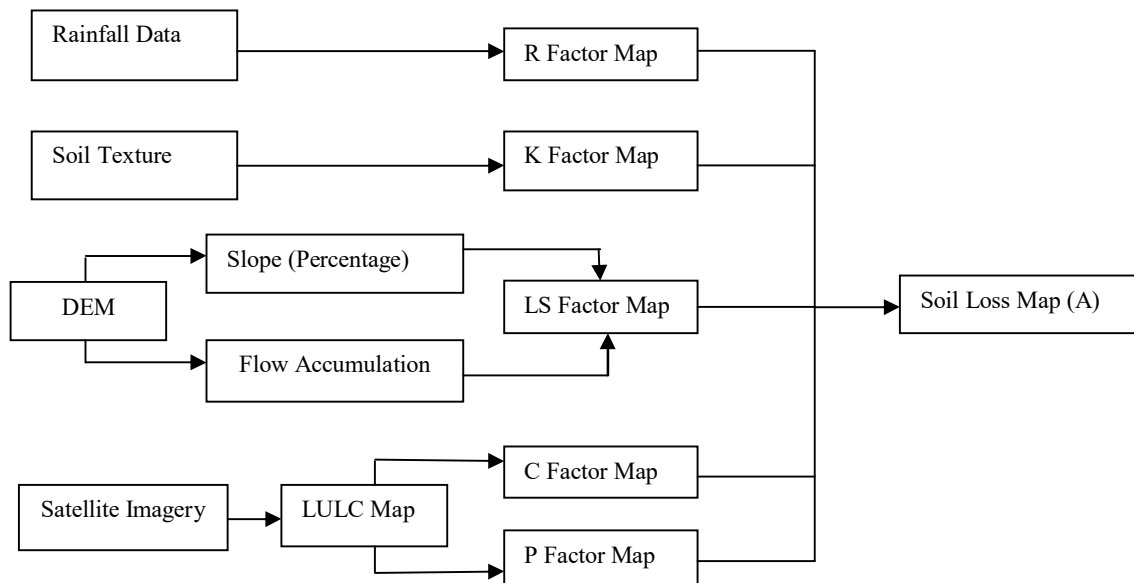


Figure 5.1 Flowchart showing procedure for RUSLE – based soil erosion modeling.

This model is widely used because of its simplicity and can be applied to broad areas with different land use patterns (Renard, et al., 1997; Dutta, et al., 2015; Prasannakumar, et al., 2011; Bera, A. 2017; Terranova, et al., 2009). It is usually denoted by

$$A=R \times K \times L \times S \times C \times P$$

Where, A is the average annual soil loss ($\text{Mg ha}^{-1} \text{ yr}^{-1}$); R is the rainfall-runoff erosivity factor ($\text{M J mm ha}^{-1} \text{ h}^{-1} \text{ year}^{-1}$); K is the soil erodibility factor ($\text{t ha h ha}^{-1} \text{ MJ}^{-1} \text{ mm}^{-1}$); L is the slope length factor; S is the steepness factor; C is the cover and management factor and P is the conservation practices factor. Among these factors L, S, C and P are dimensionless.

5.4 Rainfall-runoff erosivity factor (R)

The Rainfall runoff erosivity (R) factor represents the ability of rainfall and runoff to cause erosion on the surface of the earth. It is a function of the falling raindrop and the

rainfall intensity, and is the product of kinetic energy of the raindrop and the 30-minute maximum rainfall intensity (Wischmeier and Smith, 1978). Extreme rainfall increases the amount of erosion and sedimentation in an area (Pal and Chakraborty, 2019). For this study average yearly rainfall data for nine years (2007-2016) was used to estimate R-factor following relationship developed by Singh, et al., (1981)

$$R = 79 + 0.363P$$

Where R= Rainfall runoff erosivity factor and P= Average annual rainfall in mm.

Table 5.2 Annual Rainfall of 9 years of surrounding stations (2007-2016)

Rainfall(mm)	2007	2008	2009	2010	2011	2012	2013	2014	2015	2016	Average
Aizawl	2485.5	1569.5	1591.8	4378.4	2155.9	2543.6	2078.2	1913.7	2551.3	2844.3	2411.22
Sialsuk	4650.6	2986.7	2458.2	3276	3163	3606	3000	2993	3249.3	3162.6	3254.54
Neihbawi	4859	3784	3217	4404.3	3864	4057	4275	2976	3501	3848.7	3878.6
Darlawn	2922.6	2084.9	1921.9	2454.4	2287.4	3030.4	1697	1089	1691	2391.8	2157.04
Khawruhlian	2844.6	1894	1516	2485	1857	2128	2180	1997	2423	3010	2233.46
Sairang	2489	1661	1579	2679	2137	2266	2810	2733	2977	3217.4	2454.84

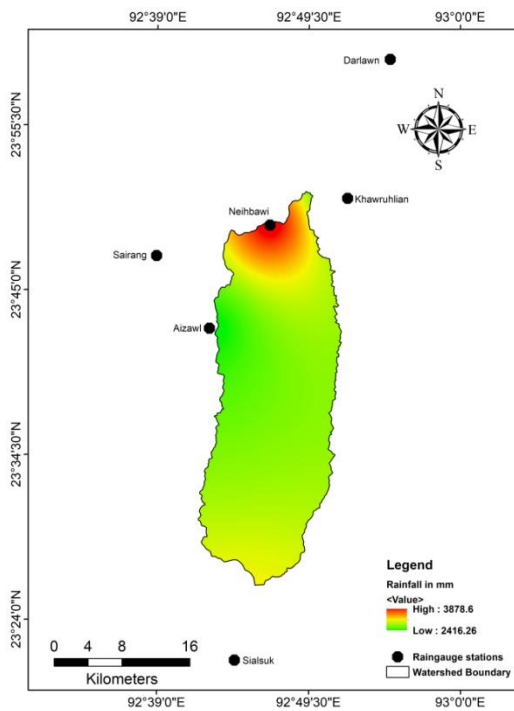


Figure 5.2 Rainfall distribution map in mm

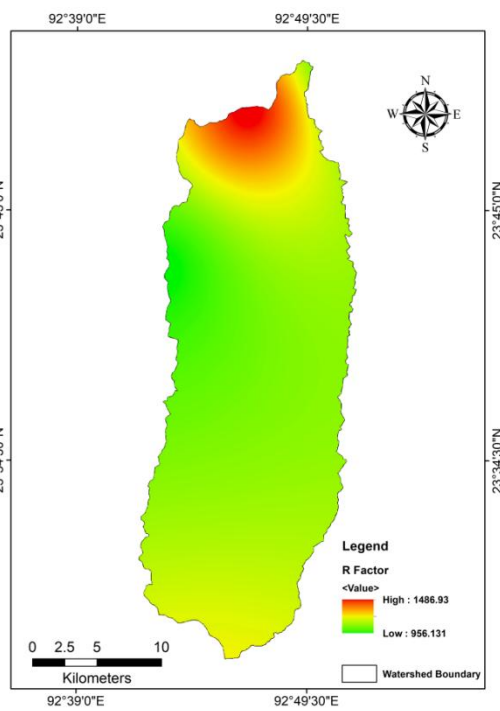


Figure 5.3 Rainfall-runoff erosivity factor map

The average annual rainfall distribution for the years 2007 to 2016 varies from 2416.26 mm to 3878.6 mm (Table 5.2) as shown in the fig. 5.2 and the R Factor ranges from 956.102 to 1486.93 M J mm ha⁻¹ h⁻¹ year⁻¹ with average value of 1116.77 M J mm ha⁻¹ h⁻¹ year⁻¹ as shown in fig. 5.3. The south (Sialsuk) and north (Neibawi) part of the river basin exposed to maximum rainfall while northwest part (Aizawl and Sairang) experienced low rainfall, and the rainfall erosivity was directly proportional to the amount of rainfall received in different parts of the river basin.

5.5 Soil Erodibility Factor (K)

The soil erodibility factor is the measure of rate of soil detached due to impact of raindrops or by surface runoff and shows change in soil erosion per unit area per applied external force. This factor is largely influenced by soil textures, soil structure, soil permeability and organic matter content.

A digitised soil textural map was prepared in Arc GIS from the data provided by NBSS & LUP and as a result we get a clear and distinct soil classification for different locations of the study area (Fig. 5.4). For this study soil erodibility factor value for different soil textures were taken from published literature (Zonunsanga, R. 2016).

The calculated K factor varied from 0.51 to 0.66, Mg ha⁻¹ MJ⁻¹ mm⁻¹ with mean value of 0.57 Mg ha⁻¹ MJ⁻¹ mm⁻¹. Lower value of K indicates soils with least prone to erosion, while higher values indicate soils which are highly prone to erosion by water (Fig. 5.5).

Table 5.3 Soil erodibility factor values assigned for different soil textures.

Soil Textures	'K' Value
Loamy soil	0.51
Fine loamy	0.57
Fine loamy to loamy skeletal	0.55
Loamy skeletal	0.54
Coarse loamy	0.66

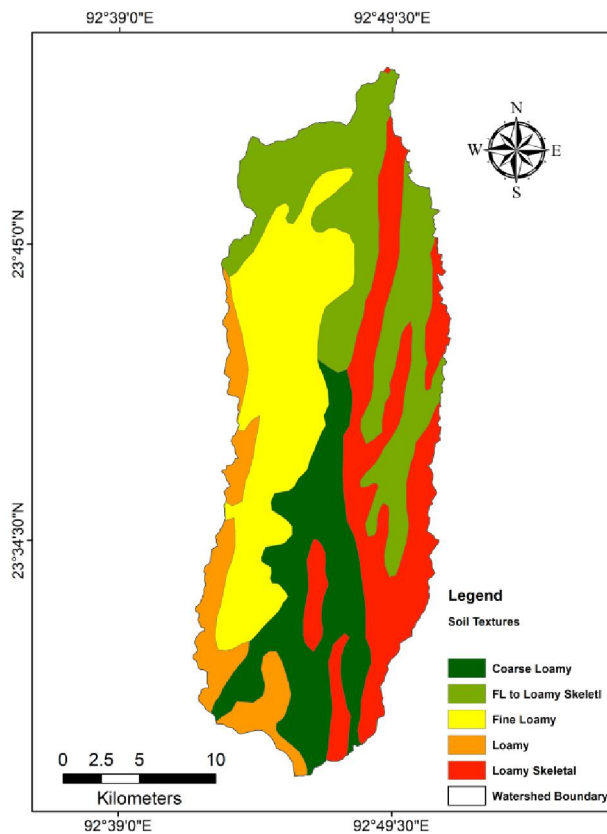


Figure 5.4 Soil Textural Map

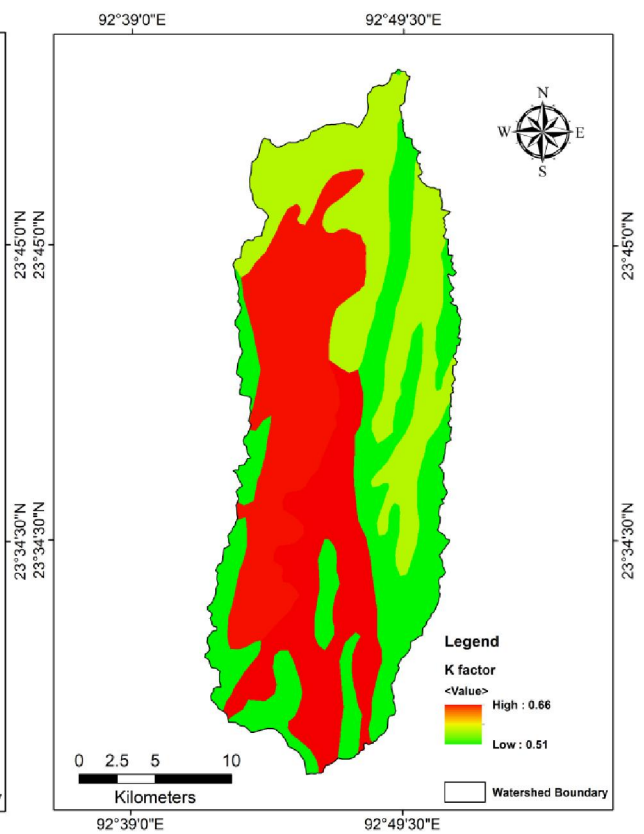


Figure 5.5 Map of soil erodibility factor.

5.6 Slope Length and Slope Steepness(LS) Factors

Slope length (L): Slope length is defined as the distance from the origin of overland flow to where the slope gradually decreases such that deposition occurs and finally enters a defined channel (Wischmeier & Smith, 1978).

Slope steepness(S): Slope steepness is a dimensionless quantity which refers to the angle of inclination of the slope or its gradients expressed in degree or percent.

The risk for erosion increases as the slope length increases and also, steeper the slope more is the erosion (Wischmeier and Smith, 1978; Renard, et al. 1997) as increase in these factors produces higher overland flow velocities and as a result higher erosion. LS factor were determined using CARTOSAT DEM data following Wischmeier & Smith, (1978) equation.

$$LS = \left(\left(\frac{\lambda}{22.13} \right)^m \right) \times (0.065 + 0.045 \times \Theta + 0.0065 \times (\Theta)^2)$$

Where, λ = Flow accumulation x Pixel size in m

Θ = Angle of slope in percentage

m = dependent on the slope

0.5 if slope > 5 %

0.4 if slope is between 3.5 % and 4.5 %

0.3 if slope is between 1 % and 3 %

0.2 if slope is less than 1 %

In this case the value of m is taken as 0.5 and the value of each pixel is 30 m. The SL factor varied from 0 to 378.661, with a mean value of 5.719 with standard error of 11.586 (Figure 5.6). The spatial distribution map clearly shows the concentration of high LS values in steeper slope areas, where there is sudden change in relief and slope angle.

5.7 Crop Management Factor (C)

Crop management or cover management factor is expressed as the ratio of soil loss of specific crop to the soil loss under the condition of continuous bare soil (Das, et al., 2018). Depending upon the type and coverage of the land surfaces, the rate and amount of soil loss also vary because region with vegetation cover prevents the direct impact of raindrops on the soil particles resulting less erosion. Whereas region having bare surfaces will have more erosion due to direct impact of raindrops on the soil surface.

For the preparation of crop management factor map, Sentinel 2A multispectral satellite data of 10 m spatial resolution acquired on 30 March 2019 was used to prepare land use and land cover map of the study area. Image classification was done based on visual interpretation of FCC image with limited field validation and also validated with Google earth pro image. Five types of land cover were identified in the study area such as Current Jhum, Settlement, natural forest, Jhum fallow and water body (Table 5.4). The C factor value corresponding to each land cover conditions were assigned as per the published literature (Zonunsanga, R. 2016; Debral, et al., 2008) who carried out similar study in this region. The magnitude and the spatial distribution of crop management factor are given in Fig.5.8. Crop management factor was found to be in the range of 0.0 to 0.3 with a mean value of 0.0327 as shown in Table 5.4.

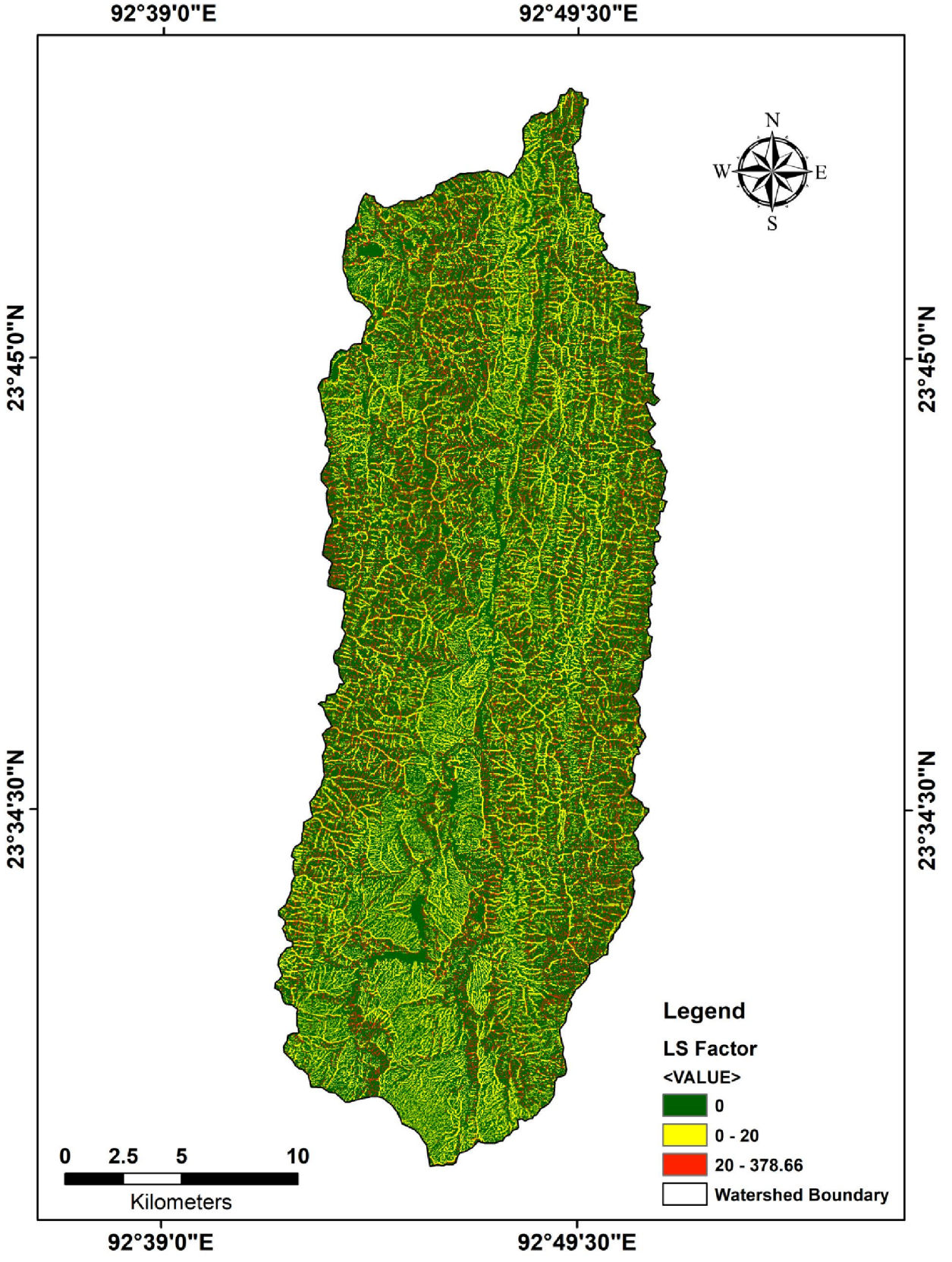


Figure 5.6 LS factor Map

Table 5.4 Image classification details and the corresponding C and P factor value.

LULC	Descriptions	C factor	P factor
Settlement	Land covered by concrete, including airport runway, residential, industrial, commercial buildings, open-roof concrete structures, other human-made structures.	0.0	1
Current jhumland	Areas characterized by grasses, herbs, and crops, including current jhum.	0.3	0.28
Jhum fallow	This category includes land with sparse vegetation, scrub land and land with barren rocks.	0.15	1
Natural forest	Land characterized by relatively moderate and thick forest vegetation.	0.005	1
Water body	Surface covered with river water only	0.280	1

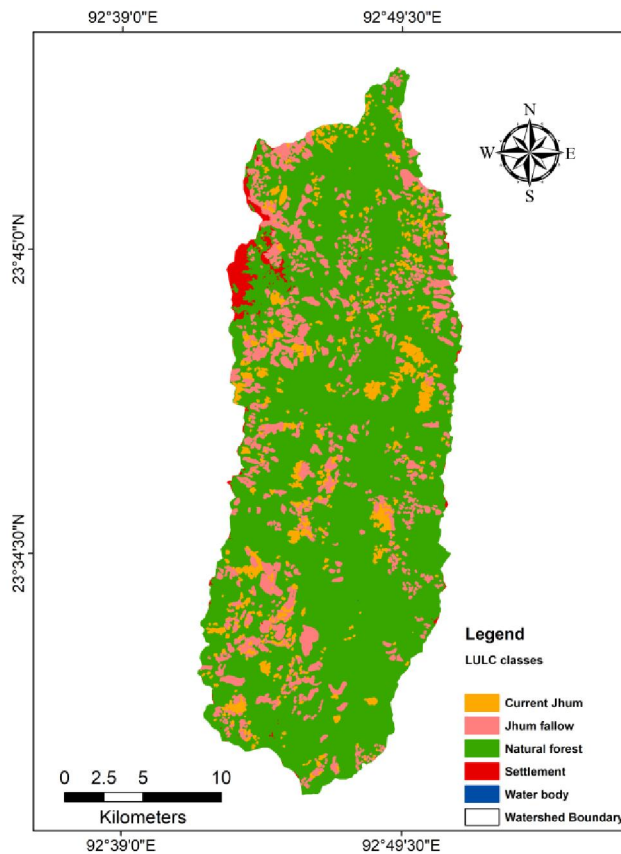


Figure 5.7 LULC Map of the study area

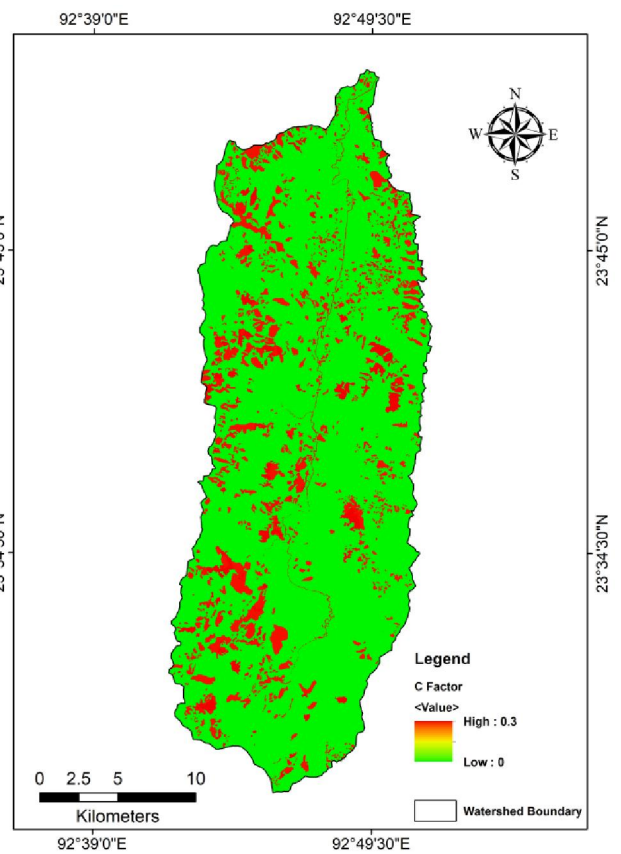


Figure 5.8 Crop management factor map

6.8 Practice management factor (P)

Practice management factor is the ratio of soil loss with a specific conservation practice to the corresponding loss with up and down slope cultivation (Debral, et al., 2008; Das, et al., 2018). This factor helps in reducing the rate of soil erosion by altering the flow direction of runoff due to preventive measures such as contour bounding, terraces, silt fences and proper drainage systems which reduces the runoff rate (Renard and Foster 1983).

In the study area, no major conservation practice is followed except terrace farming activities in jhum land in some areas. The values for P factor were assigned as 0.28 for area under jhum cultivation and 1.0 for other area (Debral, et al., 2008; Zonunsanga, R. 2016; Pandey, et al., 2009) (Table 5.4). The magnitude and the spatial distribution of P-factor are shown in Fig. 5.9 and the value ranges from 0.28 to 1 with a mean value of 0.971.

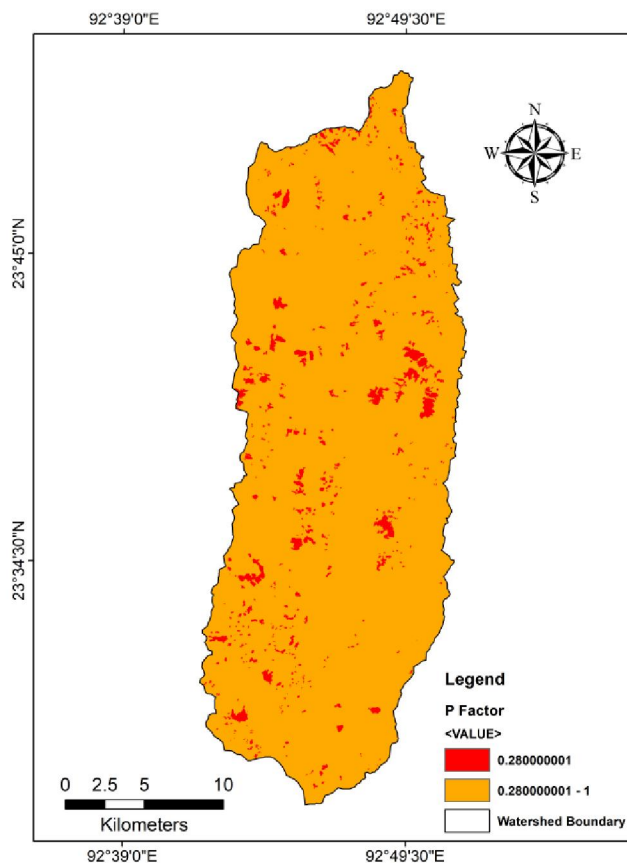


Figure 5.9 Practice management factor map

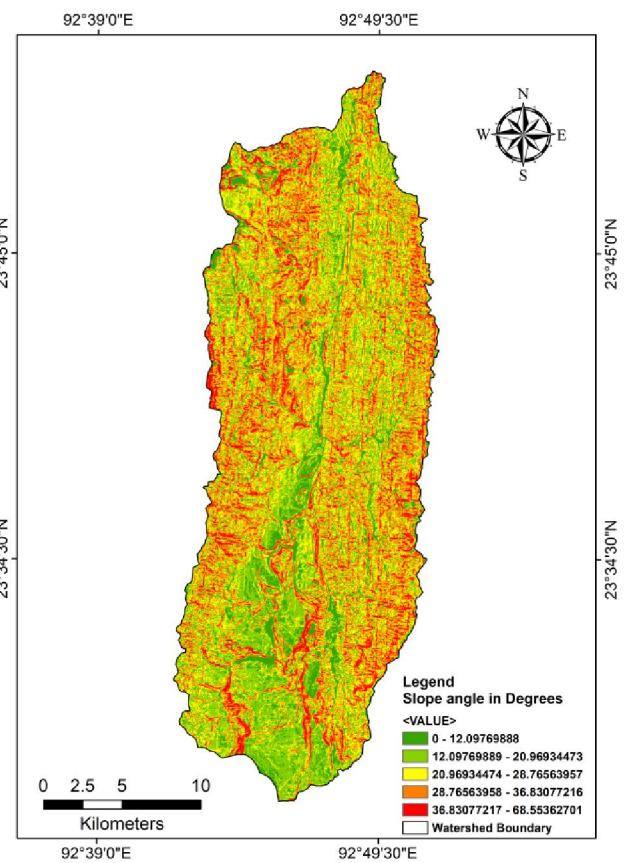


Figure 5.10 Spatially distributed soil loss Map of upper Tuirial Watershed

5.9 Average annual soil loss

Average annual soil loss was estimated by multiplying the different RULSE factors such as R, K, LS, C and P using raster calculator in Arc GIS. From figure 5.10 it can be observed that the annual soil loss of the area ranges from 0 to 34323.3 Mg ha⁻¹ yr⁻¹ with mean value of 88.875 and standard deviation of 457.65.

5.10 Erosion Risk Map

Erosion risk has been grouped into six classes based on the rate of erosion (Table 5.5). Out of the total area of the watershed, 37489.71 ha (70.21%) falls under slight/very low erosion risk zone where the erosion rate is 0 to 5 Mg ha⁻¹ yr⁻¹. A total of 3484.96 ha (6.53 %) of the area falls under very high erosion risk zone with an erosion rate of 20 to 40 Mg ha⁻¹ yr⁻¹ and 5295.41 ha (9.92%) to very severe soil erosion risk (>80 Mg ha⁻¹ yr⁻¹) zone. These values in the erosion risk map (Figure 5.11) do not represent the actual rate of erosion rather these classes are the representation of the spatial distribution of erosion risk zones for each class.

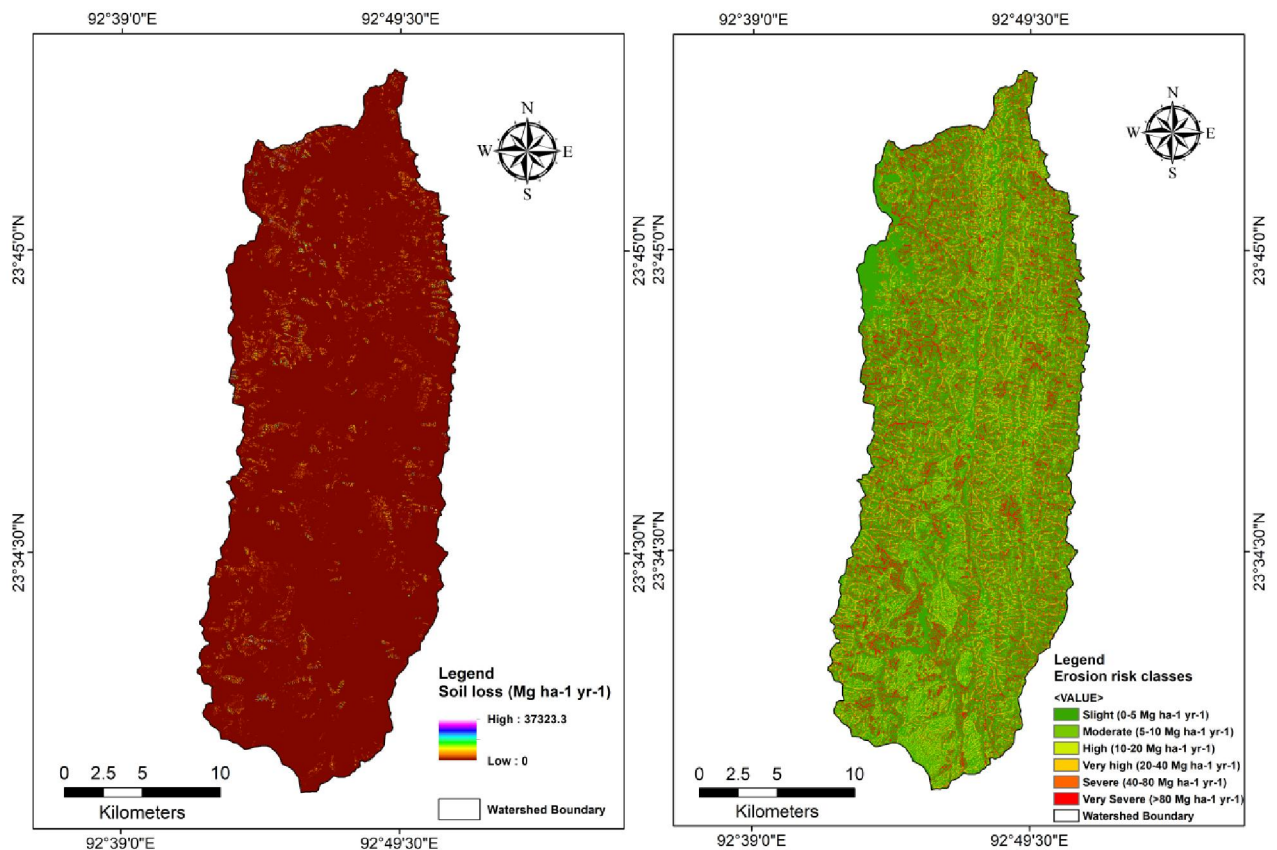


Figure 5.11 Spatial distribution of soil erosion and soil erosion risk map of the study area

Table 5.5 Spatial distribution of soil loss and erosional risk classes.

Erosion Risk Classes	Soil Loss (Tonnes/Hectare/Year)	Area in Hectare	Area in %
Slight	0-5	37489.71	70.21
Moderate	5-10	800.09	1.50
High	10-20	1877.81	3.52
Very high	20-40	3484.96	6.53
Severe	40-80	4445.08	8.33
Very severe	>80	5295.41	9.92

5.11 Results and Discussions

In Figure 5.11 (First map) the maximum value 34323.3 is the value of soil loss of only one pixel, it does not signify any overall soil loss scenario of the study area. The calculation of soil loss of that pixel is shown below:

Pixel Size = 30 m x 30 m

Area of one pixel = $900 \text{ m}^2 = 0.09 \text{ hectare}$

Therefore the soil loss in that pixel = $34323.3 \times 0.09 = 3089.07 \text{ Mg ha}^{-1} \text{ yr}^{-1}$

And mean pixel values of

$R = 1116.77 \text{ M J mm ha}^{-1} \text{ h}^{-1} \text{ year}^{-1}$

$K = 0.57 \text{ t ha h ha}^{-1} \text{ MJ}^{-1} \text{ mm}^{-1}$

$LS = 5.71$

$C = 0.0327$

$P = 0.971$

Thus average soil loss = Product of mean pixel values of R, K, LS, C and P

$= 115.4 \text{ tonnes/hectare/year}$

The total soil loss of the study watershed = Watershed Area x Mean Value

$$= 53393.09 \text{ hectare} \times 115.4 \text{ Mg ha}^{-1} \text{ yr}^{-1}$$

$$= 6.161 \text{ million Mg yr}^{-1}$$

5.12 Summary of findings

An attempt has been made to prepare an erosion risk map where the slopes and vegetation cover are taken into account. From the map, the areas prone to severe erosion are clearly visible as shown in fig.5.10. Also, field data have been collected to analyze the present condition of the erosion prone areas. It is observed that excessive erosion risk areas are characterized by large areas of fallow lands formed due to agriculture which are eroded mainly due to gulling and overland flow. Much of the areas is steeply sloping which increases the rate of erosion. The severe erosion risk areas include the land in the vicinity of rivers, where the land is very steep and moreover, small channels (rills) gear up the process. Some of the areas which are prone to erosion are shown in the following plates (Plates 5.1-5.4). Low erosion risks areas are those regions covered by thick forests.



Plate 5.1 A common phenomenon in the mountainous region shows the burning and clearing of forest cover through Jhum activity for cultivation.



Plate 5.2 Terrace farming (Top of the Photo) is more common in the hilly terrain and current jhum land (below the photograph) ready for cultivation.



Plate 5.3 Manual sand seiving is common hilly rievrr beds for construction purpose extracted form the Tuirial river bed in the study area.



Plate 5.4 Huge deposition of sediments on the river bed of Chite Lui sub-watershed, Eastern part of the Aizawl city area in Tuirial basin.

CHAPTER- 6

TEMPORAL CHANGE DETECTION OF LAND USE/LAND COVER

6.1 Introduction

Land use/land cover change is a dynamic and continuous process which changes its status with time. Analysis of Historical and current status of the land cover is essential for efficient environmental management (Gupta & Munshi, 1985; Mas, 1999; Lambin, et al., 1999; Gong, et al., 2008; Garedeew, et al., 2009; Vivekananda, et al., 2020). Updated and accurate LULC maps are of considerable significance for proper planning, global change, environment monitoring, estimation of natural resources and the estimation of forest degradation (Vivekananda, et al., 2020). Land use refers to uses of landscape for different purposes such as for developmental activities, conservation, recreation areas, wildlife habitats, agricultural land, and built-up, etc., (Reis, 2008). Land cover refers to the physical (natural) features of the land surface such as wetlands, impervious surfaces, agricultural land, soil, pastures land, water and other natural landscapes (Prakasam, 2010). The present study carried out to detect the temporal changes of land use/cover that had occurred in time span of 18 years i.e. for the year 2000 to 2018. The information and status of land use/cover (LULC) help to design an efficient and sustainable environmental management program. Satellite imagery has the potential for providing spatial and temporal consistent data for studies on monitoring changes in land use pattern (Fichera, et al., 2012; Mallupattu and Reddy, 2013; Carranza, et al., 2014). To achieve this objective, Landsat satellite imageries of two different time periods, i.e., Landsat Enhanced Thematic Mapper+ (ETM+) of 2000 and Landsat Operational Land Imager (OLI) of 2018 were acquired and the changes were quantified for statistical assessment. Various studies carried out worldwide by Landsat imagery for monitoring long term environmental changes (Sundarakumar, et al., 2012; Wang, et al., 2009; Muttitanon and Tripath, 2005; Mustafa, et al., 2007, Zhu, et al., 2016; Vicente-Serrano, et al., 2018). The various land/cover identified in the study area are built-up, jhumland, scrubland and forest. Though water body also exist in the study area as river water but the area covered is negligible hence it was not classified separately.

6.2 Materials and Methodology

Materials used in the present study include multispectral satellite imagery of Landsat 7 (ETM+) acquired on 17th March 2000 with 30 m spatial resolution, Landsat 8 (OLI)

acquired on 11th March 2018 with 30 m resolution, ground reference data (GPS coordinates) obtained from field surveys, Scan toposheets of 1:50,000 scale covering the study area prepared by SOI in 1986, Google Earth pro, ERDAS Imagine 2014 and Arc Map 10.3 software.

The quantitative method of change detection was used in this research. In the change detection method, each satellite image was classified in Erdas imagine by maximum likelihood algorithm classification method. The FCC (False Colour Composite) image of band combination 5–4–3 for Landsat 8 image and band combination of 4-3-2 for Landsat 7 image was used for the identification and classification of different land use /land cover pattern in the study area (Fig. 6.2).

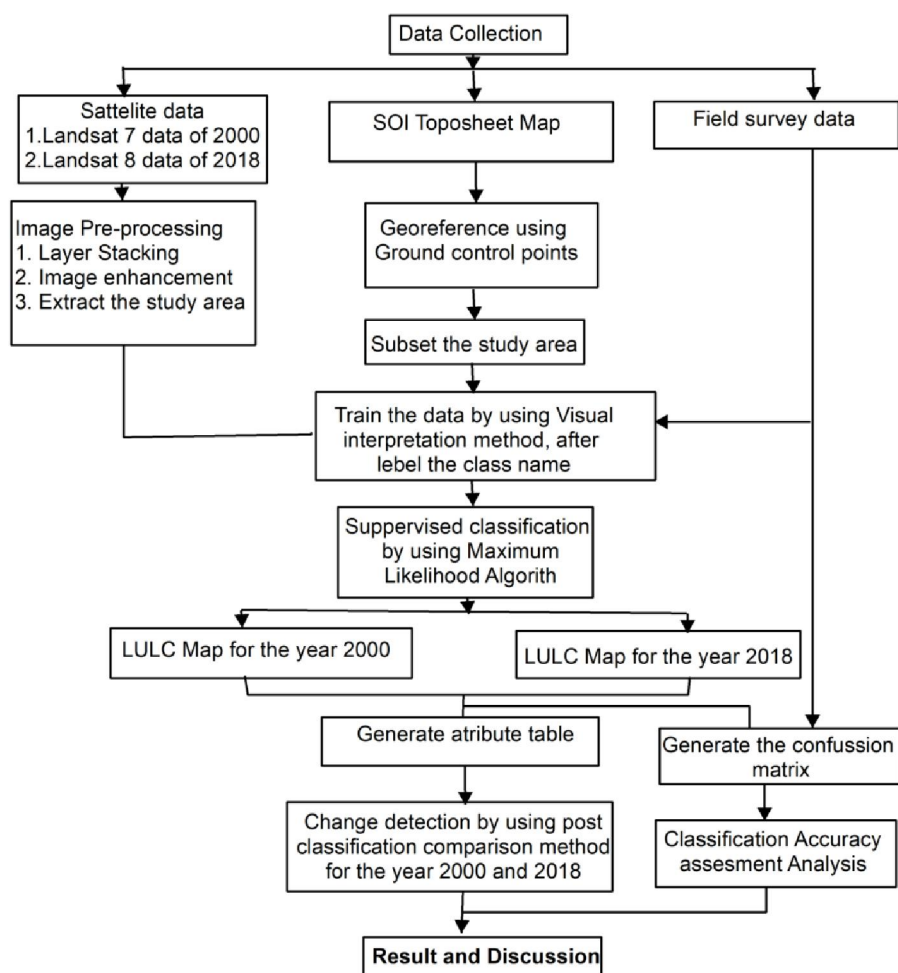


Figure 6.1 Flowchart demonstrating the methodology followed in present study.

The resulting LULC maps obtained after the classification are then compared pixel-by-pixel approach by using a change detection matrix. The methodology adopted in this study

is as follows: (1) data collection (2) pre-processing (3) selection of training data samples (4) LULC classification scheme (5) image classification, (6) accuracy assessment and (7) change detection. Figure 7.1 depicts the flow chart that illustrates the methodology included in this study.

6.3 Image classification scheme

The NRSC (National Remote Sensing Centre) Level I LULC classification scheme was adopted in this study (NRSC and ISRO, 2011). The study area was broadly classified into four different classes such as built-up, jhumland, scrubland and forest (Fig. 6.3). Multi-temporal Landsat images of the study area were used to study and classify the land cover types. The Maximum Likelihood Classifier algorithm of supervised classification was used in this study by taking spectral signature files of all the classes. Similar methodology has been widely used for the classification of medium-resolution satellite imagery (Gautam, and Narayanan, 1983; Anil, et al., 2011; Brahabhatt, et al., 2000; Ratnaparkhi, et al., 2016; Zubair Iqbal & Javed Iqbal, 2018; Bayarsaikan, et al., 2009). The detailed description of the classes is provided in Table 6.1 and the land use/land cove map of the study area is shown in Figure 6.3.

Table 6.1 Image classification details.

Built-up	Land covered by concrete, including road networks, residential, industrial, commercial buildings, educational institutes, transportation, open-roof concrete structures, other human-made structures and solid waste landfills.
Jhumland	Areas characterized by grasses, herbs, and crops, including current jhum and fallow land.
Scrubland	This category includes land with sparse vegetation and land with barren rocks.
Forest	Land characterized by relatively sparse forest vegetation.

6.4 Classification accuracy assessment

Classification accuracy assessment is an essential step after image classification. For accuracy assessment of image classification, 40 samples from each class were generated by random selection from FCC image as reference points. These points were then superimposed

on classified image to check pixel to pixel verification. Using special analyst tool in arc map, ‘extract values to points’ command was used to get the pixel value of each reference point from the classified raster image. By comparing the reference points with the pixel values, error matrix and kappa statistics for the two classified images were generated (Table 6.2 and Table 6.3). This process was performed for both the classified images (i.e., 2000 and 2018).

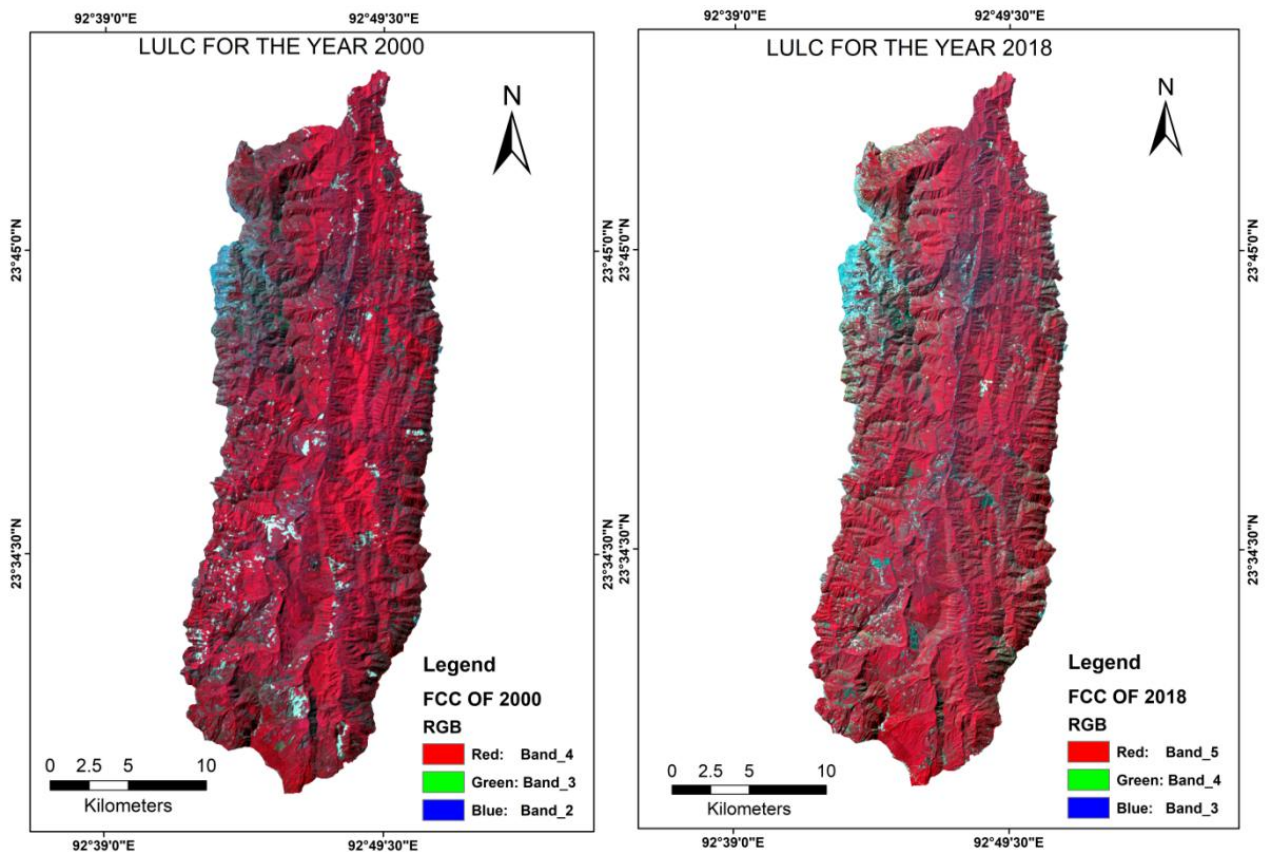


Figure 6.2 FCC images for the year 2000 and 2018

Table 6.2 Confusion matrix of 2000 LULC map of the study area.

2000	Built-up	Jhumland	Scrubland	Forest	Total (user)
Built-up	28	12	0	0	40
Jhumland	6	34	0	0	40
Scrubland	0	10	26	4	40
Forest	0	0	0	40	40
Total (producer)	34	56	26	44	160

Table 6.3 Confusion matrix of 2018 LULC map of the study area.

2018	Built-up	Jhumland	Scrubland	Forest	Total (user)
Built-up	32	8	0	0	40
Jhumland	10	24	6	0	40
Scrubland	0	2	38	0	40
Forest	0	0	0	40	40
Total (producer)	42	34	44	40	160

Values in each row represent the classes resulting from the classified image, whereas the columns represent the classes identified by the user from the reference values. The diagonal cells of the error matrix indicate the total number of correctly identified pixels for each class of the reference and classified data. The off-diagonal cells represent the incorrectly identified pixels, which indicate the error between reference data and classified data.

The user's accuracy is the accuracy from the point of view of a map user and Producer's accuracy is the map accuracy from the point of view of the map maker. The formula adopted for overall accuracy, producer's accuracy, User's accuracy and Kappa coefficient (K) is shown below.

6.5 Accuracy assessment analysis

$$\text{Overall Accuracy \%} = \frac{\text{Total number of correctly classified pixels (diagonal)}}{\text{Total number of reference fixels}} \times 100$$

$$\text{User's Accuracy \%} = \frac{\text{Number of correctly classified pixels in each category}}{\text{Total number of classified pixels in that category (the row total)}} \times 100$$

$$\text{Producer's Accuracy \%} = \frac{\text{Number of correctly classified pixels in each category}}{\text{Total number of reference fixels in that category (the column total)}} \times 100$$

$$\text{Kappa Coefficient (K)} = \frac{(\text{Total Sample} \times \text{Total Corrected Sample}) - \sum(\text{Colm.Total} \times \text{Row Total})}{\text{Total Sample} \times \text{Total Sample} - \sum(\text{Colm.Total} \times \text{Row Total})}$$

Accuracy assessment for the year 2000

$$\text{Overall accuracy} = \frac{128}{160} \times 100 = 80\%$$

Accuracy assessment for the year 2018

$$\text{Overall accuracy} = \frac{134}{160} \times 100 = 83.75 \%$$

User's Accuracy

$$\text{Built-up} = \frac{28}{40} \times 100 = 70\%$$

$$\text{Built-up} = \frac{32}{40} \times 100 = 80\%$$

$$\text{Jhumland} = \frac{34}{40} \times 100 = 85\%$$

$$\text{Jhumland} = \frac{24}{40} \times 100 = 60\%$$

$$\text{Scrubland} = \frac{26}{40} \times 100 = 65\%$$

$$\text{Scrubland} = \frac{38}{40} \times 100 = 95\%$$

$$\text{Forest} = \frac{40}{40} \times 100 = 100\%$$

$$\text{Forest} = \frac{40}{40} \times 100 = 100\%$$

Producer's accuracy

$$\text{Built-up} = \frac{28}{34} \times 100 = 82.35\%$$

$$\text{Built-up} = \frac{32}{42} \times 100 = 76.19\%$$

$$\text{Jhumland} = \frac{34}{56} \times 100 = 60.71\%$$

$$\text{Jhumland} = \frac{24}{34} \times 100 = 70.58\%$$

$$\text{Scrubland} = \frac{26}{26} \times 100 = 100\%$$

$$\text{Scrubland} = \frac{38}{44} \times 100 = 86.36\%$$

$$\text{Forest} = \frac{40}{44} \times 100 = 90.90\%$$

$$\text{Forest} = \frac{40}{40} \times 100 = 100\%$$

$$\text{Kappa Coefficient (K) of 2000} = \frac{(160 \times 128) - [(34 \times 40) + (5 \times 40) + (26 \times 40) + (44 \times 40)]}{160 \times 160 - [(34 \times 40) + (5 \times 40) + (26 \times 40) + (44 \times 40)]}$$

$$= 0.73$$

$$\text{Kappa Coefficient (K) of 2018} = \frac{(160 \times 134) - [(42 \times 40) + (34 \times 40) + (44 \times 40) + (40 \times 40)]}{160 \times 160 - [(42 \times 40) + (34 \times 40) + (44 \times 40) + (40 \times 40)]}$$

$$= 0.78$$

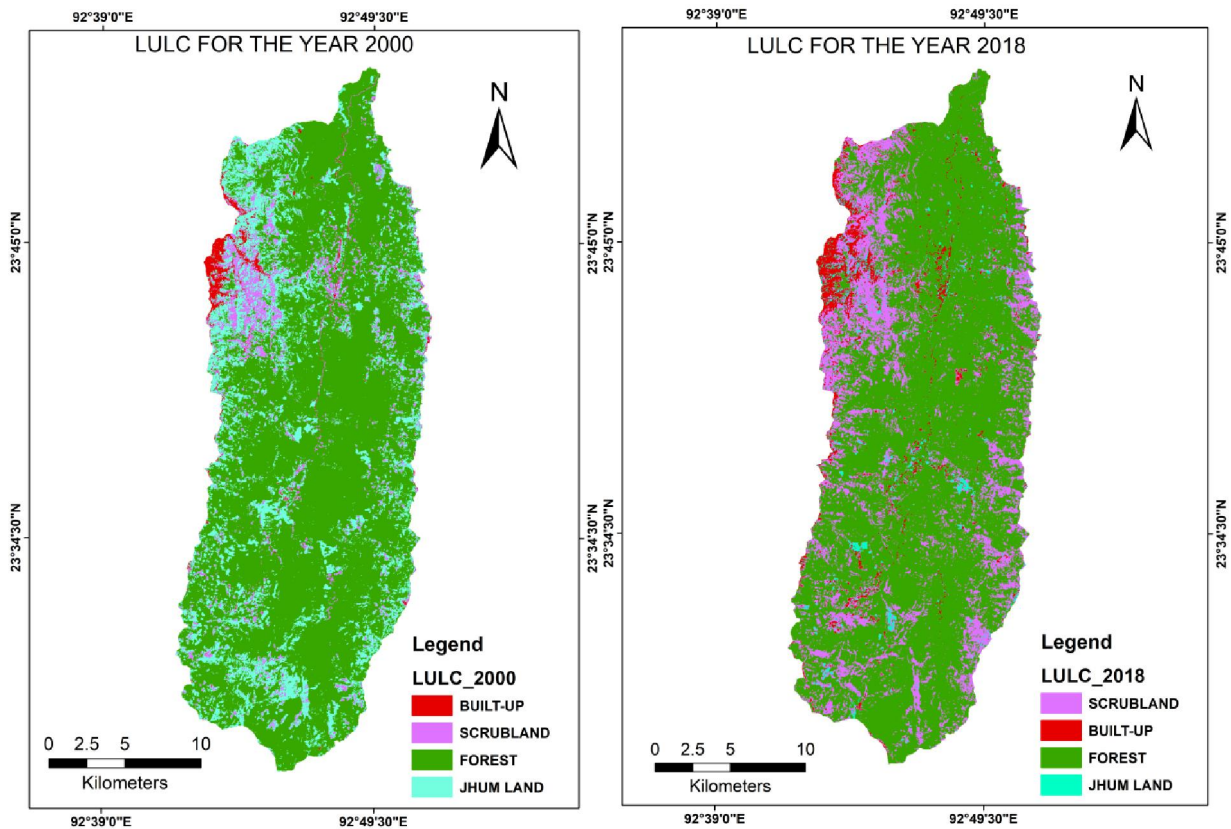


Figure 6.3 LULC classified map for the year 2000 and 2018

Table 6.4 Land use categories for 2000 and 2018 and their statistics.

LULC classes	Year 2000		Year 2018	
	Area in km ²	Area in %	Area in km ²	Area in %
Built-up	8.08	1.51	21.51	4.02
Scrubland	35	6.55	110.15	20.59
Jhumland	105.08	19.65	10.80	2.02
Forest	386.66	72.3	392.37	73.36

6.6 Results and discussions

The overall accuracy assessment of LULC classified image is found to be 80% for the image classification of Landsat 7 image of 2000 and the overall accuracy assessment for the Landsat 8 image of 2018 is 83.75%. Kappa coefficient is a measure of degree of accuracy and the value ranges from 0 to 1. Value close to 1 indicate high accuracy and vice versa. Generally kappa coefficient of more than 0.70 is considered to be good classification and accepted worldwide. Kappa coefficient value is found to be 0.73 for the year 2000 and 0.78

for the year 2018. Both the accuracy assessment show satisfactory result for the image classification.

The area under the LULC classes and its changes from 2000 to 2018 are presented in Table 6.4. The major changes observed in the study area are summarised below.

Built-up

The area under built-up increased from 8.08 km² in 2000 to 21.51 km² in 2018, which represents a net increase of 13.43 km². The area under built-up land increased due to the rise in population over time and also due to migration of population from remote villages to district head quarter.

Scrubland

The area under scrubland changes drastically from 35 km² in 2000 to 110.15 km² in 2018, which represent a net increase of 14.04%. This changed is due to unscientific agricultural activities in the past (jhum cultivation) causing destruction of natural forest into agricultural land and then abandoned as fallow land. At the later stage these fallow land converted into scrubland.

Jhumland

The area under jhumland decreases from 105.08 km² in 2000 to 10.80 km² in 2018, which represent a net decrease of 94.28 km². The area under jhumland decreased due to certain restrictions implemented by the state government against jhum practice to conserve the forest resources.

Forest

The area under forest cover increased significantly from 386.66 km² in 2000 to 392.37 km² in 2018, which represents a net increase of 5.71 km².

CHAPTER- 7

SUMMARY AND CONCLUSIONS

Upper Tuirial watershed is the western tributary of Barak River of Assam which covers an area of 534.81 km², originates in the state of Mizoram, NE India. This study was carried out to understand the sub surface lithological characteristics, hydrological behavior of catchment, morphology and evolution of the landforms. Keeping all the objectives in mind, morphometric analyses was carried out for 19 selected sub watersheds. Based on morphometric parameters and Multi Criteria Decision Making techniques, the sub-watersheds were prioritized for soil and water conservation measures. Groundwater potential zones were also identified in the study area. Morphotectonic study as one of the objective revealed that the study area is tectonically active. Quantification of soil loss was estimated using Universal Soil Loss equation model and finally the temporal change detection of LULC was analysed for a period of 2000 to 2018 using Landsat Imageries.

7.1 Conclusion about the Morphometry analysis

Based on the detail analysis of the linear, areal and relief aspects of morphometric parameters, it is found that upper Tuirial watershed, as well as those of the nineteen sub basins are characteristics of resistant and impermeable sub surface having homogeneous lithology, late youth to mature stage of erosional development and less storage capacity of water. Lower-order streams mostly dominate each basin. Based on mean weighted bifurcation ratio values it is found that sub watershed Kailian (5.34), Ngharum (5), Zilpui (5.49), Muthi (5.36) and Tuipawl (5) are structurally controlled basin. Sub watershed sakei, suibual, Belkhui, Nghalrawh, Tuiphu, Tuizual and Chite are slightly structurally distorted and the sub watersheds Nghathup, Sherbawk, Tuirial, Tulrital, Darkhuang, Suanghuan and SW18 are geologically controlled basin. High values of drainage density and drainage frequency with coarse to mostly medium texture ratio suggesting impermeable sub surface lithology, less infiltration rate, rugged topography, and high run off with high rate of erosion and dissection. Lg values for different sub watershed ranges from 0.09 km for Darkhuang to 0.20 km for Nghathup indicating high runoff, less infiltration and high rate of erosion. As the length of overland flow is very short, construction of artificial recharge structures is not feasible in the region. The constant of channel maintenance value is 0.25 km²/km i.e., only 250 square meters of area is needed to run 1000 meters of stream indicating that the area is

characterized by high surface runoff, low permeability, less infiltration and closely dissected. The circularity ratio values ranges from 0.44 for Kailian to 0.67 for Muthi indicates that the area is characterized by high to moderate relief, mature stage of geomorphic development and elongated in shape. The values of Relief ratio, gradient ratio and average slope angle indicate that the discharge capability of the watersheds is very high and ground water potential is meagre. The hypsometric integral value ranges from 0.5 to 0.55 indicating that all the sub watersheds have attained the steady state condition (mature geologic stage).

Study of the morphometric parameters are very useful for rainwater harvesting and watershed management plans. First- and second-order streams are not useful for constructing check dams in the study area because the streams are situated on high elevated area with steep slope. The unscientific landuse practices such as Juum cultivation enhances the runoff rate and hinder the rate of infiltration. This causes lowering of water table level particularly during extreme summer seasons. As a part of conservation measures, construction of artificial recharge structures and check dams at appropriate locations are advisable to increase the infiltration rate and reduce the erosion rate.

7.2 Conclusion about Soil and water conservation measures

Finally, based on morphometric analysis, the different sub watersheds were prioritized in terms of severity of erosion and found that sub-watershed Tulrital is highly susceptible to erosion followed by sub watersheds Zilpui, Tuiphu, SW18, Belkhui, Darkhuang, sakei, Chite, Ngharum, Muthi, Tuipawl, Nghalrawh, Kailian, Suanghuan, Suibual, Nghathup, Sakei, Sherbawk and the least erosive sub watershed is Tuirial.

7.3 Conclusion about Groundwater potential zones

The prioritisation of sub watersheds was carried out using 11 morphometric parameters to identify groundwater potential zones. Each morphometric parameter has significant values which are used as predicting parameters to characterise the sub subsurface lithology. Since all the parameters have different values for different sub watersheds, it is almost impossible to prioritise the best sub watershed groundwater resources. In order to deal with this type of complexity, multi criteria decision making techniques is applied. Thus, TOPSIS as one of the multi criteria decision making techniques was used in this study and is found to be very efficient in ranking and prioritising the sub-watersheds for groundwater potential zones. The result of this analysis revealed that sub watershed Kailian is the best

potential zones for groundwater resources and sub watershed Tulrital is found to be the most deficit zone of groundwater. The results of this work may be used by the decision makers, planners and public health engineering department to carry out water resources management plan for this region.

7.4 Conclusion about Morphotectonic study

From the analysis of various morphotectonic parameters, it is found that there is a strong relationship between topography and active deformation and is reflected in the geological and geomorphological set-up of the Upper Tuirial Basin. The lineament analysis indicate that there is only one set of prominent lineaments trending almost N-S direction and few lineaments oriented in all directions. The development of N-S oriented Faults/lineaments is expected in this region as the basin is under East-West tectonic compression due to collision of Indo-Burmese plates. The elongation ratio values found to be 0.56 indicating that the basin is slightly tectonically active. The Hypsometric Integral values vary from 0.50 for Suibual to 0.55 for Ngharum and 0.51 for the whole watershed indicating mature landscape and slightly tectonically active.

The values of asymmetry factor reveal that all the major channels have been shifted downstream to either right tilt or left tilt. This downstream shifting of river is possibly due to the obstruction by faulting. From the analysis of transversely topographic profiles, it is observed that sub watersheds of Tuipawl, Muthi, Chite, Suanghuan, Tuizual and Tulrital which are located on the left bank of the Upper Tuirial basin shows unpaired terraces tilting downstream eastward and another set of sub watersheds such as Nghathup, Sakei, Suibual, Ngharum, Zilpui, Tuiphu and Tuirial which are located on the right bank of the upper Tuirial watershed also shows unpaired terraces tilting westward. The presence of unpaired terraces on both the limbs suggesting that the formation of synclinal basin due to tectonic compression. Exceptionally high value of stream length gradient index is shown as knick zones along the longitudinal profile of sub watershed Chite, Muthi, Suanghuan, Tuizual, Ngharum and Tulrital. These anomalous high values cannot be due to rock resistance to erosion only, but there must be some strong tectonic activity.

The values of valley floor to valley height ratio indicate deep, narrow, V-shaped valleys due to intense incision and gradual uplift signifies strong tectonic activity. The mountain-front sinuosity values for different sub watersheds measured at different sections are found to be in the ranges of 1.02 to 1.52. These low values are the indication of active

tectonism in the watershed. Thus, the overall assessment of the geomorphic indices revealed that the tectonic uplift, lithology and climatic force played a significant role in the landscape evolution of the basin and the area has experienced differential uplift and erosion rates from time to time in the geological past.

7.5 Conclusion about Soil erosion assesent

The average annual soil loss per unit area is found to be $115.4 \text{ Mg ha}^{-1} \text{ yr}^{-1}$ with a total soil loss of 6.161 million Mg yr^{-1} . This high value is an indication of severe erosion zones. About one-fourth (24.78%) of the total basin area was projected to be very soil erosion risk area that need immediate conservation measures. Since there were no baseline field data available on soil erosion from the study area, hence no calibration/validation of the result could be made. It was also well observed that severe erosion zones are usually grounded upon areas with considerably unprotected areas like Jhum fallows and less vegetative areas with higher slope values while that of slight erosion in areas with almost negligible slope values with thick forest cover area. The areas with extreme severe soil loss should be given more importance in terms of erosion control. From this study it is also found that the severe erosion zones are mostly in areas with high slope values. While slight erosions are mostly observed in areas with low slope values.

7.6 Conclusion about LULC change detection

This study examines the LULC changes of the upper Tuirial watershed using multi-temporal satellite imagery for the period 2000-2018 that provides current and historical LULC conditions. Maximum likelihood Supervised classification algorithm was employed to monitor LULC transformations. The overall accuracy assessment and kappa coefficient values showed accepted accuracy limit. Over the study period, there is a significant changes observed in LULC classes, as evidenced by a sharp increase in built-up from 1.51% in 2000 to 4.02 % in 2018 and a net increase of 14.04% of scrubland within the landscape. The period 2000-2018 has shown a sharp decrease of jhumland from 19.65 % to 2.02% and the forest cover remains almost unchanged. This study will be useful for the forest department to carry out forestation activities in the spatially distributed scrubland and also useful in monitoring the changes that area happening in our ecosystem and environment. The quantification of LULC changes in the study area is very useful for environmental management groups, policy makers and for the general public to better understand the surrounding.

REFERENCES

- Adornado, H. A., Yoshida, M., and Apolinar, H., (2009). Erosion Vulnerability Assessment in REINA, Quezon Province, Philippines with Raster-based Tool Built within GIS Environment, *J. Agric. Res.*, **18**: 24–31.<https://doi.org/10.3173/air.18.24>
- Agarwal, C. S., (1998). Study of Drainage Pattern Through Aerial Data in Naugarh Area of Varanasi District, U. P. *Journal of the Indian Society of Remote Sensing*, **26** (4): 169-175.
- Ahmad, S. and Bhat, M. I., (2012). Tectonic geomorphology of the Rambhara basin, SW Kashmir Valley reveals emergent out-of-sequence active fault system. *Himalayan Geology*, **33** (2):162-172.
- Ahmed, F. and Rao, K. S., (2015). Prioritization of Sub watersheds based on Morphometric Analysis using Remote Sensing and Geographic Information System Techniques. *International Journal of Remote Sensing and GIS*, **4** (2): 51-65.
- Ahmed, F., Rao, U. B. Ch., and Rao, K. S., (2012). Drainage basin morphometry and tectonic implications of Tuikum watershed, Mizoram. *Journal of Geography Association of Mizoram*, Aizawl, **7**: 51 – 59.
- Akram, F., Rasul, M. G., Khan M. M. K., and Amir, M. S., (2012). Automatic delineation of drainage networks and catchments using DEM data and GIS capabilities: a case study. 18th Australasian Fluid Mechanics Conference Launceston, Australia.: 4.
- Anil, N. C., Jai Sankar, G., Jagannadha Rao, M., Prasad, I. V. R. K. V., and Sailaja, U., (2011). Studies on land use/land cover and change detection from parts of South West Godavari District, A.P-using remote sensing and GIS techniques. *Journal of Indian Geophysical Union*, **15** (4): 187–194.
- Arefin, R., Mohir, M. M. I., and Alam, J., (2020). Watershed prioritization for soil and water conservation aspect using GIS and remote sensing: PCA-based approach at northern elevated tract Bangladesh. *Appl. Water Sci.*, **10** (4):1–19.
- Arlegui, L. E., and Soriano, M. A., (1998). Characterizing lineaments from satellite images and field studies in the Central Ebro basin (NE Spain). *Int. J. Remote Sens.*, **19** (16): 3169–3185.

- Arun, P. S., Jana, R. and Nathawat, M. S., (2005). A rule based physiographic characterization of a drought prone watershed applying remote sensing and GIS. *J. Indian Soc. Remote Sens*, **33** (2): 189–201.
- Arya, V.S., Hooda, R. S., Rao, T. B. V. M., Chaudhary, B. S., Prasad, J., Tiwari, A. K., Kudrat, M., Kumar, P., Ravindran, K. V., and Manchanda, M. L., (2002). Land resources development action plan using remote sensing and GIS: a case study in Ghaggar Watershed. *Inter-national Archives of Photogrammetry, Remote Sensing and Spatial Information Science (IAPRS&SIS)*, **34**: 665–670.
- Asl-Rousta, B., and Mousavi, S. J., (2018). A TOPSIS-based multicriteria approach to the calibration of a basin-scale SWAT hydrological model. *Water Resour.Manag.*, **33**: 439–452. <https://doi.org/10.1007/s11269-018-2111-5>
- Azor, A., Keller, E. A., and Yeats, R. S., (2002). Geomorphic indicators of active fold growth: South Mountain-Oak Ridge anticline, Ventura basin, Southern California. *Geol. Soc. Amer. Bull.*, **114** (6): 745–753.
- Barman, B. K.,Gogoi, C., and Rao, K. S., (2019). Remote sensing and GIS application for morphometric analysis of Upper Mat watershed, Serchhip district, Mizoram. *Journal of Applied Geochemistry.*, **21** (2):185-195.
- Bates, R. L., and Jackson, J. A., (1987). *Glossary of geology*, 3rdEdn. American Geological Institute, Alexandria, Virginia.
- Bayarsaikan, U., Boldgiv, B., Kim, K., Park, K., and Lee, D., (2009). Change detection and classification of land cover at Hustai National Park in Mongolia. *Int. Jour. Appl. Earth Obser. and Geoinfor.*, **11**(4): 273–280. <https://doi.org/10.1016 /j.jag.2009.03.004>.
- Bera, A., (2017).Assessment of soil loss by universal soil loss equation (USLE) model using GIS techniques: A case study of Gumti river basin, Tripura, India; *Model. Earth Syst. Environ.*, **3**: 29.
- Bhatt,C. M., Chopra, R., andSharma, P. K., (2007). Morphotectonic analysis in Anandpur Sahib area, Punjab (India) using remote sensing and GIS approach. *Journal of the Indian Society of Remote Sensing*, **35** (2): 129-139.
- Bhatt, D. K., (1989). Lithostratigraphy of the Karewa Group, Kashmir valley, India and a critical review of its fossil record, 1–85.

- Bhunias, G. S., Samanta, S., and Pal, B. (2012). Quantitative Analysis of relief Characteristics using Space Technology. *Int. Jour. Phys. and Soc. Sci.*, **2**, Issue 8: 350-365.
- Bishop, M. P., Shroder, J. F., Bonk, R., and Olsenholler, J., (2002). Geomorphic change in high mountains: a western Himalayan perspective. *Global and Planetary Change*, **32**: 311–329.
- Biswas, S., Sudhakar, S., and Desai, V. R., (1999). Prioritisation of sub-watersheds based on morphometric analysis of drainage basin: A remote sensing and GIS approach. *Jour. Ind. Soc. Remote Sensing*, **27** (3): 155-166.
- Bloom, A. L., (1978). *Geomorphology, a Systematic Analysis of Late Cenozoic Landforms*. Prentice-Hall, Englewood Cliffs, NJ.
- Brahabhatt, V. S., Dalwadi, G. B., Chnabra, S. B., Ray, S. S., and Dadhwal, V. K., (2000). Land use/land cover changes mapping in Mahi canal command area, Gujarat, using multi-temporal satellite data. *Jour. Ind. Soc. Remote Sensing*, **28** (4): 221–232. <https://doi.org/10.1007/BF02990813>
- Brown, C. E., (1992). Use of principal-component, correlation and stepwise multiple regression analysis to investigate selected physical and hydraulic properties of carbonate-rock aquifers. *Jour. Hyd.*, **147** (1–4): 169–195. [https://doi.org/10.1016/0022-1694\(93\)90080-S](https://doi.org/10.1016/0022-1694(93)90080-S).
- Bull, W. B., (1977). *Tectonic geomorphology of the Mojave Desert*. U.S. Geological Survey Contract Report 14-08-001-G-394. Menlo Park, CA: Office of Earthquakes, Volcanoes, and Engineering.
- Bull, W. B., (1978). *Geomorphic tectonic classes of the south front of the San Gabriel Mountains, California*. U.S. Geological Survey Contract Report 14-08-001-G-394. Menlo Park, CA: Office of Earthquakes, Volcanoes, and Engineering.
- Bull, W. B., and McFadden, L. D., (1977). *Tectonic geomorphology north and south of Garlock fault, California*. In: Doehring, D. O., (Ed.) *Geomorphology in Arid Regions: A Proceedings volume of the 8th Annual Geomorphology Symposium*, State University of New York, Binghamton, 115-138.
- Carranza, M. L., Frate, L., Acosta, A.T.R., Hoyos, L, Ricotta, C., and Cabido, M., (2014). Measuring forest fragmentation using multitemporal remotely sensed data: three

- decades of change in the dry Chaco. *European Journal of Remote Sensing*, **47**: 793-804. doi: <http://dx.doi.org/10.5721/EuJRS20144745>.
- Chitra, C., Alaguraja, P., Ganeshkumari, K., Yuvaraj, D. and Manivel, M., (2011). Watershed characteristics of Kundah sub basin using remote sensing and GIS techniques. *Int. Jour. Geomat. Geosci.*, **2** (1): 311.
- Chopra, R., Dhiman, R. D., and Sharma, P.K., (2005). Morphometric analysis of sub-watersheds in Gurdaspur district, Punjab using remote sensing and GIS techniques, *Jour. Ind. Soc. Rem. Sens.*, **33** (4): 531-539.
- Choudhari, P. P., Nigam, G. K., Singh, S. K., and Thakur, S., (2018). Morphometric based prioritization of watershed for groundwater potential of Mula river basin, Maharashtra, India. *Geol. Ecol. Landsc.*, **2** (4): 256–267. <https://doi.org/10.1080/24749508.2018.1452482>.
- Chow, V. T., (1964). *Handbook of applied hydrology*. McGraw Hill Inc, New York.
- Clarke, J. J., (1966). *Morphometry from map. Essays in geomorphology*. Elsevier, New York. : 235–274.
- Coates, D. R., (1956). *Quantitative geomorphology of small drainage basins of southern Indiana*: Office of Naval Research, 389-042, Technical Report no. 10.
- Cox, R. T., (1994). Analysis of drainage-basin symmetry as a rapid technique to identify areas of possible quaternary tilt-block tectonics: an example from the Mississippi embayment. *Geol. Soc. Amer. Bull.*, **106** (5): 571–581.
- Crosby, B., and Whipple, K., (2006), Knickpoint initiation and distribution within fluvial networks: 236 waterfalls in the Waipaoa River, North Island, New Zealand. *Geomorphology*, **82**: 16–38.
- Cuong, N. Q., and Zuchiewicz, W. A., (2001). Morphotectonic properties of the Lo River fault near Tam Dao in North Vietnam. *Nat. Hazards Earth Syst. Sci.*, **1**: 15–22.
- Dabral, P. P., Baithuri, N., and Pandey, A., (2008). *Soil Erosion Assessment in a Hilly Catchment of North Eastern India Using USLE, GIS and Remote Sensing: Water Resource Management*, DOI 10.1007/s11269-008-9253-9.
- Dar, R. A., Romshoo, S. A., Chandra, R., and Ahmad, I., (2014). Tectono-geomorphic study of the Karewa Basin of Kashmir Valley. *Jour. Asian Earth Sci.*, **92**: 143–156.

- Das, A. K., and Mukherjee, S., (2005). Drainage morphometry using satellite data and GIS in Raigad district, Maharashtra. *J. Geol. Soc. India*, **65**: 577–586.
- Das, B., Paul, A., Bordoloi, R., Tripathi, O. P., and Pandey, P., (2018). Soil erosion risk assessment of hilly terrain through integrated approach of RUSLE and geospatial technology: A case study of Tirap District, Arunachal Pradesh; *Model. Earth Syst. Environ.*, **4** (1): 373–381.
- Das, D., (2014). Identification of Erosion Prone Areas by Morphometric Analysis Using GIS. *J. Inst. Eng. India Ser.*, **95** (1): 61–74.
- Das, S., and Gupta, K., (2019). Morphotectonic analysis of the Sali River basin, Bankura district, West Bengal. *Arabian Journal of Geosciences*, **12**: 244.
- Dehbozorgi, M., Pourkermani, M., Arian, M., Matkan, A. A., Motamedi, H., and Hosseiniasl, A., (2010). Quantitative analysis of relative tectonic activity in the Sarvestan area, central Zagros, Iran. *Geomorphology*.
- Delcaillau, B., Carozza, J. M., and Laville, E., (2006). Recent fold growth and drainage development: The Janauri and Chandigarh anticlines in the Siwalik foothills, northwest India. *Geomorphology*, **76**: 241-256.
- Derakshani, R., Shafi, H., and Farhoudi, G., (2010). Evaluation of tectonic activity of Babakouhi anticline using morphometric parameters. *World Applied Sci. J.*, **10**: 655-658.
- Dornkamp, J.C., and King, C.A.M., (1971). Numerical analyses in geomorphology, an introduction. St.Martins Press, New York.,: 372.
- Dove, N., (1957). The ratio of relative and absolute altitude of Mt. Camel. *Geog. Rev.*,**47**: 564- 569.
- Dutta, D., Das, S., Kundu, A., and Taj, A. (2015). Soil erosion risk assessment in Sanjal watershed, Jharkhand (India) using geo-informatics, RUSLE model and TRMM data. *Model Earth Syst. Environ.*,**1** (4): 37.
- Dutta, N., and Sarma, J. N., (2015). A Morphometric study of the Sonai River Basin, Barak Valley, NE India. *Jour. Assam Sci. Soc.*, **56** (2) : 74-89.

- Dutta, N., and Sarma, J. N., (2016). Morphotectonic analysis of the Madhura river basin, Barak valley, north-east India. *SE. Asian Jour. of Sedimentary Basin Research* 2-3-4(1): 23-27.
- El Hamdouni, R., Irigaray, C., Fernández, T., Chacón, J., and Keller, E., (2008). Assessment of relative active tectonics, southwest border of Sierra Nevada (southern Spain). *Geomorphology*, **96** (1–2): 150–173.
- Evans, P., (1932). Tertiary Succession in Assam, *Trans. Mining and Geological Institute India*. **27**: 161– 246.
- Evans, P. (1964). The tectonic framework of Assam. *Jour. Geol. Soc. India*. **5**: 80-96.
- Fagbohun, B. J., Anifowose, A. Y. B., Odeyemi, C., Aladejana, O. O., and Aladeboyeje, A. I., (2016). GIS-based estimation of soil erosion rates and identification of critical areas in Anambra sub-basin, Nigeria. *Modelling Earth Systems and Environment*. **2** (3): 1-10.
- Farhan, Y, Anbar, A., Al-Shaikh, N., Almohammad, H., Alshawamreh, S. and Barghouthi, M., (2018). Prioritization of sub-watersheds in a large semi-arid drainage basin (Southern Jordan) using morphometric analysis, GIS, and multivariate statistics. *Agricultural Science*, **09** (04): 437– 468. <https://doi.org/10.4236/as.2018.94031>
- Farhan, Y., and Nawaiseh, S., (2015). Spatial assessment of soil erosion risk using RUSLE and GIS techniques, *Environ. Earth. Sci.*, **74**: 4649–4669,
- Farhan, Y., and Anaba, O., (2016). A Remote Sensing and GIS approach for prioritization of WadiShueib mini-watersheds (Central Jordan) based on morphometric and soil erosion susceptibility analysis. *Jour.Geogr. Inf. Syst.*,**8** (01): 1–19.
- Farhan, Y., Anbar. A., Al-Shaikh, N., and Mousa, R., (2017). Prioritization of semi-arid agricultural watershed using morphometric and principal component analysis, Remote Sensing, and GIS techniques, the Zerqa river watershed, Northern Jordan. *Agricultural Science*, **8** (1): 113–148. <https://doi.org/10.4236/as.2017.81009>
- Farooqi, I. A., and Desai, R. N., (1974). Stratigraphy of Karewas, India. 299–305.
- Fichera, C. R., Modica, G., and Pollino, M., (2012). Land Cover classification and change-detection analysis using multi-temporal remote sensed imagery and landscape metrics. *European Journal of Remote Sensing*, **45**: 1-18.

- Gajbhiye, S., Mishra, S. K., and Pandey, A., (2014). Hypsometric analysis of Shakkar river catchment through geographical information system. *Jour. Geol. Soc. Ind.*, **84**: 192-196.
- Gajbhiye, S., Mishra, S. K. and Pandey, A. (2014). Prioritizing erosion-prone area through morphometric analysis: A Remote Sensing and GIS perspective. *Appl. Water Sci.*, **4** (1): 51–61. <https://doi.org/10.1007/s13201-013-0129-7>
- Ganguly, S., (1993). Stratigraphy, sedimentation and hydrocarbon prospects of the Tertiary succession of Tripura and Cachar (Assam). *Indian Jour. Geol.*, **65** (3):145-180.
- Ganguly, S., (1983). Geology and hydrocarbon prospects of Tripura - Cachar - Mizoram region. *Jour. Petrol. Asia*, **6** (IV): 105 - 109.
- Ganguly, S., (1975). Tectonic evolution of Mizo Hills. *Bull. Geol. Min. Met. Soc. India*. **48**: 28 - 40.
- Ganju, J. L., (1975). Geology of Mizoram. *Bull. Geol. Min. Met. Soc. Ind.* **48**: 17 - 26.
- Garedew, E., Sandewall, M., Soderberg, U. and Campbell, B. M., (2009). Land-use and land cover dynamics in the Central Rift Valley of Ethiopia. *Environment Management*, **44**: 683-694. doi: <http://dx.doi.org/10.1007/s00267-009-9355-z>.
- Gautam, N. C., and Narayanan, L. R. A., (1983). Landsat MSS Data for Land Use/Land Cover Inventory and Mapping: A Case Study of Andhra Pradesh. *Journal of Indian Society of Remote Sensing*, **11**: 15-28.
- Glock, W. S., (1932). Available relief as a factor of control in the profile of a landform. *Jour. Geol.*, **40**: 74-83.
- Gopinath, G., Nair, A. G., Ambili, G. K., and Swetha, T. V., (2016). Watershed prioritization based on morphometric analysis coupled with multi criteria decision making. *Arabian Journal of Geosciences*. **9** (2): 129.
- Gopinath, G., Swetha, T.V. & Ashitha, M. K., (2014). Automated extraction of watershed boundary and drainage network from SRTM and comparison with Survey of India toposheet. *Arab Jour.Geosci.* **7**: 2625–2632. <https://doi.org/10.1007/s12517-013-0919-0>
- Gottschalk, L. C., (1964). Reservoir sedimentation in handbook of applied hydrology. McGraw Hill Book Company, New York (Section 7-1).

- Gupta, D. M., and Munshi, M. K., (1985). Urban change detection and land-use mapping of Delhi. *International Journal of Remote Sensing*, **6** (3–4): 529–534. <https://doi.org/10.1080/01431168508948474>
- Gurmessa, T. K., and Bárdossy, A., (2009). A principal component regression approach to simulate the bed-evolution of reservoirs. *Jour.Hydrol.*, **368** (1–4): 30–41.
- Hack, J. T., (1973). Stream profile analysis and stream- gradient index. *U.S. Geol.Surv. Jour. Res.*, **1**: 421–429.
- Hadley, R. F., and Schumm, S. A., (1961). Sediment sources and drainage basin characteristics in upper Cheyenne River basin, US Geological Survey Water-Supply Paper, **1531**: 198
- Hare, P. W., and Gardner, T. W., (1985). Geomorphic indicators of vertical neotectonism along converging plate margins, Nicoya Peninsula, Costa Rica. In: M. Morisawa and J. T. Hack (Eds.), *Tectonic geomorphology. Proceedings of the 15th Annual Binghamton Geomorphology Symposium*. Boston, MA: Allen & Unwin. 75–104.
- Horton, R. E., (1932). Drainage basin characteristics. *Tran. Amer.Geophys.Uni.*, **13**: 350–361.
- Horton, R. E., (1945). Erosional development of streams and their drainage basins; hydrophysical approach to quantitative morphology. *Geol.Soc. Amer. Bull.*, **56**: 275–370.
- Hung, L. Q., Batelaan, O., and De Smedt, F., (2005). Lineament extraction and analysis, comparison of LANDSAT ETM and ASTER imagery. In: Ehlers M, Michel U (Ed.) *Suoimuoi tropical karst catchment, Vietnam. Remote Sensing for environmental monitoring, GIS applications and geology, Proceedings of S. P. I. E.*
- Hwang, C. L., Yoon, K. S., (1981). *Multiple attribute decision-making: methods and applications*. Springer, New York.
- Jain, P. and Ramsankaran, R., (2019). GIS-based integrated multi-criteria modelling framework for watershed prioritisation in India-a demonstration in Marol watershed. *Jour.Hydrol.* <https://doi.org/10.1016/j.jhydrol.2019.124131>
- Jain, S., and Verma, P. K., (2009). Drainage Characteristics of Tectonically Active Areas: An Example from Rajasthan, India. *Int. Jour. Econ. and Environ. Geol.*, **1**: 11-16.

- Javed, A., Khanday, M. Y., and Ahmed, R., (2011). Watershed prioritization using morphometric and land use/land cover parameters: A Remote Sensing and GIS-based approach. *J Geol. Soc. India.* **78** (1): 63–75.
- John Wilson, J. S., Chandrasekar, N., and Magesh, N. S., (2012). Morphometric analysis of major Sub Watersheds in Aiyar and Karai Pottanar Basin, Central Tamil Nadu, India using Remote Sensing & GIS Techniques. *Bonfring Int. J. Ind. Eng. Manag. Sci.*, **2** (special issue 1): 8–15.
- Karunakaran, (1974). Geology and Mineral Resources of the North Eastern States of India. Misc. Publ., Geol. Surv. India. **30** (4): 93 - 101.
- Keller, E. A., (1986). Investigation of active tectonics: Use of surficial earth process. In R. E. Wallace (Ed.), *Active tectonics*. Washington, DC: National Academy press. 136–147.
- Keller, E. A., and Pinter, N., (1996). *Active tectonics: Earthquakes Uplift and Landscapes*. Prentice Hall, New Jersey. 338.
- Keller, E. A., and Pinter, N., (2002). *Active tectonic earth quake—uplift and landscape* (2nd Ed.). Prentice Hall Inc., New Jersey, Upper Saddle River, 337.
- Kelson, K. I., and Wells, S. G., (1989). Geologic influences on fluvial hydrology and bedload transport in small mountainous watersheds, northern New Mexico, USA. *Earth Surf. Process.* **14**: 671–690.
- Krishnamurthy, J., Srinivas, G., Jayaram, V., and Chandrasekhar, M. G., (1996). Influence of rock type and structure in the development of drainage networks in typical hard rock terrain. *ITC J.* **4** (3): 252–259.
- Kumar, A., Jayappa, K., and Deepika, B., (2011). Prioritization of sub-basins based on geomorphology and morphometric analysis using remote sensing and geographic information system (GIS) techniques. *Geocarto International*, **26**: 569–592.
- Kumar, R., Lohani, A. K., Sanjay, K., Chatterjee, C., and Nema, R. K., (2001). GIS based morphometric analysis of Ajay river basin up to Sarath gauging site of south Bihar. *Jour. Applied Hydrology.* **14** (4): 45-54.

- Lambin, E. F., Turner, B. L., Geist, H. J., Agbola, S. B., Angelsen, A., Folke, C., Bruce, J. W., Coomes, O. T., Dirzo, R., George, P. S., Homewood, K., Imbernon, J., Leemans, R., Li, X., Moran, E. F., Mortimore, M., Ramakrishnan, P. S., Richards, J. F., Steffen, W., Stone, G. D., Veldkamp, T. A., (2001). The causes of land-use and land cover change: Moving beyond the myths. *Global Environment Change*, **11**(4): 261–269. [https://doi.org/10.1016/S0959-3780\(01\)00007-3](https://doi.org/10.1016/S0959-3780(01)00007-3)
- Langbein, W. B. (1947). Topographic characteristics of drainage basins, U. S. Geol. Survey, W.-S. Paper 968-C: 125-157.
- Leopold, L. B., and Maddock, T. J., (1953). The hydraulic geometry of stream channels and some physiographic implications: U. S. Geol. Survey Prof. Paper. **252** : 52.
- Magesh, N. S., Jitheshlal, K. V., Chandrasekar, N., Jini, K. V., (2012). GIS based morphometric evaluation of Chimmini and Mupily watersheds, parts of Western Ghats, Thrissur District, Kerala, India. *Earth Sci. Inform.* **5** (2): 111–121.
- Makhdumi, W., and Dwarakish, G. S., (2019). Prioritisation of watersheds using TOPSIS and VIKOR method. In: Papadavid, G., Themistocleous, K., Michaelides, S., Ambrosia, V., Hadjimitsis, D. G., (Eds.) Seventh international conference on remote sensing and geoinformation of the environment, **11174**: 6. <https://doi.org/10.1117/12.2532024>
- Mallet, F. R., (1876). Coalfields of Naga Hills, Mem. Geol. Surv. India, **2** (2).
- Mallupattu, P. K., and Reddy, J. R. S., (2013). Analysis of Land Use/Land Cover Changes Using Remote Sensing Data and GIS at an Urban Area, Tirupati, India. *Sci. World Jour.*, doi:10.1155/2013/268623
- Mardani, A., Jusoh, A., Nor, K., Khalifah, Z., Zakwan, N., and Valipour, A., (2015). Multiple criteria decision-making techniques and their applications – A review of the literature from 2000 to 2014, *Economic Research – EkonomiskaIstraživanja*, **28** (1): 516–571. <http://dx.doi.org/10.1080/1331677X.2015.1075139>
- Mas, J. F., (1999). Monitoring land-cover change: A comparison of change detection techniques. *International Journal of Remote Sensing*, **20** (1): 139–152. <https://doi.org/10.1080/014311699213659>
- Maxwell, J. C., (1960). Quantitative geomorphology of the San Dimas experimental forest, California. Dept. Geol., Columbia Univ., ONR Contract NONR 389-042, Tech. Rept. No. 19.

- Mayer, L., (1986). Tectonic geomorphology of escarpments and mountain fronts, active tectonics. National Academy Press, Washington DC.,: 125–135.
- Melton, M. A., (1957). An analysis of the relations among elements of climate, surface properties, and geomorphology. Dept. of Geol., Columbia University.
- Meshram, S. G., Alvandi, E., Meshram, C., Kahya, E., and Al-Quraishi, A. M. F., (2020). Application of SAW and TOPSIS in prioritizing water-sheds. *Water Resour.Manag.* <https://doi.org/10.1007/s11269-019-02470-x>
- Meshram, S. G., Alvandi, E., Singh, V. P., and Meshram, C., (2019). Comparison of AHP and fuzzy AHP models for prioritization of watersheds. *Soft Comput.*, **23** (24): 13615–13625.
- Meshram, S. G., and Sharma, S. K., (2015). Prioritization of watershed through morphometric parameters: A PCA-based approach. *Appl Water Sci.*, **7** (3): 1505–1519 .<https://doi.org/10.1007/s13201-015-0332-9>
- Meshram, S. G., and Sharma, S. K., (2017). Prioritization of watershed through morphometric parameters: A PCA-based approach. *Appl. Water Sci.*, **7**: 1505–1519.
- Miller, V. C., (1953). A quantitative geomorphic study of drainage basin characteristics in the Clinch Mountain area, Virginia and Tennessee; Department of Geology, Columbia University, New York.
- Mishra, N., Satyanarayana, T., and Mukharjee, R. K., (1994). Effect of topo element on the sediment production rate from sub watersheds in upper Damodar valley. *Jour.Agirc. Engg. ISAE.*, **21** (3): 65-70.
- Morisawa, M. E., (1962). Quantitative Geomorphology of some watersheds in the Appalachian Plateau. *Geol. Soc. Amer. Bull.* **73**: 1025–1046.
- Morisawa, M. E., (1985). Development of quantitative geomorphology. *Geological Society of America, Centennial Special.* **1**: 79-107.
- Munshi, M. M., (1964). Geological mapping in parts of Mizo Hills, Assam. Unpublished Progress Report of the Geological Survey of India for FS.: 1963-64.
- Mustafa, G., Tahsin, Y., and Reis, S., (2007). Using Landsat data to determine land use/land cover changes in Samsun, Turkey. *Environmental Monitoring and Assessment*, **127** (1–3): 155–167. <https://doi.org/10.1007/s10661-006-9270-1>

- Muttitanon, W., and Tripathi, N., (2005). Land use/land cover changes in the coastal zone of Ban Don Bay, Thailand using Landsat 5TM data. *International Journal of Remote Sensing*, **26** (11): 2311–2323.
- Nandy, D. R., (1972). Style of folding in the Mio-Pliocene of Tripura and Mizoram area and possible role of Basement dislocation fabrics. *Misc. Publ. Geol. Surv. Ind.* 31.
- Nandy, D. R., Gupta, S. D., Sarkar, K., and Ganguly, S., (1983). Tectonic evolution of Tripura–Mizoram Fold Belt, Surma Basin NorthEast India. *Quater. Jour. Geol. Min. Met. Soc. of India*. **35** (4): 186–194.
- Nautiyal, M. D., (1994). Morphometric analysis of a drainage basin, district Dehradun, Uttar Pradesh. *Jour. Ind. Soc. Remote Sens.* **22** (4): 251–261.
- Nitheshnirmal, S., Thilagaraj, P., Abdul Rahaman, S., and Jegankumar, R., (2019). Erosion risk assessment through morphometric indices for prioritisation of Arjuna watershed using ALOS-PALSAR DEM. *Model Earth Syst. Environ.* <https://doi.org/10.1007/s40808-019-00578-y>
- Nitheshnirmal, S., Bhardwaj, A., Pourghasemi, H. R., and Kamaraj, N. P., (2020). Morphometric attributes based soil erosion susceptibility mapping in Dyanganga watershed of India using individual and ensemble models. **79**: 360.
- NookaRatnam, K., Srivastava, Y. K., Venkateswara Rao, V., Amminedu, E., and Murthy, K. S. R., (2005). Check dam positioning by prioritization of microwatersheds using SYI model and morphometric analysis-Remote sensing and GIS perspective. *Journal of the Indian Society of Remote Sensing*. **33**: 25-38.
- National Remote Sensing Centre (NRSC) and Indian Space Research Organisation (ISRO) (2011). Manual on “Preparation of Geo Spatial Layers Using High Resolution (Cartosat-1 Pan+LISS-IVMx) Orthorectified Satellite Imagery”. Space Based Information Support for Decentralized Planning (SIS-DP), Remote Sensing and GIS Applications Area, National Remote Sensing Centre, Indian Space Research Organisation, Department of Space, Government of India, Hyderabad.
- Pakhmode, V., Kulkarni, H., and Deolankar, S. B., (2003). Hydrological drainage analysis in watershed programme planning: A case study from the Deccan basalt, India. *Hydrogeology Journal*, **11**: 595 – 604.

- Pal, S. C., and Chakraborty, R., (2019). Simulating the impact of climate change on soil erosion in sub-tropical monsoon dominated watershed based on RUSLE, SCS runoff and MIROC5 climatic model. *Advances in Space Research*. <https://doi.org/10.1016/j.asr.2019.04.033>.
- Panda, S. S., Andrianasolo, H., and Steele, D. D., (2005). Application of geotechnology to watershed soil conservation planning at the field scale, *Journal of Environmental Hydrology*, **13** (16): 1-22.
- Pande, C. B., and Moharir, K. (2017). GIS based quantitative morphometric analysis and its consequences: a case study from Shanur River Basin, Maharashtra India. *Appl. Water Sci.*, **7** (2): 861-871.
- Pandey, A., Chowdary, V. M., and Mal, B. C., (2007). Identification of critical erosion prone areas in the small agricultural watershed using USLE, GIS and Remote Sensing. *Water Resources Management*, **21**: 729-746.
- Pandey, A., Mathur, A., Mishra, S. K., and Mal, B. C., (2009). Soil erosion modelling of a Himalayan watershed using RS and GIS. *Environ. Earth Sci.*, doi:[10.1007/s12665-009-0038-0](https://doi.org/10.1007/s12665-009-0038-0)
- Pandey, P. K., and Das, S. S., (2016). Morphometric analysis of Usri River basin, Chhotanagpur Plateau, India using remote sensing and GIS. *Arab. Jour.Geosci.*, **9** (3): 240.
- Pandžić, K., and Trninić, D., (1992). Principal component analysis of a river basin discharge and precipitation anomaly fields associated with the global circulation. *Jour.Hydrol.*, **132** (1–4): 343–360. [https://doi.org/10.1016/0022-1694\(92\)90185-X](https://doi.org/10.1016/0022-1694(92)90185-X)
- Praveen, R. and Kumar, U., (2012). Integrated Approach of Universal Soil Loss Equation (USLE) and Geographical Information System (GIS) for soil loss risk assessment in Upper South Koel Basin, Jharkhand; *Jour. Geogr. Inf. Syst.*, **4** (6): 588–596.
- Patel, D. P., Gajjar, C. A., and Srivastava, P. K., (2012). Prioritization of Malesari mini-watersheds through morphometric analysis: A Remote Sensing and GIS perspective. *Environmental Earth Sciences*. doi:[10.1007/s12665-012-2086-0](https://doi.org/10.1007/s12665-012-2086-0)
- Patton, P. C., and Baker, V. R., (1976). Morphometry and floods in small drainage basins subject to diverse hydrogeomorphic controls. *Water Resour. Res.* **12**: 941–952.

- Pavano, F., Pazzaglia, F. J., and Catalano, S., (2016). Knickpoints as geomorphic markers of active tectonics: a case study from northeastern Sicily (southern Italy). *Lithosphere-US* **8**(6): 633–648. <https://doi.org/10.1130/L577.1>
- Pérez-Peña, J. V., Azor, A., Azañón, J. M., and Keller, E. A., (2010). Active tectonics in Sierra Nevada (Betic Cordillera, SE Spain): insights from geomorphic indexes and drainage pattern analysis. *Geomor.*, **119**: 74–87.
- Pike, R. J., and Wilson, S. E., (1971). Elevation-relief ratio, hypsometric integral and geomorphic area-altitude analysis, *Geological Soc. Amer. Bull.*, **82**: 1079-1084.
- Pradeep, G. S., Krishnan, M. V. N., and Vijith, H., (2014). Identification of critical soil erosion prone areas and annual average soil loss in an upland agricultural watershed of Western Ghats using analytical hierarchy process (AHP) and RUSLE techniques; *Arab. Jour. Geosci.*, **8** (6): 3697–3711.
- Prakasam, C., (2010). Land use and land cover change detection through Remote Sensing approach: A case study of Kodaikanal taluk Tamilnadu. *International Journal of Geomatics and Geosciences*, **1** (2): 150–158.
- Prasannakumar, V., Vijith, H., Abinod, S., and Geetha, N., (2011). Estimation of soil erosion risk within a small mountainous sub-watershed in Kerala, India using revised universal soil loss equation (RUSLE) and geo-information technology. *Geosci. Front.* **3**(2):209–215.
- Puno, G. R., and Puno, R. C. C., (2019). Watershed conservation prioritization using geomorphometric and land use-land cover parameters. *Glob. Jour. Environ Sci.Manag.*, **5** (3): 279–294.
- Rahaman, S. A., Ajeez, S. A., Aruchamy, S., and Jegankumar, R., (2015). Prioritization of sub watershed based on morphometric characteristics using fuzzy analytical hierarchy process and geographical information system: a study of Kallar watershed, Tamil Nadu. *Aquatic Procedia.*, **4**: 1322–1330. <https://doi.org/10.1016/j.aqpro.2015.02.172>
- Rai, P. K., Chandel, R. S., Mishra, V. N., and Singh, P., (2018). Hydrological inferences through morphometric analysis of lower Kosi river basin of India for water resource management based on Remote Sensing data. *Applied Water Science*, **8**: 15. <https://doi.org/10.1007/s13201-018-0660-7>

- Rai, P. K., Chaubey, P. K., Mohan, K., and Singh, P., (2017a). Geoinformatics for assessing the inferences of quantitative drainage morphometry of the Narmada Basin in India. *Appl. Geomat.*, **9** (3): 1–23. <https://doi.org/10.1007/s12518-017-0191-1>
- Rai, P. K., Mishra, S., Ahmad, A., and Mohan, K., (2014). A GIS-based approach in drainage morphometric analysis of Kanhar river basin, India. *Applied. Water Science*, **7**: 217–232. <https://doi.org/10.1007/s13201-014-0238-y>
- Rai, P. K., Mishra, V. N., and Mohan, K., (2017b). A study of morphometric evaluation of the Son basin, India using geospatial approach. *Remote Sens. Appl. Soc. Environ.*, **7**: 9–20. <https://doi.org/10.1016/j.rsase.2017.05.001>
- Rai, P. K., Singh, P., Mishra, V. N., Singh, A., Sajan, B., and Shahi, A. P., (2019). Geospatial approach for quantitative drainage morphometric analysis of Varuna river basin, India. *Jour. Landsc. Ecol.* **12** (2): 1–25. <https://doi.org/10.2478/jleco-1-2019-0007>
- Raj, R., Bhandari, S., Maurya, D. M., and Chamyal, L.S., (2003). Geomorphic indicators of active tectonics in the Karjan River Basin, Lower Narmada Valley, western India. *Jour. Geol. Soc. Ind.*, **62**: 739-752.
- Ram, J., and Venkataraman, B. (1984). Tectonic framework and hydrocarbon prospects of Mizoram. *Petrol. Asia Jour.* **2**: 60 - 65.
- Rao, K. S., and Lalduhawma, K., (2014). Morphometric aspects of the Tut watershed, Mizoram. *Geog. Jour.* **9**: 27 -36.
- Ratnaparkhi, N. S., Ajay, D. N., and Bharti, G., (2016). Analysis of land use/land cover changes using remote sensing and GIS techniques in Parbhani City, Maharashtra, India. *International Journal of Advanced Remote Sensing and GIS.*, **5** (1): 1702–1708. <https://doi.org/10.23953/cloud.ijarsg.54>
- Ravishankar, H. M., (1994). Watershed prioritization through the USLE using digital satellite data and an integrated approach. *Asia-Pacific Remote Sensing Journal*, **6**(2):101-108.
- Reddy, O. G. P., Maji, A. K., and Gajbhiye, S. K., (2004). Drainage morphometry and its influence on landform characteristics in a basaltic terrain, Central India - A Remote Sensing and GIS approach. *Int. Jour. Appl. Earth Obs. Geoinformatics.* **6**: 1–16.
- Reis, S., (2008). Analyzing land use/land cover changes using remote sensing and GIS in Rize, NorthEast Turkey. *Sensors*, **8** (10), 6188–6202. <https://doi.org/10.3390/s8106188>

- Renard, K. G., and Foster, G. R., (1983). Soil conservation – principles of erosion by water. In: Dryland Agriculture (Eds.) Dregne, H. E., and Wills, W. O., Amer. Soc. of Agronomy, Soil Science Society of America, Madison, WI, USA, : 155–176.
- Renard, K. G., Foster. G. R., and Y. D. C., (1997). Predicting soil erosion by water: A guide to conservation planning with the revised universal soil loss equation (RUSLE), USDA. Agriculture Handbook, **703**: 382.
- Resmi, M. R., Babeesh, C., and Achyuthan, H., (2019). Quantitative analysis of the drainage and morphometric characteristics of the Palar River basin, southern peninsular India using bAd calculator (bearing azimuth and drainage) and GIS. Geol, Ecol, Landscapes. **3** (4): 295–307.
- Rintluanga, P., (1994). Geography of Mizoram. R.T. Enterprise Publication Aizawl , Mizoram
- Rockwell, T. K., Keller, E. A., and Johnson, D. L., (1985). Tectonic geomorphology of alluvial fans and mountain fronts near Ventura, California. In: Tectonic Geomorphology. Morisawa, M. (Ed.), Proceedings of the 15th Annual Geomorphology. Symposium. Allen and Unwin Publishers, Boston, pp. 183–207.
- Roy, S., and Sahu, A. S., (2015). Quaternary tectonic control on channel morphology over sedimentary low land: A case study in the Ajay-Damodar interfluvium of eastern India. Geosci. Front. **6** (6): 927–946.
- Saaty, T. L., (1980). Fundamentals of decision making and priority theory with analytical hierarchical process: Vol. VI, RWS Publications, University of Pittsburgh, Pittsburgh, USA: 3-95.
- Samal, D. R., Gedam, S. S., and Nagarajan, R., (2015). GIS based drainage morphometry and its influence on hydrology in parts of Western Ghats region, Maharashtra, India. Geocarto. Int., **30** (7): 755–778
- Sarkar, K., and Nandy, D. R., (1977). Structures and Tectonics of Tripura-Mizoram area, India. Misc. Publ. No. 34, Geol. Survey India, pt. **1**: 141-148.
- Saxena, R. K., Verma, K. S., Chary, G. R., Srivastava, R., and Barthwal, A. K., (2000). IRS 1C Data application in watershed characterization and management. Int. Jour. Remote Sensing, **21** (17): 3197-3208.

- Schumm, S. A., (1955). The relation of drainage basin relief to sediment loss: Internal. Union Geodesy and Geophys., 10th General Assembly (Rome), Trans. **1**: 216-219.
- Schumm, S. A., (1956). Evolution of drainage systems and slopes in Badlands at Perth Amboy, New Jersey. Natl. Geol. Soc. Amer. Bull., **67**: 597–646.
- Sharma, A., Singh, P., and Rai, P. K., (2018). Morphotectonic analysis of Sheer Khadd River basin using geo-spatial tools. Spat. Inf. Res., **26** (4): 405. <https://doi.org/10.1007/s41324-018-0185-z>
- Shreve, R. L., (1967). Infinite topologically random channel networks. Journal of Geology. **75**: 178-186.
- Shrivastava, B. P., Ramachandran, K. K., and Chaturvedi, J. G., (1979). Stratigraphy of eastern Mizo Hills. Bull. O. N. G. C., **16** (2) : 87 - 94.
- Silva, P. G., Goy, J. L., Zazo, C., and Bardajm, T., (2003). Fault generated mountain fronts in southeast Spain: Geomorphologic assessment of tectonic and earthquake activity. Geomorphology. **250**: 203–226.
- Singh, G., Ram, B., and Chandra, S., (1981). Soil Loss Prediction Research in India. Bulletin Nos.T-12/D-9. Central Soil and Water Conservation Research and Training Institute, Dehradun.
- Singh, P., Gupta, A., and Singh, M., (2014). Hydrological inferences from watershed analysis for water resource management using remote sensing and GIS techniques. Egypt Jour. Remote Sens Space Sci., **17** (2): 111–121.
- Singh, S., and Singh, M. C., (1997). Morphometric analysis of Kanhar River Basin. Natl. Geogr. Jour. India, **43** (1): 31–43.
- Singh, S. K., Zeddies, M., Shankar, U., and Griffiths, G. A., (2019). Potential groundwater recharge zones within New Zealand. Geosci. Front. **10** (3): 1065–1072.
- Singh, T., and Awasthi, A. K., (2010). Stream profiles as indicator of active tectonic deformation along the inter-foreland thrust, Nahan salient, NW India. Curr. Sci., **98** (1): 95–98.
- Smith, G. H., (1935). The relative relief of Ohio. Geogr. Rev., **25**: 272-284.
- Smith, K. G., (1950). Standards for grading texture of erosional topography. Amer. Jour. Sci., **248**: 655–668.

- Snyder, N. P., Whipple, K. X., Tucker, G. E., and Merritts, D. J., (2000). Landscape response to tectonic forcing: digital elevation model analysis of stream profiles in the Mendocino triple junction region, northern California. *Geol. Soc. Amer. Bull.*, **112**: 1250–1263. <https://doi.org/10>
- Solanke, P. C., Srivastava, S., Prasad, J., Nagrajan, M. S. S., Saxena, R. K., and Barthwal, A. K., (2005). Application of Remote Sensing and GIS in watershed characterization and management. *Ind. Soc. Remote Sens.*, **33** (2): 239–244.
- Sreedevi, P. D., (1999). Assessment and management of groundwater resources of Pageru River basin, Cuddapah district, Andhra Pradesh, India. Unpublished Ph.D. Thesis, Sri Venkateswara Univ., Tirupati.
- Sreedevi, P. D., Owais, S., Khan, H. H., and Ahamed, S., (2009). Morphometric analysis of a watershed of South India using SRTM data and GIS. *Jour. Geol. Soc. Ind.*, **73**: 543–552.
- Sreedevi, P. D., Subrahmanyam, K., and Ahmed, S., (2005). The significance of morphometric analysis for obtaining groundwater potential zones in a structurally controlled terrain. *Environ. Geol.*, **47** (3): 412–420.
- Strahler, A. N., (1952). Hypsometric (area-altitude) analysis of erosional topography. *Bull. Geol. Soc. Amer.*, **63**: 1117–1142.
- Strahler, A. N., (1953). Revisions of Horton's quantitative factors in erosional terrain: Paper read before Hydrology Section of Amer. Geophys. Union, Washington, D. C., May 1953.
- Strahler, A. N., (1954). Quantitative geomorphology; proceedings, 19th International Geology Congress, Algiers, Sec., **13**: 341-354.
- Strahler, A. N., (1957). Quantitative analysis of watershed Geomorphology. *Trans. Amer. Geophys. Union.* **38**: 913–920.
- Strahler, A. N., (1964). Quantitative geomorphology of drainage basins and channel networks. In: Chow, V.T. (Ed.) *Handbook of applied hydrology*. McGraw-Hill, New York. 439–476.
- Sudheer, A. S., (1986). Hydrogeology of the Upper Araniar River basin, Chittoor district, Andhra Pradesh, India. Unpublished Ph.D. Thesis, Sri Venkateswara Univ., Tirupati.

- Sujatha, E., Selvakumar, R., Rojasimman, U., and Victor, R., (2013). Morphometric analysis of Sub-Watershed in Parts of Western Ghats, South India Using ASTER DEM. *Geomatics, Natural Hazards and Risk*, **6**: 326-341. <http://dx.doi.org/10.1080>
- Sundarakumar, K., Harika, M., Aspiya Begum, S. K., Yamini, S., and Balakrishna, K., (2012). Land use and land cover change detection and urban sprawl analysis of Vijayawada city using multitemporal Landsat data. *International Journal of Engineering Technology*, **4**(1): 166–174.
- Tandon, S.K., (1974). Lithocontrol of some Geomorphic Properties - An Illustration from Kumaon Himalayas, India, *Jour. Geomor, N.F.*, **18**: 460-471.
- Terranova, O., Antronico, L., Coscarelli, R., and Iaquina, P., (2009). Soil erosion risk scenarios in the Mediterranean environment using RUSLE and GIS: An application model for Calabria (southern Italy). *Geomorphology*. **112** (3–4): 228–245.
- Tiwari, R. P., and Jha, L. K., (1997). Morphometric analysis of watersheds in Mizoram for estimation of runoff and sediment yield. In: *Natural resource management. I, (Mizoram)*, Jha, L. K. (Ed.), A.P.H. Pub. Co., New Delhi. 332.
- Udayabahskara Rao, Ch., (2011). Drainage morphometry and tectonic implication in Lower Tlawng sub-watershed, Mizoram. *Geographic.*, **6**: 14-25.
- Verrios, S., Zygouri, V., and Kokkalas, S., (2004). Morphotectonic analysis in the Eliki fault zone (Gulf of Corinth, Greece). *Bull. Geological Society of Greece*. **36**: 1706-1715.
- Vicente-Serrano, S. M., Perez-Cabello, F., and Lasanta, T., (2008). Assessment of radiometric correction techniques in analyzing vegetation variability and change using time series of Landsat images. *Remote Sens. Environ.* **112**: 3916-3934.
- Vincy, M. V., Rajan, B., and Pradeepkumar, A. P., (2012). Geographic information system-based morphometric characterization of sub-watersheds of Meenachil river basin, Kottayam district, Kerala, India. *Geocarto Int.*, **27** (8): 661–684.
- Vittala, S. S., Govindaiah, S., and Gowda, H. H., (2004). Morphometric analysis of subwatersheds in the Pavagada area of Tumkur district, South India using remote sensing and GIS techniques. *Jour. Indian Soc. Remote Sens.*, **32** (4): 351–362.
- Vivekananda, G. N., Swathi, R., and Sujith, A. V. L. N., (2020). Multi-temporal image analysis for LULC classification and change detection. *European Journal of Remote Sensing*, DOI: 10.1080/22797254.2020.1771215

- Vivien, Y. C., Hui, P. L., Chui, H. L., James, J. H. L., Gwo, H. T., and Lung, S. Y., (2011). Fuzzy MCDM approach for selecting the best environment-watershed plan. *Jour. Appl. Soft.Comput.*, **11**: 265–275.
- Wang, L., Chen, J., Gong, P., Shimazaki, H., and Tamura, M., (2009). Land cover change detection with a cross-correlogram spectral matching algorithm. *International Journal of Remote Sensing*, **30** (12):3259–3273.
- Wani, A. A., Bali, B. S., and Mohammad, S.,(2019). Drainage Characteristics of tectonically active area: An example from Mawar Basin, Jammu and Kashmir, India. *Jour. Geol. Soc. India*, **93** (3): 313–320.
- Wells, S. G., Bullard, T. F., Menges, C. M., Drake, P. G., Karas, P. A., Kelson, K. I., Ritter, J. B., and Wesling, J. R., (1988). Regional variations in tectonic geomorphology along a segmented convergent plate boundary, Pacific coast of Costa Rica. *Geomorphology*. **1**: 239–265.
- Wentworth, C. K., (1930). A simplified method of determining the average slope of land surfaces. *Amer. Jour. Sci.*, **20**: 184-194.
- Wischmeier, W. H., and Smith, D. D., (1978). *Predicting Rainfall Erosion Losses: A Guide to Conservation Planning*. U.S. Department of Agriculture, Agriculture Handbook No. 537, USDA.
- Yadav, S. K., Dubey, A., Szilard, S., and Singh, S. K., (2016). Prioritization of sub-watersheds based on earth observation data of agricultural dominated northern river basin of India. *Geocarto International*. **33** (4): 339–356.
- Yadav, S. K., Dubey, A., Szilard, S. and Singh, S. K. (2018). Prioritisation of sub-watersheds based on earth observation data of agricultural dominated northern river basin of India. *Geocarto International*, **33** (4): 339-356
- Zaidi, F. K., (2011). Drainage basin morphometry for identifying zones for artificial recharge: A case study from the Gagas River Basin, India. *Journal of the Geological Society of India*, **77** (2): 160-166.
- Zavoianu, I., (2011). *Morphometry of drainage basins (developments in water science)*. Elsevier, Amsterdam.: 237.
- Zernitz, E. R., (1932). Drainage patterns and their significance. *Jour. Geol.*, **40** (6): 498–521.

- Zhu, Z., Fu, Y., Woodcock, C. E., Olofsson, P., Vogelmann, J. E., Holden, C., Wang, M., Dai, S., and Yu, Y., (2016). Including land cover change in analysis of greenness trends using all available Landsat 5, 7, and 8 images: A case study from Guangzhou, China (2000-2014). *Remote Sens. Environ.*, **185**: 243-257.
- Zizioli, D., (2008). DEM-based morphotectonics analysis of Western Ligurian Alps. *ScientificaActa*, **2**: 44 – 47.
- Zonunsanga, R., (2016). Estimation of Soil loss in Teirei watershed of Mizoram by using the USLE Model. *Mizoram University, Aizawl Science and Technology Journal*, **4** (I): 43-47.
- Zovoili, E., Konstantinidi, E., and Koukouvelas, I. K., (2004). Tectonic geomorphology of escarpments: the cases of Kompotades and NeaAnchialos faults. *Bull. Geol. Soc. Greece*, **36** (5): 1716–1725.
- Zubair Iqbal, M., and Javed Iqbal, M. (2018). Land use detection using remote sensing and GIS (A case study of Rawalpindi Division). *American Journal of Remote Sensing*, **6** (1): 39–51. <https://doi.org/10.11648/j.ajrs.20180601.17>

PARTICULARS OF THE CANDIDATE

NAME OF CANDIDATE : BINOY KUMAR MBARMMAN
DEGREE : Ph.D.
DEPARTMENT : GEOLOGY
TITLE OF THE THESIS : DRAINAGE MORPHOMETRY AND
MORPHOTECTONICS OF UPPER TUIRIAL RIVER
BASIN, MIZORAM

DATE OF ADMISSION : 05-08-2016


APPROVAL OF RESEARCH PROPOSAL:

1. DRC : 21-04-2017
2. BOS : 02-05-2017
3. SCHOOL BOARD : 31-05-2017

MZU REGISTRATION No.: 5604/2013

Ph.D. REGISTRATION No.
and DATE : MZU/Ph.D./ 998 of 31.05.2017

EXTENSION (If any) : NA



(Prof. SHIVA KUMAR)

Head
Department of Geology
Mizoram University

BRIEF BIODATA OF CANDIDATE

NAME : BINOY KUMAR BARMAN

FATHER'S NAME : PORESH BARMAN

DOB : 01.07.1986

ADDRESS : P.O. MAHENDRAGANJ, DIST. SOUTH WEST GARO HILLS,
MEGHALAYA

GENDER : MALE

RELIGION : HINDU

MARITAL STATUS: SINGLE

EDUCATIONAL

QUALIFICATION : M.Sc. (Geology)

Ph.D. REGISTRATION

NO. & DATE : MZU/Ph.D./998 of 31.05.2017

DEPARTMENT : GEOLOGY

TITLE OF THESIS : DRAINAGE MORPHOMETRY AND MORPHOTECTONICS OF
UPPER TUIRIAL RIVER BASIN, MIZORAM

Research Publications

1. Barman, B. K., Rao, Ch. U. B., Rao, K. S., Patel, A., Kushwaha, K., and Singh, S. K. (2021). Geomorphic Analysis, Morphometric-based Prioritization and Tectonic Implications in Chite Lui River, Northeast India. *Journal Geological Society of India*. **97**:385-395.
2. Barman, B. K., Biswakarma, P., Rao, K. S. and Joshi, V. (2020). Temporal Change Detection of Land Use/Land Cover using Remote Sensing and GIS techniques: A case study of upper Tuirial river basin, Mizoram, India. *NeBIO* 11(4)
3. Barman, B. K., Bawri, G. R., Rao, K. S., Singh, S. K., and Patel, D. (2021). Drainage network analysis to understand the Morphotectonic significance in upper Tuirial watershed, Aizawl, Mizoram. Book Chapter in “Agricultural Water Management, Theories and Practices” Academic Press. 22-46
4. Barman, B. K., Rao, K. S., Sonowal, K., Zohmingliani., Prasad, N. S. R. and Sahoo, U. K. (2020). Soil erosion assessment using Revised Universal Soil Loss Equation model and geo-spatial technology: A case study of upper Tuirial river basin, Mizoram, India. *AIMS Geosciences*, **6**(4): 525–544.
5. Biswakarma, P., Barman, B. K., Joshi, V. and Rao, K. S. (2020). Landslide Susceptibility Mapping in East Sikkim Region of Sikkim Himalaya Using High Resolution Remote Sensing Data and GIS techniques, *Applied Ecology and Environmental Sciences*, **8** (4):143-153
6. Barman, B. K. and Rao, K. S. (2021). Geology of Sedimentary formations in the state of Mizoram, NE India: A Review. Book Chapter: Mizoram, Environment, Development, and Climate Change. Today and Tomorrow's Printers and Publishers: 183-195
7. Barman, B. K., Bora, K., Rao, K. S., Baruah, A. and Gogoi, L. (2020). Drainage Morphometry and morphotectonic significance of Singen watershed in upper Subansiri District of Arunachal Pradesh. Edited Book chapter “Advances in Environmental Research of North East India”. South Eastern Book agencies, Guwahati. 255-282
8. Barman, B. K., Nath, P., Gogoi, L., and Rao, K. S., (2021). Morphometric Analysis of Tuikual watershed, Mizoram, using Remote Sensing and GIS Techniques. Edited Book Chapter “Recent Advances in Earth Science Research in North East India” South Eastern Book agencies, Guwahati. 64-76
9. Barman, B. K., Rao, K. S. and Saikia, I. J. (2019). Delineation of potential landslide prone zones using Remote Sensing and GIS Techniques: A case study from north western part of Aizawl city, Mizoram, India. *Research Review International Journal of Multidisciplinary*, **4**(4):1395-1400
10. Barman, B. K., Gogoi, C. and Rao, K. S. (2019). Remote sensing and GIS application for morphometric analysis of Upper Mat watershed, Serchhip district, Mizoram. *Journal of Applied Geochemistry*. **21** (2):185-195.
11. Barman, B. K. and Rao, K. S. (2019). Landslide hazard susceptibility mapping of upper Tuirial watershed, Mizoram, using Remote Sensing and GIS techniques. *International Journal of Research and Analytical Reviews*. **6**(1):1624-1630
12. Barman, B. K., Rao, K. S. and Prasad, N. S. R. (2017). Use of Geographic Information System in Hypsometric analysis of Chite Lui watershed, Aizawl district, Mizoram. Conference proceeding “Natural Resources Management for Sustainable Development and Rural Livelihoods” held during 26th -28th October, 2017, At the Department of Geography and Resource Management, Mizoram University.

Professional Development

1. Participated in the National Training Programme on Earthquake Risk Mitigation jointly organized by National Institute of Disaster Management, Ministry of Home Affairs, Government of India, New Delhi and North-Eastern Hill University, Shillong from July 08 -10, 2020 using online mode.
2. Attended e-Training on “Refresher Course on NGCM Data Handling and Interpretation” conducted by RTD, NER, GSITI, Shillong from 20.07.2020 to 24.07.2020.
3. Attended e-Conference on Climate Change, Environmental Health and Sustainable Development Goals in Post COVID-19 World during 4th-5th June, 2020. Organized by University School of Environment Management Guru Gobind Singh Indraprastha University, Sector 16 C, Dwarka, New Delhi – 110078
4. Attended a 3 days International workshop on “TecTask Workshop Structural Geology in the 21st Century” held during 26-28 February 2020 at the Department of Geology & Geophysics, IIT Kharagpur.
5. Attended National Conference on Emerging Trends in Environmental Research (NACETER 2019) during 31st October - 2nd November, 2019, At the Department of Environmental Science, Pachhunga University College (A Constituent College of Mizoram University), and presented the paper titled: "Drainage Morphometry and Morphotectonic Significance of Singen Watershed in Upper Subansiri District of Arunachal Pradesh".
6. Attended National Conference on “Big Geospatial Data: Analytics, Modelling and Applications (BiGMAP 2019) during September 25-26, 2019 held at Punjab Agricultural University Campus, Ludhiana and presented the paper titled “Identification of Soil Erosion Prone Zones Using Revised Universal Soil Loss Equation (RUSLE) Model and Geo-Spatial Technology. A case study on Upper Tuirial watershed, Mizoram.”
7. Attended Science Academies' Refresher Course on "Mineralogy, Petrology, Thermodynamics, Ore Geology, Structural Geology and Tectonics" Organized by Department of Geology, Mizoram University, held during September 17-30, 2018.
8. Participated in 4th webinar an online course on “Remote Sensing Technology” organized by Space Education and Research Foundation (SERF), Ahmadabad, India, held during August 20-30, 2018.
9. Participated in the debate competition on the topic “Application of Geosciences for sustainable growth is Utopian dream for country like India” held on 12th August 2018 at ONGC Jorhat, Assam.
10. Attended training programme on “Remote Sensing for Geological Applications” conducted by National Remote Sensing Centre (NRSC), Hyderabad, held during July 16-20, 2018.
11. Attended training programme on “Village Disaster Management Plan” organised by National Institute of Disaster Management (NIDM), New Delhi, held during July 9-13, 2018.
12. Attended National Seminar On “Dynamics of Surface and Sub-Surface Geological Processes” held during 8th - 9th February 2018, At the Department of Earth Sciences, Pondicherry University and presented the paper titled: Characterization of Hydrogeomorphological Aspects of the Upper Tuirial Watershed, Mizoram By Geospatial Technique
13. Participated Science academies' Refresher course on “Hydrology of Floods” organized by GB Pant university of Agriculture and Technology, Pantnagar from 8th January--19th January, 2018, at National Institute of Hydrology (NIH), Roorkee and GB Pant university of Agriculture and Technology, Pantnagar

14. Participated Science academies' Refresher course on "Modern and Ancient Environment and Ecology: Sediments and Biota" organized by the department of Geological Sciences, Jadavpur University, Kolkata from 4th December--24th December, 2017, at Jadavpur University, Kolkata and Chandipur-Baripada, Orissa.
15. Participated Science academies' two-week Refresher course on "Theoretical Structural Geology, Crystallography, Mineralogy, Thermodynamics, Experimental Petrology and Theoretical Geophysics" held during 20th November--4th December, 2017, at Indian Academy of Sciences, Bengaluru.
16. Attended the International Conference On "Natural Resources Management for Sustainable Development and Rural Livelihoods" held during 26th -28th October, 2017, At the Department of Geography and Resource Management, Mizoram University, and presented the paper titled: Application of Remote sensing and GIS for Hypsometric Analysis of ChiteLui watershed in Aizawl District of Mizoram.
17. Attended a 3 days International workshop and training on "Hydro-Meteorological Monitoring and Watershed Management" organized by Mizoram University, University of Minnesota and Mississippi Watershed Management Organization held during October 23-25, 2017.
18. Attended a short course on Challenges and Advances in Planetary Science (CAPS 2017) organized by Centre for Earth Sciences, Indian Institute of Science, Bengaluru held during September 18-22, 2017.
19. Attended the International Conference on Remote Sensing and GIS for Applications in Geo-Sciences held on 12th August 2017, At the Department Of Geology, Aligarh Muslim University, and presented the paper titled: Remote Sensing And GIS Aspects Of Morphometric Analysis In The Upper Mat Watershed, Serchhip District, Mizoram
20. Attended a one-day training program on landslide susceptible area mapping using frequency ratio modeling, held on 11th August 2017, At the Department of Geology, Aligarh Muslim University, Aligarh , Uttar Pradesh.
21. .Attended a one month training course on "Application of Remote Sensing and GIS in Mineral Exploration 2017" at Geological Survey of India Training Institute (GSITI), Hyderabad.
22. Attended a 9 days Geological Field Course on "Practical Applications of Neotectonics and Quaternary Geology in Geologic Hazards Assessment" Organized by GeoHazards Society, India, GeoHazards International and Government of Mizoram.
23. Attended one week workshop on "Official Statistics in North Eastern States" Organized by Indian Statistical Institute (ISI), Kolkata and Department of Statistics, Pachhunga University College,

ABSTRACT

DRAINAGE MORPHOMETRY AND MORPHOTECTONICS OF UPPER TUIRIAL RIVER BASIN, MIZORAM

A THESIS SUBMITTED IN PARTIAL FULFILMENT OF THE REQUIREMENTS FOR
THE DEGREE OF DOCTOR OF PHILOSOPHY

BINOY KUMAR BARMAN

MZU REGN. NO. 5604 OF 2013
Ph.D. REGN. NO. MZU/Ph.D./ 998 of 31.05.2017



**DEPARTMENT OF GEOLOGY
SCHOOL OF EARTH SCIENCES AND NATURAL RESOURCES MANAGEMENT
AUGUST, 2020**

ABSTRACT

**DRAINAGE MORPHOMETRY AND MORPHOTECTONICS OF
UPPER TUIRIAL RIVER BASIN, MIZORAM**

BY

**BINOY KUMAR BARMAN
DEPARTMENT OF GEOLOGY**

Research Supervisor

**Prof. K. Srinivasa Rao
Department of Geology, Mizoram University, Aizawl**

Joint Supervisor

**Dr. N.S.R. Prasad
Centre for Geoinformatics Applications in Rural Development,
National Institute of Rural Development and Panchayat Raj, Govt. of
India, Guwahati.**

Submitted

**In Partial fulfilment of the requirement of the degree of
Doctor of Philosophy in Geology of Mizoram University, Aizawl**

Abstract

Upper Tuirial watershed is the western tributary of Barak River of Assam which covers an area of 534.81 km², originates in the state of Mizoram, NE India. This study was carried out to understand the sub surface lithological characteristics, morphology and evolution of the landforms also to explore various important natural resources using conventional, Remote Sensing and GIS based analysis. The morphometric analysis of an area is an important criterion to monitor and understand the hydrological behaviour of the basin and to carry out management strategies of the watershed based on prioritization. A total of 19 sub-watersheds were delineated and calculated the various morphometric parameters. Following the computation of morphometric parameters and their significant values, prioritisation of Sub-watershed was done through geo-statistical techniques for immediate remedies.

This study reveals that the Upper Tuirial River is a six order river basin. The study is mainly focused on basin morphometric parameter such as linear aspects [Stream Order, Bifurcation Ratio, Stream length, Stream frequency and areal aspects [Form factor, Circulatory Ratio, Elongation Ratio and Drainage density] and Relief aspects [Relief, Relative relief, Relief ratio and Ruggedness Number]. During the study, relationships among the linear morphometric indices hold true for Horton's Law of drainage composition.

Based on the detail analysis of the linear, areal and relief aspects of morphometric parameters, it is found that upper Tuirial watershed, as well as those of the nineteen sub basins are characteristics of resistant and impermeable sub surface having homogeneous lithology, late youth to mature stage of erosional development and less storage capacity of water. Lower-order streams mostly dominate each basin. Based on mean weighted bifurcation ratio values it is found that sub watershed Kailian (5.34), Ngharum (5), Zilpui (5.49), Muthi (5.36) and Tuipawl (5) are structurally controlled basin. Sub watershed sakei, suibual, Belkhui, Nghalrawh, Tuiphu, Tuizual and Chite are slightly structurally distorted and the sub watersheds Nghathup, Sherbawk, Tuirial, Tulrital, Darkhuang, Suanghuan and SW18 are geologically controlled basin. High values of drainage density and drainage frequency with coarse to mostly medium texture ratio suggesting impermeable sub surface lithology, less infiltration rate, rugged topography, and high run off with high rate of erosion and dissection. Lg values for different sub watershed ranges from 0.09 km for Darkhuang to 0.20 km for Nghathup indicating high runoff, less infiltration and high rate of erosion. As the

length of overland flow is very short, construction of artificial recharge structures is not feasible in the region. The constant of channel maintenance value is $0.25 \text{ km}^2/\text{km}$ i.e., only 250 square meters of area is needed to run 1000 meters of stream indicating that the area is characterized by high surface runoff, low permeability, less infiltration and closely dissected. The circularity ratio values ranges from 0.44 for Kailian to 0.67 for Muthi indicates that the area is characterized by high to moderate relief, mature stage of geomorphic development and elongated in shape. The values of Relief ratio, gradient ratio and average slope angle indicate that the discharge capability of the watersheds is very high and ground water potential is meagre. The hypsometric integral value ranges from 0.5 to 0.55 indicating that all the sub watersheds have attained the steady state condition (mature geologic stage).

As an applied aspect of morphometric analysis, identification and prioritization of soil erosion prone zones and groundwater potential zones were also demarcated in the study area.

Prioritisation of different sub watersheds were carried out using Compound Factor (CF) model as Multi Criteria Decision Making (MCDM) techniques and the results showed that sub-watershed Tulrital is highly susceptible to erosion followed by sub watersheds Zilpui, Tuiphu, SW18, Belkhui, Darkhuang, sakei, Chite, Ngharum, Muthi, Tuipawl, Nghalrawh, Kailian, Suanghuan, Suibual, Nghathup, Sakei, Sherbawk and the least erosive sub watershed is Tuirial.

For the identification of groundwater potential zones, TOPSIS (Technique of Order Preference Similarity to the Ideal Solution) based multi criteria decision making tool was performed on selected morphometric parameters. The result of this analysis revealed that sub watershed Kailian is the best potential zones for groundwater resources and sub watershed Tulrital is found to be the most deficit zone of groundwater.

The second aspect of the study is the Morphotectonic study of Upper Tuirial watershed for investigating geomorphic signatures of active tectonics using geographical information system (GIS). Most commonly used geomorphic indices for morphotectonic analysis; viz. Basin elongation ratio (Re), Transverse topographic symmetry (T), Asymmetric factor (AF), Valley floor width to valley height ratio (Vf), Mountain front sinuosity (Smf), Longitudinal profile and Stream length gradient index (SL) have been used in this study. From the analysis of various morphotectonic parameters, it is found that there is a strong relationship between topography and active deformation and is reflected in the geological and

geomorphological set-up of the Upper Tuirial Basin. The lineament analyses indicate that there is only one set of prominent lineaments trending almost N-S direction and few lineaments oriented in all directions. The development of N-S oriented Faults/lineaments is expected in this region as the basin is under East-West tectonic compression due to collision of Indo-Burmese plates. The elongation ratio values found to be 0.56 indicating that the basin is slightly tectonically active. The Hypsometric Integral values vary from 0.50 for Suibual to 0.55 for Ngharum and 0.51 for the whole watershed indicating mature landscape and slightly tectonically active. Exceptionally high value of stream length gradient index is shown as knick zones along the longitudinal profile of sub watershed Chite, Muthi, Suanghuan, Tuizual, Ngharum and Tulrital. These anomalous high values cannot be due to rock resistance to erosion only, but there must be some strong tectonic activity. The values of valley floor to valley height ratio indicate deep, narrow, V-shaped valleys due to intense incision and gradual uplift signifies strong tectonic activity. The mountain-front sinuosity values for different sub watersheds measured at different sections are found to be in the ranges of 1.02 to 1.52. These low values are the indication of active tectonism in the watershed. The values of asymmetry factor revealed that all the major channels have been shifted downstream to either right tilt or left tilt. This downstream shifting of river is possibly due to the obstruction by faulting.

Soil loss assessment was also carried out in the present study. Soil erosion is a major problem in the present world which affects the agricultural production, soil fertility, excessive siltation and sedimentation in lakes and rivers. Though it is a natural process but due to anthropogenic intervention in over exploitation of natural resources, this process has been accelerated in the recent past. Degradation of land cover due to shifting cultivation is one of the triggering factors in accelerating the soil erosion in this region. A comprehensive methodology that is Revised Universal Soil Loss Equation (RUSLE) was adopted in the present study in order to estimate the soil loss of Tuirial river basin of Mizoram. The various thematic layers generated and utilized for the RUSLE model are rainfall erosivity factor (R), soil erodibility factor (K), slope length (L), slope steepness factor (S), crop management factor (C) and practice management factor (P). For analysis of each layer, rainfall data collected from Directorate of Agriculture and Crop Husbandry, govt. of Mizoram, soil textural map was generated based on the National Bureau of Soil Survey and Land Use Planning (NBSS & LUP), CARTOSAT DEM of 30 m spatial resolution for L and S factors, and Sentinel 2A multispectral satellite data for C and P factors were used. The estimated

average annual soil loss from the study area is found to be $115.4 \text{ Mg ha}^{-1} \text{ yr}^{-1}$. The estimated total loss of sediments is 6.161 million Mg yr^{-1} . From this study it is also found that the severe erosion zones are mostly in areas with high slope values. While slight erosions are mostly observed in areas with low slope values. The prominent cause of soil erosion in the study area is high intensity of rainfall, mountainous terrain with steep slopes and unscientific practices of shifting cultivations.

Land use and land cover change detection for a period of 2000 to 2018 was analysed to monitor LULC transformation. The overall accuracy assessment and kappa coefficient values showed accepted accuracy limit. Over the study period, there is a significant changes observed in LULC classes, as evidenced by a sharp increase in built-up from 1.51% in 2000 to 4.02 % in 2018 and a net increase of 14.04% of scrubland within the landscape. The period 2000-2018 has shown a sharp decrease of jhumland from 19.65 % to 2.02% and the forest cover remains almost unchanged. This study will be useful for the forest department to carry out forestation activities in the spatially distributed scrubland and also useful in monitoring the changes that area happening in our ecosystem and environment.